Functional study of chromatin modulators-histone H1 and HP1 in *Drosophila melanogaster*

Inauguraldissertation

zur

Erlangung der Würde eines Doktors der Philosophie

vorgelegt der

Philosophisch-Naturwissenschaftlichen Fakultät

der Universität Basel

von

Jian-Quan Ni

aus Beijing, People's Republic of China

Basel 2005

Friedrich Miescher Institute for Biomedical Research

Maulbeerstrasse 66

CH-4058 Basel

Genehmigt von der Philosophisch-Naturwissenschaftlichen Fakultät auf Antrag von Prof. Frederick Meins Jr, Prof. Patrick Matthias und Dr. Fang-Lin Sun.

Basel, den .11.25.2005

Prof. Dr. Hans-Jakob Wirz

Acknowledgements

Many thanks go to Prof. Dr. Frederick Meins Jr and to Prof. Dr. Patrick Matthias for serving as members in my thesis committee, they have been actively encouraging me to work creatively, intellectually and efficiently. I'm also very grateful to my thesis supervisor, Dr. Fang-Lin Sun, for introducing me to come to Friedrich Miescher Institute and for helping me in many aspects of my scientific career.

I would like to thank all the members of the Sun group, the Epigenetic groups in the FMI, who have given me a great deal of supports and friendship over the years. Certainly, these supports and friendship led me to a steady and successful academic performance and a happy life in Switzerland.

My very special thanks go to my wife Lu-Ping Liu and to our families in China for their continuous supports during my Ph.D. study.

Table of Contents

I. Summary

The impact of chromatin structure on transcriptional gene activity, and many other nuclear events, has become increasingly apparent over the past few decades. It is known that eukaryotic DNA in the cell nucleus is packaged into periodic nuclear proteins known as nucleosomes, the basic units of chromatin. Within each nucleosome, about 146 bp of DNA is wrapped around a core histone particle consisting of two molecules each of histones H2A, H2B, H3 and H4. It is believed that linker histone H1 binds to the linker DNA between nucleosomes, to stabilise the nucleosome and protect an additional 20 bp of DNA from nuclease digestion. Histone H1 promotes or facilitates the condensation of nucleosome filaments into supercoiled chromatin fibres, then further forms chromosomes, which can normally be seen under a microscope. Studies *in vitro* have shown that H1 is a transcriptional repressor, while the effect of histone H1 on transcription *in vivo* is rather gene-specific. Linker histone H1 inhibits DNA repair and homologous recombination in unicellular and simple multicellular organisms. In higher multicellular organisms, H1 appears to play a key role in apoptosis and cell differentiation. However, the dynamics of histone H1 in higher-order chromatin packaging, and its role in transcriptional gene regulation, remain largely unknown.

The eukaryotic linker histone H1 has a typical structure consisting of a tripartite structure of a trypsin-resistant central globular domain flanked by basic N- and C-terminal tails. It has been proposed that the globular domain binds the DNA where it enters and exits the nucleosome, while the C-terminal tail binds to the linker DNA and facilitates condensation of chromatin. Several models have been suggested, based on indirect biochemical evidence, for the location of H1 in nucleosomes. However, the precise location of H1 in the nucleosome and how it is involved in higher-order chromatin packaging still remain debated issues. Unlike mammalian cells which have many H1 variants, *Drosophila melanogaster* contains about 100 copies of histone H1 genes but these encode only a single type of H1 protein with a structure typical of linker histone H1 in higher

eukaryotes, and thus provides us with an ideal model system to address the function of H1 in chromatin and its impact on development. Using *in vitro* and *in vivo* biochemical and genetic approaches, we have tried to investigate the role of H1 in nucleosome dynamics and chromatin transcriptional gene silencing.

Besides linker histone H1 and core histones on chromatin, a large number of non-histone proteins, such as polycomb group protein, trithorax protein and HMG protein, are also associated with chromatin and play important roles in gene transcription. Another molecule, which we are interested in, is heterochromatin protein 1 (HP1): this is of the key components of condensed chromatin, and is primarily localised at heterochromatic domains. Our study showed that a number of regions in euchromatin also contain HP1, indicating that HP1 plays a genome-wide role in chromatin organization. Other recent papers have described the interaction of HP1 with both methylated histone H3 at lysine 9 and the methyltransferase enzyme (Su(var)3-9), and have further proposed a mechanism for maintenance and spreading of heterochromatin. To access the role of HP1 in cell proliferation and development, we conditionally deplete HP1 using the RNA interference (RNAi) approach. The effects of HP1 on chromatin structure, cell cycle regulation, genome-wide gene expression and late-stage development are being studied.

II. Introduction

1. Chromatin

Eukaryotic cells contain 10 million to 100 billion base pairs DNA in each nucleus. The DNA molecules that comprise the human genome could spread nearly 2 m in length if they were laid end to end. DNA in the cell nucleus is compacted over 10,000-fold compared to its straight form, and is only a few microns in diameter. This delicate line of DNA, encoding the blueprint of all life, is then further packaged by the histone proteins into a hierarchical structure called chromatin (Van Holde, 1998; Felsenfeld and Groudine, 2003) (Fig 1). The nucleosome, the fundamental repeating unit of chromatin, consisting of core histone proteins and DNA, leads to the 11nm chromatin fiber. The nucleosome "beads" are further packed together into higher orders of structure, which creates a barrier for the molecular machinery that needs access to the information encoded by DNA for chromatin and gene regulation events.

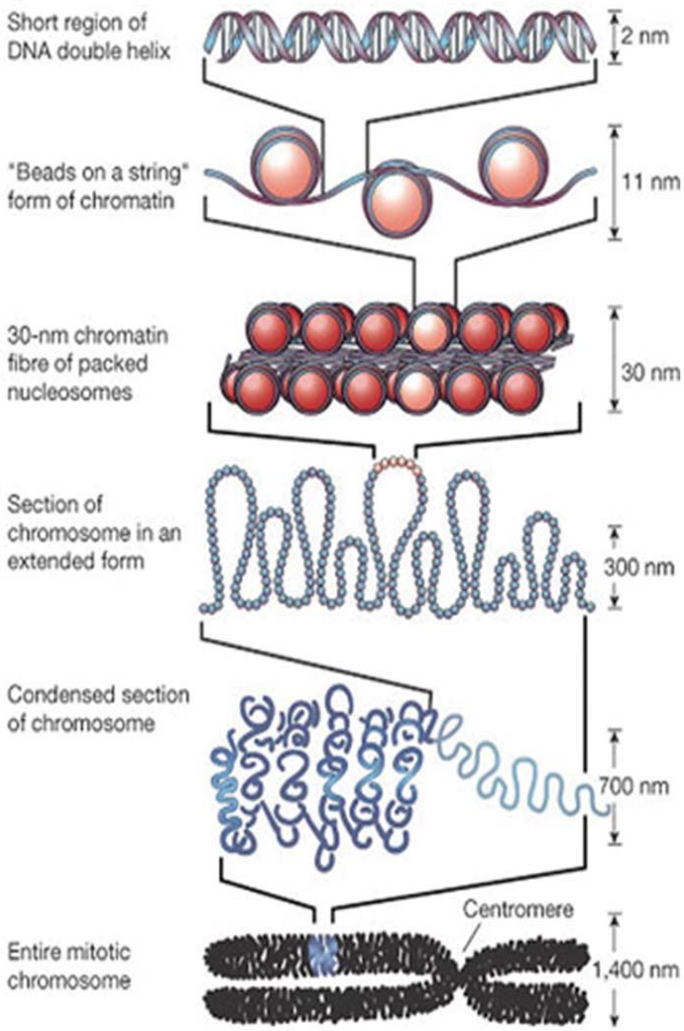

Fig 1. Chromatin structure.
Felsenfeld and groudine, 2003

The modulation of chromatin structure is central to the regulation of gene expression. At the level of the nucleosome, covalent modifications to histone

proteins can generate synergistic or antagonistic interaction affinities for regulators, which in turn dictate dynamic transitions to either transcriptionally active or transcriptionally silent states (Jenuwein and Allis, 2001). Also, normal histones exchange with their variants (Fan *et al*., 2002; McKittrick *et al.*, 2004). These variants encoded by distinct, non-allelic genes, have long been recognized (Van Holde, 1989). Variant histones are assembled into nucleosomes in a replication-independent manner, in contrast to the assembly of bulk chromatin, which is coupled to replication. Recent studies have described that variants of histones H1, H2A and H3 play important role(s) not only in the dynamics of chromatin modifications, but also in apoptosis, cell differentiation, DNA repair and the assembly of centromeres (Redon *et al*., 2002; Smith *et al*., 2002; Akimitsu *et al*., 2003; Hansol *et al*., 2004; Henikoff *et al*., 2005).

1.1. Euchromatin

The chromatin in higher eukaryotes is subdivided into euchromatin and heterochromatin. Euchromatin is a type of the decondensed state of chromatin where it enriches gene density, stains only lightly in GTG banding (Heitz, 1928), replicates early during S-phase, is generally transcription active, and is partially or fully uncoiled. (Fig 2). It is becoming clear that specific patterns of core histone modifications, such as acetylation (e.g. global histone acetylation), and methylation (e.g. H3 Lys4,79 methylation) (Jiang *et al*., 2004), mark these regions and direct the formation of distinct chromatin domains.

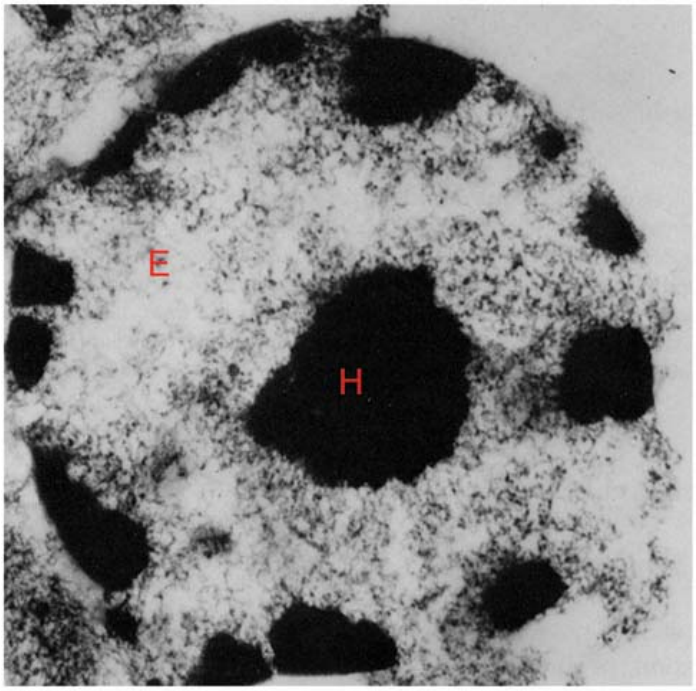

Fig 2. The distribution of euchromatin (E) and heterochromatin (H) in a normal calf thymus lymphocytes (Electron micrograph, X 5,000).

1.2. Heterochromatin

Heterochromatin comprises up to 30% of the Drosophila and mammalian genomes. In contrast to euchromatin, it is concentrated in large blocks, predominantly in the centric and subtelomeric regions of all chromosomes (Fig 2), and replicates late in the S-phase. This part of the genome has unusual cytological, molecular and genetic properties, such as late replicated, and condensed throughout the cell cycle, and has the ability to suppress the transcription of a euchromatic gene placed adjacent to these domains. Methylation of histone H3 lysine 9 generates heterochromatin domains that is recognised through the binding of heterochromatin protein- HP1. Recent studies using genetic and biochemical approaches have shown that the RNAi machinery also plays an important role in the formation of heterochromatin(Sharon *et al*., 2004) (Fig 3). RNAi not only acts post-transcriptionally (Filipowicz, 2005), but components of the RNAi machinery can also be involved in nuclear processes leading to heterochromatin formation and TGS (transcriptional gene silencing) (Taddei *et al.*, 2001; Mochizuki *et al.*, 2002; Volpe *et al*., 2002; Grewal *et al.*, 2003). Recent studies suggest that RNA-mediated heterochromatin formation appears to be a part of natural epigenetic gene regulation mechanism (James *et al.*, 2004). This mechanism is active in most eukaryotes and associated with heritable changes in gene expression that are not caused by mutations or deletions. Nuclear RNAi

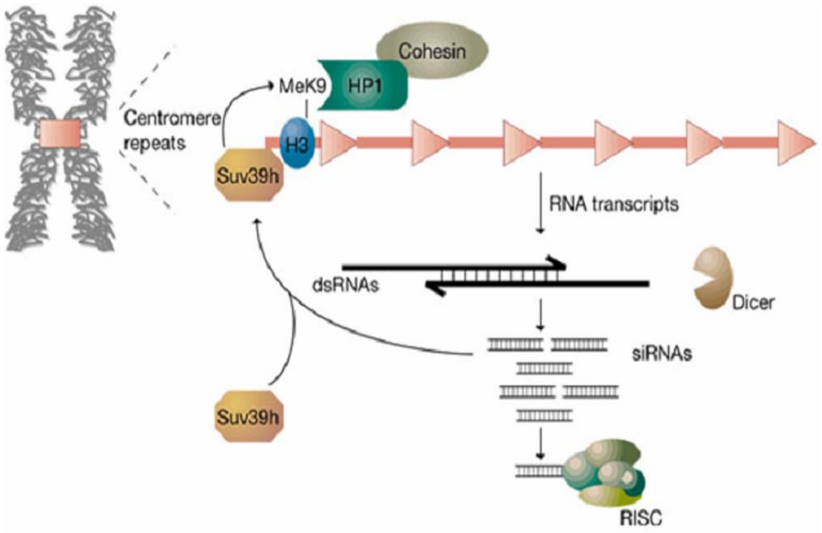

Fig 3. A model for RNAi-mediated heterochromatin assembly in vertebrates

(Sharon A. et al., 2004)

may be also functions as a surveillance mechanism against foreign DNA or RNA (retroelements and transposons), and is involved in the regulation of developmental genes, and contributes to chromosome segregation during cell division. In some organism, nuclear RNAi can engage specific processes, e.g. DNA methylation and/or RNA amplification; however, targeting of a homologous chromosomal region for chromatin modifications by an RNA inducer is a common theme (Wassenegger, 2005). In *Drosophila*, the establishment of heterochromatin also requires the recruitment of the histone H2Av variant followed by H4 Lys12 acetylation, before H3 Lys9 methylation and HP1 recruitment can take place (Swaminathan *et al.*, 2005).

On the other hand, either form of the chromatin can be converted to the other. For example, conversion of euchromatin being associated with transcriptional gene activation to heterochromatin being associated with transcriptional gene repression, or vise verse. However, the conversion between euchromatin and heterochromatin is gradual and requires specific chromatin modulators and multiple cell cycle division (Yael *et al*., 2005). Stable epigenetic inactivation of gene expression by silencing complexes involves a specialised heterochromatinization process, for example, when euchromatin is converted to the stable heterochromatin state in *Saccharomyces cerevisiae*, the induction of heterochromatin is regulated by the expression of the silencing protein Sir3, resulting in rapid loss of histone acetylation and euchromatic histone methylation. Strains lacking Sas2 histone acetylase or the histone methylases that modify Lys4 (Set1) or Lys79 (Dot1) of H3 display accelerated Sir3 accumulation at the heterochromatic *HMR* (silent mating-type locus) or the telomere, indicating that these histone modifications may exert distinct effects on heterochromatin formation. These findings supporting an ordered pathway of heterochromatin assembly, consisting of an early phase, driven by active enzymatic removal of histone acetylation and resulting in incomplete transcriptional silencing, followed by a slower maturation phase, in which gradual loss of histone methylation enhances Sir association and silencing.

In pericentic heterochromatin region, there is a unique chromosomal locus, called centromeres, that mediates multiple segregation functions, including kinetochore formation, spindle-mediated movements, sister chromatid cohesion and a mitotic checkpoint(Beth and Gary, 2004) (Fig 4). The centromeric (CEN) chromatin is embedded in heterochromatin and contains blocks of histone H3 nucleosomes interspersed with blocks of CENP-A (a histone H3 variant) nucleosomes: the H3 variant provides a structural and functional foundation for the kinetochore. In humans and *Drosophila melanogaster* CEN chromatin, the pattern of histone modification is distinct from that of both euchromatin and flanking heterochromatin (Sullivan and Gary, *et al.*, 2004): CEN chromatin fibres lack heterochromatic modifications: H3 is not di- or trimethylated at Lys9 in CEN chromatin; there is a partial overlap with di-, but not trimethylated H3 at Lys4, and H3 contains hypoacetylated histones. Heterochromatin is clearly excluded from CEN chromatin at metaphase, but is believed to play a role in the function of centromere. These distinct modification patterns may contribute to the unique domain organization and three-dimensional structure of centromeric regions, and/or to the epigenetic information that determines centromere identity.

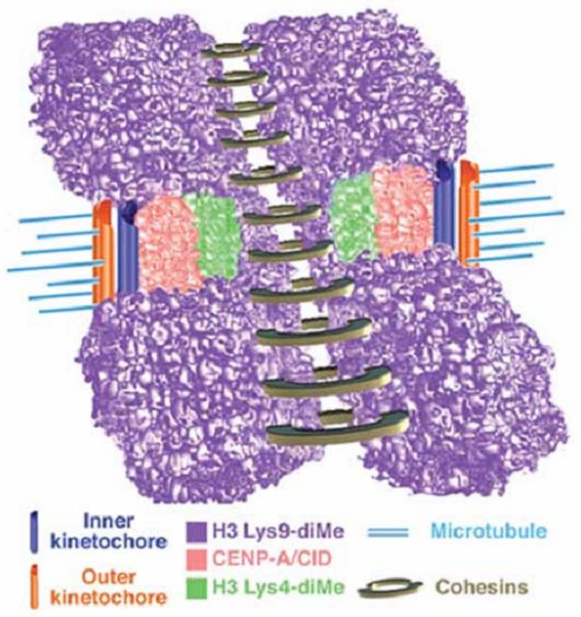

Fig 4. **Model** for three-dimensional organization of centromeric (CEN) chromatin in *D. melanogaster* and humans.

(Beth A Sullivan & Gary H Karpen, 2004)

2. Nucleosome core particle

A nucleosome core particle is the central part of a nucleosome. It consists of 147 bp double-stranded DNA and a histone core octamer (Fig 5). The histone core octamer contains four sets of dimmers, which interact with each other through the “histone fold” domain (Kornberg *et al.*, 1999). Histones H3 and H4 interact through specific domains to form a heterodimer, while histones H2A and H2B

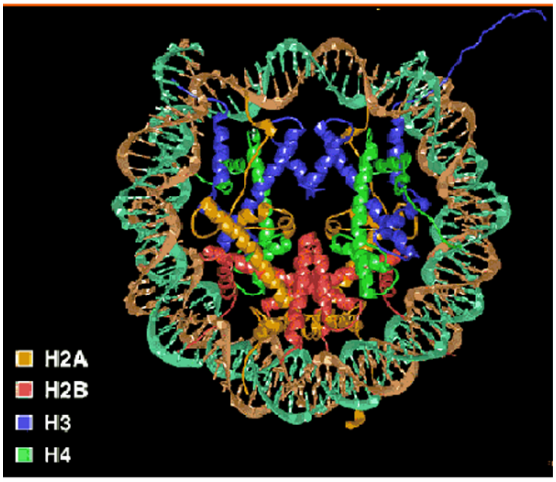

Fig 5. A top review of nucleosome core particle.
(T. Richmond's laboratory)

interact to each other to form dimers. Other interactions, including 4-helix bundle interactions between histones H3 and H3', form the core H3-H4 tetramer. The interactions between H2A/H2B and H3/H4 form the octamer, which is also called the nucleosome core particle (Luger *et al.*, 1997).

2.1. Core histone proteins

In addition to histones which are known to compact DNA, the histone proteins also undertake protein-protein interactions between themselves and other non-histone proteins. However, not all eukaryotic cells contain histones, for example dinoflagellates are reported to package the majority of their DNA with small basic proteins which are unlike histones (Vernet *et al.*, 1990); and in mammalian species the majority of DNA in spermatozoa is compacted through interaction with a basic proteins known as protamines. Each nucleosome consists of core histone proteins and the 2 full-turns of DNA sorrounding them. These core histone proteins in an octomer include two molecules of each of four different histone proteins: H2A, H2B, H3 and H4. Since histones can be removed from DNA under high concentration of salt, the major interactions between DNA and the core histones appear to be electrostatic in nature. Histones H2A and H2B dissociate first as the salt concentration is raised, followed by histones H3 and H4. Based on chemical cross-linking studies, histones H2A and H2B form a stable dimmer (H2A/H2B), whereas histones H3 and H4 form a stable tetramer ($(H3/H4)_2$) in the absence of DNA. The core histones are remarkably conserved in length and amino acid sequence through evolution. Histones H3 and H4 are the most highly conserved; for example, human and Drosophila histone H4 differ

at only one site in 102 residues. Histones H3 and H4 have a key role both within the nucleosome and in many other chromosomal processes, these functional and structural requirements possibly contributing to their remarkable sequence conservation. Histones H2A and H2B are slightly less conserved than H3 and

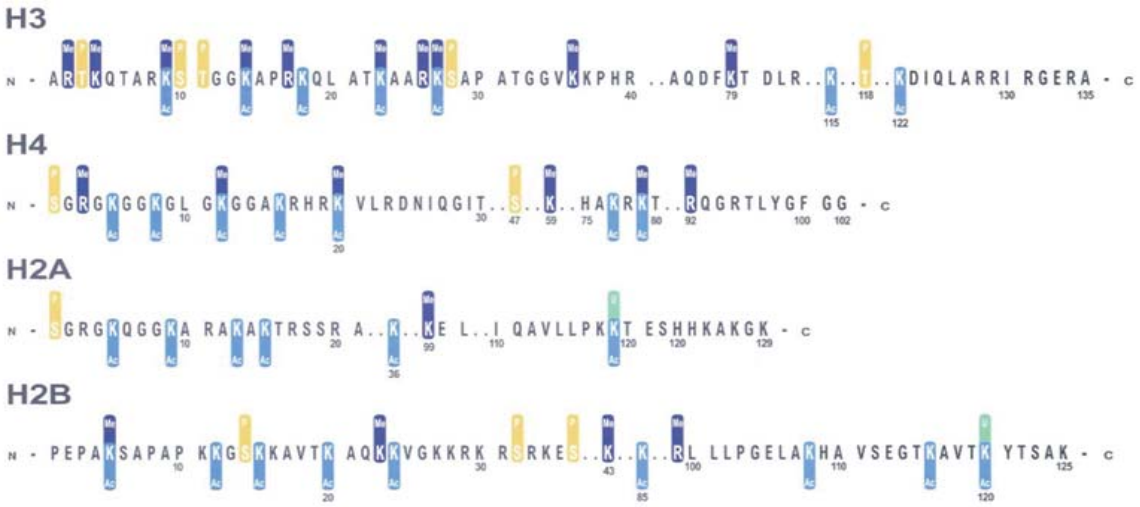

Fig 6. Core histone modification map

H4. All core histones are small basic proteins (11,000-17,000 Da molecular weight) containing higher percentage of lysine and arginine (more than 20% of the total amino acids). Histones H2A and H2B contain more lysine (13 out of 124, and 21 out of 123 amino acids, respectively, in *Drosophila*), and histones H3 and H4 contain more arginine (18 out of 136, and 14 out of 103 amino acids, respectively, in *Drosophila*). The extended histone-fold domain contains three conserved α-helices at the C-terminal tails of the protein through which histone-histone and histone-DNA interactions occur, and charged tails at the N-terminal end contain the bulk of the lysine residues (Arents *et al.*, 1991). The amino acid sequence of the charged N-terminal tails is also conserved and can be post-translational modified (Fig 6) by different regulatory proteins. The modification of core histone tails plays an important role in chromatin structure and gene regulation. Although core histones are extremely well conserved throughout eukaryotes, some variants are now known to be functionally distinct. These variants have particularly important role in chromatin structure, in cell division and development.

2.2. Histone post-translational modifications and epigenetic code

The terminus of core histones are subjected to differential modifications. Although the N-terminal tails of core histone proteins are very short (<30AA) and their domains are not necessary for maintaining the structural integrity of the nucleosome, they perform roles in higher order chromatin packaging. The modified N-terminal tails are used as docking sites for further protein-protein interactions, which links to adjacent nucleosomes and non-histone proteins, such as methyltransferase, acetyltransferase, transcription factors, remodeling complexes and polycomb proteins. The modification of the H3 and H4 tails, as a result of their interactions with histone modification enzymes, changes the folding of the chromatin fibre and therefore contribute to the local transcriptional activity. Using a genetic and biochemical approach, the important role of the core histone tails in chromatin structure and gene regulation was approved. Although tailless core histones can manage to form nucleosomes *in vitro*, the N-terminal tails of histones H3 and H4 were shown to be necessary *in vivo* for the repression of the silent mating-type loci and the telomeres in yeast (Kayne *et al*., 1988; Thompson *et al*., 1994), and enhancer-dependent activation of some genes in yeast required these N-terminal sequences as well (Durrin *et al*., 1991; Mann *et al*., 1992). Deletion of both the H3 and H4 N-terminal tails in yeast is lethal (Ling *et al*., 1996) and mutation analysis has showed that certain point mutations in the N-terminus of the H4 tail could inhibit transcriptional gene silencing (Hecht *et al*., 1995). It is known that core histones belong to some of the most evolutionarily conserved proteins but, on the level of post-translational modifications, they are among the most variable families (Fig 6). The N-terminal tails of histones can be differentially post-translationally modified, including acetylation, methylation, phosphorylation, ubiquitination and ADP-ribosylation (Berger, 2002; Iizuka *et al.*, 2003; Zhang, 2003). Some of the modified isoforms are generated immediately after their translation in cytoplasm, for example, the lysine 5 and 12 acetylated histone H4, whereas modification of others occur mainly in the cell nucleus. Based on many recent studies, it becomes clear that modifications of the tails

changing the flexibility between the DNA and the core histones and resulting in the binding of different non-histone proteins to local chromatin, therefore directly contributing to regulation of gene expression. The relationship between distinct modification patterns and physiological functions has raised the concept of "histone code" (Strahl *et al.,* 2000; Turner, 2000; Jenuwein and Allis, 2001).

Histone modifications can specifically occur at selected residues, and some of the patterns have been shown closely linked to different biological events, for example, acetylation is associated with transcription, phosphorylation is associated with chromosome condensation or DNA repair (Peterson and Cote, 2004; Christophe *et al.*, 2005). Differential patterns of K9/S10/K14 in histone H3 appear to be linked with local gene activity. An inactive state is often characterised by histone deacetylation at Lys14, which then promotes methylation at Lys9 (Noma *et al*., 2001). However, acetylation at Lys14 is preceded by, and depends on, phosphorylation at Ser10. This has been demonstrated *in vitro* for the Gcn5 acetyltransferase that cooperates with Snf1 histone kinase in this event (Lo *et al*., 2000). In the chromatin of transcriptionally active state, histone H4 is methylated at Arg3, which precedes and facilitate p300-mediated acetylation at Lys8 and Lys12. In other studies, histone H4 Lys20 hypotrimethylation was found correlate with H4 hyperacetylation; and H4 Lys20 hypertrimethylation correlates with H4 hypoacetylation (Sarg *et al.*, 2004). Modifications of histones not only affect each other in a *cis* mechanism (Cheung *et al*., 2000; Clayton *et al*., 2000; Lo *et al*., 2000; Rea *et al*., 2000; Nakayama *et al*., 2001), but recent data has also demonstrated that there are *trans* effects between the modifications. For example, there is cross-talk between histone methylation and ubiquitination: ubiquitination of histone H2B enhances H3 Lys4 methylation and is involved in gene silencing at telomeres (Sun *et al*., 2002).

The function of the histone code in activity at the affected loci could be directly through physical alteration of histone-DNA, and histone-non-histone contacts within a high order structure. Examples include the bromodomain-containing protein which is present in HATs, and specifically interacts with acetylated lysine. The second example is the chromodomain-containing protein, present in

numerous histone methyltransferases and other proteins (e.g. HP1), where HP1 binds to methylated H3 Lys9 and recruits Suvar3-9 (Bannister *et al*., 2001). Suvar3-9 methylates Lys9 and leads to further recruitment of HP1, which is known to be an important mechanism in heterochromatic DNA condensation and gene silencing.

While these epigenetic changes are heritable and normally stably maintained, they are also potentially reversible. The reversible nature of histone acetylation, phosphorylation and methylation (recently discovered) are important mechanisms for controlling gene expression and partitioning the genome into functional domains. This has been demonstrated by the success of cloning entire organisms by nuclear transfer methods using nuclei of differentiated cells (Wilmut *et al*., 2002). Therefore, understanding the basic mechanisms that mediate epigenetic regulation is also invaluable for our knowledge of cellular differentiation and genome programming.

Despite of all these known information on histone modifications, many questions, such as whether these modifications are sequentially regulated or they are rather independently regulated etc, remain to be further understood. The understanding of these events may have important implications in biomedical research. The changes in global levels of individual histone modifications are recently found to be linked with cancer, and these changes are predictive of clinical outcome-tumour stage, preoperative prostate-specific antigen levels, and capsule invasion (Seligson *et al*., 2005).

2.3. Histone methylation

Histone methylation is a covalent modification, which commonly occurs on the side-chain nitrogen atoms of lysine and arginine (Clarke *et al.*, 2001; Zhang and Reinberg, 2001) (Fig 7). There are three methylation states, mono-, di- and tri-methylation. Histone methytransferases (HMTs) display exquisite substrate specificity, which modify specific lysine residues of free histones or within nucleosomes. For example, Dot1, Set2 and PR-Set7/Set8 can only methylate histone tails presented in the context of nucleosomes (Strahl *et al.*, 2000; Fan *et*

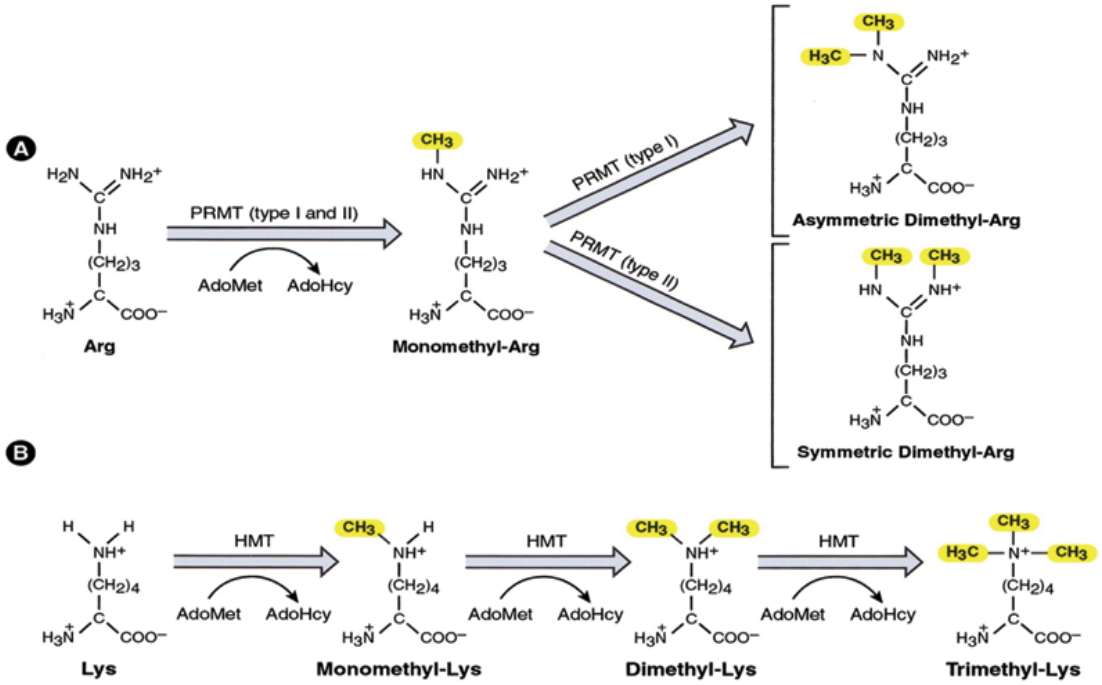

Fig 7. Methylation state on lysine and arginine .

(Zhang and Reinberg, 2001)

al., 2002; Nishioka *et al.*, 2002; van Leeuwen *et al.*, 2002), while other HMTs prefer free histones or can methylate tails from both free histones and nucleosomes. This responsible methyltransferases can be targeted in some cases to specific genes and, in other cases, to large domains of chromatin, for example, heterochromatin (Tables 1, 2). There are many sites of lysine and arginine methylation in histones. Methylation of lysine residues does not significantly change the positive charge, but progressively increases the bulk and hydrophobility, thus disrupting intra- or inter-molecular hydrogen-bond interactions of the ε-amino group, or creating new binding sites for other modulators. N-C bonds of methyl-lysine are very stable, and it had been thought that this modification was irreversible. However, Shi lab (Shi *et al.*, 2004) recently discovered a new enzyme, a demethylase, which can specifically remove mono- or di- methylation on H3 Lys4. In yeast, Epe1 is also found as a putative histone demethylase that could act by oxidative demethylation (Trewick *et al*., 2005). Thus, histone methylation appears to be more dynamic than was previously thought.

Table 1. Sites and functions of histone lysine methylation

Histone lysine	Function(s)	Histone lysine methyltransferases*
H1 K26	Transcriptional silencing	*Hs* EZH2 (catalytic subunit of Polycomb repressive complex 3)
H3 K4	Transcriptional activation	*Dm* Trx; *Hs* MLL1 (ALL-1, HRX), MLL2 (ALR-1), and MLL3 (HALR)
	Transcriptional activation and elongation	*Hs* SET1; *Sc* SET1
	Transcriptional activation	*Hs* SET7/9
	Transcriptional activation (in conjunction with ASH1-mediated methylation of H3 K9 and H4 K20)	*Dm* ASH1
H3 K9	Heterochromatic and euchromatic silencing; DNA methylation	*Dm* Su(var)3-9; *Hs* and *Mm* SUVAR39H1 and UVAR39H2; *Sp* CLR4
	Euchromatic silencing; DNA methylation	*Hs* and *Mm* G9a; *Hs* GLP1 (EuHMT1)
	Euchromatic silencing	*Hs* and *Mm* ESET (SETDB1)
	Heterochromatic silencing; DNA methylation	*Nc* DIM-5
	Heterochromatic silencing; DNA methylation	*At* KRYPTONITE
	Transcriptional activation (in conjunction with ASH1-mediated methylation of H3 K4 and H4 K20)	*Dm* ASH1
H3 K27	Euchromatic silencing	*Dm* E(z); *Hs* EZH1 and EZH2 (catalytic subunit of Polycomb repressive complex 2)
	Euchromatic silencing	*Hs* and *Mm* G9a
H3 K36	Transcriptional elongation and silencing	*Sc* SET2
	Transcriptional regulation	*Mm* NSD1
H3 K79	Demarcation of euchromatin	*Sc* and *Hs* DOT1 (a non-SET domain histone lysine methyltransferase)
H4 K20	Cell cycle-dependent silencing, mitosis and cytokinesis	*Hs* and *Dm* SET8
	Heterochromatic silencing	*Dm*, *Mm*, and *Hs* SUV4-20H1 and SUV4-20H2
	Transcriptional regulation	*Mm* NSD1
	Transcriptional activation (in conjunction with ASH1-mediated methylation of H3 K4 and H3 K9)	*Dm* ASH1
	Recruitment of checkpoint protein Crb2 to sites of DNA damage	*Sp* SET9

Species abbreviations: *At*, *Arabidopsis thaliana*; *Dm*, *Drosophila melanogaster*; *Hs*, *Homo sapiens*; *Mm*, *Mus musculus*; *Nc*, *Neurospora crassa*; *Sc*, *Saccharomyces cerevisiae*; *Sp*, *Schizosaccharomyces pombe*.

Table 2. sites and functions of histone arginine methyltranses

Histone arginine	Function(s)	Histone arginine methyltransferases
H4 Arg 3	Cooperate withPRMT4/CARM1 (human), transcriptional activation	PRMT1
H3 Arg 2	Acts as a coactivator of nuclear receptor activity (mouse)	PRMT4/CARM1
H3 Arg 17	Acts as a coactivator of nuclear receptor activity (mouse)	PRMT4/CARM1
H3 Arg 26	Acts as a coactivator of nuclear receptor activity (mouse)	PRMT4/CARM1
H2A	Cooperate with p300 acetylase to stimulate transcription by nuclear receptor (human)	PRMT5/JBP1
H4	Cooperate with p300 acetylase to stimulate transcription by nuclear receptor (human)	PRMT5/JBP1

At the global chromatin level, histone H3 Lys4 methylation is associated with euchromatin (Stallcup, 2001; Zhang, 2001). At the individual gene level, methylation of this residue is usually correlated with active transcription. Dimethylation of H3 Lys4 is associated with the coding regions of active genes (Bernstein *et al*., 2002); whereas the trimethylated Lys4, restricted primarily to the 5' end of genes, plays a direct role to control transcription. It is well known that Set1 specifically methylates Lys4 of histone H3, which is either specifically

recruited by Pol II, when the CTD is phosphorylated at Ser5, but not at Ser2 (Ng *et al*., 2003), or by the components of the Paf1 transcription elongation complex interacting with Set1 (Krogan *et al*., 2003). In human cells, the component of MLL1, MLL2, hSet1 and the WD40-repeat protein WDR5 directly associates with histone H3 di- and trimethylated at Lys4, and with H3 Lys4 dimethylated nucleosomes. WD40-repeat protein acts as a module for recognition of a specific histone modification and recruits the Set1 complex (Wysocka *et al.*, 2005). Another mechanism controlling Lys4 methylation was elucidated by the discovery that mono-ubiquitylation of histone H2B at Lys123 regulates dimethylation of histone H3 at Lys4 and Lys79 in *S. cerevisiae* (Briggs *et al*., 2002; Ng *et al*., 2002; Sun *et al*., 2002; Wood *et al*., 2003). The H2B ubiquitylation functions to create an environment in chromatin where Set1 and Dot1 methylation is possible (Ng *et al*., 2003). Recent studies have also revealed that proteasomal ATPases were recruited to ubiquitylated H2B and were required for Lys4 and Lys79 methylation of H3 (Ezhkova *et al*., 2004). These studies confirm that proteasome function links with the establishment of Lys4 and Lys79 methylation (Giannattasio *et al*., 2005). The chromatin remodelling protein chromo-ATPase/helicase-DNA binding domain 1 (Chd1) as a component of Spt-Ada-Gcn5-acetyltransferase (SAGA) and SLIK (SAGA-like), specifically interacts with the methylated Lys4 mark on histone H3 through one of the two chromodomains of Chd1 (Pray-Grant *et al.*, 2005). The SLIK complex has been shown to enhanced acetylation of a methylated substrate, and this activity is dependent upon a functional methyl-binding chromodomain, both *in vitro* and *in vivo*. Since the chromodomain can recognize methylated histone H3 (Lys 4), it is well possible that other chromodomain subfamily proteins may have similar recognition properties.

Methylation on H3 Lys79 is located in the globular domain rather than the tail of histone H3 (Feng *et al.*, 2002; Lacoste *et al*., 2002; Ng *et al*., 2003; van Leeuwen *et al*., 2002). Dot1 (disruptor of telomeric silencing 1), a unique HMT because it does not contain an SET domain, is responsible to methylate Lys79 of histone H3. The distribution of H3 Lys79 methylation is similar to that of H3 Lys4 methylation, both at global and gene specific levels, and is seen as a hallmark of

active chromatin. However, when compared with H3 Lys4 methylation, methylated Lys79 has some unique functions. The methylated Lys79 can be bound by specific proteins, for example, 53BP1, a human orthologue of the *S. cerevisiae* Rad9p and known to be involved in signalling the occurrence of DNA damage to the cell cycle checkpoint system (Huyen *et al.*, 2004). In addition, unlike the early histone H3 K4 and K9 methylation patterns, the appearance of methylated K79 during embryogenesis coincides with the maintenance phase of BX-C expression (Shanower *et al*., 2005), indicating that this chromatin modification is specifically involved in development.

The Lys36 residue of histone H3 lies at the junction between the N-terminal tail and the globular domain, and methylated by HMT-Set2 (Strahl *et al*., 2002). In *S. cerevisiae*, the methylation of Lys36 has been linked to active genes. In higher eukaryotes, Bannister and his colleagues demonstrated that active genes contain high levels of di- and tri-methyl (di- and tri-Me) H3 Lys36 modifications, when compared with inactive genes. Furthermore, in actively transcribed regions the levels of di- and tri-Me K36/H3 peak toward the 3' end of the gene, indicating a direct role in transcriptional termination and/or early RNA processing (Bannister *et al*., 2005). This unique spatial distribution of di- and tri-Me K36/H3 is in contrast to the distributions of di- and tri-Me K4/H3, which peak early in actively transcribed regions. This modification in neurospora crassa has been shown to be essential for normal growth and development (Adhvayu *et al*., 2005).

Methylation of Lys9 in the N-terminal tail of histone H3 is associated with transcriptionally silenced genes and heterochromatic domains. Suv39h HMTases selectively methylate histone H3 on Lys9 and are the major Lys9 trimethylase in pericentric heterochromatin. After methylating H3 on Lys9, they generate a binding site for HP1, a family of heterochromatic proteins implicated in both gene silencing and formation of heterochromatin structure (Lachner *et al*., 2001). In constitutive pericentric heterochromatin, Suv39h1/2 mediates trimethylation of H3 Lys9, while in euchromatin HMT G9a seems to mediate dimethylation of H3 Lys9 (Tachibana *et al*., 2002; Boulias *et al.*, 2004). It is interesting to note that, *in vitro*, both Suv39h1 and G9a can convert histone H3 peptides with dimethylated Lys9

to the trimethyl form, while *in vivo* they display different characteristics. In Suv39h1/2 double-null mouse embryo fibroblasts, trimethylation of H3 Lys9 is abolished while mono- and dimethylation were not significantly affected. In contrast, in G9a null mouse embryo fibroblasts, there was no dimethylation of H3 Lys9, a significant decrease in monomethylation, and no change in trimethylation. In mammals, trimethylation of Lys9 is a property of pericentric heterochromatin while dimethylation appeared to be dispersed throughout the euchromatin, suggesting that mono-, di- and trimethylation at Lys9 are differentially regulated and may exert different functional outcomes. Interestingly, some H3 Lys4 HMTs, such as Set7/Set9 and MLL/ALL1, are not inhibited by H3 Lys9 dimethylation *in vitro* (Nakamura *et al.*, 2002), which implies that both modifications can co-exist on the same area of tail.

How does the Suv39h1 HMT specifically recognise the chromatin regions to be methylated? Genetic evidence has indicated that HP1 lies downsteam of Suv39h1 action (Bannister *et al.*, 2001; Nakayama *et al*., 2001). Most interestingly, repetitive DNA elements, known to be the major components of heterochromatin domains, are now found to recruit Clr4 (the *S. pombe* equivalent of Suv39h1) and RNA interference (RNAi) machinery to the centromeric heterochromatic region of *S. pombe* (Allshire, 2002; Volpe *et al.*, 2002; Reinhart *et al.*, 2002). Centromeric repeats are transcribed bi-directionally to produce non-coding double-stranded RNA, then processed to small interfering RNA by the RNAi machinery. Deletion of any of the three components of the RNAi machinery [e.g. RNAseIII helicase dicer dic1, RNA-dependent RNA polymerase (rdp1) and Argonaute (ago1)] caused inappropriate activation of a reporter gene integrated within centromeric heterochromatin, and loss of centromeric localization of Swi6 (the *S. pombe* equivalent of HP1) and H3 Lys9 dimethylation, along with increased H3 Lys4 methylation of the centromeric region (Ira *et al*., 2002). These observations all support that shRNA in heterochromatic regions helps to recruit Clr4, which establishes Lys9 methylation then recruits HP1/Swi6. Consistent with the hypothesis that histone deacetylases facilitate the initial stages of assembly of heterochromatin, Clr3 (which deacetylates H3 Lys14) was found partially

required for the H3 Lys9 methylation and the further recruitment of Swi6 to the centromere. Once HP1/Swi6 has been recruited to the initiation site of heterochromatin, it then spread into adjacent domains by HP1 self-association and recruiting additional Suv39h1, which then catalyzes Lys9 methylation to attract more HP1 molecules, and so forth (Noma *et al*., 2001).

How these events lead to gene silencing has been investigation. The complex of retinoblastoma (Rb) protein, binding to E2F transcription factors and repress transcription of genes required for cell cycle progression, contains histone deacetylases and also Suv39h1. It was shown that Suv39h1 methylation of H3 Lys9 resulted in the recruitment of HP1 to the cyclin E gene promoter, and causes transcriptional repression (Nielsen *et al*., 2001; Vandel *et al.*, 2001). Similarly, KRAB-ZFP, which is a DNA sequence-specific transcriptional repressor protein, recruits the KAP1 co-repressor, brings the H3 Lys9 HMT SETDB1/ESET to promoters of specific genes and results in transcriptional silencing (Schultz *et al*., 2002).

Although most H3 Lys9 methylation appears to be involved in heterochromatin formation and gene repression, a few observations hint at possible selective involvement in gene specific transcriptional activation. Chromatin immuno-precipitation experiments have demonstrated that dimethylation of Lys4 and Lys9 of histone H3 and Lys20 of histone H4 is linked with transcriptional activation of Ash1 target genes, both for an integrated reporter gene and the endogenous Ultrabithorax (*Ubx*) gene (Beisel *et al*., 2002). Ash1, a known member of the trithorax group in Drosophila, is an unusual HMT because it can methylate histone H3 at Lys4 and Lys9 and histone H4 at Lys20 *in vitro* (Beisel *et al*., 2002). While Ash1 is responsible for the majority of H3 Lys4 methylation, it is not for the majority of H3 Lys9 or H4 Lys20 methylation *in vivo* (Byrd, 2003). In mammalian chromatin, H3K9 di- and trimethylation also occur in the transcribed region of active genes (Vakoc *et al.*, 2005). This modification is dynamic, as it increases during activation of transcription and is rapidly removed upon gene repression. HPγ, an isoform of HP1, is also present in the transcribed region of the active genes examined. Remarkably, both the presence of HP1γ and H3 K9

methylation are dependent upon elongation by RNA polymerase II. These findings therefore demonstrate novel roles for H3 Lys9 methylation in transcription activation.

Using a ChIP assay, Carvell *et al*. (2002) found that silenced genes in cancer cells also exhibit a heterochromatic structure which is characterized by histone H3 Lys9 hypermethylation and histone H3 Lys4 hypomethylation. This aberrant heterochromatin is incompatible with transcriptional initiation but does not inhibit elongation by RNA polymerase II either. Thus, H3 Lys9 methylation may play a role in the silencing of tumour-suppressor genes in cancer. Treatment with 5-aza-2'-deoxycytidine (5-Aza-CdR), previously known to inhibit cytosine methylation, induced a rapid and substantial remodelling of the heterochromatic domains in bladder cancer cells, reducing levels of dimethylated H3 Lys9 and increasing levels of dimethylated H3 Lys4 at this locus (Carvell *et al.*, 2002), indicating a strong correlation between the histone methylation and CpG island DNA methylation (Yutaka *et al.*, 2004), and the forthcoming specific inhibitors for HMT may be proven to be new drug targets for epigenetic diseases.

EZH2, a mammalian homologue of *Drosophila* enhancer of zeste [E(z)], is the HMT that mediates methylation of H3 Lys27 on the inactive X chromosome or histone H1b Lys26 (Kuzmichev *et al*., 2004). This enzyme also methylates Lys9 *in vitro*, but whether it has the same function *in vivo* is not clear (Cao *et al.*, 2002; Czermin *et al.*, 2002; Kuzmichev *et al*., 2002; Muller *et al*., 2002). Methylation of H1b Lys26 has been shown to be important for transcriptional repression. Methylation of histone H3 at lysine 27 displays functional similarities to that of lysine 9, i.e. different degrees of methylation have different distributions in chromatin. Monomethylation of Lys27 is found in pericentric heterochromatin, along with trimethylation of Lys9 (Peters *et al*., 2003; Rice *et al.*, 2003). Trimethylation of Lys27 is characteristic of facultative heterochromatin on the inactive X chromosome during the initial stage of X inactivation (Plath *et al.*, 2003; Silva *et al.*, 2003), along with dimethylated but not trimethylated Lys9 (Heard *et al*., 2001; Boggs *et al*., 2002; Peters *et al*., 2002). Similar like Suv39h1-mediated trimethylation of histone H3 Lys9 leads to recruitment of HP1 in mammals, ESC-

E(z) complex-mediated methylation of histone H3 Lys27 creates a specific binding site for recruitment of the PRC1 complex via polycomb (Pc) protein in *Drosophila* (Fischle *et al.*, 2003; Min *et al*., 2003). The chromodomain of Pc specifically recognises trimethylated H3 Lys27. Two different mechanisms exist for recruiting H3 Lys27 HMTs to their targets. At the global level EED-EZH2, the human ESC-E(z) complex, is recruited to the inactive X chromosome via *Xist* RNA to trimethylate histone H3 at Lys27, which is also similar to the mechanism by which centromeric shRNA recruits Clr4 (equivalent of human Suv39h1) to heterochromatin in fission yeast. Interestingly, the recruitment of EED-EZH2 and trimethylation of H3 Lys27 is transient, occurring only during the initial stage of X inactivation. At the individual gene level, the Drosophila ESC-E(z) complex is targeted to Pc response elements via many DNA binding proteins such as the GAGA factor, pleiohomeotic (Pho) and Zeste (Brown *et al*., 1998; Horard *et al*., 2000; Simon *et al*., 2002; Mulholland *et al*., 2003).

Methylation of histone H4 Lys20 is mediated by the PR-Set7/Set8 HMT (Fan *et al*., 2002; Nishioka *et al*., 2002; Couture *et al*., 2005). In *Drosophila* polytene chromosomes, this modification is associated with the chromocentre and euchromatic arms. Its staining in the euchromatin does not significantly co-localise with dimethylated H3 Lys4. PR-Set7/Set8 HMT was found to be cell cycle-regulated, coincident with increased H4 Lys20 methylation at mitosis and transiently decreased H4 Lys16 acetylation (Judd *et al.*, 2002). These data also indicate that H4 Lys20 methylation by PR-Set7 acts to antagonize H4 Lys16 acetylation; H4 hyperacetylation precludes histone H4 Lys20 trimethylation (Sarg *et al*., 2004), argue that this modification is involved in the silent domains of euchromatin. In the fission yeast *S. pombe*, Set9 is responsible for H4-K20 methylation, and this modification does not have any apparent role either in the regulation of gene expression or heterochromatin function, but has a role in DNA damage response (Sanders *et al.*, 2004): loss of Set9 activity or mutation of H4-K20 markedly impairs cell survival after genotoxic challenge, and compromises the ability of cells to maintain checkpoint-mediated cell cycle arrest; genetic experiments have found Set9 links to Crb2 (a homologue of the mammalian

checkpoint protein 53BP1); the localisation of Crb2 to sites of DNA damage is Set9-dependent; and these results argue that H4 Lys20 methylation may functions as a marker required for the recruitment of the checkpoint protein Crb2.

Methylation of arginine residues is a common post-translational modification in eukaryotes. Arginine methyltransferases (Table 2) can modify proteins functionally involved in a number of cellular events, including cytoplasmic and nuclear signal transduction, nuclear-cytoplasmic shuttling, transcriptional activation and multiple post-transcriptional steps in gene expression. Two types of protein arginine methyltransferases (PRMTs) transfer the methyl group from Sadenosyl-L-methionine (AdoMet) to the guanidino group of arginines in protein substrates (Fig 7). Type I PRMT enzymes form monomethylarginine and asymmetric dimethylarginine products. Type II PRMT enzymes catalyse the formation of monomethylarginine and symmetric dimethylarginine (Gary *et al*., 1998; McBride *et al*., 2001). PRMTs may be universal to all eukaryotes, since homologues are found in fungi, higher plants, invertebrates and vertebrates (Zhang *et al*., 2003). Seven mammalian PRMT genes have been identified: PRMT1, PRMT2, PRMT3, CARM1/PRMT4, JBP1/PRMT5, PRMT6 and PRMT7 (Ananthanarayanan *et al.*, 2004; Covic *et al.*, 2005); but the yeast *S. cerevisiae* has only one member: Hmt1/Rmt1. PRMT5 is the only example of a type II enzyme, whereas the other PRMTs (except PRMT7) are all type I enzymes. PRMT7 makes only monomethylarginine and contains two methyltransferase domains in a single polypeptide chain (Miranda *et al.*, 2004), therefore it may represent a third class of PRMT. Histone H3 Arg17 methylation is involved in gene activation because methylases are recruited to the promoter region as co-activators and control the level of this methylation. The human enzyme peptidylarginine deiminase 4 (PAD4/PADI4) can specifically catalyse the conversion of methylated arginines (R2, R8, R17 and R26 in the H3 tail) to citrulline (Cuthbert *et al.*, 2004; Zhang *et al*., 2004), converts histone arginine to citrulline, and antagonises arginine methylation.

2.4. Histone acetylation

The ε-amino group of specific lysines within the N terminus of histones can be acetylated by acetyltransferase, and this modification can be reversed by deacetyltransferase. The enzymes that catalyse histone acetylation are classified into four families (Table 3): the GNAT (GCN5-related N-terminal acetyltransferases)-MYST superfamily encompasses enzymes that catalyse the transfer of an acetyl group from acetyl-CoA to a primary amine of non-histone proteins and small molecules (Dyda *et al.*, 2000); the p300/CBP proteins, and other proteins which are distinct but related to proteins p300 and CBP, such as p270, are a protein family that participates in many physiological processes, including proliferation, differentiation and apoptosis (Janknecht and Hunter, 1996; Shikama *et al*., 1997; Giordano *et al.*, 1999; Goodman and Smolik, 2000); the general transcription factors HATs, which include TAF250, the largest of the TATA binding protein-associated factors (TAFs) within the transcription factor complex TFIID, can acetylate lysine residues in the N-terminal tails of histones H3 and H4 *in vitro* (Mizzen *et al*., 1996). These three families are widespread in eukaryotic genomes, and their homologous proteins are also involved in non-HAT reactions in prokaryotes and Archaea. The other family is, found particularly in mammals, nuclear receptor co-activators such as the steroid receptor co-

TABLE 3. Characteristics of HAT families

HAT group	HAT and it's complex	Recombinant HAT	Histones acetylated by HAT complex	Interactions with other HATs
GNAT	Gcn5 (SAGA, ADA, A2)	H3 >> H4	H3, H2B	p300; CBP
	PCAF (PCAF)	H3 >> H4	H3, H4	p300; CBP
	Hat1 (HatB)	H4 >> H2A	H4, H2A (human)	
	Elp3 (elongator)	H2A, H2B, H3, H4		
	Hpa2	H3 > H4		
MYST	Esa1 (NuA4)	H4 >> H3, H2A	H2A, H4	
	MOF (MSL)	H4 >> H3, H2A	H4	
	Sas2		H4	Cac1 (Large subunit of CAF1)
	Sas3 (NuA3)		H3	
	MORF	H4 > H3		
	Tip60	H4 >> H3, H2A		
	Hbo1 (ORC)		H3, H4	
p300/CBP	p300	H2A, H2B, H3, H4		PCAF; GCN5
	CBP	H2A, H2B, H3, H4		PCAF; GCN5
Basal	TAFII250 (TFIID)	H3 > H2A		
transcription	TFIIIC		H3 H4 > H2A	
Nuclear	ACTR (RAC3, AIB1, PCIP, and TRAM)	H3 > H4		p300; CBP; PCAF
receptor		H3 > H4		p300; CBP; PCAF

activator (SRC-1) and ACTR (SRC-3), a thyroid hormone and retinoic acid co-activator that can not only recruit HAT proteins CBP/p300 and P/CAF, but itself is a HAT (Chen *et al*., 1997). Recent data have also indicated that the HAT domain containing protein-NCOAT (nuclear cytoplasmic O-GlcNAcase and acetyltransferase) has a double function (Toleman *et al.*, 2004): O-GlcNAcase and HAT activities.

Since Allfrey and co-workers observed a link between reversible acetylation and mRNA synthesis (Allfrey *et al*., 1964), there has been an increasing amount of studies supporting a general model in which histone acetylation contributes mainly to the formation of a transcriptionally competent environment by 'opening' chromatin and allowing general transcription factors to gain access to promoter regions and, hence, initiate transcription. In addition, the unfolding of chromosomal domains facilitates the process of transcription elongation, DNA repair (H3 K56) (Masumoto *et al*., 2005), and chromatin assembly (H4 K91) (Ye *et al*., 2005). Conversely, histone deacetylation contributes to a 'closed' chromatin state and transcriptional gene repression. Condensed heterchromatin regions are generally hypoacetylated, whereas euchromatin active domains are associated with hyperacetylated histones. Highly acetylated histones are not limited to the coding region, they are also found along the entire loop domain, but they are never found close to repressive heterochromatic structures in nuclei (Schubeler *et al*., 2000). Using the chromatin immunopreciption (ChIP) approach, the distribution of histone acetylation and its correlation with gene activity and chromatin structure have been mapped in more detail in yeast (Suka *et al*., 2001) and, later on, in *Drosophila melanogaster* embryonic cells (Schubeler *et al*., 2004). Using ChIP analysis, the histone H3 Lys9 and Lys14 in *MFA2* promoter (Yu *et al.*, 2005), but not the relevant sites from histone H4 in nucleosomes in this region, are hyperacetylated after UV irradiation, and the level of histone hyperacetylation diminishes gradually as repair proceeds. This change leads to the promoter becoming more accessible to restriction enzymes after UV irradiation and returns to the pre-UV state gradually (Berden *et al*., 2002; Yu *et al*., 2005). UV-related histone hyperacetylation and chromatin remodelling in the

MFA2 promoter depend on Gcn5p and, partially, on Swi2p. Deletion of *GCN5*, but not of *SWI2*, impairs the repair of DNA damage in the *MFA2* promoter. The post-UV histone modifications and chromatin remodelling at the repressed *MFA2* promoter do not activate *MFA2* transcriptionally, nor do they require damage recognition by Rad4p or Rad14p.

The major groups of HDACs include the RPD3/HDA1 superfamily, the Silent Information Regulator 2 (SIR2) family and the HD2 family. RPD3/HDA1-like

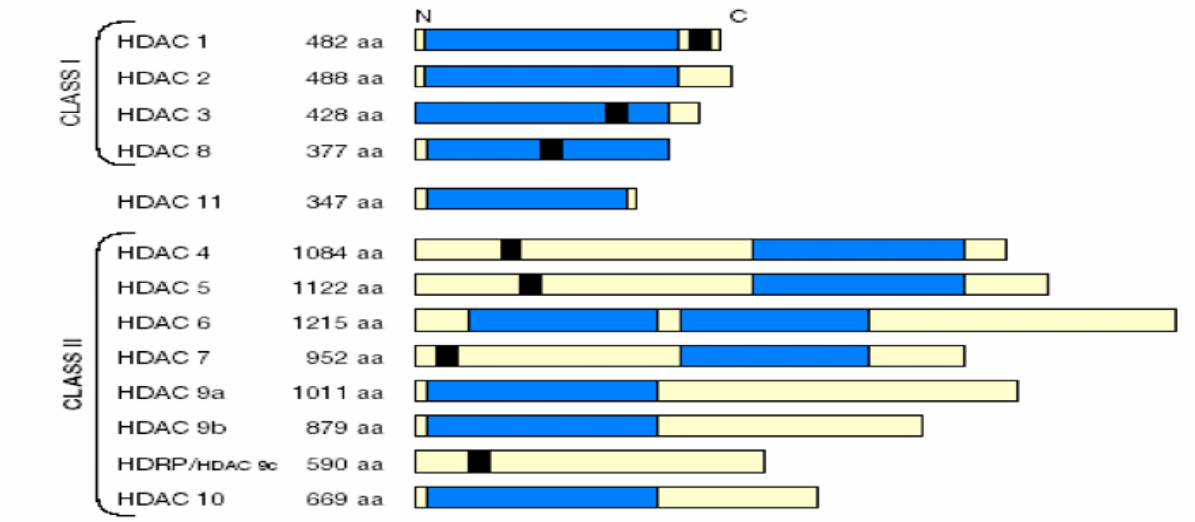

Fig 8. Classification of histone deacetylases. The catalytic domain is shown in blue, black depicts NLS (Annemieke *et al*., 2003).

HDACs are found in all eukaryotic genomes and are further divided into two classes: class I HDACs (HDAC-1, -2, -3 and -8) are similar to the yeast RPD3 protein; class II HDACs [HDAC-4, -5, -6, -7 (also involved in apoptosis) (Bakin *et al*., 2004), -9 and -10] are homologous to yeast HDAC1 protein (Fig 8).

What's the mechanism that histone acetylation regulates chromatin structure and gene regulation? The "direct" model indicates that acetylation results in the neutralisation of lysine residues located in the N-terminal tails of the histones. This kind of change weakens interactions between the positive charged histone tails and the negatively charged double-strand DNA. The second model proposes that acetylation could change histone interactions between neighbouring nucleosomes as well as interactions between histones and other regulatory proteins, therefore modulating the higher-order chromatin structure, this is supported by acetylation of histones H3 and H4 counteracts the tendency

of chromatin fibres to form highly compact structures *in vitro* by disrupting internucleosomal interactions made through the histone tails (Tse *et al*., 1998). Acetylation, usually combined with other modifications, is exposed to the environment outside of the chromatin polymer, and therefore likely provides a special signalling platform that can mediate critical interactions with proteins or protein complexes. For example, specific acetylation patterns on core histone tails may also function to recruit further modulators of chromatin structure, including complexes essential for other covalent modifications, such as phosphorylation and methylation. The bromodomain, a domain that is present in all nuclear HATs, was recently reported *in vitro* to bind with acetylated lysines within H3 and H4 amino-terminal peptides, indicating that this interaction may constitute a targeting step following histone acetylation and recruit other factors such as those involved in nucleosome remodelling and other covalent modifications.

Protein components of transcription factor complexes and many other non-histone proteins are also substrates for HDACs and HATs, therefore providing the molecular mechanisms that switch on or off inflammatory genes that can be exploited in therapy (Barnes *et al*., 2005). Specific enzyme inhibitors, such as HDAC inhibitors, represent a new class of targeted anti-cancer agents because they can induce growth arrest, differentiation, apoptosis and autophagocytic cell death of cancer cells (Dokmanovic *et al*., 2005). Several of these compounds are in clinical trials, with significant activity against a spectrum of both hematologic and solid tumours at doses that are well tolerated by the patients.

2.5. Histone phosphorylation

Phosphorylation occurs on core histones and linker histone H1 within S/T residues in tails (Fig 9). This modification has recently been shown to play an important role in chromatin-associated processes. Distinct sets of kinases have been implicated in these events. Cdc2 protein kinase phosphorylates histone H1 during mitosis of most cells, consistent with this phosphorylation playing a role in both chromosome condensation and transcriptional regulation. Within the histone

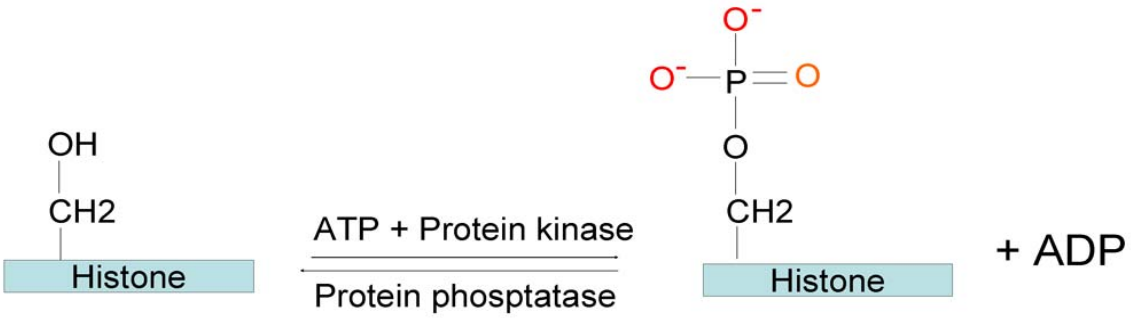

Fig 9. Histone Phosphorylation

H3 tail, serines 10 and 28 are both proceeded by the same three amino acids (A-R-K). Both of these motifs are highly conserved throughout evolution, being identical from yeast to human. They play important role in condensation of chromosomes during mitosis and meiosis, and regulate transcriptional activation upon stimulation of these two serine residues (Pascreau *et al.*, 2003).

Two classes of kinases, previously known to be required for chromosome condensation, have been shown to phosphorylate histone H3 serine 10 during the cell cycle. In *Aspergillus nidulans*, the *nimA* gene encodes a Ser/Thr-specific protein kinase (NIMA kinase) phosphorylates serine 10 *in vitro*, and is required for H3 phosphorylation *in vivo* (De Souza *et al*., 2000). In yeast and *C. elegans*, the Ip11/Aurora kinase family, and the opposing G1c7/PP1 phosphatases, have been shown to establish the level of mitotic serine 10 phosphorylation (Hsu *et al*., 2000). In mammals, serine 28 is a second site of phosphorylation, which also occurs during chromosome condensation at early mitosis (Goto *et al*., 1999). Aurora B is also implicated in mitotic serine 28 phosphorylation. In mammals, the mitogen-activated protein kinase-mixed lineage kinase-like mitogen-activated protein triple kinase (MLTK)-alpha specifically phosphorylates histone H3 at Ser28, but not at Ser10 (Choi *et al*., 2005). Besides these enzymes, the levels of phospho-S10-H3 and phospho-S28-H3 in chromatin are also modulated by nucleosome binding proteins HMGN1, which alter the ability of enzymatic complexes to access and modify their nucleosomal targets (Lim *et al.*, 2004).

Although a clear link between mitogen- or stress-inducible histone H3 phosphorylation and gene transcription has been established, its exact molecular functions remain unclear. It has been suggested that phosphorylation may

mediate changes in nucleosome and chromatin structure by disrupting or altering histone-DNA interactions, thus facilitating the access of transcription factors to the underlying DNA sequences. A second function, based on the histone code hypothesis, is that the phosphoacetyl epitope on histone H3 at Ser10 (as well as on Ser6 of HMG-14) serves as a docking site for recruitment of co-activator complexes. For example, the inducible genes such as c-fos and c-myc showed enhanced acetylation upon activation, which could be the consequence of phosphorylation on H3 Ser10, to stimulate the activity of acetyltransferase Gcn5 on H3 K9 and K14 (Clements *et al*., 2003), in addition histone H3 Thr11 is necessary for optimal transcription at yGcn5-dependent promoters requiring Ser10 phosphorylation (Clements *et al*., 2003).

Casein kinase II (CK2) can phosphorylate histone H4 S1 (Cheung *et al*., 2005), and the CK2 has been implicated in regulating DNA-damage response. Null or temperature-sensitive CK2 yeast mutants no longer induce H4 S1 phosphorylation upon DNA damage *in vivo*, indicating that histone H4 S1 phosphorylation belongs to a part of the DNA-repair histone code.

Phosphorylation of histone H2B on Ser33 (H2B-S33) is regulated by the carboxyl-terminal kinase domain (CTK) of the *Drosophila* TFIID subunit TAF1. This modification occurs at the promoter region of the cell cycle regulatory gene *string* and the segmentation gene *giant* coinciding with transcriptional activation. Elimination of TAF1 CTK activity in *Drosophila* cells and embryos reduces transcriptional activation and phosphorylation of H2B-S33, indicating that H2B-S33 is a physiological substrate for the TAF1 CTK, and that phosphorylated H2B-S33 is essential for transcriptional activation events, which promote cell cycle progression and development. H2B phosphorylation also occurs universally in apoptotic cells and is associated with an apoptosis-specific nucleosomal DNA fragmentation, indicating that phosphorylation of H2B is a hallmark of apoptotic cells.

Phosphorylation on H3 is linked to transcriptional gene activation, while the mitogen- and stress-induced kinase-MSK1 inhibited transcription through phosphorylated histone H2A on serine 1 (Zhang *et al.*, 2004)**.** Mutating H2A Ser1

to alanine or increasing acetylation of histone H3 can block the inhibition of transcription by MSK1. Another function of phosphorylation on H2A is that it is involved in DNA repair (Bassing and Alt, 2004; Fernandez-Capetillo *et al.*, 2004), a process must take place within the context of chromatin. It was shown that DNA damage checkpoint kinases Mec1p and Tel1p phosphorylate the SQ motif in H2AX (one of the H2A variants) (Shroff *et al.*, 2004; Unal *et al*., 2004), a marker for the presence of double-strand DNA breaks (DSBs), in DNA-damage responses. This modification is an early response to the induction of DNA damage, and occurs in a wide range of eukaryotic organisms (Foster *et al*., 2005). Such breaks can arise from mistakes during DNA replication, from external agents such as ionising radiation, or during genomic rearrangements in immune cells. If left unrepaired, DSBs could result in the loss of entire centromere-distal chromosomal regions or the presence of deleterious chromosomal rearrangements, which potentially lead to cancer or other diseases.

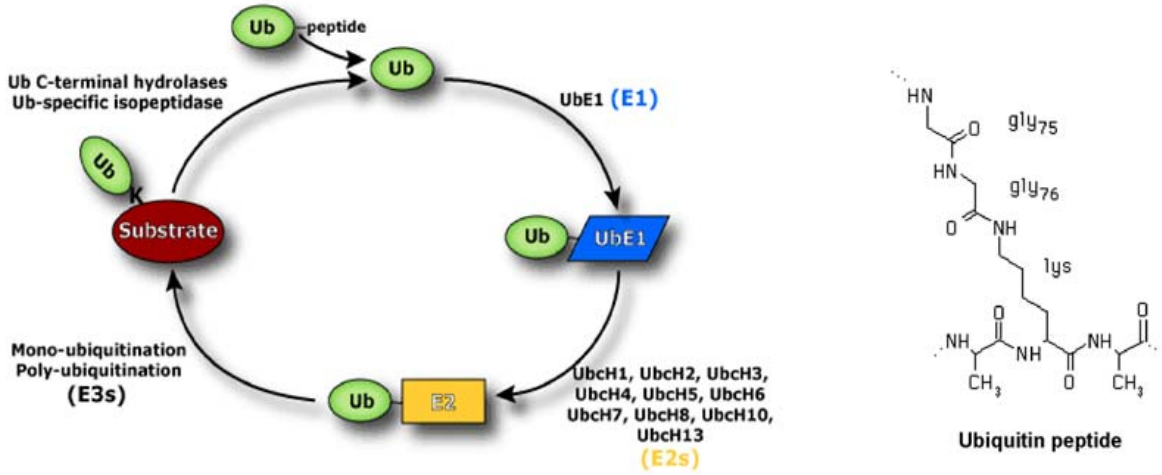

Fig 10. Protein ubiquitination and deubiquitination

2.6. Histone ubiquitination

Ubiquitin is a small, 76 amino acid long polypeptide, which is attached as a polymer to the ε-amino group of lysine residues in polypeptides targeted for proteasomal degradation (Fig 10). Histone ubiquitination represents the most

bulky structural change to histones. Histone H2A was the first histone found to be post-translationally modified by covalent ligation with ubiquitin, which is largely mono-ubiquitination, and affects about 5-15% of this histone in most eukaryotic cells. Ubiquitinated H2B is another most abundant ubiquitin conjugates in eukaryotes and has been identified in many eukaryotic organisms except *S. pomber* and *Arabidopsis thaliana* (reviewed in Jason *et al*., 2002 and Zhang, 2003). The lysine residues to which ubiquitin is conjugated in H2A and H2B are highly conserved. Polyubiquitination has also been detected on histones H2A, H2A.Z and H2B in preparations of bovine thymus, chicken erythrocytes, *Tetrahymena* macronuclei and micronuclei, trout testis, trout liver and trout hepatocellular carcinoma. Recently, ubiquitination of H3 was also reported to occur *in vivo* within elongating spermatids of rat testes, but could not be detected in mouse (Chen *et al*., 1998). In Drosophila embryos, the ubiquitin-conjugating activity of TAFII 250 is involved in the ubiquitination of linker histone H1 (Pham and Sauer, 2000). However, the sites of H3 and H1 ubiquitination are presently unknown. In general protein ubiquitination reactions, E1, E2 and E3 are necessary for ubiquitination on the histones. E1 is found in almost all compartments of the eukaryotic cell, including the nucleus, and it has also been found to be associated with condensed chromosomes during mitosis. Although many E2 isoenzymes have been identified, only a subset is involved in histone ubiquitination. In *S. cerevisiae*, Rad6p/Ubc2p and Cdc34p/Ubc3p are homologous to mammalian reticulocyte E220KD and E232kD isoenzymes, which can ubiquitinate histone H2B *in vitro* without any help from the E3 ligase. However, Rad6 is indispensable for H2B ubiquitination *in vivo* (Robzyk *et al*., 2000). Recent studies have indicated that a Rad6-associated RING finger protein Bre1 is likely to be the E3 ligase involved in H2B ubiquitination, because mutation in the RING domain of Bre1 abolished H2B ubiquitination *in vivo* (Wang *et al*., 2003; Wood *et al*., 2003). Ubiquitin protease Ubp10/Dot4p is important for telomeric silencing through its interaction with Sir4p. Recent evidence supports the idea that Ubp10p removes ubiquitin from histone H2B; cells with deleted *UBP10* have increased steady-state levels of H2B ubiquitination. As a

consequence, *ubp10*Δ cells also have increased steady-state levels of methylation of histone H3 Lys4 and Lys79. The ubiquitin protease Ubp8p has been shown to remove ubiquitin from H2B, because *ubp8*Δ cells have increased levels of H2B ubiquitination similar to those in *ubp10*Δ cells. Unlike *ubp10*Δ cells, however, *ubp8*Δ cells do not have increased steady-state levels of H3 Lys4 and Lys79 methylation, nor is telomeric silencing affected. Despite their separate functions in silencing and SAGA-mediated transcription respectively, deletion of both *UBP10* and *UBP8* results in a synergistic increase in the levels of H2B ubiquitination and in the number of genes with altered expression (Henry *et al.*,

Table 4. Examples of E3 ubiquitin ligases implicated in the regulation of Pol II transcription.

ubiquitin ligases	Class	Target
E6-AP/E6	HECT	p53
Rsp5	HECT	RNA polymerase II large subunit
WWP1	HECT	Lung Kruppel-like factor (LKLF)
Smurf2	HECT	Smad1, Smad2
Mdm2/hdm2	RING	p53
		HIF1α and HIF2α ?
Siah-1	RING	c-myb
Siah-2	RING	N-CoR
SCF^{Cdc4}	RING, Skp1-based	Gcn4
SCF^{Met30}	RING, Skp1-based	Met4
$SCF^{\beta\text{-TRCP}}$	RING, Skp1-based	IkB, ATF4, β-catenin, Smad3, NF- B p105
VHL-EloBC-Cul2-Rbx1	RING, Elo BC-based	HIF1α , HIF2α
E4orf6/E1B55K-EloBC-Cul5-Rbx1	RING, Elo BC-based	p53
Med8-EloBC-Cul2-Rbx1	RING, Elo BC-based	?
Siah/SIP/Skp1/Ebi	RING, Skp1-based variant	β-catenin, Tramtrack?
$TAF_{II}250$	Novel	Histone H1

2003; Daniel *et al*., 2004), indicating that Ubp10p and Ubp8p probably functionally overlap in some chromatin regions (Richard *et al.*, 2005).

uH2A presents on the inactive X chromosome in female mammals and this correlates with recruitment of Polycomb group (PcG) proteins belonging to the Polycomb repressor complex 1 (PRC1) (de Napoles *et al*., 2004). The physiological E2 and E3 enzymes involved in H2A ubiquitination have been identified (Wang *et al.*, 2004), and the E3 ubiquitin ligase complex is specific for histone H2A. This complex, termed human Polycomb repressive complex 1-like (hPRC1L), is consists of several Polycomb-group proteins, including Ring1,

Ring2, Bmi1 and HPH2, and monoubiquitinates nucleosomal histone H2A at lysine 119. Reducing the expression of Ring2 results in a dramatic decrease in the level of ubiquitinated H2A in HeLa cells. Removal of *Drosophila* dRing in SL2 tissue culture cells also resulted in a loss of H2A ubiquitination concomitant with depression of *Ubx*, indicating that the hPRC1L mediated monoubiquitination of nucleosomal histone H2A may link Polycomb with gene silencing. Notably, uH2A was also present in histone H1-containing nucleosomes. *In vitro* experiments using nucleosomes reconstituted with 167-bp random sequence and 208-bp (5S rRNA gene) DNA fragments showed that ubiquitination of H2A did not prevent binding of histone H1, on the contrary, enhanced the H1 binding, and neither affected the positioning of the histone octamer in the nucleosome (Jason *et al*., 2005). In mammals, H2A ubiquitination occurs during the post-meiotic period of spermatogenesis, when protamines replace histones. If a mouse homologue of the yeast E2 enzyme RAD6, mHR6B, is inactivated by gene targeting, male mice become sterile. This effect was initially thought due to abnormal histone displacement during spermatogenesis, but it was subsequently shown that the overall pattern of histone ubiquitination was not affected in HR6B-knockout mice, indicating that the ubiquitin-conjugating activity of HR6B affects other aspects of male fertility, and that another E2 enzyme must be responsible for global H2A ubiquitination.

The levels of ubiquitinated histones have been found to vary at different stages, and to different extents, during spermatogenesis in vertebrate species such as the rooster, trout, rat and mouse. Like acetylation and phosphorylation, histone ubiquitination is a reversible modification (Fig 10). Steady-state histone ubiquitination levels are determined by the availability of free ubiquitin and enzymatic activities involved in both adding and removing the ubiquitin moiety from histones. Berger and his colleagues (Henry *et al*., 2003) reported that Ubp8, a component of the SAGA complex, is a histone H2B ubiquitin protease and deubiquitylates H2B. Surprisingly, unlike other reversible histone modifications in which addition or removal of a group from a histone molecule results in opposing transcriptional effects, sequential ubiquitination and deubiquitination are both

involved in transcriptional activation. They provide evidence that the effect of ubiquitination and deubiquitination signals is probably mediated through histone methylation. Thus, sequential ubiquitination and deubiquitination of histones, as well as cooperation with different histone modifications, all play an essential role in transcriptional regulation (Fig 10, Table 4). Although the exact role of histone ubiquitination on transcription activation, is, so far, still controversial, it has been suggested that histone ubiquitination most likely regulates gene transcription both in a positive and negative fashion, depending on its genomic location.

There are at least three possible explanations for histone ubiquitination in control transcription. First, histone ubiquitination may affect higher-order chromatin folding, therefore resulting in greater access of the underlying DNA to the transcription machinery. Second, ubiquitination may function as a signal for the recruitment of regulatory molecules that affect transcription. And the third possibility is that histone ubiquitination affects transcription through its impact on other histone modifications. Although the first two possibilities have not been ruled out, recent studies have given the most support for the third possibility.

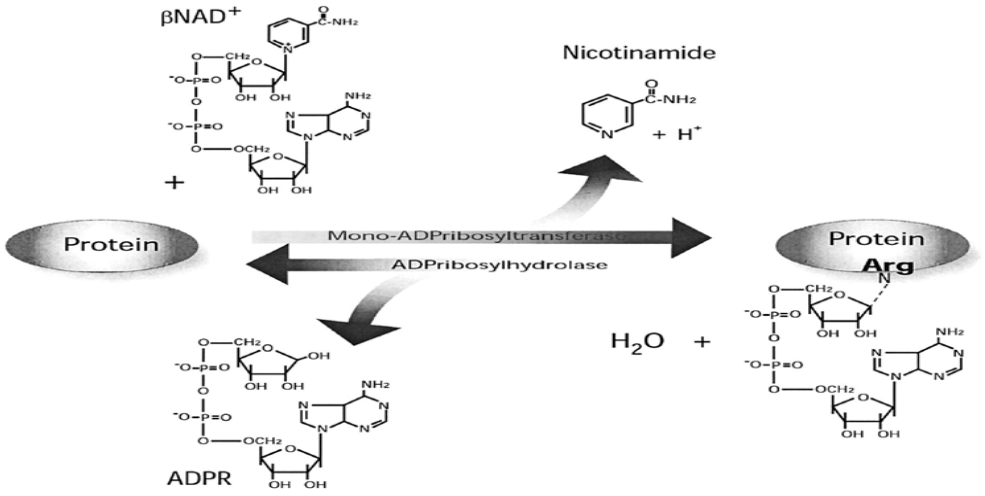

Fig 11. The reversible mono-ADP-ribosylation reaction catalysed by an arginine-specific mono-ADP-ribosyltransferase and an ADP-ribosylhydrolase

2.7. ADP-ribosylation

The ADP-ribosylation of proteins is catalyzed by ADP-ribosyltransferases [ART, mono(ADP-ribosyl)transferases], which transfer the ADP-ribose moiety of NAD to a specific amino acid residue on the target protein, via *N*- or *S*-glycosidic

Table 5. Mono-ADP-ribosylation: enzymes and substrates

Enzymes	Source	Substrate/amino acid	Function
ART1	Human, rat, mouse	Integrin, defensin/Arg	Inhibits substrate activity
ART2(A,B)	Rat, mouse	Unknown/Arg	Role in T cell proliferation
ART3	Human, rat, mouse	Unknown	Unknown
ART4	Human, rat, mouse	Unknown	Unknown
ART5	Human	Unknown/Arg	Unknown
ART6(A,B)	Chicken	p33/actin/Arg28-206	Inhibits substrate activity
ART7	Chicken	Unknown	Inhibits substrate activity
Sir2p	Yeast	Histones/Sir2p/acetyl-lysine	Involved in histone deacetylation
Sirtuin2	Human	Albumin/acetyl-lysine	Involved in histone deacetylation
Pierisin1,2	Cabbage butterfly	DNA	Cytotoxic
Arginine-specific	Hamster, human	Gß/Arg129	Inhibits substrate activity
Cysteine-specific	Human	GDH/Cys	Inhibits substrate activity

linkages, and at the same time release nicotinamide (Fig 11, Table 5). Another separate class of enzymes, namely poly-(ADP-ribose)-polymerase [PARP, poly(ADP-ribosyl)transferase], yields chains of ADP-ribose units linked to each other by *O*-glycosidic linkages (Alvarez-Gonzalez *et al.*, 1994). Poly(ADP-ribosyl)ation of nuclear proteins has been implicated in the regulation of both physiological and pathological events, such as gene expression/amplification, cellular division/differentiation, DNA replication, malignant transformation, apoptosis, and long term memory (Meyer-Ficca *et al*., 2005; Visochek *et al*., 2005). The macro domain containing proteins have a high affinity for ADP-ribose binding (Karras *et al.*, 2005). PARPs are generally activated after DNA damage, the product of this reaction being poly(ADP-ribose), and they play a fundamental role, particularly PARP1, in recruiting protein targets to specific sites and in interacting physically with structural and regulatory factors, through highly reproducible and inheritable mechanisms (Faraone-Mennella *et al.*, 2005).

In contrast to other known proteins of this family, TbSIR2RP1 is a chromosome-associated NAD-dependent enzyme, which catalyses both ADP-ribosylation and deacetylation of histones, particularly H2A and H2B (Jose *et al*., 2003). Depletion of TbSIR2RP1 resulted in an increased sensitivity to the DNA alkylating agent MMS, while overexpression of TbSIR2RP1 resulted in an increased resistance to this agent. Moreover, both effects correlated with the extent of ADP-ribosylation of histones. However, overexpression of an inactive mutant form of this protein did not increase resistance to MMS or the ribosylation status of histones, indicating the direct role of histone ADP-ribosylation appears to reduce the condensation of chromatin in the region of the damage. TbSIR2RP1 is a known component of the chromatin remodelling machinery that reassembles nucleosomes, by affecting the acetylation and ribosylation status of specific residues of histones, to generate sufficient space for subsequent binding of other NER (nucleotide excision repair) factors and other regulators. These data therefore also provide evidence that histone ADP-ribosylation, methylation, acetylation, phosphorylation and ubiquitination are functionally linked, and serve as binding domains for other regulators of chromatin and transcription (Jenuwein and Allis, 2001).

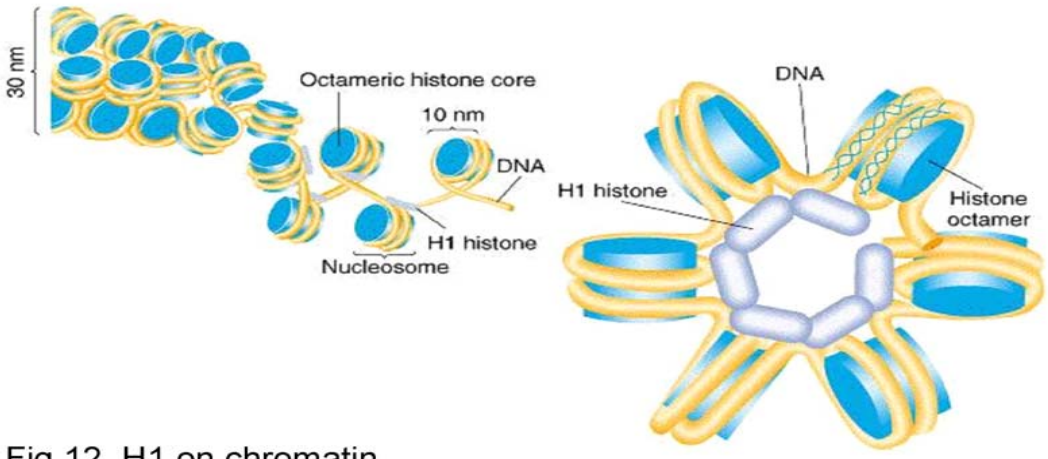

Fig 12. H1 on chromatin

3. Linker histone H1

In eukaryotes, cells contain a fifth histone called the linker histone H1. It binds to each nucleosome, and is believed to link these nucleosomes together, and to

facilitate/maintain the 30 nm chromatin fibre, which is fundamental to the structural organization of chromosomes (Fig 1, 12). During the past 20 years, many studies have been performed to examine the properties of linker histone H1, especially studies from chicken erythrocytes. The structure of its globular domain (H1G) has now been determined to a high resolution by NMR spectroscopy and x-ray crystallography (Zarbock *et al*., 1986; Clore *et al*., 1987). Both histone H1 and its variants are highly basic, particularly rich in lysine and slightly larger than core histones (>20,000 Da molecular weight). Linker histones are the least tightly bound to DNA of all the histones, and are readily dissociated by solutions of moderate ionic strength (≥0.35 M NaCl).

It is essential to identify the exact location of the linker histone within nucleosomes, the fundamental packing units of chromatin. The traditional model for H1 binding to nucleosomes cores (Fig 13A) proposed that the globular domain of the linker histone binds to the outward-facing DNA, at the site where DNA enters and leaves the nucleosome core. In this model, the linker histone spans the entering and exiting DNA, holding the DNA in place, resulting in the higher order structure of 30 nm chromatin fibre (Thomas *et al*., 1992). Zhou and

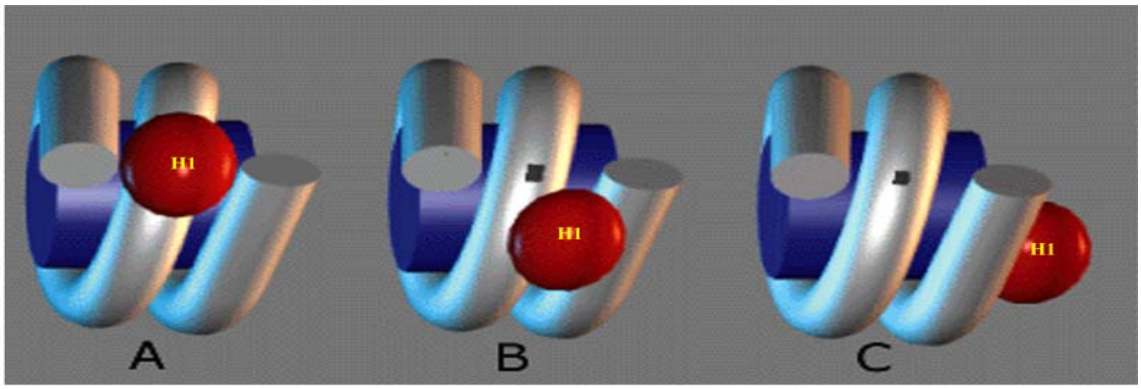

Fig 13. The models of H1 localization

co-workers, using a site-specific protein-DNA photo cross-linking method, have mapped the binding site and the orientation of the globular domain of histone H1 (H1G) on chicken nucleosomes. In contrast to an earlier model where H1G forms a bridge between one terminus of chromosomal DNA and the DNA in the vicinity of the dyad axis of symmetry of the core particle, helix III of the H1G binds in the major groove of the first helical turn of the chromosomal DNA, whereas the

secondary DNA-binding site on the opposite face of the H1G contacts the nucleosomal DNA close to its midpoint (Fig 13B). This location places the basic carboxy-terminal region of the globular domain in a position from which it could simultaneously bind the nucleosome-linking DNA strands that exit and enter the nucleosome (Zhou *et al.*, 1998). Using neutron scattering microscopy, Graziano *et al*. (Graziano *et al*., 1994) found that H1 might actually nestle inside the coils of the DNA, which wrap around core histones (Fig 13C). Other studies suggested that H1 may be not symmetrically associated with entering and exiting DNA, which is displaced by approximately 60 nucleotides from the centre (dyad axis) of the nucleosome-bound DNA (Hayes, 1996; Pruss *et al*., 1996).

Crystal structure analysis has shown that each linker histone consists of a globular “winged-helix” central domain flanked by basic N- and C-terminal tail domains (Hartman *et al*., 1977; Ramakrishnan *et al*., 1993) (Fig 14). The short N-terminal tail (length depend on species: *Drosophila*, 39AA; chicken, 25AA; mammals, 38-39AA) contains Ser, Thr and Lys which can be potentially modified by enzymes (Tuck *et al.*, 1985; Arion *et al*., 1988). It is believed that H1 is unstructured in solution, but the conformation of the Pro of this region appears to play an important role as the dominant antimicrobial peptide in skin mucous from Atlantic salmon (Torben *et al*., 2005). The model of an asymmetric nucleosome described above might impart directionality to the folding of the chromatin fibre, consistent with a polar head-to-tail arrangement of linker histone molecules. Both H1 and H1G bind cooperatively to two molecules of double-stranded DNA at once (Goytisolo *et al*., 1996), indicating that H1G must have at least two DNA-binding surfaces, and that these

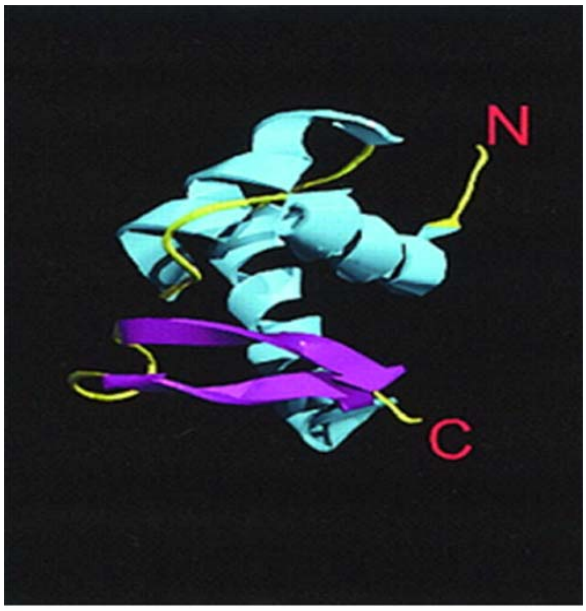

Fig 14. Crystal structure of H1 (chicken)

might both be required for targeting chromatin. Analysis of the structure of H1G has confirmed a potential second DNA binding surface in addition to the one identified by homology to the other structurally similar known DNA binding domains. Mutation of this second site shows that it is required for the formation of the cooperative complexes with pairs of DNA molecules and for proper binding to H1-depleted nucleosomes. New electron and atomic force microscopy studies further confirmed and extend the earlier findings that H1 influences the entry/exit angle of linker DNA. When H1 is present, the points at which DNA enters and exits the nucleosome are close, whereas when H1 is removed, the points of DNA entry and exit are further apart, appearing to be on approximately opposite sides of the nucleosome from each other. All of these data are consistent with the earlier model in which H1G is located over the nucleosomal dyad, binding simultaneously to the pair of DNA segments on the nucleosome. However, using chemical cross-linking methods to map the location of H1G in the nucleosome yielded a very different location (Hayes 1996; Pruss *et al*., 1996.). At present, this is still a debated issue. The orientation of the winged-helix domain would favour interaction between the basic C-terminal tail of the linker histone and linker DNA (the DNA between nucleosomes), facilitating chromatin compaction. The binding of the winged-helix domain in the major groove may account for sequence selectivity of nucleosome position and the restriction of nucleosome mobility that is dependent on linker histones.

It was shown using a mixture of calf thymus histone H1 variants isotypes that the globular domain and C-terminus can stabilize chromatin folding to the same extent as the full-length H1s, while neither the globular domain alone nor the globular domain plus the N-terminus could facilitate chromatin folding (Allan *et al*., 1980; 1986). These studies indicate that the ability of linker histones to stabilize chromatin folding resides in the C-terminal domain of the protein, and the C-termini performs its function by shielding negative charges on the DNA backbone. Does the C-terminal tail of linker histone function as random coils or do they contain secondary structure? The C-termini contains high percentages of evenly distributed lysine and arginine residues thus believed that has no

secondary structure in solution. However, resent data suggest that this is not true. The long C-terminal extensions of the proteins have a propensity towards alpha helix formation upon interaction with other components of the chromatin fiber. Hill *et al*. (Hill *et al*., 1989) found that a proline-free region of 57 residues in sea urchin sperm-specific H1 contains some α-helical structure in a low salt solution. However, there is noproline-free region in the H1 C-termini from higher organisms. Studies using circular dichroism (CD), infrared (IR) spectroscopy, or NMR have shown that trifluoroethanol, NaClO and dsDNA can induce formation of an α-helix within the linker histone C-terminus (Clark *et al*., 1988; Vila *et al.*, 2000; 2001). Using Fouriertransform IR spectroscopy to study a 23 amino acid residue peptide from the H1° C-terminus, Vila *et al.* found that in aqueous solution this peptide is mainly in random coil conformations, with some turn structures that are in rapid equilibrium with unfolded structures (Vila *et al*., 2000; 2001). However, in the presence of DNA, this peptide displays stable helical and turn structures. Noteworthy, the turn structure is attributed to the TPKK motif, which is commonly found in linker histones as an S/TPKK motif, and is considered to be a DNA binding domain (Suzuki 1989; 1993).

Unlike core histones, such as H3 and H4, which are relatively conserved among different species, histone H1 has a numerous variants (Lennox *et al*., 1983, 1984; Tanaka *et al*., 2001). Among the different H1 isotypes, the N- and C-termini show the most variation in length and amino acid sequence, while the globular domain is the most conserved (Wolffe *et al*., 1997) (Fig 15). Khadake and Rao compared the ability of rat linker histone isotypes to condense naked DNA into its liquid crystal form, they found that the somatic linker histone isotypes H1b, H1e have greater abilities to compact naked DNA than H1a and H1t (testes-specific variant). Similar results were obtained using short linker histone stripped chromatin fibers prepared from rat liver. These differences in the ability to compact DNA presumably result from variations in the C-terminal tails of these linker histone isotypes. Indeed, the sequences of the H1d and H1t C-terminal tails differ significantly. Interestingly, three imperfect octapeptide repeats containing an S/TPKK motif were found in H1d C-terminus, while none were

found in H1t. In a subsequent study using similar techniques, Bharath *et al*. (Bharath *et al*., 2002) showed that when a stretch of 34 amino acid residues containing the H1d octapeptide repeats was deleted, H1d essentially loses its naked DNA compacting ability even though only1/3 of the total amino acid residues in the C-terminal tails have been deleted. The spacer between two of the repeats also plays an important role. When the normal spacer of 10 amino acid residues was deleted, the DNA compacting ability of the mutant was reduced by 70%. These results suggest that the specific secondary structure motifs in the C-termini is important for linker histone dependent DNA compaction (Khadake and Rao, 1995; Bharath *et al*., 2002).

To further address the role of the linker histone C-terminal domain in chromatin condensation, Hansen's group studied recombinant mouse histone H1 comparing with the mutant H1 histones containing progressive deletions of the C-terminus. They compared the binding ability of the native and mutant H1 histones to nucleosomal arrays, and subsequently stabilize salt-dependent intra-array folding and inter-array oligo-merization. They found that although both the wild type and the four mutant H1 histones can bind to nucleosomal arrays, the systematic deletion of the C-terminus leads to a systematic decrease in the relative binding affinity of the mutant H1 histones for the arrays (Lu and Hansen, 2003).

The ability of the 1–96 mutant to bind nucleosomal arrays indicates that the H1 globular domain also contributes to nucleosome binding. It is well documented that nucleosomal arrays and chromatin fibers can undergo both salt-induced folding and intermolecular oligomerization *in vitro*, which can mimic the short- and long-range interaction in chromatin *in vivo* (Hansen, 2002): Deletion of residues 97–121 and 146–169 within the C-terminus significantly compromises the ability of H1 to stabilize chromatin folding; In contrast, only deletion of residues 97–121 affected oligomerization. These results demonstrate that different, discrete subdomains within the linker histone H1 C-terminus mediate stabilization of salt-dependent chromatin condensation.

In *vitro* experiments had suggested that H1 played an essential role in the 30 nm fiber, through its effects on the organization of nucleosomal linker DNA, however,

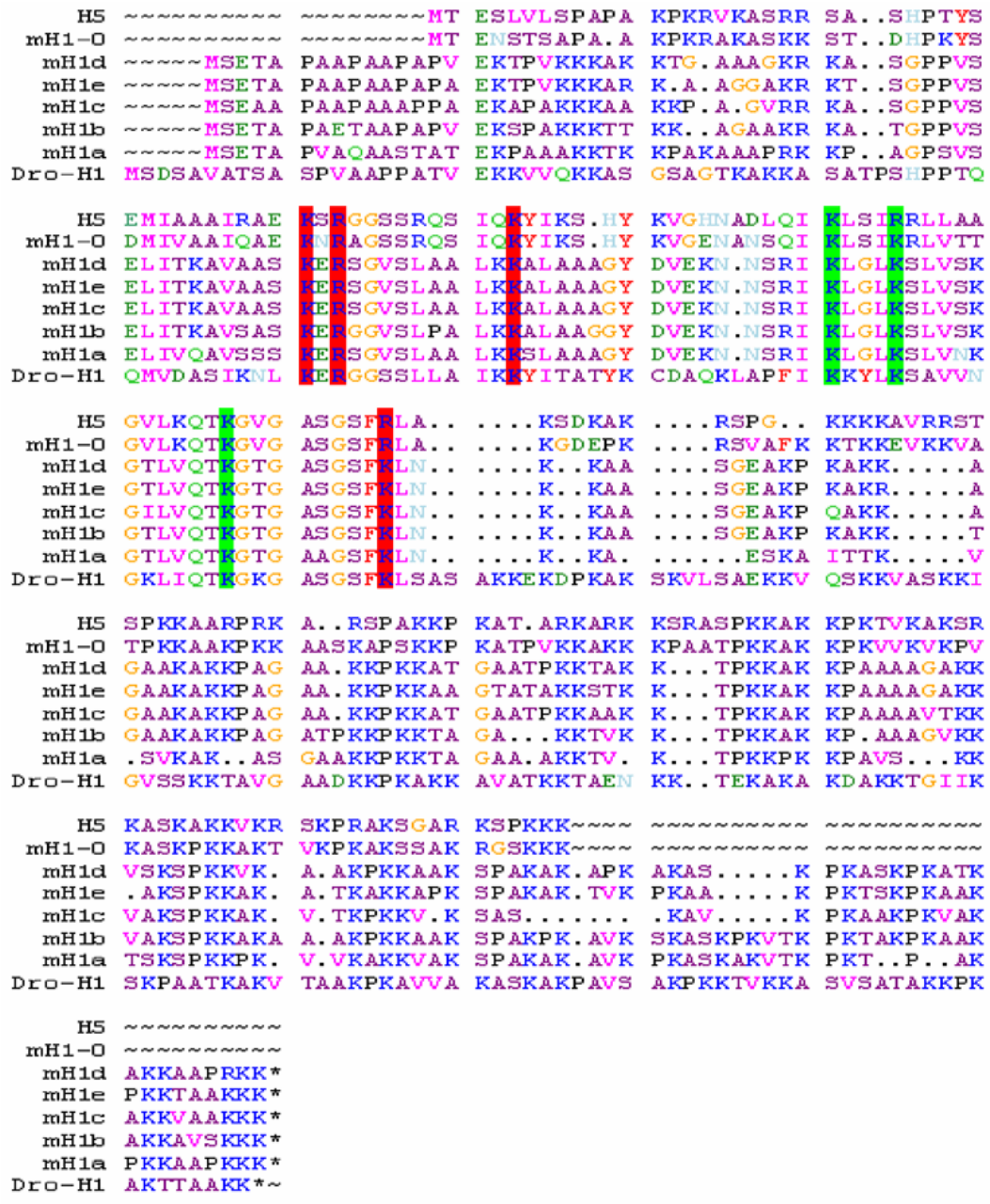

Fig 15. Comparison H1 protein in different organisms

studies *in vivo* challenged to the role of H1. In yeast *Saccharomyces cerevisiae,* only one protein having significant homology to the conserved globular domain of typical histone H1, this protein has now been eliminated by knockout, and cells remain viable, although there are detectable alterations in gene regulation.

Knockout histone H1 In *Tetrahymena thermophila* (Shen and Gorovsky, 1995;1996), the mutant strains grow at normal rates and reach near-normal cell densities, arguing that H1 in this organism is not essential for cell survival. Similarly, H1 does not have a major effect on global transcription although can act as either a positive or negative regulator of transcription in *vivo*. However, it was noticed that the histone H1 like protein in *S. cerevisiae* contains two globular domains, without N and C terminal tails of a typical H1 in higher eukaryotes; in *Tetrahymena,* the histone H1 like protein contains only N and C terminal tails, but without globular domain (Fig 15). Therefore, it has been considered that they may be not the real linker histone H1.

In multi-cellular organisms such as plants and mammals, linker H1 have been shown to be functional. In mice, there are at least eight histone H1 variants that are differentially regulated during development and differentiation(Fig 15). Mouse H1a, H1b, H1c, H1d, and H1e, these somatic linker histones, are ubiquitously expressed but at different levels in different tissues (Lennox and Cohen 1983; Wang *et al*., 1997). H1°, the replacement linker histone, tends to be highly expressed in fully differentiated cells (Zlatanova & Doenecke, 1994), while H1t and H1oo are expressed specifically in developing spermatocytes and oocytes, respectively (Tanaka *et al.*, 2001). This heterogeneity in expression pattern is matched by a strong divergence among the subtypes at the structural level. Although they all share the same basic organization of metazoan H1s consisting of a globular core flanked by two "unorganized" tails, both the globular domain and the tails exhibit significant differences among the various mammalian linker histones, with H1° being the most divergent (Wang, 1997). To investigate the roles of the individual linker-histone subtypes in mammals, Fan and coworkers have systematically deleted linker-histone genes in mouse embryonic stem cells and generated mice null for H1°, H1a, H1c, H1d, H1e, or H1t, as well as several double mutants of H1 variants. Surprisingly, mice lacking any one of these subtypes develop normally (Sirotkin *et al*., 1995; Lin *et al*., 2000; Fan *et al*., 2001), whereas the disruption of multiple but not individual H1 isoforms in the mouse leads to embryonic lethality. Studies of chromatin in specific tissues of

single H1-null animals suggested that the lack of a phenotype in these mice is due to compensation by the remaining subtypes. Using mice lacking specific H1 subtypes, they further investigate the role of histone H1 in position effects on gene expression. Some but not all histone H1 subtypes can attenuate or accentuate position effects. These results suggest that the linker histone subtypes play differential roles in the control of gene expression, and that linker histones on the chromatin fiber might regulate higher order chromatin structure and fine tune of the individual gene expressing level (Raouf Alami, *et al*., 2003).

Although H1 is a key architectural component of chromatin, it clearly has additional complex regulatory functions (Zlatanova, 1992; Wolffe, 1997). For example, linker histone H1 stoichiometrily regulates core histone acetylation *in vivo*. Gunjan *et al.* demonstrated that exponentially growing cell lines induced to overproduce either variants, H1° or H1c, displayed significantly reduced rates of acetylation on core histones; pulse-chase experiments indicated that the rates of histone deacetylation were similar in all cell lines. Reduced levels of acetylation in H1 overproducing cell lines do not appear to depend on higher order chromatin structure, because it persists even after digestion of the chromatin with micrococcal nuclease (Gunjan *et al*., 2001).

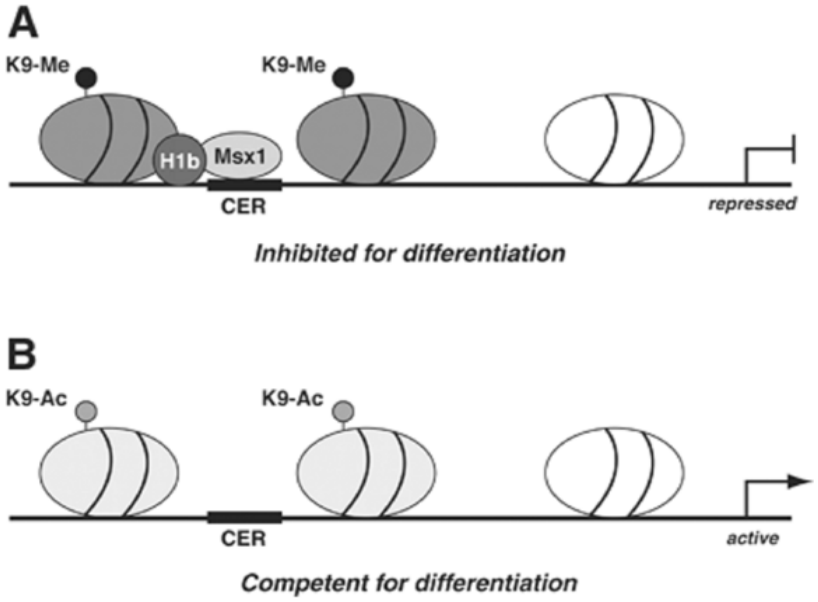

Fig 16. Histone H1b interacts with Msx1 and is involved in differentiation (Hansol L, *et al*., 2004)

Histone H1b co-operates with Msx1 for inhibition of transcription (Fig 16). H1b and Msx1 bind to a key regulatory element of MyoD, a central regulator of skeletal muscle differentiation, where

they induce repressed chromatin (Hansol *et al*., 2004). Moreover, Msx1 and H1b co-operate to inhibit muscle differentiation in cell culture and in Xenopus caps. This study provided evidence that one isoform-H1b can function as a gene-specific regulator, supporting to the idea that H1 isoforms may have distinct functions *in vivo*, and the complexity of H1 function is attributed, in part, to differential activities of its isoforms and their partners, which thereby impart distinct developmental outcomes. This study also supports a long-standing prediction that the developmental expression of H1 isoforms is indicative of differential regulatory functions in higher organisms.

Specific variant of linker histone H1 seems also functional associated with DNA-damage-induced apoptosis. DNA damage presents a vital threat to long-lived multi-cellular organisms because of the consequences of cancer. Mammalian has an excess capacity for the individual cells, with an alternative and more certain strategy to eliminate risks by eliminating the damaged cells through apoptosis pathway. p53 has been shown to play a key role in this process (Oren, *et al*., 2003). Recently, Konishi and his colleagues demonstrated a role for the linker histone H1c in triggering apoptosis in response to DNA damage (Konishi *et al*., 2003). Using biochemical approaches, cytosol from irradiated rat thymocytes was fractionated and assayed for induction of cytochrome c, which is released from purified mitochondria. Surprisingly, the most potent activity detected was due to the presence of H1c, but not other histone H1 variants. After depletion H1c in living cells and mice, both thymocytes and cells in the small intestine in H1c-deficient mice showed remarkable resistance to the X-rays. Therefore, H1c emerges not only as a component of chromatin, but capable of transforming cells to death.

It is not clear how does a nuclear H1 protein acts on mitochondria. H1c itself does not show any obvious posttranslational modification as a consequence of DNA damage, raising the possibility that DNA damage may cause physical remodelling or modification of other chromatin components, which results in some H1c to leave from chromatin. The relocalization of H1c from the nucleus to the cytoplasm appears to be p53 dependent, arguing that perhaps p53 mediated

DNA repair is involved in displacing H1c from chromatin. On the other hand, given that p53 itself undergoes active nucleo-cytoplasmic shuttling (Liang *et al*., 2001), thus p53 might play a direct role in regulating H1c translocation after damage.

In *Drosophila*, histone H1 is absent from early embryos, but appears during midblastula transition, when zygotic messenger RNA synthesis becomes activated. The H1 competitor on chromatin- high mobility group protein (HMG), present at high levels prior to midblastula transition declines in prevalence relative to H1 concentration. It is thought that this change in protein concentrations is an important factor in activation of zygotic transcription. Because the binding site of HMG with nucleosome is partially overlap with histone H1 (Alfonso *et al*., 1994), and HMG proteins conteract the repression role of H1 in chromatin (Ding *et al*., 1997).

The dynamics of histone H1 in the nucleus of living cells has been investigated using fusion proteins of histone H1 and green fluorescent protein (GFP), since they were shown to associate with chromatin in an apparently identical fashion to native H1. Using human cells expressing a stably integrated H1a–GFP fusion protein, the movement of H1 was monitored directly by fluorescence recovery after photobleaching in the living cells (Melodya *et al*., 2000). They showed that histone H1 exchange is rapid in both condensed and decondensed chromatin, occurs throughout the cell cycle, and does not require fibre–fibre interactions. However, it was also noticed that histone H1 seems to recover relatively slower in heterochromatic domains than that in euchromatic domains. Treatment with drugs that alter H1 phosphorylation significantly reduces exchange rates. These results suggest that histone H1 exchange *in vivo* is rapid, occurs through a soluble intermediate, and is modulated by the phosphorylation.

In order to examine the effect of H1 phosphorylation on the role of the histone in nuclear dynamics, Alejandro et al. produced a mutant histone H1, referred to as M1-5, in which the five cyclin-dependent kinase phosphorylation consensus sites were mutated from serine or threonine residues into alanines (Alejandro *et al*., 2003). Cyclin E/CDK2 or cyclin A/CDK2 cannot phosphorylate the mutant *in vitro*.

Using the technique of fluorescence recovery after photobleaching, the mobility of GFP–M1-5 fusion protein is decreased compared to that of a GFP–wild-type H1 fusion protein. In addition, the recovery of H1 correlated with CDK2 activity, as GFP-H1 mobility was decreased in cells with low CDK2 activity. Blocking the activity of CDK2 by p21 expression decreased the mobility of GFP-H1 but not that of GFP–M1-5. In heterochromatic regions, the level and rate of recovery of cyan fluorescent protein (CFP)–M1-5 were lower than those of CFP-H1. These data suggest that CDK2 phosphorylates histone H1 *in vivo*, resulting in a more open chromatin structure by destabilizing H1-chromatin interactions.

4. Ribosomal protein dynamics

Cell growth (increase in cell size and mass) is controlled in response to nutrients, growth factors, and other environmental conditions. A key component of cell growth control is the regulation of ribosome biogenesis. This is not only because ribosomes are directly required for protein synthesis and cell growth, but also because ribosome biogenesis is a major consumer of cellular energy. To maintain robust growth in response to favorable conditions, cells synthesize approximately 2000 ribosomes per minute. This requires the coordinated activity of all three RNA polymerases transcribing several hundred genes, including 45S rRNA genes by Pol I, ribosomal protein (RP) genes by Pol II, and 5S rRNA and tRNA genes by Pol III (Jorgensen *et al*., 2004; Nomura, 2001; Warner, 1999). Thus, in a growing cell, approximately 95% of total transcription and a large portion of total cellular energy are dedicated to ribosome biogenesis, underscoring the need for tight regulation of ribosomal genes in response to nutrient and energy conditions (Dietmar *et al*., 2004). Despite the fundamental importance of this regulation, the functional dynamics of ribosomes and other related protein synthesis machineries in cells remains poorly understood.

Ribosome subunits are believed to be assembled in the nuclear compartment-nucleolus, where RNA Pol I-mediated rDNA transcription occurs(Fig 17). Although the morphology of nucleoli varies among cell types, it generally consists

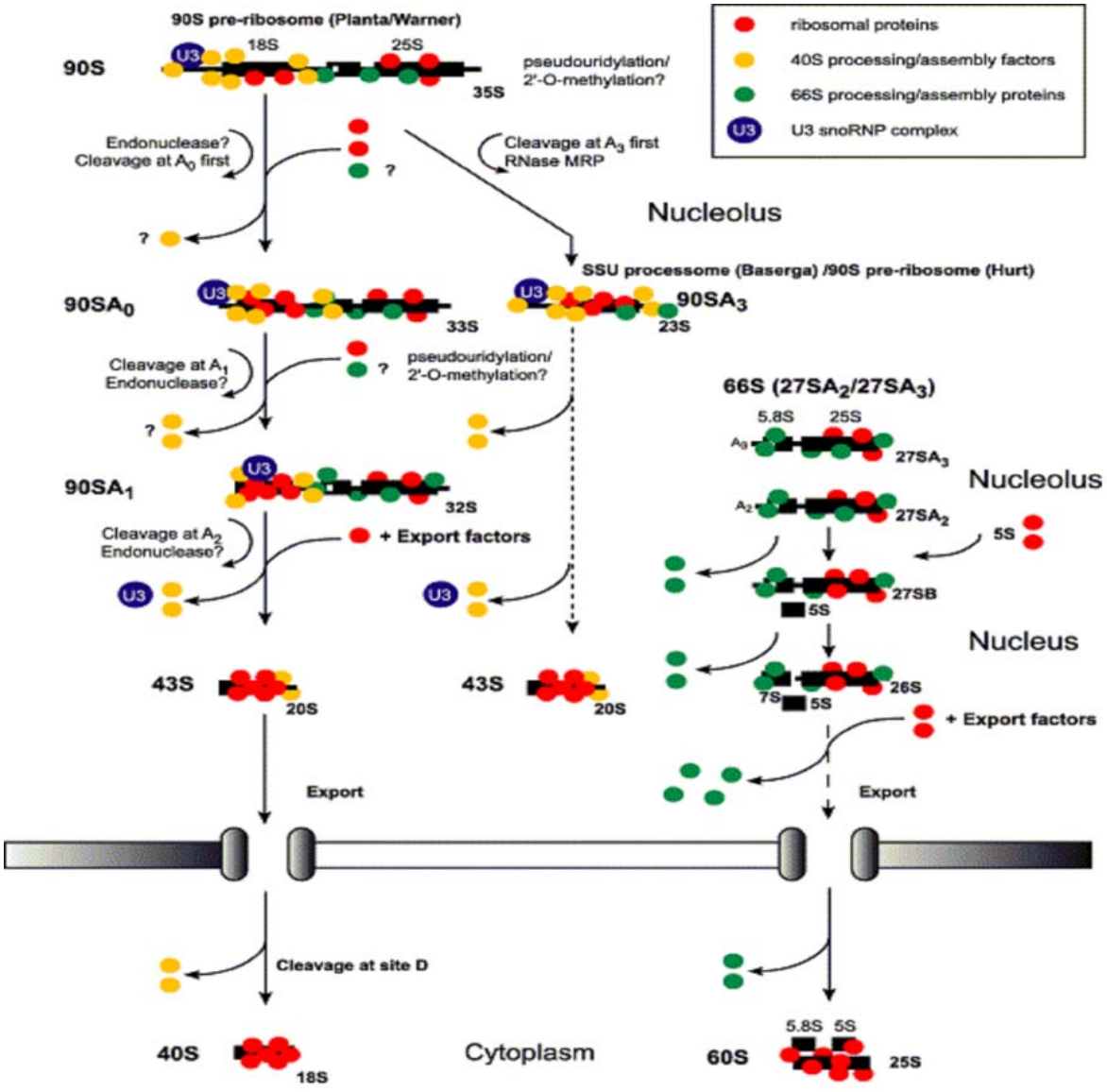

Fig 17. Dynamic nature of ribosome biogenesis (Sander 2004).

of three domains: the innermost is the fibrillar center (FC), which contains both inactive and active rDNA genes; the processing and assembly of rRNA take place in the surrounding dense fibrillar component (DFC); the latter steps of ribosome maturation occur in the outermost granular component (GC). In budding yeast, the nucleolus is a crescent-shaped structure abutting the nuclear

envelope, occupying roughly one third of the nucleus. Plant and animal nuclei contain multiple nucleoli, often adjacent to heterochromatin. In all cases, nucleolar morphology is influenced by the growth rate of the cell.

Ribosomes are known located on the endoplasmic reticulum (ER) of eukaryotic cells, and are made of large number of ribosomal proteins as well as a special type of RNA- ribosomal RNAs. In eukaryotes, 28S, 18S, 5.8S and 5S rRNA are known associated with ribosomes. The 5.8S, 18S, and 28S rRNAs are transcribed as a single unit within the nucleolus by RNA polymerase I, yielding a 45S ribosomal precursor RNA. The 45S pre-rRNA is further processed to the 18S, 5.8S and 28S rRNA. 18S rRNA along with about 30 different ribosomal protein molecules, make the 40S (small) ribosomal subunit. 5.8S and 28S rRNAs are components of the 60S (large) ribosomal subunit (references)(Fig 17). One of the 60S subunit- L22, has a globular domain that sits on the surface of the large ribosomal subunit and an extended loop that penetrates its core. The tips of it's loops contribute to the lining of the peptide exit tunnel and have been implicated in a gating mechanism that might regulate the exit of nascent peptides (Zengel *et al.*, 2003). Transcription of the 5S rRNA, which is present in the 60S ribosomal subunit, takes place outside of the nucleolus and is catalyzed by RNA polymerase III. In addition as a key component of ribosome, the rRNA molecules have several roles in protein synthesis: the 28s rRNA has a catalytic role, it forms part of the peptidyl transferrase activity of the 60 s subunit; 18s rRNA has a recognition role, involved in correct positioning of the mRNA and the peptidyl tRNA; finally, the rRNA molecules also have a structural role, they fold into three-dimensional shapes forming the scaffold on which the ribosomal proteins assembled.

The structure and function of the mature ribosome in cytoplasm, the machinery that synthesizes proteins, is well known. In contrast, our knowledge on the formation and maturation of these molecular machines is only slowly emerging. To produce a ribosome, eukaryotic cells must assemble more than 70 ribosomal proteins (r-proteins) with the four different rRNA species (25S/28S, 18S, 5.8S and 5S) described above. Unlike assembly in prokaryotes, this process cannot

occur spontaneously in eukaryotes, but requires numerous non-rRNA and protein factors (Fig 17). In addition, a number of ribosomal protein subunits contain posttranslational modification, such as acetylation, methylation, and phosphorylation (Odintsova *et al.*, 2003). Notably, the biogenesis of eukaryotic ribosomes depends on the concerted action of all three transcription machineries (RNA polymerases I, II and III), which have to be co-ordinated to ensure the high efficiency and accuracy of ribosome production. The outcome of such a spatially and temporally coordinated effort is that, for example, in a growing yeast cell, every second ~40 nascent ribosomes leave the nucleolus, and export into the cytoplasm (Tschochner *et al.*, 2003).

It is generally believed that eukaryotic ribosome first associate with mRNA in the cytoplasm. However, most recent study using immunostaining and in situ hybridization found that ribosomal subunits are also present at transcription sites on *D*rosophila salivary gland chromosomes- polytene chromosomes (Brogna *et al.*, 2002), and associate with nascent RNP complexes within the nucleus, arguing a new role for ribosome in cell nucleus.

III. Results

1. *Drosophila* ribosomal proteins are associated with chromatin through histone H1 and suppress global transcription

Jian-Quan Ni[1], Lu-Ping Liu[1], Daniel Hess[1], and Fang-Lin Sun[1,*]

[1]Friedrich Miescher Institute for Biomedical Research, Maulbeerstrasse 66, Basel, CH-4058, Switzerland

*****Corresponding author

Mailing address: Friedrich Miescher Institute for Biomedical Research, Maulbeerstrasse 66, Basel, CH-4058, Switzerland. E-mail: fang-lin.sun@fmi.ch

FAX: +41 (0) 61 697 3976

Tel: +41 (0) 61 697 7590 or +41 (0) 61 697 7565

Summary

The assembly and maturation of ribosomes in eukaryotes is believed to take place largely in the nucleolus and cytoplasm. Little is known of the dynamics and function of ribosome proteins in the cell nucleus. Here we provide evidence that components of *Drosophila melanogaster* 40S and 60S ribosomes co-purify with histone H1 in the cell nucleus. Using various experimental approaches, we demonstrate that the association of ribosomal proteins with histone H1 is nuclear-specific, and show co-localization on condensed chromatin. ChIP analysis confirmed that ribosomal proteins are directly associated with chromatin in a histone H1-dependent manner. Further studies revealed that the presence of H1 and ribosomal proteins on chromatin is coupled to suppression of transcription and changes in chromatin structure. Overall, this study provides evidence for a previously undefined link between ribosomal proteins and chromatin, and suggests a role for this association in transcriptional repression in higher eukaryotes.

Introduction

In eukaryotes, the assembly and maturation of ribosome complexes involves a large number of proteins, including those associated with small nucleolar RNAs, endo- and exoribonucleases, and putative ATP-dependent RNA helicases (Woolford, 1991; Venema and Tollervey, 1999; Kressler et al., 1999). Pre-40S particles are believed to be processed in the cytoplasm, whereas maturation of the 60S subunit continues in the nucleus prior to export to the cytoplasm from the nucleolus (Fromont-Racine et al., 2003). In contrast to our understanding of the process of the assembly, processing, and maturation of ribosome particles, and their transportation between nucleolus and cytoplasm, very little is known about the dynamics of ribosomal proteins in the cell nucleus.

Previous studies have shown that a number of ribosome components, as well as other proteins of the translation apparatus, are present in the cell nucleus (Ringborg et al., 1970; Lejbkowicz et al., 1992; Sanders et al., 1996; Lund and Dahlberg, 1998; Dostie et al., 2000). In yeast, ribosomal proteins co-purify with a subunit of chromatin assembly factor 1 (CAF1) (Schaper et al., 2001). Complexes of the origin recognition complex (ORC)-interacting protein Yph1p also contain 60S ribosomal proteins and pre-ribosomal particle proteins (Du and Stillman, 2002). It is generally believed that ribosome particles in the cell nucleus are confined to the nucleolus and may not be functional; however, polysomes have been found in the nucleus, and the presence of ribosomes in the nucleus was reported to be associated with nuclear translation (Goldstein, 1970; Allen, 1978; Golid, 1978; Iborra et al., 2001). A recent study using antibodies against more than 20 human ribosomal proteins demonstrated that ribosomal proteins are associated with nascent RNA transcripts on *Drosophila* polytene chromosomes, and are also coupled to amino acid incorporation at these chromosomal locations (Brogan et al., 2002).

Since functional ribosomes are the only known means to detect termination codons in mRNA, it has been proposed that the presence of ribosomes in the cell nucleus may be linked to nonsense-mediated mRNA decay (NMD)/mRNA surveillance (Wilkonson and Shyu, 2002), a phenomenon in which mRNA

degradation is triggered by premature codons occurring in messenger RNAs (Schell et al., 2002; Wagner and Lykke-Anderson, 2002; Baker and Parker, 2004; Maquat, 1995).

Linker histone H1 is a basic component of nucleosomes that is believed to bind to nucleosomal DNA, protecting an additional 20 bp of DNA, and to have a fundamental role in promoting or facilitating the condensation of nucleosome filaments into supercoiled chromatin fibers (Thomas, 1999; Luger, 2003; Bustin, 2005; Vignali and Workman, 1998). Previous studies have shown that H1 limits nucleosome mobility (Pennings et al., 1994), reduces transient exposure of DNA on the surface of nucleosomes (Juan et al., 1997; Polach and Widom, 1995), and also directly occludes the binding of transcription factors, suggesting that H1 functions as a general repressor of transcription (Juan et al., 1997; Laybourn and Kadonaga, 1991). *In vivo* studies suggested that H1 is also essential for lifespan, suppression of homologous recombination, and transmitting apoptotic signals from the nucleus to the mitochondria following DNA double-strand breaks (Shen and Gorovsky, 1996; Barra et al., 2000; Downs et al., 2003; Konishi et al., 2003;). Although mutation of H1 in unicellular organisms had only limited effects on transcription (Hellauer et al., 2000; Shen and Gorovsky, 1996), in higher multicellular organisms H1 appears to be essential for cell differentiation and normal development (Fan et al., 2003; Jedrusik and Schulze, 2003; Steinbach et al., 1997).

Here, we investigated the role of histone H1 in chromatin *in vivo* using *D. melanogaster* as a model system. Unexpectedly, we found that H1 co-purified with a large number of nuclear proteins identified as components of 40S and 60S ribosomes. Further immuno-fluorescent staining and chromatin immuno-precipitation (ChIP) analyses demonstrated that ribosomal proteins and H1 are both directly associated with chromatin. Upon depletion of H1, ribosomal protein association with chromatin was lost. Furthermore, we show that ribosomal proteins in the cell nucleus co-localize with condensed chromatin, where histones are hypo-acetylated or methylated. Overexpression of ribosomal proteins caused a global suppression of gene transcription, overlapping with suppression by

histone H1. Consistently, H1 and ribosomal proteins are both lost from chromatin during transcriptional activation of endogenous genes, while ribosomal proteins bind to newly synthesized RNA transcripts in the cell nucleus. This is the first report demonstrating that ribosomal proteins are directly associated with chromatin and functionally coupled with global transcriptional repression.

Results

Linker histone H1 co-purifies with specific ribosomal proteins

Immunoprecipitation (IP) experiments aimed at co-purifying the partners of *D. melanogaster* histone H1 in the cell nucleus were performed using newly derived polyclonal antibodies specifically recognizing the N terminus (AA 33–47, H1N) and C terminus (AA 242–256, H1C) of H1 (Figure 1A, B). Since histone H1 is known to be lysine-rich and to have strong DNA-binding activity (Hill et al., 1991), nuclear extracts from *D. melanogaster* Kc cells were treated with ethidium bromide (EB, see Experimental Procedures) to reduce potential DNA-protein interactions (Du and Stillman, 2002). IP fractions obtained using anti-H1C or anti-H1N antibodies were separated by SDS-PAGE (Figure 1C, D and data not shown). Mass spectrometry was used to identify the most prominent bands present between the sizes of 15 and 50 kDa in the gels. In addition to core histones H2B and H3, we found that histone H1 co-purifies with 40S and 60S ribosome components (Figure 1C, D). hnRNP48 and hnRNP36 (Matunis et al., 1993), which are known to be involved in mRNA quality control (Krecic and Swanson, 1999; Lykke-Andersen, 2001), were also among the pulled down proteins (Figure 1D).

In these IP experiments, 40S and 60S ribosomal proteins were unlikely to have been pulled down as a result of non-specific interactions between the H1 antibodies and cytoplasmic ribosomal proteins because no ribosomal proteins were pulled down from cytoplasmic extracts of Kc cells by either the anti-H1N or the anti-H1C antibody (data not shown).

Tagged ribosomal proteins are present in the nucleus and interact specifically with histone H1

To further determine the specificity of the interaction between ribosomal proteins and histone H1, we transiently expressed V5-HA-tagged ribosomal proteins L7 (T-L7) and L22 (T-L22) in Kc cells. Ribosomal proteins L22 and L7 were chosen simply because of their presence at high frequency in the complexes of histone H1 under differential experimental conditions (Figure 1C, D, and data not shown).

Immunofluorescent staining experiments using formaldehyde-fixed Kc cells showed the expected distribution pattern of tagged ribosomal proteins within cells, i.e. both cytoplasmic and nucleolar localization (Figure 2A, B, and Figure S1). However, in more than 10% of cells, ribosomal proteins also showed a clear nuclear localization (Figure 2A, B). Ribosomal proteins fused with GFP or LacZ tags have been shown to be functional (Gadal et al., 2002; Milkereit et al., 2001; Stage-Zimmermann et al., 2000; Tsay et al., 1994). To confirm that the tagged ribosomal proteins are functional in our case, we performed co-sedimentation experiments in sucrose density gradients using cytoplasmic cell extract; T-L22 was present in both 60S ribosomes and polysomes (Figure 2C). Using the same experimental approach, we then performed a sedimentation experiment with nuclear extract from Kc cells. Notably, nuclear fractions containing histone H1 all contained T-L22, regardless of the salt conditions used [e.g., 360mM $(NH_4)_2SO_4$, or 300mM NaCl] (Figure 2D, and data not shown), supporting the notion of a specific interaction between nuclear ribosomal proteins and histone H1. Furthermore, IP experiments performed using nuclear extracts (EB-treated) from Kc cells expressing T-L22 and T-L7 showed that ribosomal proteins can reverse pull down histone H1 (Figure 2E).

To investigate whether any interaction occurs between H1 and cytoplasmic ribosomes, we isolated native histone H1 from the nuclei of Kc cells (see Experimental Procedures) and mixed this H1 with cytoplasm collected from T-L22 cells. Immunoblotting of fractions collected following sucrose gradient sedimentation showed that the purified H1 failed to interact with 40S, 60S or 80S ribosomes in the cytoplasm (Figure 2F), implying that interaction between H1 and ribosomal proteins is indeed specific to the nucleus. This result also served to confirm that the observed interaction between nuclear ribosomal proteins and H1 did not result from contaminating ribosomal proteins from the cytoplasm.

Ribosomal proteins are dynamically associated with condensed chromatin, and co-localize with H1 in the cell nucleus

To examine association of nuclear ribosomal proteins and histone H1 *in vivo*, we derived antibodies using peptides corresponding to the N- (1-15; L22N) and C- (285-299; L22C) termini of *D. melanogaster* ribosomal protein L22 (see Figure S2 for antibody specificity verification).

Using these specific L22N and L22C antibodies, we performed immuno-fluorescent staining experiments to study the cytological distribution of endogenous ribosomal proteins in wild type Kc cells. The results showed L22 to be predominantly distributed in the nucleus in more than 10% of cells, while other cells showed both nuclear and cytoplasmic localization of L22 (Figure 3A, B). Interestingly, the nuclear ribosomal protein L22 often co-localized with intensive DAPI signals, which often represent the most condensed chromatin in the cell nucleus. In some cells, the localization of L22 fully overlapped with DAPI staining (Figure 3A, B).

Using the same antibodies, and Kc cells expressing GFP-tagged H1 (H1-GFP), we next compared the distribution of L22 with that of histone H1 in the cell nucleus. The nuclear fraction of L22 and H1 partially co-localized in the cell nucleus in cells where L22 is distributed in both cytoplasm and nucleus. However, in cells in which L22 is mostly nuclear, it almost entirely overlaps with H1 in regions of highly condensed chromatin, as indicated by DAPI staining (Figure 3C). The results support the view that histone H1 and ribosomal proteins are dynamically associated with each other, and that their interaction likely occurs on chromatin *in vivo*.

Ribosomal proteins are directly associated with chromatin

Histone H1 is a known component of chromatin (Zlatanova and Van Holde, 1992; Wolffe, 1997; Vagnali and Workman, 1998; Thomas, 1999). To confirm that the interaction between histone H1 and ribosomal proteins is associated with chromatin in the cell nucleus, we performed ChIP analysis using the stable Kc cell line T-L22 to detect any physical association of L22 with chromatin. ChIP analysis was performed using anti-HA (to detect T-L22) and anti-H1 antibodies, and fragmented chromatin extracts from formaldehyde-fixed T-L22 cells and

control Kc cells. The resulting isolated ChIP DNA was subjected to PCR analysis with primers specific for ten genes known to be enriched for H1 binding (J-Q Ni and F-L Sun, unpublished data) to test their physical association with ribosomal protein T-L22. Most of the H1-enriched genes were found to be associated with T-L22 (Figure 4A), thus supporting our hypothesis that ribosomal proteins are directly associated with chromatin.

The association of ribosomal proteins on chromatin is H1-dependent

We next determined whether the presence of histone H1 is essential for the association of ribosomal proteins on chromatin. Using T-L22 cells and an RNAi procedure (see Experimental Procedures), we depleted histone H1 by approximately 80%. Western blotting analysis using anti-V5 and anti-H3 antibodies suggested no obvious global change in the expression of T-L22 after H1 depletion (data not shown), and these cells were therefore used in further ChIP analysis. As controls for the ChIP assay, we used polyclonal anti-H3 (positive control), anti-GFP, and monoclonal anti-Xpress antibodies (negative controls). We chose four genes, *CG8066*, *Act57B*, *Klp38B* and *CG4914*, known to bind histone H1 and ribosomal protein T-L22 on chromatin in wild type Kc cells to monitor changes in binding of H1 and ribosomal proteins in H1-depleted cells. Depletion of histone H1 resulted in increased transcription of *Act57B*, *CG8066*, and *CG4914* (approximately 10-, 4-, and 2.5-fold, respectively), and a 4-fold decrease in transcription of *Klp38B* (J-Q Ni and F-L Sun, unpublished data). PCR analysis of the ChIP DNA showed that the association of H1 was dramatically reduced following H1 depletion, and association of ribosomal protein T-L22 with chromatin was reduced by 4- to 8-fold in *CG8066*, *Act57B* and *Klp38B* (Figure 4B), suggesting that H1 is required for the association of ribosomal proteins with chromatin. For *CG4914*, only a minor change in T-L22 association was observed, possibly due to some H1 remaining associated with this gene following RNAi treatment (Figure 4B).

Histone H1 and nuclear ribosomal proteins are repressors of histone modifications

To understand the biological function of the association of ribosomal proteins with H1 on chromatin, we investigated the relationship between histone H1, ribosomal protein L22 and core histone modifications, including hallmarks of active chromatin, such as histone H3K4 methylation and H4 acetylation, and inactive chromatin, such as H3K9 methylation.

Histone H1 has been suggested to be a repressor of specific histone modifications in mammals (Gunjan et al., 2001; Herrera et al., 2000; Vaquero et al., 2004). Using cells expressing H1-GFP in Kc cells, we compared the H1 localization pattern with that of histone H3K4 methylation (polyclonal antibodies) and H4K8 acetylation, both hallmarks of active chromatin. The results showed that H1 is largely excluded from domains where histone H3K4 is hypermethylated, or H4 is hyperacetylated (Figure 5A), implying that histone H1 may be a repressor of H3K4 methylation and H4 acetylation in *D. melanogaster*.

Using wild type Kc cells, we also compared the localization of L22 with H3K4 methylation (monoclonal antibodies). The results showed that in cells where L22 was distributed in both nucleus and cytoplasm, the nuclear fraction of L22 seemed to only partially overlap with H3K4 methylation (Figure 5A). However, among cells in which L22 is mainly localized in the nucleus, L22 was largely excluded from chromatin where H3K4 is hypermethylated, implying that ribosomal proteins, like histone H1, may be involved in maintaining inactive chromatin or transcriptional repression.

To test this hypothesis, we next attempted to determine whether a dosage effect of histone H1 and ribosomal proteins on histone modifications exists. Extracts from stably transfected Kc cells overexpressing T-L22, and cells overexpressing H1-GFP were used to perform the assays. The results showed that ectopic expression of histone H1 caused a global reduction in H3K4 methylation, acetylation of H4 at lysine 8, 12, and pan-acetylated histone H4, all hallmarks of active chromatin (Figure 5B). However, the global level of H3K9 methylation,

which is believed to be associated with pericentric heterochromatin, seemed not to be affected (Figure 5B).

Using the same experimental strategy, we then analyzed the impact of overexpression of T-L22 on histone modifications. In contrast to histone H1, overexpression of T-L22 caused only a minor reduction in histone H4K8, H4K12 and pan-acetylated H4, and no obvious change in global H3K4 methylation (Figure 5C). This difference from histone H1 may be due to the lower level of overexpression of L22, since it showed no more than a 2-fold increase compared to endogenous L22. However, other possibilities, such as the use of a histone modification-independent pathway, should not be fully excluded.

Overall, the above results confirm that, like histone H1, nuclear ribosomal proteins are associated with inactive chromatin and suppress the histone modifications characteristic of active chromatin.

Overexpression of H1 and ribosomal protein L22 causes transcriptional repression of the same set of genes

To test whether, like histone H1, ribosomal proteins are directly involved in transcriptional repression, we performed microarray analysis using total RNA extracted from Kc cells stably overexpressing GFP (control), T-L22 or H1-GFP. The results showed that more than 1344 genes were significantly affected when overexpressing H1-GFP. Upon overexpression of T-L22, 1161 genes were affected. Notably, among the genes affected by H1-GFP and T-L22, over 1000 genes were commonly affected by both proteins (Figure 6A and Supplementary Table 1-2), and nearly 70% of these commonly affected genes (690/1007 genes) were down-regulated (Figure 6A, B), supporting an overlapping role of ribosomal proteins and histone H1 in transcriptional repression.

To be sure that the suppression caused by histone H1 and ribosomal proteins is due to direct binding of the affected genes, we next performed ChIP experiments to detect the presence of these proteins on chromatin using formaldehyde pre-fixed wild type Kc cells and specific antibodies against histone H1 and ribosomal protein L22. Among nine randomly selected genes whose transcription was

affected at least 9-fold in cells overexpressing H1-GFP and T-L22, seven genes showed the presence of both histone H1 and L22 on their chromatin (Figure 6C), supporting a direct role for H1 and L22 in their transcriptional regulation. The other two showed the presence of H1, but with less, or no, binding of L22, implying that the altered transcription of these genes may be due to secondary effects.

The presence of histone H1 and nuclear ribosomal proteins on chromatin is coupled to the transcriptional status of endogenous genes

We next examined the role of H1 and ribosomal proteins in transcriptional repression of endogenous genes in wild type cells. Upon heat shock, transcription of heat-shock-inducible genes increases at least 100-fold (Lis and Wu, 1993), and histone H1 is known to be released from the chromatin of these genes immediately after their activation (Karpov et al., 1984). Using cell extract from heat-shocked and non-heat-shocked T-L22 cells, and antibodies against histone H1 (H1N) and pan-acetylated histone H4 (H4Ac), as well as Xpress antibodies and anti-HA antibodies (detecting T-L22), we performed ChIP analysis to detect any change in H1 and ribosomal protein L22 binding on local chromatin before and after heat shock (Figure 7A). The efficiency of the heat shock treatment was monitored by RT-PCR, which confirmed the dramatic increase in the transcription of the heat-shock genes (data not shown). However, heat shock had no effect on the global levels of tagged L22, H1, or acetylated histone H4 (data not shown). To detect changes in H1 and L22 binding on chromatin, we performed PCR analysis using ChIP DNA and primers covering the transcribed regions of two heat shock genes, *Hsp70Aa* (*CG31366*) and *Hsp70Ab* (*CG18743*), and two non-heat shock genes, *CG8190* and *CG8066*. Both H1 and ribosomal protein T-L22 were associated with chromatin of the *Hsp70* genes before heat shock treatment; however, binding decreased at least 10-fold following heat shock treatment (Figure 7A). Histone H4 acetylation in the heat shock genes increased more than 3-fold after heat shock, presumably because of the loss of histone H1 and/or T-L22, which would result in a relatively “open” chromatin

structure. The non-heat shock genes *CG8190* and *CG8066* showed no changes in L22 or histone H1 enrichment, or in histone H4 acetylation, before and after heat-shock treatment (Figure 7A).

The relationship between histone H1, L22 and transcriptional activation of the endogenous heat shock genes was also verified using specific antibodies (L22C) against endogenous ribosomal protein L22 instead of the anti-HA tag antibody. The results show that, as in cells expressing T-L22, L22 is associated with the chromatin of heat shock genes before their activation, but not after transcription is initiated (Figure 7B). Overall, the above results support a role of histone H1 and ribosomal proteins in transcriptional repression of endogenous genes.

Nuclear ribosomal protein L22, but not H1, is associated with newly synthesized RNA transcripts

A previous study showed an association of functional ribosomes with newly synthesized RNA on Drosophila polytene chromosomes isolated from salivery gland cells (Brogna et al., 2002). We wondered whether such an association also occurs in diploid Kc cells, which are derived from *Drosophila melanogaster* embryos. Using cells stably expressing T-L22, we analyzed the presence of ribosomal protein T-L22 and H1 on transcripts of the heat shock genes *Hsp70Aa, Hsp70Ab*, and *Hsp23*. The non-heat shock gene *CG8066* was used as a control. RNA-ChIP analysis show that T-L22 becomes associated with *Hsp70* and *Hsp23* after heat shock, (Figure 7C), confirming association of this ribosomal protein with newly synthesized RNA transcripts. However, histone H1 was not found with any of the RNA transcripts tested, either before or after heat shock (Figure 7C). This result confirms the presence of ribosomal proteins on newly synthesized RNA. On the other hand, the above result also implies that the interaction between histone H1 and ribosomal proteins is chromatin-based, but does not occur through RNA transcripts.

Discussion

The work in this study provides evidence that ribosomal proteins are present within the complexes of chromatin component- histone H1. Several experimental approaches were used to corroborate this finding. Pre-treatment of nuclear extract with EB or DNAse I prior to IP experiments did not affect the interaction between H1 and ribosomal proteins (Figure 1C, D, and data not shown), arguing against a DNA-mediated interaction. RNA-ChIP experiments further ruled out the possibility that the interaction might occur through RNA transcripts because nuclear RNAs associated only with ribosomal proteins, but not histone H1. We have also observed that a mutated *Drosophila* H1 in which the DNA binding sites within the globular domain of H1 are mutated simultaneously, is largely shifted into the nucleolus (J-Q Ni and F-L Sun, unpublished data), further supporting an *in vivo* interaction. Overall, our results suggest that ribosomal proteins are specifically associated with histone H1 in the cell nucleus.

Ribosomal proteins seem also to be directly associated with chromatin; histone H1 and ribosomal proteins co-localize at regions stained with DAPI -- often indicative of chromatin domains with condensed structure. Notably, the interaction is highly dynamic, and in many cases only a partial overlap was observed (Figure 3C). We further confirmed the chromatin association of ribosomal proteins using a ChIP assay; genes bound by H1 were found also to be bound by ribosomal proteins (Figure 4A). The association of ribosomal proteins and chromatin clearly depends on histone H1 because depletion of H1 caused loss of ribosomal proteins from chromatin (Figure 4B), while partial depletion of ribosomal proteins seemed not to affect the presence of H1 on chromatin dramatically (Figure 4 and data not shown).

The interaction of H1 and ribosomal proteins on chromatin occurred in the absence of transcription. After initiation of transcription of endogenous heat-shock genes, ribosomal proteins become associated with newly synthesized RNA in the cell nucleus, but histone H1 did not (Figure 7C). This result is consistent with a previous report of the presence of ribosomal proteins together with RNA on *Drosophila* polytene chromosomes (Brogna et al., 2002); on the

other hand, it supports the hypothesis that the machineries of gene expression, encompassing chromatin organization, transcription, mRNA transport, and protein synthesis, are likely to be highly coordinated (Maniatis and Reed, 2002; Jensen et al., 2003).

The above observation also leads to a further question: what is the biological function of the interaction between histone H1 and ribosomal complexes on chromatin? As seen in immuno-fluorescent staining experiments, in some cases ribosomal proteins fully overlap with H1 at regions of highly condensed chromatin (Figure 3C). This result implies that, similar to histone H1, ribosomal proteins on chromatin may function in transcriptional repression. Indeed, overexpression of either H1 or L22 caused de-regulation of more than a thousand genes. Remarkably, nearly 90% of the genes affected by ribosomal proteins were the same as those affected by histone H1 (Figure 6A, B), supporting an overlapping role of histone H1 and ribosomal proteins in transcriptional gene regulation. Nearly 70% of the commonly affected genes were suppressed by overexpression of H1 or L22. The repressive role of these proteins in transcription may be mediated through controlling changes in chromatin structure since overexpression of histone H1 caused a several-fold reduction in histone modifications of active chromatin at the global level. Overexpression of ribosomal protein L22 seemed to affect specific histone modifications to a much lesser degree (Figure 5B, C), which possibly implies that ribosomal proteins may suppress gene transcription through promoting or stabilizing H1-associated higher-order chromatin, or other pathways, without dramatically affecting histone modifications. On the other hand, this result may simply be due to the lower level of overexpression of ribosomal proteins in Kc cells since overexpression of ribosomal proteins to higher levels seemed to be toxic (data not shown).

The association of ribosomal proteins with histone H1 in the cell nucleus may be part of the ribosome complex assembly/maturation process, for example, to mediate the further packaging or modifying of ribosome complexes before they are imported into nucleolus or exported to the cytoplasm for protein synthesis. This is also supported by our observation that mutated histone H1 can be

"brought" into the nucleolus when the mutated histone H1 fails to bind chromatin (J-Q Ni and F-L Sun, unpublished data), although the exact nature of the dynamic interaction of H1 and ribosomal proteins *in vivo* requires further study. Alternatively, ribosomal proteins on chromatin may have a "scanning" function, acting in concert with hnRNPs to monitor the quality of newly synthesized RNA during transcription, or they may be involved in nonsense-mediated mRNA decay (NMD) (Maquat, 1995; Hilleren and Parker, 1999; Muhlemann et al., 2001; Wilusz et al., 2001) as suggested previously (Wilkinson and Shyu, 2002; Brogna et al., 2002; Iborra et al., 2004). Other possibilities, such as ribosomal proteins on chromatin functioning as a reserve "ribosomal protein pool" in the nucleus that can be delivered immediately onto newly synthesized transcripts before transport to the cytoplasm for protein synthesis, should also not be excluded.

In summary, we demonstrate evidence that ribosomal proteins in *Drosophila melanogaster* are also components of histone H1 complex, and are directly associated with chromatin in the cell nucleus. We further show that ribosomal proteins and histone H1 are both repressors of transcription *in vivo*, and target the same set of genes within the genome. The study therefore supports a role for ribosomal proteins in chromatin and transcriptional gene regulation. It remains to be seen whether this function of ribosomal proteins is also conserved in other higher eukaryotes.

Experimental Procedures

Constructs

Vectors for expression of L7 and L22 in Kc cells were constructed by subcloning the RT-PCR-amplified coding regions of *L7* and *L22,* fused with an HA tag, into pIB/V5-His-TOPO (Invitrogen). pIB/V5-His-TOPO constructs expressing GFP were constructed by subcloning the GFP coding sequence from pcDNA3.1/NT-GFP-TOPO (Invitrogen). The pIB/V5-His-TOPO construct expressing H1-GFP was constructed by fusing the GFP-tag with the *D. melanogaster* H1 coding sequence, and then subcloning into the vector.

Preparation of stable Kc cell lines

All Kc cells were grown in a 25°C incubator. Transfection of constructs into Kc cells was performed according to a standard protocol (Invitrogen) with some modifications. Briefly, 1×10^6 Kc cells [in 2 ml Schneider's *Drosophila* Medium (Gibco), with 10% fetal calf serum and 200 mM glutamine], were first seeded into a six-well plate for 1 h at 25°C. Purified plasmid DNA (5 μg) was then diluted into 100 μl of serum-free medium (Gibco), and mixed with 100 μl of serum-free medium containing 8 μl cellfectin (Invitrogen). The mixture was incubated at room temperature for 40 min. After removing the medium from the six-well plate, the cells were washed once with 2 ml serum-free medium, and then with 0.8 ml of serum-free medium plus the 200 μl of medium containing plasmid DNA and cellfectin. The remaining procedures followed the standard Invitrogen protocol (available online at http://www.invitrogen.com/transfection/celltypes).

RNAi in Kc cells

The coding sequence of *Drosophila* histone H1 was first amplified with primers containing the gene sequence plus the sequence of a T7 promoter. Single-stranded RNA (ssRNA) was then produced using a MEGAscript T7 kit (Ambion). To prepare dsRNA, the ssRNAs were incubated in annealing buffer (100 mM potassium acetate, 30 mM HEPES-KOH at pH 7.4, 2 mM magnesium acetate) at

a concentration of 10 µg/µl at 65ºC for 30 min and 95ºC for 5 min, and the tube was then immediately placed into a glass beaker filled with water at 75ºC, and allowed to cool slowly to room temperature. The products were then aliquoted at 10 µl/tube and stored in a –80ºC freezer.

RNAi was performed according to the protocol of Dixon (http://dixonlab.biochem.med.umich.edu). For H1 RNAi, 1×10^6 Kc cells cultured at 25ºC were suspended in 1 ml pre-warmed (25ºC) serum-free medium, and seeded into one well of a six-well plate. H1 dsRNA (45 µg) was then added to each well and gently mixed. After 1 h incubation at 25ºC, a further 2 ml of complete Kc cell culture medium was added to each well. The medium was removed after 2 days of incubation in a 25ºC incubator, and the cells were washed once with serum-free medium before adding another 1 ml of fresh serum-free medium containing 45 µg H1 dsRNA. Subsequent procedures were as described above, and the RNAi treatment was performed for the third time on day 4. Cells were harvested on day 8.5 for further analysis.

Antibodies

Drosophila histone H1 and L22 peptide sequences were: H1 N terminus (CAGTKAKKSATPSHP; H1N), H1 C terminus (CATAKKPKAKTTAAKK; H1C), L22 N terminus (MAPTAKTNKGDTKTA; L22N), L22 C terminus (YFRISSNDDEDDDAE; L22C). Injection of rabbits with these peptides and antibody purification were performed by Eurogentec (www.eurogentec.com). Anti-V5 and anti-Xpress monoclonal antibodies were purchased from Invitrogen. Anti-H4Ac, anti-H3K4met (polyclonal antibodies), anti-H3K9met, anti-H4K8Ac and anti-H4K12Ac were purchased from Upstate. Anti-H3, anti-GFP, anti-fibrillarin, anti-H3K4met and anti-HA monoclonal antibodies (HA-m) were all purchased from Abcam. Anti-HA polyclonal antibodies (HA-p) were purchased from Sigma.

Western blots

Kc cells were lysed in NP-40/300 mM NaCl buffer (1% NP-40, 300 mM NaCl, 50 mM Tris, pH7.8). Bacteria were lysed in denaturing buffer (8 M urea, 100 mM NaH_2PO_4, 10 mM Tris, pH 8.0). The protein concentration of the supernatant was measured using Coomassie Plus^{TM} Protein Assay Reagent (Pierce). For SDS-PAGE, 20 μg/lane for Kc cell extracts, and 30 μg/lane for bacterial extracts were loaded. For modification checking, cells were lysed in HEMGN buffer (25 mM Hepes, pH7.6, 0.1 mM EDTA, 12.5 mM $MgCl_2$, 10% Glycerol, 0.1% NP-40, 1 mM DTT, 0.3 M KCl), mixed with Laemmli buffer (Bio-Rad) and boiled for 5 min; 2 μg was used for loading. After electrophoresis, proteins were transferred from the gel onto Hybond-P PVDF membrane (Amersham), then hybridized with primary antibodies at the dilutions indicated: H1N (1:10,000), H1C (1:10,000), anti-Xpress (1:5,000), anti-V5 (1:10,000), L22N (1:100), L22C (1:100), H3K4met polyclonal antibodies (1:3,000), H4K8Ac (1:3,000), H4K12Ac (1:2,000), H3K9met (1:2,000) and anti-H4Ac (1:5000). The secondary antibodies used were peroxidase-conjugated affinipure goat anti-rabbit IgG (H+L) (1:10,000), and peroxidase-conjugated affinipure goat anti-mouse IgG (H+L) (1:10,000). The ECL detection system (Amersham) was used to detect signals on the blots. Loading on the gel was monitored by staining the same membrane with Coomassie blue (Coomassie Plus^{TM} Protein Assay Reagent, Pierce).

Immunofluorescence staining

Immunofluorescence staining was performed according to a standard procedure (Harlow and Lane, 1999). Kc cells (100 μl; 6×10^6/ml) were seeded on a polylysine slide for 10 min at room temperature, and fixed with 4% formaldehyde for 12 min. The primary antibodies used were: anti-H1C (1:500), anti-H1N (1:500), anti-L22N (1:10), anti-L22C (1:10), anti-V5 (1:500), anti-H3K4met polyclonal (1:500), anti-H4K8Ac (1:300), anti-H3K4met monoclonal (1:200), and anti-fibrillarin (1:400). The DNA staining marker DAPI (Sigma) was used at a concerntration of 1×10^{-4} μg/μl. Secondary antibodies coupled to FITC (green, 1:100 dilution) and anti-rabbit Texas red (red, 1:400 dilution) were purchased

from Milan. All images were taken under a deconvolution microscope (Olympus, ×71), and processed using Adobe Photoshop software.

Purification of H1 complex

Nuclear extracts from Kc cells used for IP were prepared following a standard protocol (for details see Current Protocols In Pharmacology). Kc cells (4×10^8) were collected and washed once with 1×PBS, then with 10 ml hypotonic buffer (10 mM HEPES, pH 7.9, 1.5 mM $MgCl_2$, 10 mM KCl, 0.5 mM DTT, protease inhibitors); the pellet was then suspended in 5 ml hypotonic buffer, placed for 10 min on ice, homogenized and pelleted by centrifugation (3600 g, 15 min at 4°C). The supernatant (cytoplasmic extract) was collected. The pellet (nuclei) was then further purified by resuspension in 5 ml buffer A1 (60 mM KCl, 15 mM NaCl, 15 mM Tris pH 7.8, 1 mM EDTA, 0.1 mM EGTA, 0.5 mM spermidine, 0.15 mM spermine, 0.5 mM DTT, 0.5% Triton X-100, 0.2 mM PMSF), and then gently layered onto 5 ml buffer A2 (buffer A1 + 0.3 M sucrose). Cell debris was removed by centrifugation (9000 g, 15 min at 4°C). The nuclear pellet was washed with 5 ml buffer A2 (60 mM KCl, 15 mM NaCl, 15 mM Tris pH 7.8, 0.5 mM spermidine, 0.15 mM spermine, 0.5 mM DTT, 0.5% Triton X-100, 0.2 mM PMSF) to remove EDTA and EGTA. The nuclei were then resuspended in 3 ml NP-40/300 mM NaCl buffer with 300 µg/ml ethidium bromide, vortexed three times, and freeze/thawed on dry ice; this procedure was repeated a further three times. The lysate was centrifuged at 19,000 g for 15 min at 4ºC. The supernatant was then pre-cleared using protein-A-sepharose beads (Amersham) at 4ºC (50 µl beads/ml lysis buffer). IP experiments were performed with anti-H1C (10 µg), 35 µl protein A beads, and 600 µl nuclear extract (1 µg/µl). As a control, 10 µg anti-H1C antibodies were pre-blocked with 1 µg of the peptide used to derive the H1C antibodies. IP was performed in NP-40/300 mM NaCl buffer (see above) with overnight incubation at 4ºC, followed by washing with NP-40 buffer for 6× 8 min at 4ºC. The pellets were boiled in Laemmli buffer (Bio-Rad) and loaded onto a 15% SDS PAGE gel. The gel was stained with Gelcode Blue Stain Reagent (Pierce) and photographed.

For digestion of the immunoprecipitate with RNase A and DNase I, the pellet was washed with NP-40/300 mM buffer five times, then resuspended in RNase A buffer and digested with 100 µg/ml RNase A for 30 min at 25°C. After removing the RNase A buffer by centrifugation, DNase I buffer (10mM Tris, pH7.5, 2.5mM $MgCl_2$, 0.5mM $CaCl_2$) and DNase I (100 U/ml) were added and incubated for 30 min at 25°C. DNase I buffer was removed and the pellet washed once with wash buffer before being suspended in Laemmli buffer, boiled and loaded onto a 15% PAGE gel. The gel was stained and photographed.

Sucrose gradient and polysome analysis

Nuclear extract was prepared using 2×10^8 T-L22 cells. Cells were washed once with 1×PBS and then with 10 ml hypotonic buffer. The pellet was resuspended in 2 ml hypotonic buffer (HB), incubated for 10 min on ice, homogenized and then pelleted by centrifugation (3600 g, 15 min at 4°C). The supernatant (cytoplasmic extraction) was collected. The pellet was then resuspended and homogenized in buffer HB and gently loaded onto buffer HB+0.3 M sucrose. The nuclei were purified by centrifugation (9000 g, 15 min at 4°C), washed once with buffer HB, and resuspended in 1 ml buffer B (15 mM HEPES pH 7.6, 110 mM KCl, 3 mM $MgCl_2$, 0.1 mM EDTA, 1 mM dithiothreitol). Ammonium sulfate (4 M, pH 7.6) was then added to a final concentration of 0.36 M. The lysis of nuclei was performed by gently vortexing the tube for 1 h at 4°C (Topol et al., 1985). The extract was centrifuged at 22,000 g for 30 min at 4°C. The supernatant was loaded into Spectra/Por®CE (Cellulose Ester) Float A Lyzer™ in dialysis buffer (20 mM Tris-HCl (pH 7.4), 80 mM NaCl, 5 mM $MgCl_2$) for 10 h at 4°C. Dialyzed nuclear extract (450 µl, 2 µg/µl) was loaded onto a 17–51% linear sucrose density gradient with 20 mM Tris-HCl (pH 7.4), 80 mM NaCl, and 5 mM $MgCl_2$. The lysates were centrifuged at 36,000 rpm (SW41 rotor, Beckman) for 6 h at 4°C. Thirty fractions (400 µl/tube) were then collected from the top to the bottom (numbered from 1 to 30) using a gradient collector (FRAC-100, Pharmacia) with continuous monitoring by a UV/Vis detector (UA-6, IG instrument) measuring absorbance at A_{254}.

Sedimentation of cytoplasmic extracts from T-L22 was performed as described by Pelczar and Filipowicz (1998). We used 2×10^8 cells, which were washed once with 1×PBS, then with 10 ml hypotonic buffer; the pellet was resuspended with 2 ml hypotonic buffer, incubated on ice for 10 min, then homogenized and pelleted by centrifugation (3600 g, 15 min for 4°C). The supernatant was collected, 450 µl (4 µg/µl) loaded onto a 17–51% linear sucrose density gradient prepared in 20 mM Tris-HCl (pH 7.4), 80 mM NaCl, 5 mM $MgCl_2$. The lysates were centrifuged at 4°C for 6 h at 36,000 rpm in an SW41 rotor (Beckman). Thirty fractions (400 µl/tube) were collected as described above. A 40-µl sample from each of the selected fractions was boiled in loading buffer and run on a 15% SDS PAGE gel.

Interaction between histone H1 and cytoplasmic ribosomes

For purification of nuclear histone H1, 1×10^9 Kc cells were washed once with 1×PBS, then suspended in 20 ml low-salt buffer (10 mM HEPES pH 7.9, 1.5 mM $MgCl_2$, 10 mM KCl, 0.5 mM DTT, 0.5% Triton X-100, protease inhibitors), placed for 10 min on ice, homogenized and pelleted by centrifugation (3600 g, 15 min for 4°C). The pellet was washed twice with wash buffer (10 mM Tris, 1 mM EDTA, 0.5 mM EGTA, 0.2 M NaCl, protease inhibitors) and then resuspended in 2 ml extract buffer (50 mM Tris, 50 mM EDTA, pH 7.4). Thirty microliters of 98% H_2SO_4 was added, the mixture incubated for 1 h on ice, then spun at 19,000 g for 15min at 4°C). The supernatant was precipitated with acetone and dissolved in NP-40 buffer, mixed with Laemmli buffer and then loaded onto a 15% SDS-PAGE gel, electrophoresed at 150 V for 100 min and stained with $CuCl_2$ (0.3 M); protein bands were isolated and eluted from the gel using an Electro-Eluter (Model 422, Bio-Rad). Purified proteins were precipitated using methanol-chloroform (www.1s.huji.ac.il/~purification/protocols/precipitation.html) and then dissolved in standard NP-40 buffer (1% NP-40, 150 mM NaCl, 50 mM Tris, pH 7.8), and stored at –80°C.

The interaction between H1 and ribosomes in cytoplasm extracted from cells expressing T-L22 was determined as follows. Cytoplasmic extract obtained as described above was adjusted to a final concentration of 150 mM NaCl with 3 M

NaCl stock solution, and NP-40 was then added to a final concentration of 1%. NP-40 buffer (80 µl) containing 30 µg purified histone H1 or 80 µl NP-40 buffer control was then added separately to 400 µl of cytoplasmic extract. The mixes were rotated for 2 h at 4°C, after which 450 µl (4 µg/µl protein) of extract was used for sucrose density gradient centrifugation as described above. A 30µl sample from each selected fraction was used for western analysis.

ChIP

ChIP analysis followed an Upstate protocol (www.upstate.com) with some modifications. Approximately 2×10^8 Kc cells were fixed in 1% formaldehyde, and the reaction terminated by adding 2.5 M glycine to a final concerntration of 0.125 M. The Kc cells were washed once with 5 ml hypotonic buffer, and then resuspended with 5 ml hypotonic buffer, incubated in ice for 10 min, homogenized, and pelleted by centrifugation. The nuclei were purified as described above and were then resuspended in 3 ml sonication buffer (50 mM Tris, pH 8.0, 10 mM EDTA, 1% SDS, protease inhibitors). Subsequent steps were as described in the Upstate ChIP protocol. The size of the chromatin fragments after sonication (Branson, sonifier 250, setting at 0-1) was checked in an agarose gel using DNA purified from the chromatin fractions, digested by proteinase K (100 µg/ml) at 45°C for 2 h, followed by a phenol/chloroform extraction. In our experiments, we used fractions with a chromatin size range between 0.3 and 0.8 kb. Chromatin fractions were diluted 10 times then 100 µl aliquots were used in each ChIP reaction Five micrograms of each of the following antibodies were used in IP reactions: polyclonal anti-GFP (mock control), polyclonal anti-H1N, polyclonal anti-H3, polyclonal anti-HA, monoclonal anti-HA, and monoclonal anti-Xpress (mock control). ChIP DNA was precipitated using 2 µl of color precipitant and ethanol. The pellet was dissolved in 80 µl 1×TE; 2 µl was used in each 50-µl PCR reaction. The number of cycles used for amplification was between 30 and 35, depending on the amplification efficiency of the primers of the different genes relative to input DNA. From a total of 50 µl PCR products, 6 µl was loaded onto a 2% agarose gel, stained with EB and

photographed. Signals were quantified using a Molecular Dynamics Phosphorimager and data analyzed using ImageQuant version 5.2 software. Sequences of primers used to amplify ChIP DNA are given in Supplementary Material.

For the heat shock experiments in ChIP and RNA-ChIP assays (see below), 2×10^8 Kc cells in two T_{75} flasks were incubated in a 37°C water bath for 1 h and then immediately fixed with 1% formaldehyde. Subsequent processing was as described above.

RNA-ChIP

RNA-ChIP was performed as described for the ChIP procedures, but with the addition of 0.5 U/μl RNASIN in all the buffers used. Nuclei from T-L22 Kc cells were first isolated from 1% formaldehyde-fixed cells, and used for chromatin fragmentation. Fragment size was between 0.3 and 0.8 kb. The amount of chromatin extract and antibodies used in each reaction was the same as in ChIP assays. After IP, washing, and elution, the precipitated RNA/DNA pellets were resuspended in 70 μl H_2O (nuclease-free) with1 μl of 40 U/μl RNASIN, 5 μl of 1 M Tris-HCl (RNase-free), pH 7.5, 20 μl of 50 mM (RNase-free) $MgCl_2$, and 4 μl of 10 U/μl DNase I (RNase-free). The mixture was incubated at 37°C for 30 min and extracted once with phenol/choloroform (5:1). RNA was precipitated with ethanol and dissolved in 30 μl nuclease-free water. Twenty-seven microliters of the RNA was used for a 60-μl cDNA synthesis reaction; 2 μl from a total of 60 μl of cDNA reaction was used in each RT-PCR reaction. The PCR reactions were performed for between 30-32 cycles. Of 50 μl products, 6 μl was loaded onto a 2% agarose gel, stained with EB, and photographed. The primer sequences used are given in Supplementary Material.

RT-PCR

Total RNA from 4×10^6 non-heat-shocked and heat-shocked Kc cells was isolated using Trizol reagent (Invitrogen). Total RNA was then digested with DNase I, phenol/chloroform extracted, and precipitated with ethanol. Total RNA (5 μg) was

used to synthesize cDNA in a volume of 20 μl (Superscript II Reverse Transcriptase, Invitrogen). For each 50-μl PCR reaction, 2 μl cDNA was used for 20–25 cycles. PCR products (6 μl) were loaded onto a 2% agarose gel, stained with EB and photographed. The sequences of primers used for RT-PCR are given in Supplementary Material.

Microarray analysis

Extraction of total RNA was performed following a standard protocol (Current protocols library). Total RNA was isolated from two or three independent populations of Kc cells which express GFP, H1-GFP and T-L22. In brief, cells were resuspended in Trizol reagent by pipetting, and were extracted with phenol-chloroform. The precipitated RNA was washed, and then dissolved in RNase-free water. Five micrograms of total RNA from each experimental sample were reverse-transcribed using the SuperScript Choice cDNA synthesis kit from Stratagene. One microgram of double-stranded cDNA was *in vitro*-transcribed using the Affymetrix IVT kit and labeled by the incorporation of biotinylated-UTP. Fifteen micrograms of cRNA were then fragmented and hybridized to Affymetrix DG GeneChips as per the manufacturer's instructions (Affymetrix, Santa Clara CA, USA).

Supplementary Data

Supplemental Data including two figures, two tables and primer sequences are available online with this article.

Acknowledgements

We thank in particular Witold Filipowicz and Barbara Hohn who provided many useful suggestions throughout this study. We would like to thank Dr. Ramesh Pillai for his technical help, and Dr. Edward Oakeley for his assistance with the micro array analysis. This work was supported by the Novartis Research Foundation.

References

Allen, W. (1978). Does protein synthesis occur within the nucleus? Unambiguous evidence is still needed. Trends Biol. Sci. ***3***, pp. N225–N228.

Baker, K.E. and Parker, R. (2004). Nonsense-mediated mRNA decay: terminating erroneous gene expression. Curr. Opin. Cell Biol. *16*, 293-299.

Barra, J.L., Rhounim, L., Rossignol, J.L., and Faugeron, G. (2000). Histone H1 is dispensable for methylation-associated gene silencing in *Ascobolus immersus* and essential for long life span. Mol. Cell Biol. *20*, 61-69.

Brogna, S., Sato, T.A., and Rosbash, M. (2002). Ribosome components are associated with sites of transcription. Mol Cell. *10*, 93-104.

Bustin, M. (2005). The dynamics of histone H1 function in chromatin. Mol Cell. *17*, 617-620.

Dostie, J., Lejbkowicz, F. and Sonenberg, N. (2000). Nuclear eukaryotic initiation factor 4E (eIF4E) colocalizes with splicing factors in speckles. J. Cell Biol. *148*, 239-247.

Downs, J.A., Kosmidou, E., Morgan, A., and Jackson, S.P. (2003). Suppression of homologous recombination by the *Saccharomyces cerevisiae* linker histone. Mol Cell *11*, 1685-1692.

Du, Y. C., and Stillman, B. (2002). Yph1p, an ORC-interacting protein: potential links between cell proliferation control, DNA replication, and ribosome biogenesis. Cell *109*, 835-848.

Fan, Y., Nikitina, T., Morin-Kensicki, E.M., Zhao, J., Magnuson, T.R., Woodcock, C.L., and Skoultchi, A.I. (2003). H1 linker histones are essential for mouse

development and affect nucleosome spacing in vivo. Mol Cell Biol. *23*, 4559-4572.

Fromont-Racine, M., Senger, B., Saveanu, C., and Fasiolo, F. (2003). Ribosome assembly in eukaryotes. Gene. *313*, 17-42.

Gadal, O., Strauss, D., Petfalski, E., Gleizes, P.E., Gas, N., Tollervey, D., and Hurt, E. (2002). Rlp7p is associated with 60S preribosomes, restricted to the granular component of the nucleolus, and required for pre-rRNA processing. J. Cell Biol. 157, 941-951.

Goild, J. (1978). Does protein synthesis occur within the nucleus? Good evidence that it does. Trends Biol. Sci*. 3*, pp. N225–N228.

Goldstein, L. (1970). On the Question of Protein Synthesis by Cell Nuclei, Advances in Cell Biology Vol. 1, Appleton-Century-Crofts, New York pp. 187–210.

Gunjan, A., Sittman, D.B., and Brown, D.T. (2001). Core histone acetylation is regulated by linker histone stoichiometry *in vivo*. J. Biol. Chem. *276*, 3635-3640.

Harlow, E.D., and D. Lane. (1999). Using antibodies. Staining Cells (CRC Press), pp.103-149.

Herrera, J. E., West, K. L., Schiltz, R.L., Nakatani, Y., and Bustin, M. (2000). Histone H1 is a specific repressor of core histone acetylation in chromatin. Mol. Cell. Biol. *20*, 523-529.

Hellauer, K., Sirard, E., and Turcotte, B. (2001). Decreased expression of specific genes in yeast cells lacking histone H1. J. Biol. Chem**.** *276*, 13587-13592.

Hill, C.S., Rimmer, J.M., Green, B.N., Finch, J.T., and Thomas, J.O. (1991). Histone-DNA interactions and their modulation by phosphorylation of -Ser-Pro-X-Lys/Arg- motifs. EMBO J. *10*, 1939-1948.

Hilleren, P., and Parker, R. (1999). Mechanisms of mRNA surveillance in eukaryotes. Annu Rev Genet. *33*, 229-260.

Iborra, F.J., Jackson, D.A., and Cook, P.R. (2001). Coupled transcription and translation within nuclei of mammalian cells. Science. *293*, 1139-1142.

Jedrusik, M.A., and Schulze, E. (2003). Telomeric position effect variegation in Saccharomyces cerevisiae by Caenorhabditis elegans linker histones suggests a mechanistic connection between germ line and telomeric silencing. Mol. Cell. Biol*. 23*, 3681-3691.

Jensen, T.H., Dower, K., Libri, D., and Rosbash, M. (2003). Early formation of mRNP: license for export or quality control? Mol Cell. *11*, 1129-1138.

Juan, L.J., Utley, R.T., Vignali, M., Bohm, L., and Workman, J.L. (1997). H1-mediated repression of transcription factor binding to a stably positioned nucleosome. J. Biol. Chem*. 272*, 3635-3640.

Karpov, V.L., Preobrazhenskaya, O.V., and Mirzabekov, A.D. (1984). Chromatin structure of hsp70 genes, activated by heat shock: selective removal of histones from the coding region and their absence from the 5' region. Cell *36*, 423-431.

Konishi, A., Shimizu, S., Hirota, J., Takao, T., Fan, Y., Matsuoka, Y., Zhang, L., Yoneda, Y., Fujii, Y., Skoultchi, A.I., and Tsujimoto, Y. (2003). Involvement of histone H1.2 in apoptosis induced by DNA double-strand breaks. Cell *114*, 673-688.

Krecic, A. M., and Swanson, M. S.. (1999). hnRNP complexes: composition, structure, and function. Curr. Opin. Cell Biol. *11*, 363-371.

Kressler, D., Linder, P., and De La Cruz, J. (1999). Protein trans-acting factors involved in ribosome biogenesis in Saccharomyces cerevisiae. Mol. Cell. Biol. *19*, 7897-912.

Laybourn, P.J., and Kadonaga, J.T. (1991). Role of nucleosomal cores and histone H1 in regulation of transcription by RNA polymerase II. Science *254*, 238-245.

Lejbkowicz, F., Goyer, C., Darveau, A., Neron, S., Lemieux, R., and Sonenberg, N. (1992). A fraction of the mRNA 5' cap-binding protein, eukaryotic initiation factor 4E, localizes to the nucleus. Proc. Natl. Acad. Sci. U S A *89*, 9612-9616.

Lis, J., and Wu, C. (1993). Protein traffic on the heat shock promoter: parking, stalling, and trucking along. Cell *74*, 1-4.

Lykke-Andersen, J. (2001). mRNA quality control: Marking the message for life or death. Curr. Biol. *11*, R88-91.

Luger, K. (2003). Structure and dynamic behavior of nucleosomes. Curr. Opin. Genet. Dev. *13*, 127-35.

Lund, E., and Dahlberg, J.E. (1998). Proofreading and aminoacylation of tRNAs before export from the nucleus. Science 282, 2082-2085.

Maniatis, T., and Reed, R. (2002). An extensive network of coupling among gene expression machines. Nature *416*, 499-506.

Matunis, E. L., Matunis, M. J., and Dreyfuss, G. (1993). Association of individual hnRNP proteins and snRNPs with nascent transcripts. J. Cell Biol. *121*, 219-228.

Maquat, L. E. (1995). When cells stop making sense: effects of nonsense codons on RNA metabolism in vertebrate cells. RNA *1*, 453-465.

Milkereit, P., Gadal, O., Podtelejnikov, A., Trumtel, S., Gas, N., Petfalski, E., Tollervey, D., Mann, M., Hurt, E., and Tschochner, H. (2001). Maturation and intranuclear transport of pre-ribosomes requires Noc proteins. Cell *105*, 499-509.

Muhlemann, O., Mock-Casagrande, C.S., Li, J., Wang, S., Custodio, N., Carmo-Fonseca, M., Wilkinson, M.F., and Moore, M.J. (2001). Precursor RNAs harboring nonsense codons accumulate near the site of transcription. Mol. Cell *8*, 33-43.

Pelczar, P., and Filipowicz, W. (1998). The host gene for intronic U17 small nucleolar RNAs in mammals has no protein-coding potential and is a member of the 5'-terminal oligopyrimidine gene family. Mol. Cell. Biol. *18*, 4509-4518.

Pennings, S., Meersseman, G., and Bradbury, E.M. (1994). Linker histones H1 and H5 prevent the mobility of positioned nucleosomes. Proc. Natl. Acad. Sci. U S A *91*, 10275-1029.

Polach, K.J., and Widom, J. (1995). Mechanism of protein access to specific DNA sequences in chromatin: a dynamic equilibrium model for gene regulation. J. Mol. Biol. *254*, 130-149.

Ringborg, U., Daneholt, B., Edstrom, J.E., Egyhazi, E., and Rydlander, L. (1970). Evidence for transport of preribosomal RNA from the nucleolus to the chromosomes in Chironomus tentans salivary gland cells. J. Mol. Biol. *51*, 679-686.

Sanders, J., Brandsma, M., Janssen, G.M., Dijk, J., and Moller, W. (1996). Immunofluorescence studies of human fibroblasts demonstrate the presence of the complex of elongation factor-1 beta gamma delta in the endoplasmic reticulum. J. Cell Sci. *109*, 1113-1117.

Schaper, S., Fromont-Racine, M., Linder, P., de la Cruz, J., Namane, A., and Yaniv, M. (2001). A yeast homolog of chromatin assembly factor 1 is involved in early ribosome assembly. Curr. Biol. *11*, 1885-1890.

Schell T, Kulozik, A.E., and Hentze, M.W. (2002). Integration of splicing, transport and translation to achieve mRNA quality control by the nonsense-mediated decay pathway. Genome Biol. 3:REVIEWS1006.

Shen, X., and Gorovsky, M.A. (1996). Linker histone H1 regulates specific gene expression but not global transcription in vivo. Cell *86*, 475-483.

Stage-Zimmermann, T., Schmidt, U., and Silver, P.A. (2000). Factors affecting nuclear export of the 60S ribosomal subunit in vivo. Mol. Biol. Cell *11*, 3777-3789.

Steinbach, O.C., Wolffe, A.P., and Rupp, R.A. (1997). Somatic linker histones cause loss of mesodermal competence in Xenopus. Nature *389*, 395-399.

Thomas, J.O. (1999). Histone H1: location and role. Curr. Opin. Cell Biol. *11*, 312-317.

Topol, J., Ruden, D.M., and Parker, C.S. (1985). Sequences required for in vitro transcriptional activation of a Drosophila hsp 70 gene. Cell *42*, 527-537.

Tsay, Y.F., Shankweiler, G., Lake, J., and Woolford, J.L. Jr. (1994). Localization of Saccharomyces cerevisiae ribosomal protein L16 on the surface of 60 S ribosomal subunits by immunoelectron microscopy. J. Biol. Chem. *269*, 7579-7586.

Vaquero A., Scher, M., Lee, D., Erdjument-Bromage, H., Tempst, P., Reinberg, D. (2004). Human SirT1 Interacts with Histone H1 and Promotes Formation of Facultative Heterochromatin. Mol. Cell *16*, 93-105.

Venema, J., and Tollervey, D. (1999). Ribosome synthesis in Saccharomyces cerevisiae. Annu. Rev. Genet. *33*, 261-311.

Vignali, M., and Workman, J.L. (1998). Location and function of linker histones. Nat. Struct. Biol*. 5*, 1025-1028.

Wagner E, Lykke-Andersen J. (2002). mRNA surveillance: the perfect persist. J. Cell Sci. *115*, 3033-3038.

Wilkinson, M.F., and Shyu, A.B. (2002). RNA surveillance by nuclear scanning? Nat. Cell Biol. *4*, E144-147.

Wilusz, C.J., Wang, W., and Peltz, S.W. (2001). Curbing the nonsense: the activation and regulation of mRNA surveillance. Genes Dev. *15*, 2781-2785.

Wolffe A.P. (1997). Histone H1. Int. J. Biochem. Cell Biol. *29*, 1463-1466.

Woolford, J.L. Jr. (1991). The structure and biogenesis of yeast ribosomes. Adv. Genet. *29*, 63-118.

Zlatanova, J., and Van Holde, K. (1992). Histone H1 and transcription: still an enigma? J. Cell Sci. *103*, 889-895.

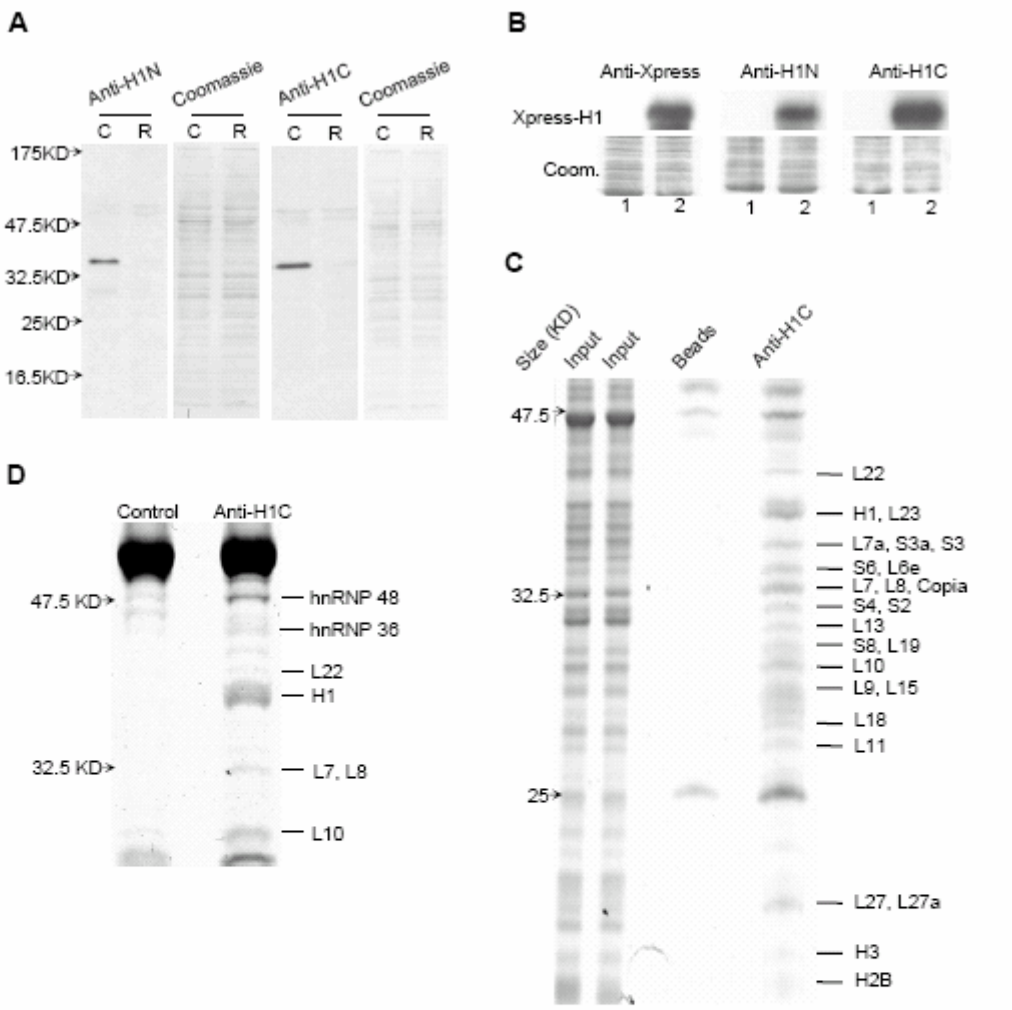

Figure 1. ***Drosophila*** **histone H1 co-purifies with 40S and 60S ribosomal subunit proteins.**

(A) Anti-H1N and anti-H1C antibodies specifically recognize H1. Extracts from control Kc cells (C) and Kc cells depleted of H1 using an RNAi approach (R) were separated on a 15% SDS PAGE, and subjected to Western analysis with anti-H1N or anti-H1C antibodies. The same membranes stained with Coomassie Blue are also shown. The positions of molecular weight markers (in kDa) are indicated on the left of the gels. (B) Anti-H1N and anti-H1C antibodies specifically recognize bacterially expressed ***Drosophila*** **histone H1. Upper panel: Western blot analysis of bacterial cell extracts from control bacteria not expressing** ***Drosophila*** **H1 (lanes 1) and bacteria expressing His-Xpress-tagged histone H1 (lanes 2) with anti-Xpress, anti-H1N and anti-H1C antibodies. Lower panel: The same membranes stained with Coomassie Blue. (C), (D) Drosophila Kc cell nuclear extract treated with (D) and without (C) 300 μg/ml of EB was used to perform IP reactions with anti-H1C antibodies. As controls, anti-H1C antibodies pre-blocked with the peptide used to raise the antibody (D) or Protein-A-Sepharose beads (C, Beads) were used. IP fractions were resolved by 15% SDS PAGE, stained with Gelcode Blue Staining Reagent (Pierce) and photographed. Prominent bands were excised and identified by mass spectrometry (as indicated on the right of the gels). Size markers are shown to the left. Panel C also shows diluted inputs.**

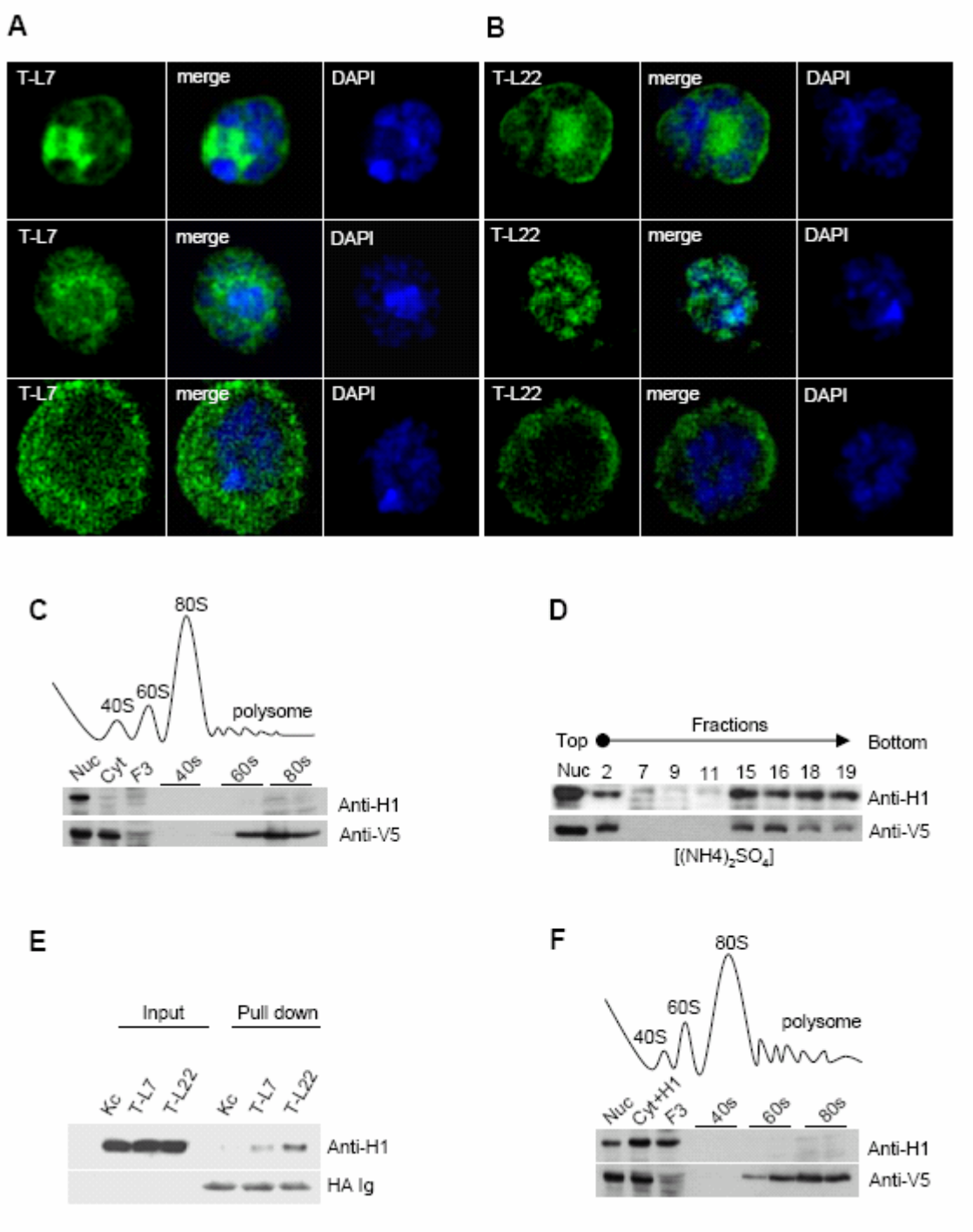
A
T-L7
merge
DAPI
B
T-L22
C
80S
60S
40S
polysome
Nuc
Cyt
F3
40s
60s
80s
Anti-H1
Anti-V5
D
Fractions
Top
Bottom
Nuc 2 7 9 11 15 16 18 19
[(NH4)2SO4]
E
Input
Pull down
Kc
HA Ig
F
Cyt+H1

Figure 2. Co-localization and interaction of ribosomal proteins with histone H1 in the cell nucleus.
(**A-B**) Distribution of V5-HA-tagged ribosomal proteins L7 (T-L7) (**A**) and L22 (T-L22) (**B**) in individual Kc cells. The localization of tagged proteins is illustrated in green (FITC) and DAPI staining is in blue. (**C**) Ribosomal protein T-L22 is incorporated into 60S and 80S ribosomes and polysomes in the cytoplasm. The input from nuclear (Nuc) and cytoplasmic (Cyt) extracts, and fractions from sucrose gradient sedimentation were assayed by western blot with anti-V5 antibodies to reveal the tagged T-L22 protein and H1N (anti-H1) to reveal H1. Lane F3 represents fraction 3 of the gradient. The A254 absorbance profile shows the distribution of 40S, 60S, 80S and polysomes in the gradient. (**D**) Ribosomal protein T-L22 is present in all nuclear fractions containing histone H1. Selected fractions (as indicated) were resolved on a 15% SDS PAGE gel and subjected to Western blot analysis using antibodies against H1N (anti-H1) and V5 (anti-V5). Diluted nuclear extract (Nuc) was used as a control. (**E**) T-L7 and T-L22 reverse pull down histone H1 in the cell nucleus. Nuclear extracts from Kc cells (or Kc cells expressing T-L7 or T-L22) were subjected to IP using anti-HA antibodies. IP products were resolved by 15% SDS PAGE and subjected to Western blotting using anti-H1N antibodies to detect H1. The inputs (0.5% of total nuclear extract) from different cell lines are shown, and the amount of anti-HA antibodies used in each reaction is indicated by HA Ig. (**F**) No interaction occurs between nuclear histone H1 and 40S, 60S, or 80S ribosomes from the cytoplasm of T-L22 Kc cells. Cytoplasmic extract from cell line T-L22 pre-mixed with purified H1 (Cyt+H1) was separated by sucrose gradient sedimentation. The upper and lower panels show western blot analysis of gradient fractions with H1N (Anti-H1) and Anti-V5 antibodies, respectively. Nuclear extract (Nuc), input extract (Cyt+H1), and fraction 3 (F3) from the gradient were also loaded onto the 15% SDS PAGE as controls.

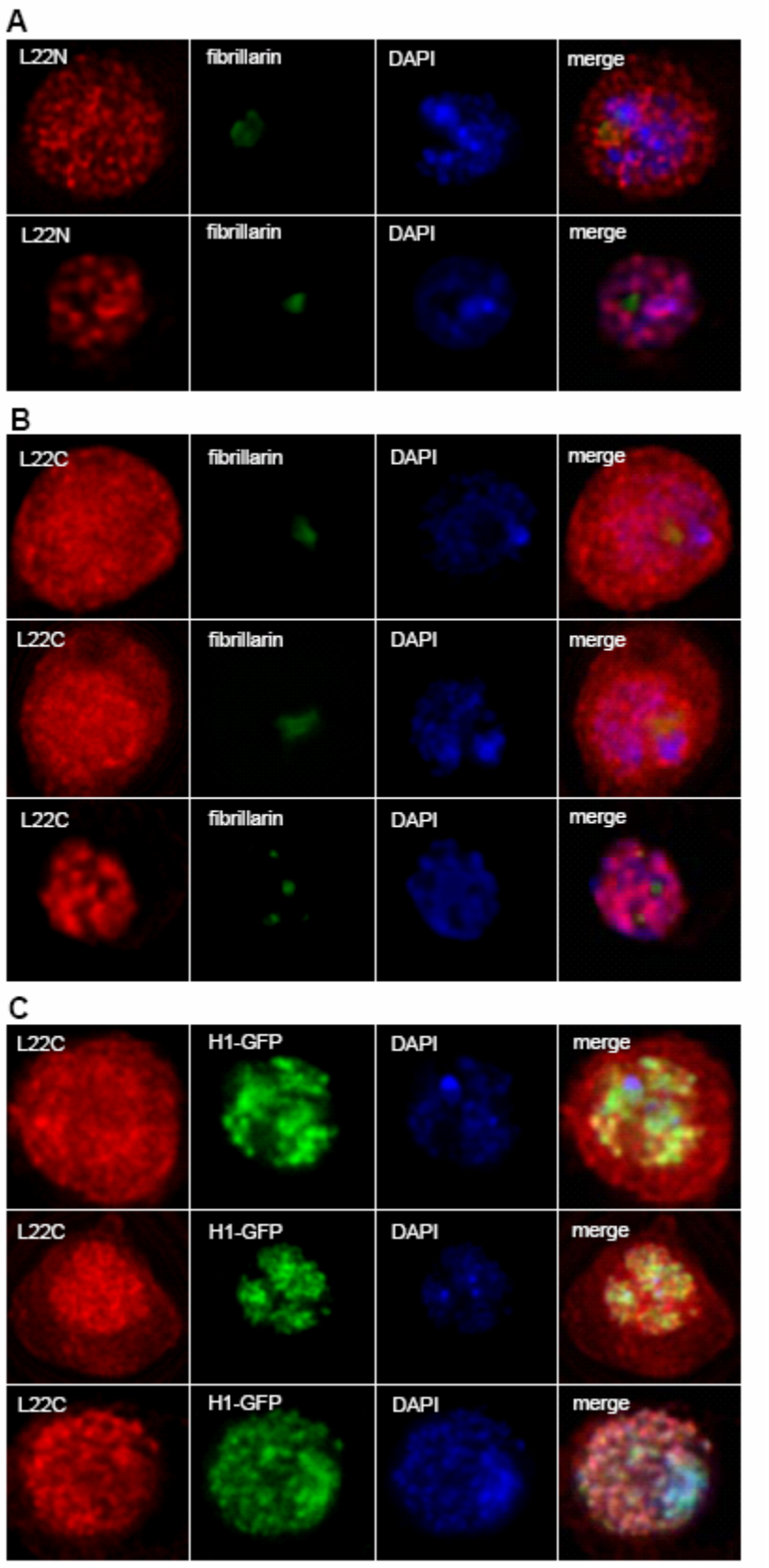
A
L22N
fibrillarin
DAPI
merge
L22N
fibrillarin
DAPI
merge
B
L22C
fibrillarin
DAPI
merge
L22C
fibrillarin
DAPI
merge
L22C
fibrillarin
DAPI
merge
C
L22C
H1-GFP
DAPI
merge
L22C
H1-GFP
DAPI
merge
L22C
H1-GFP
DAPI
merge

Figure 3. Co-localization of ribosomal protein L22 and H1 in the cell nucleus.
(**A**-**B**) The dynamic localization of L22 in Kc cells, as determined by anti-L22N (**A**) and anti-L22C (**B**) antibody (red), is compared with anti-fibrillarin (green), a nucleolar marker. DAPI is indicated in blue. (C) Co-localization of nuclear L22 with H1. L22 (L22C) is shown in red, H1-GFP in green, and DAPI is indicated in blue.

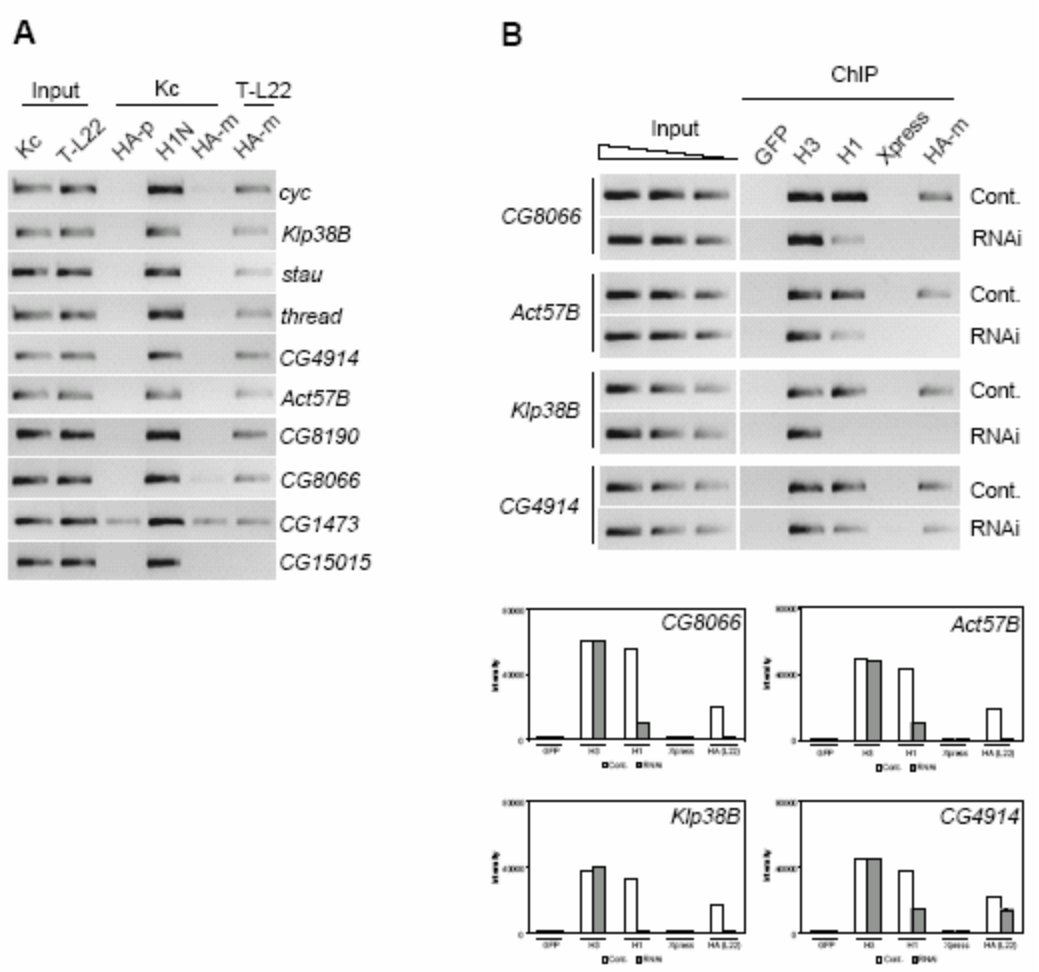

Figure 4. Ribosomal protein L22 is associated with chromatin enriched in histone H1 binding.
(**A**) Fragmented chromatin extracts from formaldehyde-fixed control Kc cells (Kc) were immunoprecipitated with polyclonal anti-HA antibodies (HA-p) (used as mock control for polyclonal antibodies in wild type Kc cells), anti-H1N, or monoclonal anti-HA antibodies (HA-m). Kc cells expressing T-L22 were immunoprecipitated with monoclonal anti-HA antibodies (HA-m) The resulting isolated ChIP DNA was subjected to PCR analysis with primers specific for ten genes known to be enriched in H1 binding (names/CG numbers indicated on the left of the panel). PCR products from the input DNA (0.1% of total chromatin DNA) were loaded into the first two lanes on the left side of the gel. (**B**) The association of ribosomal proteins with chromatin depends on histone H1. Chromatin extracts from control T-L22 cells (Cont.) and from dsH1RNA-treated cells (RNAi) were used to perform ChIP assays. Anti-GFP (GFP) and anti-Xpress antibodies (Xpress) were used as a negative controls, and polyclonal antibodies against histone H3 (H3) were used as a positive control. Anti-HA monoclonal antibodies (HA-m) were used to immunoprecipitate L22. ChIP DNA was subjected to PCR analysis with primers specific for genes *CG8066*, *Act57B*, *Klp38B* and *CG4914*. PCR products from the diluted inputs used in each ChIP reaction are also shown. A quantitative representation of PCR product intensity is shown beneath the gel pictures.

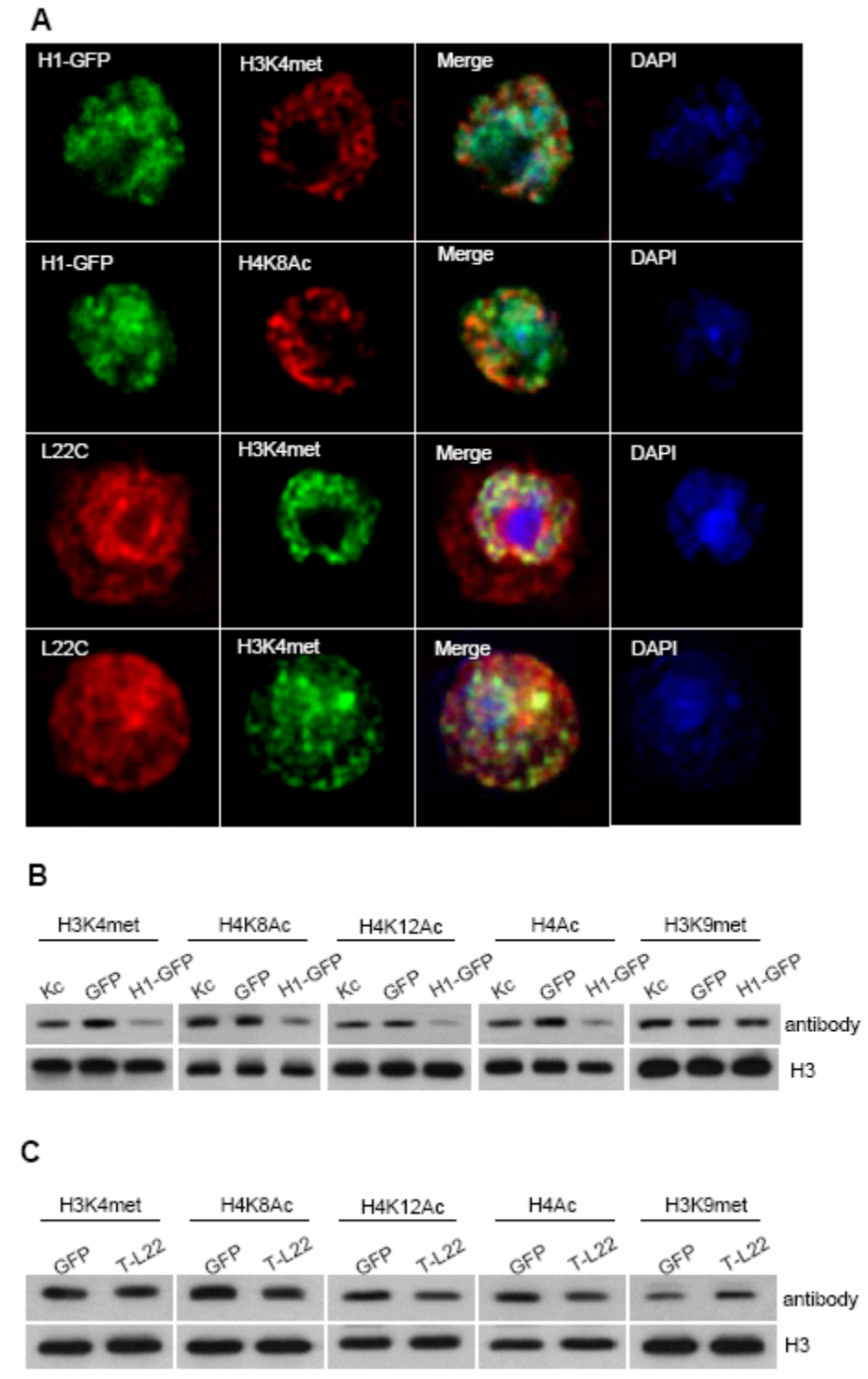
A
H1-GFP
H3K4met
Merge
DAPI
H1-GFP
H4K8Ac
Merge
DAPI
L22C
H3K4met
Merge
DAPI
L22C
H3K4met
Merge
DAPI
B
H3K4met
H4K8Ac
H4K12Ac
H4Ac
H3K9met
Kc
GFP
H1-GFP
antibody
H3
C
H3K4met
H4K8Ac
H4K12Ac
H4Ac
H3K9met
GFP
T-L22
antibody
H3

Figure 5. H1 and L22 in suppression of histone modifications.

(**A**) The top two panels show the distribution of H1 (H1-GFP; green) compared to that of methylated H3K4 (H3K4met; red) and acetylated H4K8 (H4K8Ac; red). The bottom two panels compare the localization of L22 (L22C) with that of methylated H3K4 (H3K4met; green). DAPI is in blue. (**B**) Overexpression of H1 causes global suppression of histone modifications. Equal amounts of cell extracts from control Kc cells (Kc), or cells expressing GFP (GFP) or GFP-tagged H1 (H1-GFP) were used in Western blot assays. Antibodies against the methylated (met) or acetylated (Ac) histones H3 and H4 are indicated on the top of the panel. Anti-H3 (H3) antibody was used as a loading control. (C) Overexpression of L22 slightly affects global histone modifications. Extracts from Kc cells expressing GFP or T-L22 were subjected to western analysis with the same antibodies as in (B).

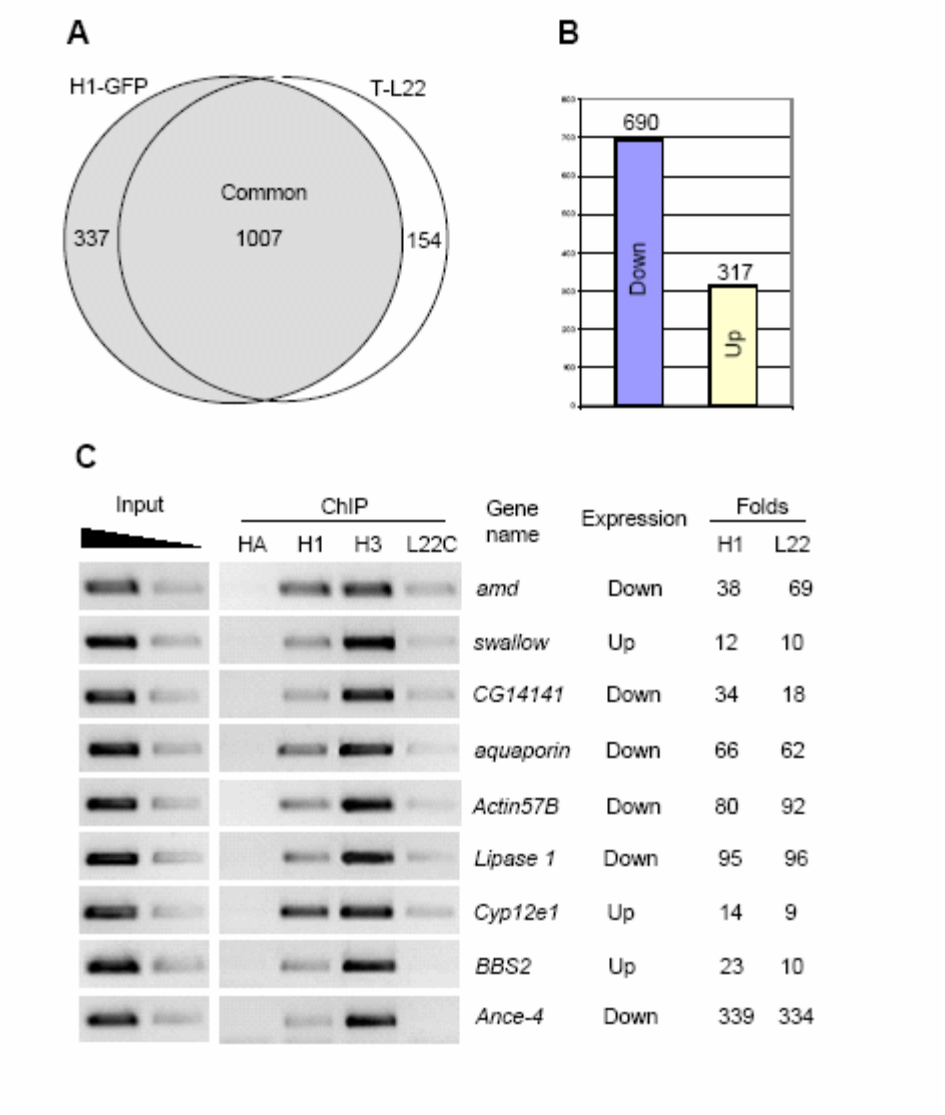

Figure 6. Overexpresion of H1 and L22 causes transcriptional repression of the same set of genes.

(**A**) The number of genes specifically affected in cells overexpressing H1 (H1-GFP), that in cells overexpresing T-L22, and those commonly affected (common) are all indicated in the Venn digram. (B) The number of genes down-regulated (Down; blue bar) and up-regulated (Up; light yellow) by H1 and L22 of the 1007 commonly affected genes. (C) ChIP analysis shows that the affected genes are directly associated with H1 and L22. The antibodies used to perform the assays, the names/CG numbers of the genes tested, the fold change in their transcription, and the PCR products from the diluted inputs (0.4, 0.05%) are all indicated.

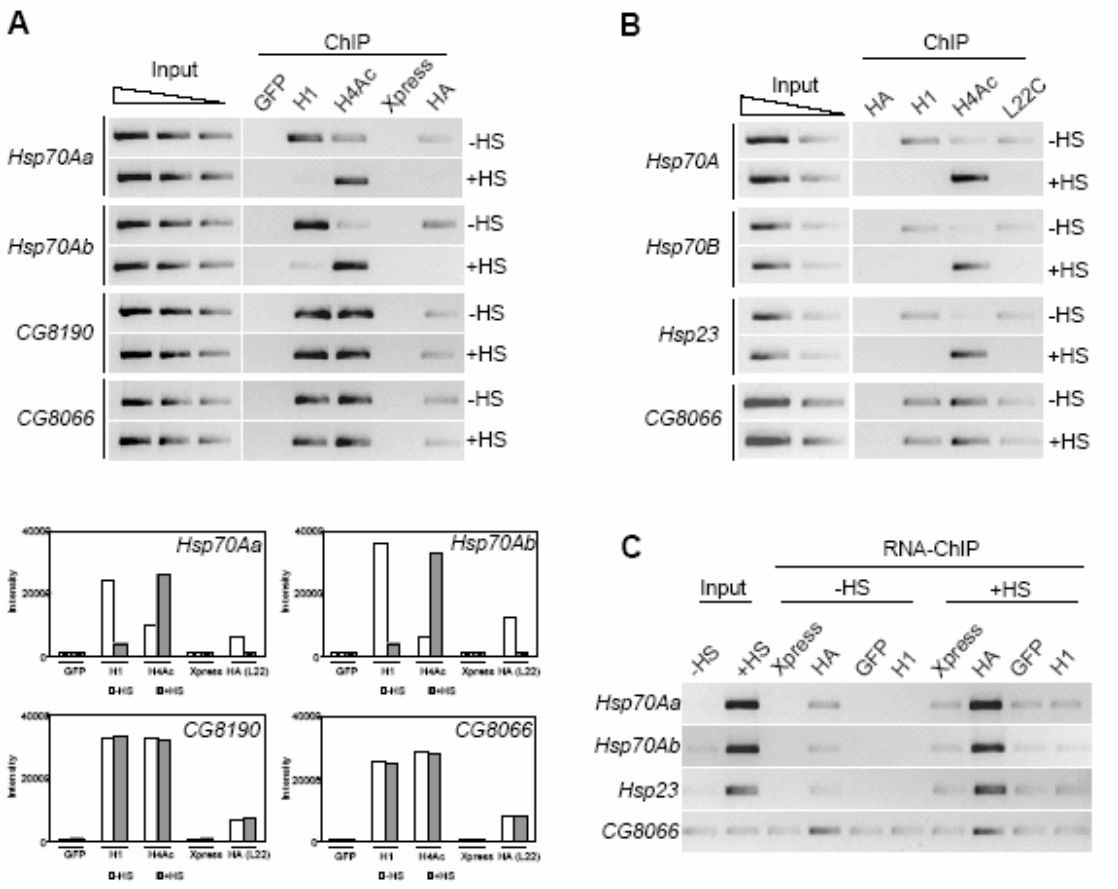

Figure 7. (**A**) Loss of association of L22 with heat shock genes correlates with the absence of H1 on chromatin. ChIP assays were performed using chromatin extract from fixed non-heat-shocked (-HS) and heat-shocked (+HS) T-L22 cells. Antibodies against H1N (H1), pan-acetylated histone H4 (H4Ac), and HA-tagged (HA; monitoring L22) were used in the assay as indicated. Anti-GFP and anti-Xpress antibodies were used as negative controls. The PCR products from the diluted input (0.4, 0.2, and 0.1%) are shown on the left. A quantitative representation of the PCR product intensity is shown beneath the gel pictures. (**B**) ChIP analysis performed using wild type Kc cells and antibodies against endogenous L22 (L22C). Chromatin extract from non-heat-shocked (-HS) and heat-shocked (+HS) Kc cells was treated with the antibodies shown. The genes tested are indicated on the left. (**C**) Ribosomal protein L22 becomes associated with newly synthesized *Hsp70* and *Hsp23* transcripts after heat shock. Nuclei from formaldehyde-fixed T-L22 cells without (-HS) or with heat shock (+HS) treatment were used to perform RNA-ChIP analysis using anti-Xpress, anti-HA, anti-GFP and anti-H1 antibodies. Histone H1 was not associated with any of the transcripts tested, before or after heat shock in comparison to the control (Anti-GFP). Anti-Xpress (monoclonal) was used as control for anti-HA (monoclonal). RT-PCR products from the input RNA are shown in the two lanes on the left of the gel.

Figure S1

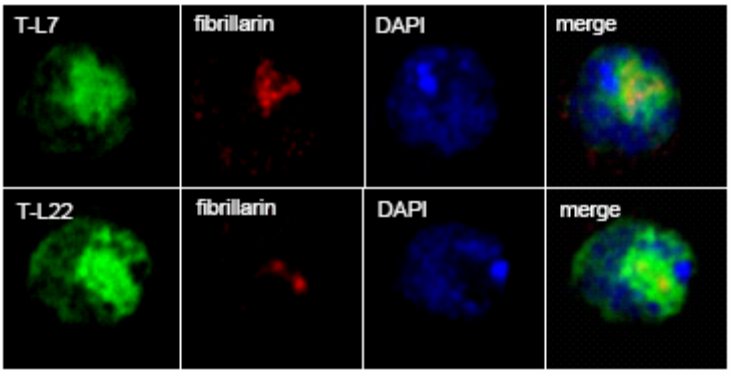

Figure S2

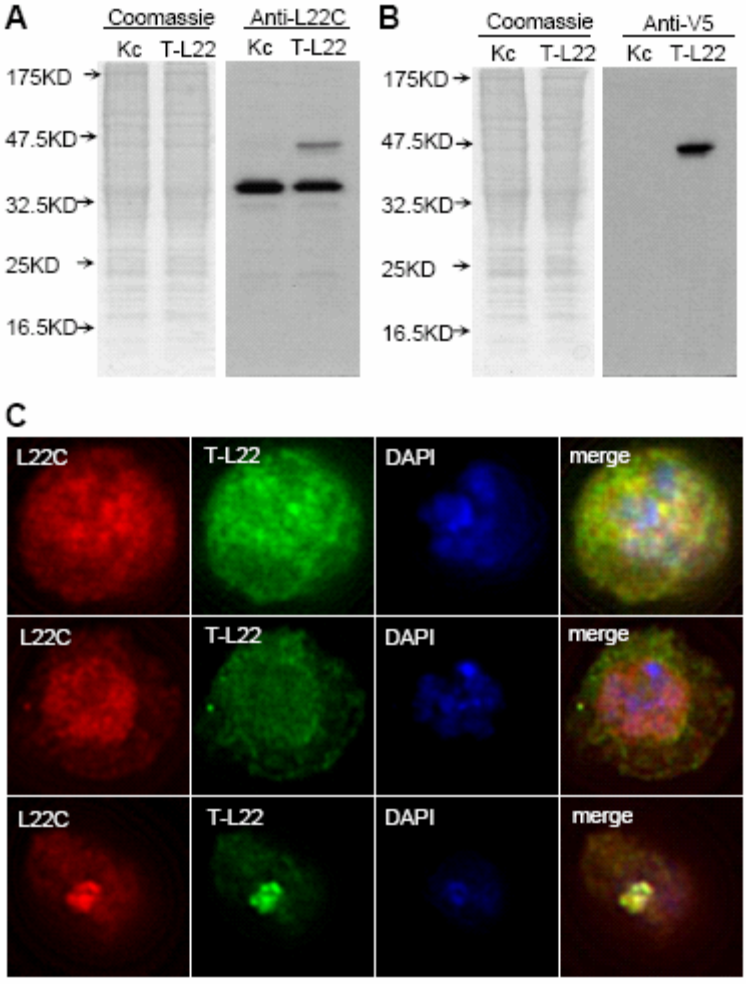

Figure S1.

Co-localization of ribosomal proteins T-L7 and T-L22 with fibrillarin in the nucleolus. Immunostaining of formaldehyde-fixed Kc cells with anti-V5 monclonal antibodies (green) and polyclonal anti-fibrillarin (Texas red). DAPI is in blue.

Figure S2.

The newly derived polyclonal antibodies against *Drosophila* L22 are specific. (**A**) The panel on the left shows the loading of the extract from Kc cells (Kc) and V5-HA-tagged L22(T-L22); the membrane was stained with Coomassie Blue. The Western blot in the right panel shows the same membrane hybridized with Drosophila polyclonal anti-L22C antibody. Size markers are shown to the left. (**B**) The left panel shows the loading of cell extract [labels as in (**A**)]. The Western blot in the right panel shows the membrane hybridized with anti-V5 antibody. (**C**) The *Drosophila* L22C antibody is specific to L22 in cytological assays. Kc cells expressing T-L22 were fixed with formaldehyde and immuno-stained with anti-L22C (red), anti-V5 (green), and DAPI (blue). Signals detected using antibody against L22 (L22C) specifically recognize the T- L22 protein.

Supplementary Table 1

Affymetrix ID	GFP Normalized	H1-GFP Normalized	T-L22 Normalized	Gene	Product
1634561_s_at	1.616926	0.800748	0.890318	CG32675	---
1641445_s_at	1.629097	0.86602	0.768235	CG7192	---
1634209_at	1.833276	0.69747	0.936877	CG5052	pimples
1634002_at	1.790175	0.67934	0.978071	CG13315	---
1641293_at	1.691378	0.739881	0.932756	CG4583	---
1633554_at	1.705358	0.777091	0.904245	CG1708	costa
1635365_at	1.777114	0.844012	0.722531	CG5198	---
1626823_a_at	1.477823	0.708429	0.952613	CG7945	---
1630287_at	1.882365	0.849911	0.748236	CG2013	Ubiquitin conjugating enzyme
1639816_at	1.695163	0.873977	0.84552	CG3733	Chromodomain-helicase-DNA-binding protein
1635051_a_at	1.747139	0.914083	0.772103	CG14536	---
1639286_s_at	2.074266	0.720381	0.860197	CG31689	---
1627665_at	1.445623	0.614756	0.954174	CG17486	---
1625047_at	1.734853	0.535448	0.915513	CG5821	---
1630530_at	1.685619	0.705028	0.946128	CG9296	---
1640222_s_at	1.885156	0.858071	0.813802	CG13124	---
1635109_at	1.531874	0.732873	0.955944	CG5888	---
1630340_at	1.4965	0.674578	0.962151	CG11927	---
1638953_a_at	2.257573	0.53367	0.924352	CG2086	draper
1627627_at	1.723497	0.798932	0.941122	CG10466	---
1630839_at	1.928318	0.683011	0.958817	CG14804	---
1629466_at	1.863817	0.942176	0.752185	CG6759	---
1626216_at	1.782335	0.806559	0.933899	S.CX001053	---
1629715_at	1.71076	0.792634	0.94108	CG7891	---
1635856_at	2.004532	0.945555	0.716336	CG13163	---
1624335_at	1.976463	0.979316	0.830657	CG11188	---
1633055_at	2.293788	0.534637	0.975594	CG10874	---
1630027_s_at	1.873911	0.731032	0.974515	CG33113	---
1631828_s_at	2.019896	0.575417	0.968063	CG8830	---
1634404_at	1.854387	0.991396	0.592488	CG4573	---
1626940_at	1.681273	0.748338	0.931737	CG2910	spenito
1631763_at	1.478661	0.991524	0.682003	CG31793	---
1628986_at	1.701514	0.822792	0.986655	CG7897	---
1637150_at	1.968058	0.908358	0.864035	CG13928	---
1637771_s_at	1.817601	0.972829	0.860412	CG7220	---
1631649_at	2.089322	0.95851	0.820629	CG8271	---
1627337_at	1.582184	0.992661	0.764753	CG11555	---
1634001_at	1.60801	0.995652	0.745749	CG9062	---
1637456_at	1.839019	0.728901	0.947047	CG8878	---
1635260_at	2.15955	0.822463	0.881288	CG6521	Signal transducing adaptor molecule
1636242_at	1.815833	0.521172	0.858779	CG14049	---
1637556_at	1.666801	0.777294	0.954544	CG11857	---
1640231_a_at	1.887448	0.912211	0.851566	CG8908	---
1636960_a_at	1.876296	0.930061	0.822317	CG11763	---
1626565_at	2.037151	0.859357	0.928568	CG2790	---
1641018_s_at	1.786777	0.833085	0.971886	CG8468	---

1641381_s_at	2.889322	0.572891	0.983295	CG13213	---
1633520_at	1.786116	0.971257	0.787184	CG32027	---
1637473_s_at	2.156434	0.92335	0.832959	CG18789	---
1638964_at	2.302577	0.804894	0.897199	CG7800	---
1628092_at	1.994173	0.995644	0.883591	CG5041	---
1625175_s_at	2.374872	0.817874	0.905864	CG7082	---
1635120_at	1.897172	0.835275	0.930014	CG8446	---
1625533_at	2.190296	0.628679	0.970029	CG5680	basket
1626325_a_at	2.377475	0.693186	0.939563	CG7849	---
1625068_a_at	2.702113	0.987876	0.647897	CG1836	---
1625524_at	2.307925	0.814281	0.961378	CG3165	---
1631030_at	3.152713	0.726636	0.896242	CG17023	---
1625889_at	2.744585	0.641914	0.876032	CG4863	Ribosomal protein L3
1629732_at	3.497339	0.630857	0.9509	CG8791	---
1640929_at	1.840145	0.978922	0.846869	CG7564	---
1623402_at	2.204171	0.882827	0.905981	CG10954	---
1634794_at	4.694866	0.968733	0.712296	CG10924	---
1630884_at	2.192898	0.922105	0.929665	CG17436	---
1625211_s_at	1.566737	0.77581	0.977936	CT34594	---
1629797_at	1.913334	0.87887	0.968503	CG6601	Rab-protein 6
1630802_at	2.176303	0.817175	0.957667	CG12800	---
1635813_at	2.235708	0.946085	0.949871	CG10390	TBP-associated factor 6-like
1629864_at	2.027705	0.790401	0.958181	CG2685	---
1625281_at	1.84613	0.999863	0.829808	CG6191	---
1637383_at	1.592682	0.761968	0.963825	CG11168	---
1624231_s_at	2.117585	0.826357	0.929839	CG8385	ADP ribosylation factor 79F
1636912_at	2.101952	0.709308	0.955682	CG7745	---
1625720_at	1.971639	0.909956	0.91089	CG12259	---
1640300_at	3.060875	0.588285	0.919208	CG33144	---
1628536_s_at	2.29408	0.830687	0.942981	CG11880	---
1631716_at	1.791815	0.955802	0.848348	CG2709	---
1628660_at	1.970128	0.945699	0.855807	CG7130	---
1639484_at	2.700802	0.96728	0.743428	CG1635	---
1629904_at	2.126979	0.716137	0.950478	CG14307	fruitless
1639759_s_at	2.446379	0.874307	0.898646	CG8390	vulcan
1630640_at	1.911556	0.88163	0.959733	CG4594	---
1628924_a_at	1.85637	0.994181	0.788344	CG13567	---
1628279_s_at	2.595946	0.924458	0.856383	CG11076	---
1636289_s_at	2.213677	0.980467	0.823377	CG7602	---
1634858_s_at	6.264344	0.751585	0.87002	CG5344	---
1636153_at	3.245445	0.741448	0.927005	CG6984	---
1641281_at	2.151871	0.967478	0.841022	CG12391	---
1624884_at	3.709973	0.772631	0.931245	CG32712	---
1629121_at	2.560154	0.795643	0.956223	CG10337	---
1630732_at	1.662357	0.998317	0.811486	CG2848	---
1628013_at	5.666623	0.753448	0.904378	CG3597	---
1628194_at	1.765177	0.878931	0.986917	CG2918	---
1626731_at	2.954593	0.748308	0.957728	CG5433	Kinesin light chain
1623013_s_at	1.971102	0.93286	0.967913	CG3907	---
1626653_a_at	2.909828	0.83441	0.907934	CG2098	ferrochelatase

1636044_at	1.829433	0.866289	0.960328	CG3539	---
1631614_at	2.161791	0.994103	0.7468	CG5190	---
1633563_at	2.043103	0.909455	0.931442	CG1637	---
1628938_at	1.798573	0.999324	0.817911	CG10882	---
1629207_at	2.361791	0.951153	0.86675	CG6287	---
1632633_at	3.254947	0.97523	0.697919	CG6514	---
1623737_a_at	2.486499	0.730619	0.922976	CG4212	Rab-protein 14
1634528_at	2.886365	0.818108	0.905897	CG8412	---
1630245_at	2.095458	0.887548	0.96485	CG4735	shutdown
1630990_at	2.892524	0.777884	0.936832	CG3411	blistered
1630390_at	2.13077	0.955261	0.892436	CG5602	---
1639188_at	1.948053	0.945284	0.956451	CG3308	---
1637461_at	2.291827	0.720111	0.949985	CG9527	---
1635508_at	2.014728	0.953265	0.957813	CG2859	TBP-associated factor 10
1629239_s_at	1.842794	0.912109	0.953728	CG2246	---
1641326_at	2.651272	0.902873	0.894905	CG30118	---
1637739_at	2.04895	0.87244	0.977439	CG16721	---
1635861_a_at	2.088091	0.994877	0.841	CG4599	Tetratricopeptide repeat protein 2
1640230_at	2.267273	0.855426	0.953446	HDC05827	---
1636025_at	2.604926	0.83351	0.975057	CG1167	Ras oncogene at 64B
1623322_at	2.213173	0.957153	0.888059	CG9067	---
1625975_at	3.179753	0.754543	0.930408	CG31052	---
1629189_at	1.790781	0.99603	0.835095	CG8843	---
1633711_a_at	5.405934	0.765683	0.921657	CG31012	---
1628017_a_at	2.705765	0.929272	0.970459	CG4916	maternal expression at 31B
1633865_at	2.185859	0.722618	0.923089	CG16734	---
1641336_at	1.811979	0.904989	0.954864	CG6443	---
1631388_at	1.826887	0.999623	0.904713	CG8432	Rab escort protein
1627617_at	2.035396	0.988698	0.884387	CG6264	Bestrophin 1
1629464_a_at	2.300276	0.999971	0.817753	CG32473	---
1635052_a_at	1.875183	0.962908	0.930669	CG15747	---
1640233_at	2.344764	0.795403	0.977263	CG5174	---
1634565_at	1.997625	0.986913	0.924064	CG4957	---
1640650_at	2.004111	0.886953	0.965917	CG6342	---
1632298_s_at	4.897889	0.824625	0.925869	CG3359	midline fasciclin
1633047_at	4.64565	0.997748	0.827278	CG1809	---
1632637_at	3.062966	0.905825	0.931069	CG32592	highwire
1623479_at	5.570684	0.813365	0.87447	CG7413	Retinoblastoma-family protein
1630984_at	2.328628	0.997499	0.849795	CG11154	---
1630572_at	2.249362	0.841967	0.974391	CG17158	capping protein beta
1629106_at	3.017938	0.991161	0.871414	CG2233	---
1624901_at	1.895239	0.927476	0.989414	CG9272	---
1639266_at	1.839865	0.993427	0.900354	LD29955	---
1623971_at	2.638012	0.831493	0.954272	CG9150	---
1630841_at	3.986891	0.676552	0.959647	CG8668	---
1641287_at	4.071113	0.945448	0.90651	CG8301	---
1641578_at	5.818995	0.806193	0.92539	CG4531	argos
1636392_at	3.948593	0.815641	0.92928	CT36057	---
1640829_at	5.819819	0.806964	0.904154	CG12075	---
1640264_at	3.446449	0.886398	0.915789	CG31160	---

1626550_at	2.840271	0.750685	0.965354	CG32705	---
1627564_s_at	2.630332	0.774928	0.968615	CG8954	---
1627528_at	3.502128	0.973789	0.908845	CG8257	---
1633355_at	2.103624	0.943704	0.925765	CG10802	---
1634468_at	2.884984	0.919789	0.925085	CG13397	---
1635964_at	2.371725	0.889142	0.970987	CG10951	---
1627582_a_at	4.786915	0.982661	0.713447	CG30035	---
1625851_s_at	2.039187	0.892682	0.989161	CG13383	---
1632748_at	2.578722	0.902678	0.987393	CG15084	---
1629040_at	2.009397	0.950251	0.961872	CG3476	---
1633403_at	2.146423	0.872606	0.984701	CG2160	Suppressor of Cytokine Signaling at 44A
1631741_a_at	5.591301	0.633106	0.939678	CG6899	Protein tyrosine phosphatase 4E
1638431_at	3.253167	0.979435	0.866951	CG2911	---
1635745_a_at	2.142546	0.948111	0.954258	CG4389	---
1625195_s_at	2.956384	0.855091	0.956391	X59545	---
1637513_at	6.777068	0.955372	0.75075	CG11275	---
1626850_s_at	2.164174	0.870981	0.951956	CG31953	---
1623960_s_at	2.522635	0.98429	0.876778	AJ010298	---
1633673_a_at	2.237086	0.911712	0.952007	CG11154	---
1623081_at	2.038961	0.890185	0.980783	CG3776	---
1633017_at	4.438125	0.876633	0.948945	CG3666	Transferrin 3
1623364_at	9.015281	0.737281	0.895215	CG4250	---
1623910_at	3.718391	0.99999	0.87694	CG9476	Tubulin at 85E
1626985_a_at	2.724306	0.915362	0.971888	CG7263	---
1641450_s_at	5.844041	0.902633	0.876916	X14037	---
1629886_s_at	7.328844	0.960448	0.829674	CG10033	foraging
1627489_a_at	2.854954	0.915961	0.970375	CG10433	---
1632626_at	2.062927	0.967987	0.939771	CG17712	---
1632646_at	3.917925	0.878881	0.943398	CG13687	---
1629803_a_at	23.36608	0.935481	0.661215	CG8095	scab
1625828_at	10.43705	0.726373	0.964249	CG11841	---
1638856_at	2.928651	0.959786	0.965012	CG2650	---
1623996_at	7.342343	0.776025	0.943805	CG5001	---
1637304_at	7.476367	0.99924	0.796194	CG14911	---
1636255_s_at	3.393265	0.999976	0.829335	CG7997	---
1628581_at	3.884987	0.923444	0.920625	CG3884	---
1624517_at	2.133683	0.851528	0.967653	CG3132	---
1626766_s_at	5.711606	0.996546	0.763338	CG16987	Activin Like Protein at 23B
1640048_s_at	1.975148	0.966101	0.984169	CT35401	---
1634208_a_at	4.39994	0.849421	0.962928	CG1093	pollux
1637389_at	8.094103	0.917322	0.845142	CG11575	---
1623957_s_at	6.284543	0.607782	0.602948	CG8938	Glutathione S transferase S1
1629042_at	5.257637	0.692746	0.629047	CG15674	---
1639996_at	7.725657	0.664633	0.904702	CG14016	---
1626566_at	1.891472	0.901714	0.977043	CG12262	---
1623693_a_at	3.068968	0.840787	0.966159	CG3365	drongo
1638693_s_at	2.410937	0.889276	0.974238	CG1882	---
1629731_at	9.927184	0.622104	0.562292	CG14565	---
1623080_at	8.462172	0.711327	0.636045	CG18410	---
1638354_at	2.299701	0.998119	0.898022	CG12007	---

1623731_at	3.662839	0.99819	0.835454	CG5619	trunk
1624159_at	10.03253	0.863344	0.835972	CG17577	---
1629924_at	35.60874	0.98173	0.682524	CG10238	---
1626724_at	8.998812	0.914725	0.787674	CG32687	---
1629705_at	3.134502	0.967129	0.949582	CG6084	---
1640661_at	2.284556	0.981598	0.959653	CG14992	---
1635079_at	2.630793	0.999954	0.956542	CG1550	---
1635763_at	5.876021	0.553836	0.647615	CG13226	---
1639180_at	2.072062	0.999991	0.928587	CG12505	---
1626560_at	54.45332	0.825216	0.877737	CG12251	aquaporin
1638329_at	2.735816	0.909004	0.970155	CG11420	pan gu
1641464_s_at	16.90086	0.778768	0.957696	CG32850	---
1641722_at	9.29493	0.882505	0.95208	CG3200	---
1639036_at	3.642617	0.970165	0.94961	CG8857	---
1635399_s_at	5.243729	0.999466	0.861158	CG11006	---
1630354_at	13.49791	0.999982	0.81867	CG13353	---
1629903_at	13.66721	0.997909	0.782164	CG30359	---
1626341_at	19.20744	0.939702	0.867793	CG14122	---
1625691_at	2.230646	0.925844	0.983452	CG3171	heat shock construct of Ishimoto
1633805_a_at	8.871606	0.995194	0.851759	CG1891	saxophone
1635900_at	6.63149	0.999997	0.856801	CG8846	Thor
1640896_at	28.89739	0.740511	0.654149	CG4462	---
1629469_s_at	6.669255	0.978	0.948802	CG10960	---
1630130_at	15.97415	0.712478	0.825572	CG4404	---
1627687_at	11.7294	0.617515	0.696667	CG14101	---
1637031_at	26.42961	0.537771	0.547753	CG2692	---
1628428_at	4.606153	0.931052	0.977185	CG12389	Farnesyl pyrophosphate synthase
1625873_at	4.90879	0.963038	0.981151	CG15661	---
1629710_at	86.93045	0.912685	0.909853	CG7279	Lipase 1
1641268_at	36.68143	0.949742	0.95005	CG13313	---
1623555_at	38.83801	0.831458	0.960526	CG10131	---
1641280_at	171.3833	0.505465	0.512343	CG8196	---
1639976_at	1.334483	0.643881	0.946728	CG7222	---
1635567_s_at	1.609156	0.573104	0.989554	CG10084	---
1636020_s_at	1.580307	0.533351	0.973882	CG15845	Adh transcription factor 1
1623777_s_at	1.505513	0.504298	0.908587	CG1358	---
1623826_at	1.610534	0.559043	0.956887	CG5203	---
1630942_at	1.313821	0.628831	0.949179	CG5742	---
1626323_s_at	1.558692	0.626171	0.962515	CG17255	---
1640364_at	1.599276	0.486161	0.909387	CG9258	nervana 1
1631351_s_at	1.388134	0.603031	0.955698	CG12118	---
1627668_s_at	1.528047	0.587543	0.968758	CG32527	---
1628184_at	1.499948	0.451517	0.877037	CG10742	Tetraspanin 3A
1632322_at	1.574269	0.520288	0.96272	CG16953	---
1637118_at	1.414953	0.641669	0.938831	CG30010	---
1627598_at	1.465882	0.657828	0.979624	CG11490	---
1639332_at	1.780382	0.609944	0.960024	CG3204	Ras-associated protein 2-like
1625810_s_at	1.433552	0.504262	0.981086	CG13937	---
1638591_at	1.392065	0.531192	0.976485	CG3278	---
1636352_at	1.442851	0.603685	0.935446	CG15443	---

1640042_at	1.736164	0.584947	0.975664	CG12299	---
1633680_at	1.710387	0.669073	0.978445	CG12818	---
1639908_a_at	1.5219	0.731345	0.973486	CG9705	---
1632394_s_at	2.043502	0.435741	0.977917	CG31919	---
1637778_a_at	1.707477	0.387111	0.941235	CG1969	---
1639370_at	1.356313	0.501373	0.958642	CG1239	---
1628482_at	1.501361	0.519149	0.975747	CG12156	---
1640871_at	1.40303	0.660344	0.966567	CG3637	Cortactin
1632712_s_at	1.465191	0.566917	0.988411	CG17836	---
1639265_at	1.369418	0.671454	0.95973	CG15536	---
1623551_at	1.285753	0.563654	0.955837	CG18081	---
1627433_at	1.351053	0.99979	0.64926	CG3163	---
1638327_a_at	1.302055	0.568641	0.937511	CG17754	---
1636967_a_at	2.576845	0.285937	0.955024	CG5315	---
1632790_at	1.541583	0.691396	0.95259	CG7863	---
1626371_at	1.548797	0.731467	0.977848	CG8507	---
1631151_at	1.625581	0.572996	0.936994	CG4951	---
1629241_at	1.313475	0.998579	0.650382	CG3289	Phosphotyrosyl phosphatase activator
1627165_a_at	1.554887	0.745921	0.963221	CG13645	---
1631179_s_at	2.023667	0.495859	0.906623	CG6680	---
1636296_at	1.806596	0.251763	0.942053	CG12945	---
1640925_at	1.508688	0.99195	0.701686	CG10927	---
1633794_a_at	1.991468	0.604122	0.936039	CG4710	---
1627002_at	1.395356	0.590699	0.984175	CG17446	---
1627470_at	1.65113	0.991954	0.494898	CG2845	pole hole
1632281_at	1.53548	0.54759	0.981485	CG4266	---
1629065_s_at	1.385198	0.48108	0.95001	CG1088	Vacuolar H<up>+</up>-ATPase 26kD E subunit
1640146_at	1.729244	0.583868	0.972161	CG33116	---
1633401_s_at	1.565253	0.992924	0.72818	CG30489	---
1636807_at	1.81941	0.432618	0.921944	CG1795	---
1626833_at	1.835096	0.562578	0.941679	CG11839	---
1625651_at	2.168483	0.395928	0.885003	CG18317	---
1636145_at	1.650452	0.595329	0.944101	CG7219	---
1638464_a_at	1.505287	0.369406	0.941888	CG14039	quick-to-court
1632380_at	1.362015	0.474183	0.963425	CG7826	minibrain
1638857_at	1.583573	0.992581	0.56123	CG3605	---
1634173_at	1.377176	0.999969	0.682389	CG3152	---
1638053_at	1.890457	0.997578	0.525194	CG10842	Cytochrome P450-4p1
1640251_s_at	1.934405	0.50305	0.980687	CG9553	chickadee
1631006_a_at	1.369433	0.538615	0.959158	CG10171	---
1636379_a_at	1.237479	0.61225	0.988751	CG12240	---
1623975_at	1.476208	0.694745	0.95985	CG1605	---
1640326_at	1.398723	0.597287	0.968004	Stencil:2R:2991693:2991352:GENSCAN	---
1641169_s_at	1.702944	0.756687	0.984053	CG11050	---
1627636_at	1.95068	0.999622	0.554205	CG14636	---
1631243_s_at	1.348052	0.459912	0.983951	CG7129	---
1636180_at	1.641328	0.679438	0.95072	CG4600	yippee interacting protein 2
1632332_at	2.242828	0.485297	0.948668	CG5447	---
1623743_at	2.471207	0.529018	0.960542	CG3191	---

1625151_at	1.485299	0.499676	0.962785	CG32770	---
1639256_at	1.627406	0.578869	0.987194	CG5676	---
1638173_s_at	1.320583	0.444455	0.965058	CG2950	---
1626617_at	1.981225	0.379665	0.952736	CG3929	deltex
1633294_at	1.700941	0.560617	0.949948	CG2812	---
1624537_s_at	1.767817	0.998599	0.754165	CG9866	---
1633836_a_at	1.317961	0.993479	0.652946	CG9847	---
1626404_a_at	1.994487	0.50214	0.902629	CG5680	---
1626683_at	1.639754	0.617302	0.939067	CG1514	---
1639432_at	1.247432	0.461709	0.936502	CG6437	---
1641164_s_at	1.751544	0.671723	0.949377	CG11163	---
1638513_s_at	1.37945	0.33172	0.961352	CG6668	---
1632630_at	1.401776	0.6024	0.962852	CG7039	---
1637085_at	1.199827	0.571361	0.978165	CG8203	Cyclin-dependent kinase 5
1636002_at	1.321708	0.658882	0.968638	CG4281	---
1637469_at	1.45339	0.331899	0.982992	CG33198	---
1636101_a_at	1.314465	0.608702	0.981835	CG31729	---
1633918_s_at	2.337157	0.519724	0.976421	CG7115	---
1629650_at	1.812159	0.995477	0.76421	CG3248	---
1629309_at	1.338124	0.996446	0.661123	CG7627	---
1637703_a_at	1.721119	0.618307	0.974407	CG15154	Suppressor of cytokine signaling at 36E
1636173_s_at	2.001606	0.53878	0.933046	CG5475	heat shock construct of Han
1623422_a_at	1.427666	0.642474	0.976409	CG31908	---
1638044_a_at	1.383975	0.642543	0.979452	CG5902	---
1633835_s_at	1.316543	0.590273	0.962915	CG2694	---
1624156_at	2.212746	0.982338	0.59892	CG18578	---
1639118_a_at	1.436579	0.360546	0.957466	CG12749	Heterogeneous nuclear ribonucleoprotein at 87F
1627512_at	1.472918	0.700386	0.995671	CG31915	---
1631412_at	1.686868	0.56886	0.969308	CG10695	---
1636837_at	2.36047	0.445375	0.938819	CG32177	---
1625876_at	1.740173	0.994001	0.6652	CG5864	---
1631321_s_at	1.3919	0.349273	0.91652	CR31614	---
1641123_at	1.36201	0.574388	0.98735	HDC06513	---
1638822_at	2.165407	0.609034	0.962211	CG6859	---
1632179_at	2.351016	0.679113	0.964805	CG12117	Sepiapterin reductase
1629619_at	1.872302	0.401361	0.8977	CG9735	---
1638839_at	1.420254	0.998945	0.658785	CG8092	---
1630764_at	2.003715	0.99831	0.743779	CG31756	---
1637430_s_at	1.627187	0.996281	0.722422	CG1572	---
1638446_a_at	1.737781	0.99557	0.733436	CG3542	---
1632234_at	1.486383	0.99885	0.716314	CG4561	---
1632974_s_at	6.58803	0.407442	0.968897	CG30015	---
1638637_at	2.377832	0.656972	0.973762	S.C3L002039	---
1634443_a_at	2.346956	0.631293	0.990477	CG3320	Rab-protein 1
1628352_a_at	1.571625	0.994501	0.586146	CG8798	---
1631555_at	1.548924	0.995504	0.675725	CG10062	---
1636384_at	2.184137	0.9862	0.638638	CG32703	---
1632343_at	1.310771	0.623853	0.951185	CG3017	Aminolevulinate synthase
1636933_at	1.559323	0.35173	0.936437	CG13562	---
1628351_at	1.683944	0.996061	0.788377	CG6198	---

1633613_at	1.816438	0.770804	0.98417	CG2765	---
1624899_at	1.412812	0.40403	0.976044	CG9375	Ras oncogene at 85D
1625080_at	2.00134	0.411395	0.977595	CG10686	---
1626706_at	1.293228	0.600308	0.986421	CG10229	---
1625165_at	1.604779	0.620905	0.985894	CG17187	---
1624142_a_at	2.905254	0.62094	0.939453	CG7085	---
1631334_at	1.821279	0.6974	0.968828	CG10260	---
1623384_at	1.629691	0.454237	0.991439	CG18426	yantar
1629968_s_at	1.207136	0.486308	0.971575	CG17370	---
1630403_s_at	1.190809	0.559091	0.982465	CG12746	---
1638701_at	2.820391	0.650079	0.952604	CG3825	---
1637598_at	1.449006	0.476155	0.980323	CG15715	---
1635939_a_at	1.636665	0.500073	0.980326	CG9641	---
1639193_a_at	2.01158	0.540479	0.981195	CG1971	---
1625388_at	1.380298	0.999685	0.653968	CG4893	---
1626682_s_at	1.398472	0.306542	0.938095	CG9135	---
1636647_s_at	1.760254	0.596634	0.958458	CG40160	---
1639876_a_at	1.457375	0.679982	0.979517	CG3510	Cyclin B
1640247_at	2.485166	0.674986	0.966255	CG9712	tumor suppressor protein 101
1626839_s_at	4.05555	0.565722	0.91252	CG3897	bloated tubules
1627015_at	1.292834	0.645911	0.985852	CG10964	sniffer
1631380_s_at	1.656109	0.99954	0.695562	CG7123	Laminin B1
1633847_at	2.875747	0.675672	0.966577	CG11284	---
1639997_s_at	1.396676	0.998172	0.69706	CT39116	---
1623683_at	2.055323	0.451878	0.943255	CG3712	mitochondrial ribosomal protein L33
1624378_at	1.257773	0.306963	0.915781	CG4399	enhanced adult sensory threshold
1635407_at	1.302477	0.393821	0.968867	CG32772	---
1639890_at	1.684048	0.444845	0.975365	CG17508	---
1623900_a_at	7.055604	0.25789	0.89849	CG14935	---
1627421_at	1.233192	0.570213	0.970825	CG18292	---
1633992_at	1.70497	0.998291	0.793709	CG2137	---
1626096_at	1.306607	0.538052	0.972299	CG5220	---
1634217_s_at	2.015113	0.549771	0.945888	CG1587	---
1637747_s_at	1.298659	0.61923	0.981967	CG8841	---
1635910_at	1.95053	0.367826	0.958458	CG7331	---
1639195_a_at	1.503047	0.522627	0.945543	CG5940	Cyclin A
1625830_a_at	3.340919	0.47282	0.923964	CG5186	scruin like at the midline
1625793_at	1.494823	0.999546	0.653599	CG5838	DNA replication-related element factor
1631565_a_at	1.220879	0.537796	0.989474	CG8669	cryptocephal
1627939_a_at	1.576107	0.999684	0.523366	CG2098	ferrochelatase
1633599_a_at	3.909624	0.395656	0.976351	CG17725	Phosphoenolpyruvate carboxykinase
1629663_at	1.444391	0.392756	0.95573	CG1832	---
1626649_s_at	1.796361	0.519136	0.965601	CG31232	---
1632345_at	2.763572	0.406587	0.946087	CG8353	---
1627837_at	1.800502	0.2815	0.957643	CG5527	---
1628453_at	1.880012	0.429105	0.992333	CG2221	---
1639714_at	2.758253	0.998762	0.715074	CG13201	intersex
1635723_s_at	1.279472	0.483383	0.975374	CG33129	---
1626241_at	1.900457	0.996799	0.737395	CG13263	---
1623308_at	2.090976	0.428323	0.9518	HDC12790	---

1635903_at	1.283472	0.466122	0.980631	CG4720	Protein kinase at 92B
1635652_at	1.393974	0.583294	0.953588	CG3585	---
1625034_s_at	1.261709	0.346567	0.977778	CG9765	transforming acidic coiled-coil protein
1632403_at	1.731302	0.995642	0.574507	CG12263	---
1634868_at	1.369923	1	0.684523	CG13016	---
1630877_a_at	1.53071	0.310456	0.980468	CG8455	---
1638581_at	1.23677	0.421792	0.986974	CG14224	---
1626835_at	1.607098	0.724795	0.973068	CG12210	Synaptobrevin
1631118_s_at	1.387189	0.574143	0.980083	CG3086	---
1635310_s_at	1.518675	0.588287	0.985786	CG31688	---
1633333_a_at	3.273783	0.561653	0.958715	CG7231	---
1623291_at	1.399177	0.540253	0.986195	CG31673	---
1634003_at	1.701171	0.277918	0.978465	CG32685	---
1633985_at	2.199683	0.593668	0.956143	HDC15359	---
1630433_at	1.857066	0.726507	0.986854	CG11963	---
1623238_at	2.515641	0.346013	0.894791	CG5618	---
1628483_at	1.331029	0.506294	0.997507	CG3004	---
1634925_at	1.422951	0.411076	0.959164	CG11176	---
1635191_at	1.307167	0.999638	0.587527	CG12846	Tetraspanin 42Ed
1628382_at	1.84355	0.9991	0.740877	CG4602	---
1639467_at	1.431294	0.470405	0.97425	CG32672	---
1640257_at	1.431024	0.998754	0.654964	CG9858	cricklet
1623565_at	1.56347	0.323979	0.973343	CG17278	---
1630707_at	1.957596	0.74351	0.966404	CG15085	modulator of the activity of Ets
1624145_a_at	1.505882	0.386872	0.960665	CG11025	---
1638220_at	2.235068	0.587379	0.947413	CG16888	---
1627934_at	1.775897	0.751497	0.969921	CG11723	---
1632180_at	1.23837	0.999996	0.468834	CG7791	---
1625845_s_at	1.215444	0.342194	0.978415	CG9745	D1 chromosomal protein
1624982_s_at	1.600781	0.558244	0.968662	CG5080	---
1623887_at	1.736978	0.689881	0.998441	CG12367	---
1635223_at	1.363697	0.291763	0.968573	CG30285	---
1626390_at	1.374079	0.997568	0.680285	CG5336	---
1629342_s_at	1.496003	0.674086	0.980151	CG1746	---
1632337_at	3.33959	0.999813	0.687006	CG5772	Sulfonylurea receptor
1628929_s_at	1.40885	0.388331	0.98395	CG1902	---
1630348_a_at	1.646396	0.35024	0.956056	CG5059	---
1628044_at	1.481855	0.99892	0.718587	CG10214	---
1635049_at	2.679493	0.996033	0.544322	CG13877	---
1623626_a_at	1.397718	0.504306	0.952607	CG11412	---
1628774_a_at	1.510662	0.486051	0.97135	CG32796	---
1623020_at	1.728606	0.999994	0.829685	CG31937	---
1636186_s_at	1.584247	0.998602	0.567064	CG1469	Ferritin 2 light chain homologue
1623053_a_at	1.589806	0.68528	0.967704	CG5174	---
1632028_a_at	1.388264	0.570998	0.97742	CG15441	---
1625078_at	1.307489	0.999433	0.615115	CG9124	---
1623762_at	2.08069	0.663191	0.96616	CG16910	kenny
1636883_s_at	1.34564	0.367492	0.978977	CG17950	High mobility group protein D
1637402_at	1.233673	0.345567	0.957045	CG32109	---
1632070_at	1.696927	0.559344	0.974012	CG4414	---

1632907_a_at	1.936267	0.612411	0.962418	CG13204	---
1633549_s_at	2.055535	0.476405	0.977438	CG1871	enhancer of rudimentary
1630949_s_at	1.547663	0.501493	0.970294	CG1081	---
1632908_s_at	1.908441	0.319647	0.961371	CG31072	---
1638663_at	1.249955	0.581277	0.978145	CG9539	---
1633565_at	1.576209	0.998884	0.663375	CG7741	---
1631672_at	1.645835	0.999714	0.769729	CG9867	---
1632158_a_at	1.552437	0.479754	0.95586	CG6755	---
1640142_at	1.244706	0.999551	0.462439	CG2957	mitochondrial ribosomal protein S9
1638844_s_at	2.31723	0.994807	0.709046	CG3714	---
1639984_at	1.374585	0.266667	0.994525	CG5692	rapsynoid
1624669_at	1.923926	0.721272	0.971308	CG7009	---
1636872_at	1.252854	0.998533	0.617423	CG13348	---
1638937_at	2.705406	0.603068	0.995351	CG3488	---
1638485_s_at	6.320378	0.496392	0.944041	CG5473	---
1640002_at	2.487485	0.577166	0.947221	CG4586	---
1635253_a_at	1.568129	0.559514	0.965334	CG7010	---
1630941_s_at	1.303939	0.533728	0.988885	CG16944	stress-sensitive B
1636268_at	1.767285	0.997933	0.699852	CG10570	---
1639255_s_at	2.06842	0.424311	0.971832	CG1516	---
1623320_at	2.472935	0.344154	0.981391	CG3711	---
1637499_s_at	2.412259	0.264565	0.966575	CG5953	---
1637036_s_at	2.05827	0.998766	0.655022	CG16784	purple
1639911_at	2.337851	0.20918	0.969658	CG17029	---
1637307_at	1.469158	0.998449	0.587577	CG31694	---
1640523_at	1.271074	0.997682	0.57953	CG3782	mitochondrial ribosomal protein L28
1626570_s_at	1.64596	0.323276	0.946754	CG17299	SNF4/AMP-activated protein kinase gamma subunit
1626981_s_at	1.184547	0.366924	0.965611	CG8979	---
1634722_s_at	1.648411	0.797771	0.990614	CG4143	multiprotein bridging factor 1
1632515_a_at	1.600859	0.790123	0.987612	CG18619	---
1631073_at	1.151536	0.412722	0.981498	CG10997	---
1635996_at	1.433086	0.540377	0.980356	CG6638	---
1632188_at	1.61302	0.53554	0.976945	CG1318	Hexosaminidase 1
1625348_s_at	1.678765	0.666029	0.977568	CG8892	---
1632341_at	4.557342	0.437201	0.907503	CG13559	---
1640169_s_at	1.093882	0.508663	0.972529	CG9983	Heterogeneous nuclear ribonucleoprotein at 98DE
1637689_at	1.459923	0.999648	0.679024	CG5317	---
1637191_at	1.296718	0.510922	0.967652	CG3433	Coproporphyrinogen oxidase
1635363_a_at	1.657085	0.272064	0.952196	CG31363	---
1636961_a_at	1.617757	0.999504	0.310795	CG9027	---
1623212_s_at	1.935427	0.686029	0.980712	CG4057	---
1624618_at	1.729741	0.489957	0.952991	CG3870	chrowded
1630695_at	1.759027	0.828962	0.984761	CG1970	---
1636137_at	1.564214	0.779924	0.978311	CG12390	defective in the avoidance of repellents
1638143_a_at	2.214536	0.997265	0.832887	CG8222	PDGF- and VEGF-receptor related
1641126_at	2.115813	0.520108	0.941688	CG15735	---
1628229_at	2.030657	0.600567	0.963743	CG11331	Serpin-27A
1628828_s_at	1.641155	0.53811	0.965597	CG6957	---
1639733_s_at	3.499974	0.996446	0.585262	CG14275	---

1633734_at	1.316213	0.999347	0.592917	CG7261	---
1627212_at	1.937392	0.999527	0.702153	CG10360	refractory to sigma P
1633763_at	2.159315	0.548458	0.947519	CG2855	---
1626729_at	1.579941	1	0.699802	CG3803	---
1638642_at	1.556571	0.999476	0.756131	CG17259	---
1626023_at	5.750418	0.373525	0.908958	CG14932	---
1629061_s_at	2.378903	0.99799	0.686949	CG32041	---
1623643_s_at	1.276093	0.99999	0.624724	CG4559	Imaginal disc growth factor 3
1628623_at	2.224028	0.679912	0.982302	CG9904	---
1638315_s_at	1.497731	0.999836	0.727226	CG8493	---
1625827_s_at	2.077184	0.375697	0.957233	CG31992	---
1628516_at	1.861687	0.77198	0.964153	CG15432	---
1635828_at	1.681346	0.755668	0.994009	CG14996	---
1630946_at	1.243389	0.462106	0.986779	SD02875	---
1632694_at	1.559061	0.473701	0.972455	CG31918	---
1630457_s_at	3.108982	0.705912	0.948281	CR_tc_RE65113	---
1630131_at	1.267821	0.378795	0.95953	CG6567	---
1640227_at	1.214204	0.999937	0.587967	CG8801	---
1640497_at	1.876203	0.862085	0.989369	CG17492	---
1631377_a_at	1.29498	0.437421	0.989503	CG17146	Adenylate kinase-1
1631007_at	1.51073	0.998698	0.490056	CG5371	Ribonucleoside diphosphate reductase large subunit
1639171_at	1.725658	0.999652	0.840125	CG14048	mitochondrial ribosomal protein L14
1633237_at	1.387053	0.997508	0.326745	CG4472	Imaginal disc growth factor 1
1631227_at	1.179022	0.5821	0.985054	CG5793	---
1623349_x_at	1.57634	0.381765	0.982859	AC005734	---
1628583_at	1.688941	0.469209	0.976326	CG31688	---
1630299_at	2.041302	0.993616	0.253668	CG17325	---
1634845_at	1.739011	0.804923	0.981544	CG12845	Tetraspanin 42Ef
1628602_a_at	2.308442	0.747553	0.962335	CG9248	---
1631535_at	1.417146	0.999922	0.701195	CG3299	Vinculin
1623388_at	2.586636	0.356422	0.996073	CG15861	---
1626707_a_at	1.199343	0.582543	0.978832	CG5730	Annexin IX
1634757_a_at	2.339548	0.783371	0.960848	CG16747	Ornithine decarboxylase antizyme
1624288_at	1.835076	0.292669	0.92823	CG10654	---
1640435_at	1.119543	0.505486	0.998904	CG8053	---
1636176_at	1.349864	0.999844	0.651959	CG4153	---
1625414_at	1.288116	0.350237	0.984266	CG9078	infertile crescent
1624101_at	1.289045	0.999958	0.527553	CG10242	---
1624296_at	1.638066	0.595444	0.96336	CG14508	---
1631342_at	1.209087	0.40775	0.992973	CG4204	---
1640032_a_at	3.196769	0.627027	0.954616	CG3814	---
1630677_at	1.339315	0.998618	0.583521	CG15100	---
1626767_at	1.88908	0.51583	0.97393	CG11415	Tetraspanin 2A
1628169_at	1.231123	0.572127	0.981749	CG12261	mitochondrial ribosomal protein S22
1628696_at	3.466108	0.459519	0.95626	CG12643	---
1640379_s_at	1.879733	0.999994	0.870257	CG11079	---
1629440_at	1.785882	0.552208	0.979945	CG2937	mitochondrial ribosomal protein S2
1628466_s_at	1.942443	0.550289	0.974691	CG10149	Proteasome p44.5 subunit
1640103_s_at	1.356223	0.608994	0.976787	CG17224	---
1640610_at	1.186242	0.267745	0.957394	CG6613	---

1634298_at	1.97557	0.421961	0.975343	CG12375	---
1632429_at	2.21703	0.999164	0.854136	CG5915	Rab-protein 7
1633005_at	1.458525	0.601151	0.972375	CG6903	---
1639897_at	1.97202	0.449839	0.949419	CG3091	---
1636724_at	2.719222	0.589744	0.960528	CG8292	---
1625658_at	1.395059	0.598468	0.982417	CG5181	---
1630750_at	2.060763	0.817419	0.979974	CG5323	---
1626133_s_at	2.760131	0.540247	0.98338	GH06606	---
1637671_a_at	1.725093	0.999754	0.618603	CG14767	---
1633012_at	1.690614	0.648123	0.97239	CG3662	---
1639184_at	1.38017	0.677217	0.981729	CG16787	---
1637276_at	1.421463	0.458291	0.995406	CG4799	Pendulin
1631541_at	1.48344	0.597783	0.998401	CG4494	---
1631488_at	1.319788	0.999734	0.4546	CG15618	---
1627922_at	3.369298	0.557431	0.967377	CG32544	---
1636382_at	2.097177	0.682164	0.986031	CG17574	---
1626867_at	2.051136	0.523816	0.973742	CG31613	---
1629625_at	1.827918	0.532387	0.969333	CG13211	---
1631627_at	3.153223	0.723769	0.959898	CG5335	---
1637510_s_at	1.599888	0.535812	0.983607	CG1318	Hexosaminidase 1
1629144_at	1.581778	0.678593	0.97158	CG15440	---
1639087_at	1.698908	0.697392	0.988327	CG5499	Histone H2A variant
1630212_at	5.213203	0.997344	0.661215	CG2065	---
1638295_s_at	1.342033	0.412	0.982675	CG1129	---
1639503_at	4.43191	0.993487	0.760852	CG3401	Tubulin at 60D
1630795_at	2.863721	0.765229	0.966441	CG12125	---
1630450_s_at	5.210383	0.701863	0.963259	HDC16707	---
1635116_a_at	1.33268	0.443873	0.987007	CG7518	---
1639522_at	1.787512	0.731393	0.979538	CG31950	---
1630093_at	1.184687	0.999999	0.522778	CG3751	---
1631832_at	1.258074	0.249776	0.977564	CG3201	---
1637193_at	1.122999	0.370864	0.985027	CG4954	---
1626844_at	2.2508	0.814132	0.990265	CG5748	Heat shock factor
1626851_at	3.383091	0.997783	0.576854	CG9460	---
1637642_at	6.402336	0.998086	0.688771	CG15047	---
1634048_a_at	4.992964	0.750308	0.955582	CG4501	---
1638883_at	1.803913	0.999882	0.892701	CG8636	---
1631598_at	1.232368	0.571101	0.981027	CG3184	---
1639353_at	6.476416	0.447457	0.936334	CG17032	---
1626383_at	2.181511	0.999732	0.881577	CG4096	---
1640286_at	1.119126	0.362979	0.994309	CG32174	---
1641647_at	2.502883	0.736396	0.979322	CG9232	---
1623193_at	2.600844	0.997618	0.614716	CG33123	---
1635227_at	2.149864	0.999972	0.88726	CG10160	Ecdysone-inducible gene L3
1640857_at	2.228194	0.653727	0.980625	CG10208	---
1638351_s_at	2.031396	0.998978	0.807307	CG8280	Elongation factor 1&agr;48D
1628589_at	1.569026	0.356839	0.972532	CG5010	---
1626840_a_at	1.860144	0.999991	0.793807	CG8479	---
1626902_a_at	1.669682	0.475893	0.988381	CG5771	Rab-protein 11
1636149_at	2.440768	0.752979	0.99053	CG31705	---

1625839_at	1.703164	0.999956	0.788505	CG3267	---
1632952_at	1.380439	0.634511	0.98056	CG4598	---
1637627_at	4.392174	0.742192	0.960548	CG6899	Protein tyrosine phosphatase 4E
1641017_at	2.555588	0.602261	0.963714	CG12352	separation anxiety
1623813_at	1.869467	0.537719	0.984256	CG16887	---
1630085_s_at	9.265461	0.649192	0.947459	CG17058	---
1624800_at	1.809906	0.999831	0.551103	CG5224	---
1626886_at	1.384431	0.487775	0.989009	CG3663	---
1634219_a_at	2.018872	0.999991	0.854508	CG1633	thioredoxin peroxidase 1
1628314_a_at	1.766277	0.663563	0.974508	CG6891	---
1631426_at	2.379937	0.483623	0.991275	CG32412	---
1626324_at	7.788203	0.99306	0.295756	CG9964	---
1634041_at	1.161369	0.578096	0.986852	CG31548	---
1625954_at	3.606174	0.661971	0.994072	CG2681	---
1623901_s_at	1.562202	0.528878	0.98583	CG7073	---
1627280_s_at	1.27121	0.446853	0.980186	CG8705	peanut
1622907_at	1.555868	0.492744	0.984936	CG5189	---
1639654_at	1.158594	0.411069	0.97685	CG3603	---
1637491_s_at	1.14895	0.412662	0.97731	CG3835	---
1632949_at	1.928697	0.775852	0.987434	CG3240	---
1630397_at	2.336562	0.999367	0.820146	CG13625	---
1640175_at	1.623252	0.518202	0.979579	CG13220	---
1639877_at	1.180743	0.541454	0.980881	CG2917	Origin recognition complex subunit 4
1641256_at	1.283299	0.486832	0.979753	CG7842	---
1623045_at	1.692534	0.999682	0.663545	CG5277	Intronic Protein 259
1630038_at	2.409412	0.999696	0.499631	CG3027	---
AFFX-Dm- AF 292560-1_s_at	19.55942	0.988879	0.05441		---
1624077_at	1.544064	0.469609	0.973917	CG13390	---
1634574_a_at	21.79876	0.987623	0.599674	CG18255	---
1639097_at	1.232338	0.541871	0.982499	CG2707	female sterile (1) Young arrest
1626808_s_at	2.036456	0.703498	0.989694	CG8416	glass multimer reporter construct of Hariharan
1633770_at	1.221298	0.999988	0.367892	CG11967	---
1629906_s_at	6.166993	0.992188	0.272371	CG33045	---
1636015_s_at	12.45233	0.992786	0.385866	NO_REP_ID	---
1634314_s_at	1.357432	0.615083	0.984007	CG7176	Isocitrate dehydrogenase
1622962_a_at	2.65051	0.385348	0.97554	CG17221	---
1635355_a_at	1.228296	0.594914	0.990253	CG9415	X box binding protein-1
1636202_s_at	2.346028	0.999999	0.436926	CG15009	Ecdysone-inducible gene L2
1629430_s_at	1.465967	0.058105	0.981257	HDC18536	---
1626768_at	2.078129	0.999791	0.767609	CG7044	---
1627493_at	2.796129	0.458631	0.972142	CG5958	---
1628657_at	1.804467	0.998787	0.398055	CG17534	---
1633916_at	14.51609	0.707867	0.93338	CG18605	---
1641428_at	3.274435	0.999345	0.281298	CG3616	Cytochrome P450-9c1
1638400_at	17.96442	0.647168	0.939695	CG8503	---
1623816_s_at	2.380975	0.783899	0.995789	CG1943	---
1623613_at	4.457943	0.140569	0.958938	CG13762	---
1628316_at	1.283789	0.369731	0.992478	CG7670	---
1635677_a_at	1.221478	0.189663	0.988904	CG1921	sprouty
1639085_at	1.831229	0.999954	0.723477	CG7221	---

1641245_a_at	3.247714	0.208884	0.98274	CG40115	---
1631266_a_at	1.165006	0.250441	0.975982	CG5840	---
1633547_a_at	1.801293	0.519377	0.991501	CG13211	---
1625354_at	10.09685	0.489248	0.984629	CG1257	---
1640884_at	1.441041	0.371661	0.985932	CG15784	---
1632532_s_at	1.18904	0.589135	0.988522	CG8996	walrus
1636040_at	1.526417	0.508425	0.99224	CG10527	---
1637086_at	5.736434	0.27995	0.957488	CG11843	---
1627872_at	1.119071	0.514278	0.995073	CG3770	---
1624993_at	10.84851	0.995515	0.681244	CG4377	---
1635507_at	9.837928	0.998969	0.253082	CG4269	---
1640486_s_at	11.77816	0.341968	0.935494	CG7125	---
1641102_at	17.1942	0.477595	0.966274	CG14141	---
1641446_s_at	16.55449	0.995835	0.257944	CG5171	---
1640720_a_at	5.874631	0.999986	0.836336	CG14872	---
1624070_at	1.64807	0.999862	0.822394	CG3395	Ribosomal protein S9
1628493_at	7.317271	0.998643	0.68576	CG6173	---
1634107_at	1.60263	0.486531	0.988291	CG3083	Peroxiredoxin 6005
1624907_at	4.460779	0.527269	0.985848	CG10106	Tetraspanin 42Ee
1637145_at	1.718019	0.100509	0.967725	CG14787	---
1628315_at	2.158031	0.724954	0.983296	CG17264	---
1631121_at	1.122852	0.999116	0.211837	CG7267	---
1627017_at	1.329327	0.613382	0.99184	CG12363	Dynein light chain 90F
1632652_s_at	1.35941	0.99989	0.339019	CG40100	---
1638543_at	6.470858	0.999559	0.831746	Stencil:2R:7629614:7629144:GENSCAN	---
1641134_at	1.397779	0.386548	0.983001	CG7277	---
1630393_a_at	1.47831	0.429237	0.983786	CG2903	Hepatocyte growth factor regulated tyrosine kinase substrate
1638308_s_at	1.911768	0.525337	0.989069	CG31613	---
1640363_a_at	4.435267	0.999734	0.521049	CG6330	---
AFFX-Dm-M62653-1_s_at	31.15908	0.998019	0.209377		---
1626442_at	4.336589	0.740682	0.994022	CG7224	---
1629889_s_at	1.130535	0.346273	0.987807	CG1803	---
1634033_s_at	11.6877	1	0.529504	CG1086	Glucose transporter 1
1625712_at	2.633712	0.356486	0.995009	CG14780	---
1638367_at	2.734136	0.602323	0.994602	CG7686	---
1628558_at	1.46889	0.999959	0.375263	CG30022	---
1625050_s_at	2.376782	0.999819	0.426794	X07656	---
1623222_s_at	1.392934	0.148259	0.996625	CG8989	Histone H3.3B
1633039_at	3.69147	0.999785	0.451005	CG5646	---
1631281_a_at	38.44731	0.997999	0.550384	CG10501	&agr; methyl dopa-resistant
1624290_at	55.36108	0.706489	0.970206	CG4752	---
1625582_at	2.113325	0.050647	0.986911	CG32187	---
1634869_at	1.407252	0.427216	0.994712	CG4581	Thiolase
1634250_at	54.61255	0.67809	0.590339	CG10067	Actin 57B
1624505_at	9.681196	0.995818	0.404422	CG6113	---
1635218_at	1.159445	0.518013	0.984818	CG11009	---

Supplementary Table 2

Affymetrix ID	GFP Normalized	H1-GFP Normalized	T-L22 Normalized	Gene	Product
1638652_at	0.63171	1.475537	1.047293	CG40006	---
1636972_at	0.727647	1.471171	1.056459	CG8003	---
1627553_at	0.576939	1.211363	1.125587	CG7919	farinelli
1630752_at	0.49642	0.977116	1.353092	CG6982	---
1625075_at	0.454185	1.078868	1.264265	CG9761	Neprilysin 2
1637501_a_at	0.468632	1.183593	1.072703	CG1835	---
1635356_at	0.481503	1.1205	1.066714	CG8816	---
1641379_a_at	0.524616	1.049566	1.165291	CG17419	---
1633989_at	0.524637	0.998259	1.220143	CG1124	---
1637226_at	0.601767	1.265243	1.005284	CG11885	---
1630178_at	0.592289	1.353277	1.081006	CG12082	---
1636726_at	0.552482	1.014383	1.107276	CG17180	---
1638312_at	0.536726	1.044912	1.088672	CG13189	---
1634557_at	0.421794	0.999983	1.456039	CG8497	Rhophilin
1623943_at	0.521383	1.101409	1.079794	CG17556	---
1637056_s_at	0.55151	1.184782	1.067815	CG11200	---
1641317_at	0.48075	1.041182	1.100033	HDC02844	---
1634100_at	0.309647	0.994874	1.174575	CG13865	---
1641630_at	0.60806	1.248359	1.033796	CG4237	GTPase-activating protein 69C
1628106_at	0.565967	0.996608	1.178793	CG12034	---
1637035_at	0.495239	1.023927	1.038353	CG1501	---
1641108_at	0.366696	1.201947	1.045455	CG17928	---
1640073_at	0.552407	0.997598	1.152242	CG14164	---
1625752_at	0.195769	0.980488	1.722664	CG2981	Troponin C at 41C
1625895_a_at	0.493943	1.000752	1.11687	CG31211	---
1637255_a_at	0.25218	0.998169	1.400903	CG1112	---
1623864_at	0.516229	1.025304	1.104358	CG6321	---
1636415_at	0.390456	1.066362	1.086124	CG14225	---
1627679_at	0.180722	0.99982	1.451756	CG12470	---
1624756_at	0.582878	1.176992	1.041469	CG5009	---
1626304_at	0.398072	0.993311	1.212402	CG32446	---
1636311_at	0.486908	1.019339	1.10236	CG9042	Glycerol 3 phosphate dehydrogenase
1627873_at	0.510181	1.00345	1.108543	CG5641	---
1633417_at	0.170758	1.138649	1.013756	CG5272	---
1629804_s_at	0.252165	1.200462	1.043625	CG6329	---
1637367_at	0.228265	1.461047	1.006836	CG10799	---
1639837_at	0.280455	1.163205	1.049749	CG11556	---
1636591_at	0.180601	0.999716	1.15723	CG8881	---
1640242_s_at	0.272357	1.393684	1.021772	AF222049	---
1628686_a_at	0.460738	1.057462	1.082232	CG17170	---
1624280_at	0.517759	0.998878	1.15598	CG2263	---
1630713_at	0.381756	1.234001	1.028083	CG33162	Signal recognition particle receptor &bgr;
1636906_s_at	0.149464	1.586156	1.037804	CG13320	---
1637896_at	0.452356	1.174825	1.018378	CG15804	Dynein heavy chain at 62B
1629671_at	0.092366	1.084613	1.028175	CG14193	---
1623022_at	0.327986	0.999951	1.232931	CG15820	---

1633893_at	0.138095	0.99626	1.236215	CG31217	---
1637309_a_at	0.110489	1.535009	1.013222	CG14680	---
1636899_s_at	0.27357	0.999433	1.271323	CG1623	---
1630808_at	0.48901	1.152553	1.008242	CG11495	rasp
1629468_at	0.080332	0.999868	1.181906	CG9372	---
1625950_a_at	0.235519	1.206869	1.029977	CG7777	---
1641117_a_at	0.507431	1.070254	1.002446	CG17600	---
1623961_at	0.092669	0.999674	1.372623	CG8936	---
1629852_at	0.413979	1.034306	1.05591	CG9018	---
1639801_at	0.406972	1.015179	1.042085	CG17168	---
1633458_at	0.100004	1.249114	1.008338	CG3429	swallow
1636943_s_at	0.159994	0.998385	1.136488	CG18525	Serine protease inhibitor 5
1635788_a_at	0.46754	1.102933	1.00776	CG6584	---
1623065_at	0.101277	1.001719	1.097656	CG13692	---
1640455_a_at	0.128331	1.065792	1.076086	CG17931	---
1637826_at	0.526034	0.999955	1.052476	CG10623	---
AFFX-Dros-GAPDH_M_at	0.402714	1.075081	1.015267		Eukaryotic initiation factor 4a
1630370_at	0.309162	1.058886	1.018786	CG9796	---
1637370_at	0.145836	0.999624	1.104485	CG18550	---
1633391_at	0.032612	1.07966	1.010684	CG8913	---
1629387_s_at	0.014576	1.158992	1.018525	CG4276	arouser
1638278_s_at	0.172765	1.007244	1.021877	CG9155	Myosin 61F
1630997_at	0.665732	1.439756	1.034385	CG7429	---
1631579_a_at	0.747321	1.497699	1.044796	CG32045	furry
1630624_s_at	0.682789	1.724956	1.056506	CG10151	---
1632198_at	0.705062	1.631664	1.055616	CG13902	---
1629613_at	0.714393	1.500566	1.028472	CG9591	---
1627799_at	0.588279	0.9922	1.654061	CG12161	---
1639116_at	0.473693	1.537898	1.005114	CG40041	---
1633137_at	0.354234	0.946615	2.33844	CG1442	---
1632271_a_at	0.74733	0.994195	1.537828	CG7971	---
1623520_a_at	0.652399	1.308148	1.024127	CG10336	---
1631271_a_at	0.74678	1.572715	1.006617	CG32575	---
1626883_at	0.780149	1.644767	1.035396	CG1620	---
1623742_at	0.785959	1.988019	1.030595	CG4813	---
1625680_a_at	0.752093	2.169112	1.02893	CG5792	---
1622912_at	0.749348	0.99894	1.508304	CG6492	---
1639067_at	0.719992	0.998963	1.561461	CG11589	---
1635410_at	0.572286	1.890312	1.03025	CG12766	---
1635593_at	0.565632	1.693113	1.070623	CG4373	---
1641267_at	0.678313	1.36244	1.023827	CG18572	rudimentary
1630987_at	0.782074	1.637906	1.044191	CG12297	heat shock construct of Hu
1624138_at	0.84512	1.890835	1.062311	CG5800	---
1624665_at	0.796827	1.999659	1.024537	CG9257	---
1636237_s_at	0.637693	1.460024	1.022937	CG8465	---
1637417_at	0.861594	1.797132	1.038147	CG6565	---
1630067_a_at	0.645247	1.942472	1.041245	CG7052	Thiolester containing protein II
1629740_at	0.705215	1.967613	1.057063	CG31617	---
1627723_at	0.617418	1.46118	1.060306	CG14701	---
1627900_at	0.814703	1.898896	1.021868	CG3058	---

1632182_at	0.699218	1.946085	1.032238	CG12096	---
1629395_at	0.477025	2.584851	1.079194	CG9743	---
1640260_at	0.773907	1.844445	1.021368	CG9703	Abnormal X segregation
1633394_a_at	0.682426	1.482486	1.02838	CG13900	---
1633641_a_at	0.530136	2.095681	1.0158	CG15611	---
1635913_at	0.770552	1.701311	1.033472	CG10814	---
1641459_at	0.701019	1.524993	1.023008	CG10372	Fas-associated factor
1628645_at	0.708264	0.999924	1.969103	CG6018	---
1638283_at	0.665431	2.075775	1.056027	CG9799	---
1631479_at	0.624747	1.377402	1.019914	CG4195	lethal (3) 73Ah
1629841_at	0.800728	1.609084	1.030911	CG32418	---
1627142_at	0.558161	1.560896	1.029854	CG2943	---
1626817_at	0.669755	2.040029	1.033144	CG9606	---
1633380_at	0.826356	2.150061	1.030763	CG12128	---
1629623_at	0.864611	1.745817	1.028869	CG15916	---
1630917_at	0.625078	1.302541	1.014467	CG7889	---
1638198_at	0.617533	1.458122	1.016829	CG12768	---
1626645_at	0.751849	1.848024	1.014143	CG8596	---
1627354_at	0.50488	0.990796	1.815195	CG5835	---
1625088_at	0.607438	1.431545	1.021956	CG17996	---
1631831_at	0.810391	2.392129	1.062545	CG31040	---
1629974_at	0.559415	1.364456	1.036697	CG6711	TBP-associated factor 2
1630421_at	0.693753	0.998406	1.657307	CG33170	---
1639406_at	0.710425	0.996862	1.568335	CG2374	late bloomer
1638737_at	0.783478	1.571742	1.027313	CG17209	---
1641294_a_at	0.580589	0.996884	1.291533	CG3625	---
1638052_at	0.738946	0.99936	1.72128	RH61753	---
1626375_a_at	0.615239	0.997915	1.365487	CG17592	---
1633741_at	0.440752	1.357058	1.030268	CG31032	---
1628018_at	0.524283	3.252586	1.039008	CG7002	Hemolectin
1628925_at	0.46505	0.983982	2.470614	CG17625	---
1624435_at	0.613667	1.257064	1.016749	CG12143	Tetraspanin 42Ej
1632342_a_at	0.596405	0.999937	1.373901	CG33080	---
1641324_at	0.597227	1.270252	1.005505	CG10236	Laminin A
1633389_at	0.742134	1.576603	1.042624	CG12404	---
1637482_at	0.69447	1.606847	1.017744	CG32300	peptide O-xylosyltransferase
1623724_at	0.739815	1.632164	1.040367	CG15027	---
1633696_at	0.717938	0.99996	3.048869	CG11303	Transmembrane 4 superfamily
1631244_a_at	0.578957	0.999878	1.660425	CG2163	---
1638341_s_at	0.599492	2.510981	1.034662	CT41625	---
1627176_at	0.352444	2.061492	1.022654	CG31431	---
1629413_at	0.80023	1.717407	1.018102	CG12703	---
1633822_at	0.66266	1.490692	1.018266	CG7519	---
1629517_at	0.695168	2.061579	1.036877	CG5118	---
1634630_at	0.357707	0.998237	1.412607	CG5707	---
1631146_at	0.40334	4.347784	1.066896	CG1906	---
1640489_at	0.756801	0.999849	1.760565	CG18522	---
1625923_s_at	0.536752	0.983594	9.640876	CG32593	---
1629444_at	0.56848	0.997889	1.51132	CG11756	---
1633473_s_at	0.606756	3.229446	1.029918	CG6058	Aldolase

1634988_a_at	0.647848	2.14544	1.023312	CG17352	---
1628638_at	0.64294	2.027842	1.034306	CG7200	---
1632390_at	0.774906	0.998261	1.632662	CG10460	---
1626871_at	0.631596	1.715278	1.02781	CG4924	---
1634152_at	0.311572	1.862481	1.028608	CG12242	Glutathione S transferase D5
1637645_at	0.602654	1.360781	1.031964	CG18321	---
1629597_a_at	0.274204	1.903721	1.068777	CG8421	Aspartyl hydroxylase
1632663_at	0.546933	0.997217	1.30282	CG7407	---
1625688_at	0.135866	1.828622	1.016058	CG6293	---
1631549_s_at	0.480849	1.982192	1.047012	CG18278	---
1639509_at	0.75068	3.479157	1.009271	CG12396	---
1628463_at	0.569687	1.19011	1.02462	CG7242	---
1638801_at	0.608301	1.260968	1.008374	CG14229	---
1629298_at	0.28109	1.40711	1.049376	CG31280	Gustatory receptor 94a
1629153_s_at	0.742156	1.559415	1.029208	CG5991	---
1638265_s_at	0.590927	0.999402	1.231571	CG31311	---
1632263_at	0.791831	1.697927	1.014529	CG1381	---
1639944_at	0.609958	0.999214	1.793076	CG11466	---
1638962_at	0.717823	1.462469	1.022429	CG6227	---
1634187_x_at	0.337603	0.995697	1.265564	NO_REP_ID	---
1635210_a_at	0.305738	1.911542	1.026497	CG33103	Papilin
1630159_at	0.452134	0.996784	2.047185	CG11672	---
1630312_s_at	0.441949	1.389456	1.020678	CG11989	---
1627277_s_at	0.302667	1.928369	1.0195	CG2930	---
1628332_at	0.152745	1.629063	1.010154	CG14990	---
1639460_a_at	0.781861	0.999842	1.571903	CG17218	---
1638690_at	0.698842	1.435348	1.01577	CG5537	---
1623342_at	0.565827	1.755045	1.024761	CG8369	---
1631123_at	0.454508	0.99595	1.992127	CG2105	---
1632775_at	0.722856	0.999652	1.471943	CG12854	---
1636579_s_at	0.344707	1.418925	1.000894	CG31991	midway
1632818_at	0.543458	1.354686	1.020026	CG32281	---
1623486_at	0.730654	0.998192	2.161053	CG7900	---
1631700_at	0.454811	2.457563	1.0081	LP09368	---
1635057_s_at	0.732379	1.672397	1.016158	CG15445	---
1624027_at	0.561331	1.244884	1.017945	CG4780	---
1636843_a_at	0.650739	0.996351	2.176969	CG10512	---
1631328_s_at	0.506788	1.27766	1.020372	CG9828	---
1627476_at	0.103321	2.347975	1.057921	CG13691	---
1635058_at	0.774276	1.587421	1.010772	CG6937	---
1630745_at	0.593388	1.232128	1.023542	CG9099	---
1623956_at	0.559527	1.519101	1.035339	CG1685	penguin
1627235_at	0.392131	0.999993	3.350831	AT11646	---
1629272_at	0.562306	1.28203	1.027334	CG14230	---
1624530_at	0.824918	1.818037	1.017959	CG5701	---
1637269_at	0.597781	0.999898	1.619756	CG6310	---
1624413_at	0.48816	5.894964	1.040949	CG14527	---
1632431_s_at	0.774208	2.684719	1.036095	CG8827	Angiotensin converting enzyme
1635370_at	0.564204	1.220891	1.016166	CG12840	Tetraspanin 42El
1635940_at	0.441454	0.989152	5.370565	CG5367	---

1638810_at	0.803361	1.657652	1.018815	CG14993	Fumarylacetoacetase
1624778_at	0.569752	1.600301	1.013007	CG3291	pacman
1638236_at	0.744156	1.729991	1.017134	CG9302	---
1627032_a_at	0.65574	1.979528	1.009684	CG8611	---
1639587_s_at	0.622969	1.432864	1.017424	CG7458	---
1633293_at	0.385097	1.250813	1.023178	CG10157	---
1640170_at	0.512677	0.98861	6.491959	CG10311	---
1640695_at	0.752238	1.761659	1.017076	CG10425	---
1625410_at	0.667177	1.463711	1.015273	CG5147	---
1630438_at	0.688774	1.603844	1.014288	CG32409	---
1634672_at	0.925518	1.903612	1.012746	CG5064	---
1632593_at	0.841635	0.999369	1.709765	CG32147	---
1634958_at	0.383052	2.563235	1.013336	CG9455	---
1637217_at	0.497176	1.547277	1.024419	CG5714	---
1630375_at	0.503728	1.437874	1.02567	CG7635	---
1638837_a_at	0.646479	1.506222	1.007703	CG33066	---
1634546_at	0.760039	3.111774	1.028266	CG11527	Tiggrin
AFFX-Dros-GAPDH_5_at	0.659534	0.999268	1.685566		Eukaryotic initiation factor 4a
1623194_at	0.852948	2.060526	1.011408	CG7637	---
1626251_at	0.298219	0.999648	1.627344	CG9668	Rhodopsin 4
1626600_at	0.472037	0.995656	3.044077	CG30016	---
1640972_at	0.649966	0.999597	2.988924	CG10308	Cyclin J
1625096_at	0.729965	3.299355	1.029492	CG9300	---
1640776_at	0.150258	0.988093	1.965049	S.C3L000065	---
1627111_at	0.862589	1.905544	1.016531	CG5258	---
1639159_at	0.896356	2.161715	1.016716	CG4069	---
1639096_at	0.58815	0.998781	2.928302	CG14096	---
1626162_s_at	0.278045	3.720288	1.038956	CG1906	---
1630150_s_at	0.710127	1.523494	1.017069	CG4145	Collagen type IV
1629606_at	0.727762	0.999981	1.510364	CG13890	---
1624594_at	0.73613	0.999705	1.640991	CG32484	Sphingosine kinase 2
1634942_at	0.751083	2.653191	1.033221	CG5114	---
1634733_at	0.249387	1.807675	1.055612	CG3831	---
1634230_s_at	0.54477	1.267197	1.001627	CG17161	grapes
1627265_at	0.488632	0.999999	1.327008	CG9139	---
1624310_s_at	0.190214	0.999375	1.598972	CG4753	---
1637650_at	0.784139	2.042764	1.003856	CG4164	---
1639251_at	0.444597	0.996462	3.01767	CG17462	---
1630858_s_at	0.792183	0.999933	1.590851	CG7816	---
1640220_a_at	0.684332	1.771309	1.019256	CG11779	---
1633222_at	0.776705	1.971302	1.022227	CG6073	---
1627741_at	0.312012	0.998395	2.948699	CG13086	---
1641491_at	0.875217	1.84522	1.021391	CG7911	---
1636031_at	0.226166	0.996514	2.898135	CG1294	---
1627027_at	0.819543	1.98973	1.014057	CG15168	---
1635020_s_at	0.817519	1.900433	1.01114	CG2488	---
1633994_at	0.227474	0.98787	5.125312	CG4940	---
1627726_a_at	0.679285	1.482566	1.016818	CG6404	---
1639229_at	0.506907	1.833573	1.018152	CG16858	viking
1627916_s_at	0.786786	2.016316	1.010867	CG1799	raspberry

1638117_at	0.506936	1.647521	1.013945	CG14451	---
1641199_a_at	0.500421	1.393799	1.015863	CG1544	---
1624609_at	0.584332	0.999383	1.909368	CG31279	---
1623746_a_at	0.16168	1.728962	1.037683	CG6167	---
1628036_at	0.275954	0.997864	1.952895	CG15329	---
1634087_at	0.499675	0.999538	1.584901	CG1311	---
1627152_at	0.651492	1.397504	1.012287	CG12918	---
1628298_at	0.405264	0.999327	3.162257	CG2952	---
1634658_a_at	0.723004	2.45998	1.001233	CG8772	---
1628487_s_at	0.311534	0.999856	1.210174	CG1216	---
1626255_at	0.097814	0.998341	2.144622	CG13888	Gustatory receptor 61a
1627884_at	0.103315	0.999159	1.507119	CG5281	---
1634253_at	0.547894	0.999988	1.645709	CG9917	---
1632377_at	0.400283	1.526897	1.014947	CG8399	---
1624568_at	0.315341	0.99979	1.426286	CG7985	---
1634186_a_at	0.222823	3.292563	1.030232	CG17119	---
1632665_a_at	0.674717	1	1.368571	CG6340	---
1640747_s_at	0.094724	1.531812	1.032714	CG8547	---
1634739_a_at	0.35981	4.16582	1.032957	CG4001	Phosphofructokinase
1622921_at	0.463437	1.962428	1.018331	CG32022	---
1629685_at	0.880864	0.999995	1.797229	CG16986	---
1641733_a_at	0.413563	0.99973	1.163374	CG15645	---
1624079_a_at	0.153143	1.245849	1.016568	CG17515	---
1629916_at	0.541584	0.999758	1.361304	CG33134	death executioner Bcl-2 homologue
1624357_at	0.114855	0.998763	1.828706	CG7676	---
1626473_a_at	0.908038	3.635692	1.016151	CG15825	---
1636566_at	0.745141	0.999286	4.502129	CG32368	---
1630797_at	0.247097	0.998145	1.469842	CG32582	---
AFFX-Dros-GAPDH_3_at	0.446863	1.185643	1.010395		Eukaryotic initiation factor 4a
1631392_at	0.538414	1.502127	1.003701	CG11089	---
1625023_a_at	0.289619	0.998978	1.871905	CG11822	---
1628764_at	0.681086	1.420652	1.006812	CG2245	---
1632667_s_at	0.484768	1.101062	1.006013	CG8893	Glyceraldehyde 3 phosphate dehydrogenase 2
1636689_at	0.543065	0.999886	1.390664	CG4259	---
1640478_at	0.096566	0.998317	1.702246	CG31777	---
1630412_at	0.166791	1.95598	1.026322	CG16873	---
1623296_at	0.221479	0.997891	1.339889	CG32625	---
1636997_at	0.356027	1.288248	1.013431	CG18528	---
1627352_at	0.419803	0.999459	1.845362	CG8782	---
1630167_at	0.343401	0.999476	2.061446	CG1963	pterin-4a-carbinolamine dehydratase
1625134_at	0.352858	1.329199	1.007232	CG10873	---
1637816_s_at	0.518926	2.331852	1.015693	CG2171	Triose phosphate isomerase
1630044_s_at	0.463394	1.374164	1.004003	CG6904	---
1627060_s_at	0.298779	0.996805	2.533976	CG1106	Gelsolin
1641259_at	0.180993	2.924636	1.02859	CG5210	Chitinase-like
1626607_at	0.567721	1.282818	1.002044	CG8583	---
1626917_at	0.301607	3.628388	1.041932	CG31337	---
1630950_at	0.899261	2.580393	1.013711	CG10206	---
1629796_s_at	0.310006	1.579973	1.006208	CG2945	cinnamon

1632882_at	0.240415	0.999546	1.18544	CG11671	---
1636730_at	0.533587	1.531536	1.013349	CG13373	---
1635140_at	0.070312	2.50935	1.007595	CG15515	---
1635263_at	0.62212	7.818044	1.013121	CG11825	---
1632313_at	0.075214	0.998039	1.404873	CG1998	---
1634329_at	0.38073	0.999724	1.141262	CG32579	---
1635946_at	0.569378	61.36537	0.812246	CG17923	---
1625572_s_at	0.140997	0.99946	1.67995	CG8627	Diazepam-binding inhibitor
1626022_at	0.069598	1.26192	1.004882	CG14680	---
1640405_at	0.251565	1.353157	1.006524	CG5304	---
1641192_at	0.095548	2.653384	1.019136	CG14523	---
1641232_s_at	0.309328	0.999944	1.394434	CG6999	---
1634464_at	0.205633	0.999971	1.974453	CG5338	---
1624688_at	0.095635	0.999992	1.188082	CG9360	---
1636900_at	0.31415	0.999999	1.41171	CG5390	---
1640104_at	0.767521	0.999844	18.50757	CG7014	---
1637003_at	0.125007	1	1.695839	CG6927	---
1624628_at	0.07164	0.999994	1.757579	CG10396	---
1633347_at	0.404629	1.025347	1.058624	Stencil:3L:10591603:10592020:GENSCAN	---
1625995_a_at	0.475518	1.058487	1.018404	CG12529	Zwischenferment
1634302_s_at	0.169717	1.050747	1.087776	CG14516	---
1637610_at	0.467534	1.011717	1.048518	CG15736	---

Supplementary Table 1-2

The tables show the genes/predicted transcripts (with known CG number) affected when overexpressing histone H1 and ribosomal protein L22. The Affymetrix ID number of each gene/predicted transcript, their CG number, and known/predicted function are included in the table. All the listed genes past the ANOVA test. The genes down-regulated are listed in Table 1; those up-regulated are listed in Table 2. Normalized: normalized expression value.

Microarray analysis was performed using DrosophilaGenome1 (DG1) GeneChips™ (Affymetrix, Santa Clara, USA). The 15 μg of total RNA from each sample was reverse-transcribed and 5 μg of biotin-labeled cRNA was fragmented and hybridized to the Affymetrix *DrosophilaGenome* (DG) GeneChips. Expression values were estimated using the robust multi-chip average method with quantile normalization as implemented in the R BioConductor package (R.A.Irizarry et al., 2003, Nucl Acid Res 31:e15). These data were then imported into GeneSpring 7 (Agilent Technologies) with the default per chip and per gene

normalization steps. Genes were considered to have significantly ($p < 0.05$) changed in their expression values if they reached an expression value of >50 in one or more conditions, and passed a one-way ANOVA ($p<0.05$). A Benjamini and Hochberg false discovery rate correction was applied to deal with multiple testing errors. To find the origins of the significant changes, we performed a Tukey *post-hoc* analysis on the ANOVA results.

Primer Sequences

GFP, H1-GFP, T-L7, T-L22 in pIB/V5-His-TOPO vector

GFP

Forward primer 5'- ACCATGGCTAGCAAAGGAGAAGAA -3'

Reverse primer 5'- TTATTTGTAGAGCTCATCCATG -3'

H1-GFP

Forward primer 5'- ACCATGGGAATGTCTGATTCTGCAGTTGC -3'

Reverse primer 5'- CGGAATTCCGCTTTTTGGCAGCCGTAGTC -3'

Forward primer 5'- CGGAATTCCATGGCTAGCAAAGGAGAAGAA -3'

Reverse primer 5'- TTATTTGTAGAGCTCATCCATG -3'

T-L7

Forward primer 5'- ACCATGGGAATGCCTGCTCCGGTCGTC -3'

Reverse primer

5'- TGCGTAGTCAGGCACATCATACGGATAGACCATCTTGCGCAGCAGA -3'

T-L22

Forward primer 5'- ACCATGGCTCCTACCGCCAAG -3'

Reverse primer

5'- TGCGTAGTCAGGCACATCATACGGATACTCGGCATCGTCGTCCTC -3'

RNAi primer

GFP

Forward primer

5'- ATTGTAATACGACTCACTATAGATGGCCAGCAAAGGAGAAGA -3'

Reverse primer

5’- ATTGTAATACGACTCACTATAGGCTTTTGTAGAGCTCATCCAT -3’

H1

Forward primer

5’- ATTGTAATACGACTCACTATAGATGTCTGATTCTGCAGTTGC -3’

Reverse primer

5’- ATTGTAATACGACTCACTATAGTTACTTTTTGGCAGCCGTAG -3’

ChIP primer

cyc

Forward primer 5’- TCTAGCTGACTTCTCCTCGT -3’

Reverse primer 5’- TGCAGCCACGTTCACACTG -3’

Klp38B

Forward primer 5’- TGCGAGGTCGTTTCACTTTG -3’

Reverse primer 5’- CCACACACATTCACACGTAG -3’

stau

Forward primer 5’- TTCAAGGACCCAGACCCAAA -3’

Reverse primer 5’- ATCGACTATTGTGCAGCCCT -3’

thread

Forward primer 5’- CGTGTTGGAGAGAGAAAGGT -3’

Reverse primer 5’- CGAGAACGCAGAACCGACA -3’

CG4914

Forward primer 5’- TCTTCTGCCTGCTGGTTATG -3’

Reverse primer 5’- TGTGGGGGCTTGGGTAAAAT -3’

Act57B

Forward primer 5’- CCTCGCTGTGTGTATTCGTT -3’

Reverse primer 5’- GCTGTTGGGTCCTTTGTCTA -3’

CG8190

Forward primer 5’- GCAAAAAGGGTCATCTGACTT -3’

Reverse primer 5’- CCAGTACCACAACAATGACC -3’

CG8066

Forward primer 5’- ATCTCGGATCCATTGTCCAG -3’

Reverse primer 5'- CACTCCAACAAAAGCTCCAG -3'

CG1473

Forward primer 5'- CGAAATTGGTGCTCTTCTCTT -3'

Reverse primer 5'- GCAGGAGGAACACGTCAGA -3'

CG15015

Forward primer 5'- GATAGAGAGCGATGCAACTG -3'

Reverse primer 5'- GGTCTCTGGTCACACTGCA -3'

amd

Forward primer 5'- GGAGTTCCCCCCCAAACT -3'

Reverse primer 5'- CGCTCCAAGGATAAAAGTCCA -3'

swallow

Forward primer 5'- AATGGCGCTGTATCCCGC -3'

Reverse primer 5'- CTGACATCCGGCGTTAGTG -3'

CG14141

Forward primer 5'- TGAAATGTGGAAATGCGGCG -3'

Reverse primer 5'- CGTGGCCAGCATTAATAGCC -3'

aquaporin

Forward primer 5'- GAATGCAGTGCACAAGCAAG -3'

Reverse primer 5'- ACGTCAGGACCCAGTGGAT -3'

Lipase 1

Forward primer 5'- ACCACACTGAGAGTCGAATC -3'

Reverse primer 5'- GCGCAATGTTGTTGTCTGATC -3'

Cyp12e1

Forward primer 5'- TCACCCGCTGAGAAAAAGAG -3'

Reverse primer 5'- GGGTCCCGGAATATCAGCA -3'

BBS2

Forward primer 5'- CTCGTTCTATGTGGAATTCTC -3'

Reverse primer 5'- GGCCAATGCGTTGCAAATTG -3'

Ance-4

Forward primer 5'- GCTGCAGTTGCGCACTAAAA -3'

Reverse primer 5'- CTCGCTGATTAGGCTTATCA -3'

Hsp70-1

Forward primer 5'- TGCGAGAGCCGTCCCTTG -3'

Reverse primer 5'- CGACATCGTGCTCGTCGG -3'

Hsp70-4

Forward primer 5'- CCACTCGCATTCCCAAGGT -3'

Reverse primer 5'- TCTAGAGGTTATTCGCTGGC -3'

RNA ChIP primer

Hsp23

Forward primer 5'- TACGCTTACATCCCATGGGT -3'

Reverse primer 5'- GACATCGAGAAGGGACACG -3'

Hsp70-1

Forward primer 5'- TGCGAGAGCCGTCCCTTG -3'

Reverse primer 5'- CGACATCGTGCTCGTCGG -3'

Hsp70-4

Forward primer 5'- CCACTCGCATTCCCAAGGT -3'

Reverse primer 5'- TCTAGAGGTTATTCGCTGGC -3'

CG8066

Forward primer 5'- CAACGTTCCAATTGTAGGCG -3'

Reverse primer 5'- GTAAAACCTTCTACCAGGTGT -3'

CG8190

Forward primer 5'- GAGTTCCAGGCCGTAGTTTT -3'

Reverse primer 5'- ATAGGCTGACATTGCTGACG -3'

2. Sex-specific role of *Drosophila* HP1 in regulating chromatin structure and gene transcription (*Nature Genetics*, in press)

Lu-Ping Liu[1,3], Jian-Quan Ni[1,3], Yan-Dong Shi[1,2], Edward. J. Oakeley[1] & Fang-Lin Sun[1]

[1]Friedrich Miescher Institute for Biomedical Research, Maulbeerstrasse 66, Basel, CH 4058, Switzerland.

[2]Present address: Institut für Zellbiologie, Schafmattstr. 18, ETH Hönggerberg HPM F 28, Zürich, CH-8093, Switzerland.

[3]Both authors contributed equally to this work.

Abstract

Drosophila heterochromatin protein 1- HP1[1] is believed to be involved in active transcription, transcriptional gene silencing, and the formation of heterochromatin[2-7]. However, little is known about the function of HP1 during development. Using a Gal4-induced RNA interference system, we show that conditional depletion of HP1 in transgenic flies results in preferential lethality in male flies. Cytological analysis of mitotic chromosomes reveals that HP1 depletion causes sex-biased chromosomal defects, including telomere fusions. The global levels of specific histone modifications, particularly the hallmarks of active chromatin, are preferentially increased in males as well. Expression analysis revealed that approximately twice as many genes are specifically regulated by HP1 in males compared to females. Furthermore, HP1-regulated genes showed greater enrichment for HP1 binding in males. Taken together, these results reveal that HP1 modulates chromosomal integrity, histone modifications, and transcription in a sex-specific manner.

Text

Mutations in *Drosophila HP1* cause lethality at larval stages, precluding a systematic functional analysis of *HP1* during development[2,8]. To circumvent this limitation, we have studied the role of HP1 using a Gal4-inducible RNA interference (RNAi) system (see legend to Fig. 1*a*), which enables to deplete HP1 in a tissue- and development-specific manner.

Drosophila melanogaster y w^{67c23} embryos were transformed with a construct expressing dsRNA from an HP1 cDNA[9] (Fig. 1*a*). To deplete HP1, four independent transgenic lines (*HP1-2, -11, -21* and *-31*) were crossed with an act-Gal4 line (*y w; +/+; act-Gal4/TM6B*), expressing Gal4 ubiquitously during *Drosophila* development. Resulting larval progeny from lines *HP1-11* and *HP1-21* showed approximately 90% reduction in HP1 levels, *HP1-31* a 60% reduction, and *HP1-2* no reduction (Fig. 1*b*). Those progeny with a 60-90% reduction in HP1 generally survived to the 3rd-instar larval stage. However, progeny with a 90% reduction rarely survived to the adult stage (Table 1). The lethality mainly occurred at the pupal stage, apparently due to a failure to eclose (data not shown). Adult progeny of *HP1-31/act-Gal4* were also viable. Surprisingly, however, the female/male ratio (2.4:1) was highly skewed (cf. 0.9:1 for this genotype at the larval stage). An alteration in the sex ratio was also evident in adult flies from the *HP1-11/act-Gal4* line, with all 21 survivors being female (Table 1). There were no adult *HP1-21/act-Gal4* survivors when progeny were grown at 25°C. However, 30 escapers were obtained at 18°C, all of which were again female. Collectively, these results suggested an association between sex-biased lethality and HP1 dosage.

To assess the cause of lethality on depletion of HP1, lines *HP1-21* and *HP1-11* were crossed with lines inducing RNAi exclusively in eye imaginal discs (ey-Gal4) and in the posterior compartment of developing wings (en-Gal4)[10,11]. The effect of HP1 depletion in these tissues was examined in 3rd-instar larvae. In HP1-depleted imaginal discs, we consistently found an increased number of dying cells (Fig. 1*c-f*) using acridine orange (AO) staining, which is often used to detect apoptotic cells[12]. Tissue growth defects were also observed in the eyes

and wings of adult flies (Fig. 1*i-l*), although defects in both of these tissues appeared more severe in males than in females (data not shown). The apoptosis seems to be mediated through a caspase-dependent pathway since tissue growth defects could be partially rescued by the addition of p35 (*y w; UAS-P35/UAS-P35; +/TM6B*; Fig. 1*m,n*), a cysteine protease apoptosis inhibitor[13]. These results suggest that the observed lethality and growth defects in both sexes are linked to apoptosis.

We next asked whether sex-specific lethality involves specific mitotic chromosome defects as have been observed previously in *HP1* mutants[8]. Indeed, we found a variable number of "ring-like chromosomes" and other aberrant segregated chromosomes (e.g., chromatin bridges; Fig. 2 and data not shown) in the metaphase spreads from 3rd-instar larval neuroblast cells of HP1 depleted larvae. Interestingly, the relative frequency of defective mitotic chromosomes in HP1-depleted males was approximately twice that in females, indicating that differential chromosomal segregation defects may underlie sex-biased lethality.

However, since the *HP1* mutant lethal allele *Su(var)2-5^{02}* does not result in telomeric fusions, thus lethality cannot be solely due to this cause[8]. To explore if additional mechanism(s) may be involved in the sex-biased lethality, we next measured the impact of HP1 depletion on core histone modifications, since increases in histone acetylation have been shown to cause apoptosis[14]. Using cell extracts from larval imaginal discs of HP1 RNAi mutants and control larvae, we compared the global levels of several core histone modifications in males and females. The levels of histone modifications acH4K8, metH3K4, and metH3K79 (hallmarks of active chromatin[15,16]), are all increased in males following HP1 depletion. However, levels of metH4K20 and metH3K9 (hallmarks of heterochromatin[15]) show a global decrease when cells were lysed in 300 mM salt buffer (Fig. 3a), and no change when lysed in SDS buffer (see Supplementary Fig. S1 online), suggesting that it is the changes in histone modifications associate with the active state that may play a role in the observed lethality. These effects are not caused by misregulation of genes encoding known histone-

modifying enzymes, including histone methylases, acetylases, or deacetylases, etc. as these were unaffected by HP1 depletion (see Supplementary Fig. S1 online and data not shown).

We then wondered whether any change in histone H3K9 methylation occurs on chromatin, since H3K9 methylation is known to be interdependent with the dymanics of HP1[17,18]. In polytene chromosomes from HP1-depleted mutants, H3K9 methylation remained at the pericentric heterochromatin region in both sexes (Fig. 3*b*), consistent with previous reports[17,18]. However, the intensity of the pericentric H3K9 methylation signal in males was lower than that in females (Fig. 3*b*). Histone H4K16 acetylation, a modification linked to X-chromosome dosage compensation in males[19], showed no obvious change either on western blot or in polytene chromosomes (see Supplementary Fig. S1 online).

To test the possibility that the HP1-induced preferential lethality in males is linked to the disruption of specific functional genes in males, total RNA isolated from two independent populations of male and female 3rd-instar larvae of *HP1-21/act-Gal4* (the line showing the strongest developmental defects following HP1 depletion), was compared using microarray analysis (see Methods and Supplementary Table 1-3 online). Over 200 predicted transcripts/genes were found to be specifically affected in males, but only 119 in females; 127 genes appeared to be affected in both males and females (Fig. 3*c*; see Supplementary Tables 1-3 online).

Among the affected genes with known function, genes essential for DNA replication, such as *Mus209* and *Mcm6*[20], were down-regulated in both sexes; *W* (*wrinkled*), and *Rep4*, both regulators of apoptosis[21], were up-regulated. Notably, a number of genes encoding cell cycle regulators, such as *fzy*, *pimples* (*pim*), cyclin-dependent kinase (*Cks*) subunit (*CG3738*), and the DNA replication initiation inhibitor *Geminin*, were all specifically affected only in males, suggesting a role for these genes in the observed differential lethality. Genes known to regulate the sex ratio, such as MSL[22], were not affected.

Of the 127 genes affected in both males and females, transcription of nearly two-thirds was up-regulated in the absence of HP1 (see Supplementary Table 1

online). In addition, 22 out of 24 genes which showed lower expression in wild type females were up-regulated in the female RNAi mutants (see Supplementary Table 3 online), all consistent with a known role of HP1 in transcriptional gene silencing. However, it was also noticed that nearly half of the affected genes were down-regulated in the absence of HP1, supporting the view that HP1 may play a role both in negative and positive regulation of transcription[2-7].

To determine whether the sex-biased effects of HP1 on histone modification and transcription are due to a differential distribution of HP1 on chromatin in males and females, we next performed chromatin immunoprecipitation (ChIP) analysis[23]. Sonicated chromatin extracts of nuclei isolated from male and female 3rd-instar *yw*^{67c23} larvae (see Methods) were immmunoprecipitated with polyclonal antibodies against *Drosophila* HP1 (#192; Supplementary Fig. S2 online). Among the eight genes tested that were affected in both males and females, four showed similar levels of HP1 binding enrichment in the two sexes, implying a direct role of HP1 in their transcription (Fig. 4*a*). Of 12 genes specifically affected in females, six were enriched in HP1 binding to similar levels in both sexes, the other six being HP1 negative (Fig. 4*c*). Interestingly, 11 out of 18 genes specifically affected in males showed a severalfold enrichment of HP1 binding in males compared to females, five were similarly enriched in both sexes, and two were not associated with HP1 (Fig. 4*b*). While the ChIP results indicate that genes specifically affected in males appear to be enriched in HP1 binding in males compared to females, genes specifically affected in females fail to show a “female-specific” HP1 binding pattern, indicating that HP1 might invoke sex-specific mechanisms in the regulation of chromatin/transcription.

Our results show that HP1 plays a rather different role in males and females. RNAi knock-down of HP1 results in sex-biased defective chromosome segregation, alterations in histone modifications, specific changes in transcription, and a skewed sex ratio in surviving progeny. Two recent studies[24,25] suggest that chromosomal segregation defects, particular telomeric fusion, may play a major role in the observed apoptosis and sex-biased lethality observed in this study. Overexpression of the heterochromatin protein Su(var)3-7

also induces lethality in males, with a shortened or condensed X-chromosome[26]. However, the morphology of the X-chromosome (see Supplementary Fig. S1 online and data not shown) and the global level of histone H4K16 acetylation, and its distribution (see Supplementary Fig. S1 online), seem unaffected in male HP1 knock-down progeny, suggesting an alternative mechanism.

The differential change in histone H3K9 methylation on chromatin may be due to an alteration in Su(var)3-9 localization, since HP1 is known to be essential for maintaining its dynamics[17,18]. Changes in global histone acetylation and phosphorylation could result from an HP1-induced global change in chromatin structure, or from secondary effects; the absence of a Su(var)3-9 homologue in mammals also caused changes in different histone modifications, in addition to H3K9 methylation[27]. Intriguingly, all of these changes occur in a sex-biased manner. We attribute this to the sex-specific distribution of HP1 on chromatin, demonstrated by the ChIP analysis. Based on this hypothesis, one expects to see that the male genome, relatively enriched in HP1, is subject to more changes in histone modifications, more chromosome segregation defects, and more changes in transcription in the absence of HP1, which seems to be the case (Fig. 2, Fig. 3, and see Supplementary Fig. S1 online). The presence of the heterochromatic Y chromosome in males may be involved in the sex-biased distribution of HP1 in the genome of both sexes, which alters the distribution of remaining HP1 and other heterochromatin proteins.

A previous cytological study of mealybugs revealed a conspicuous HP1-associated “mass/aggregate” structure in male chromosomes, contrasting with a scattered localization along female chromosomes[28]. This result and the results presented here both support a hypothesis that HP1 may play a distinct regulatory role in male and female chromatin. Whether the sex-specific distribution of HP1 on chromatin directly regulates the sex-biased differences in global transcription, showing relatively lower transcription in males than in females (Liu L-P and Sun F-L, unpublished data), is not clear. The fact that HP1 is known to be involved in transcriptional gene silencing[2,3], and that the depletion of HP1 also resulted in up-regulation of some male genes, normally transcribed at a lower level in males

than in females, seems to support a role of HP1 in the phenomenon. However, these sex-biased regulation mechanisms also seem to require other sex-specific regulators (e.g. proteins or RNA). Future studies are required to define those regulators and to understand their role in the organization of sex-biased chromatin and transcriptional regulation. Understanding the mechanism(s) of this regulation may also yield important clues as to the basis of sexual dimorphism in animals.

Methods:

Drosophila stocks

All fly stocks were raised on cornmeal sucrose-based medium[29] and the crosses were performed at 25°C, unless otherwise stated. Larvae or adults of the same age were used for all experiments.

P-element transformation

The P-element vector was constructed by subcloning the 617 bp of the *HP1* coding sequence into *sym-pUAST*[9] vector, in which HP1 is flanked by inverted *UAS* activator sequences and a minimal TATA box from the *hsp70* gene. Two *SV40* polyadenylation signals are used to terminate the complementary transcripts. The purified plasmid DNA was injected into *y* w^{67C23} embryos to generate transgenic flies according to the standard germline transformation procedure. Male stocks of act-Gal4 (*y w; +/+; act-Gal4/TM6B*), en-Gal4 (*y w; en-Gal4/en-Gal4*), and ey-Gal4 (*y w; ey-Gal4/ey-Gal4*) were crossed with female transgenic lines carrying the P-element. Detailed genetic information of these Gal4 stocks can be found at Fly Base: http://fly.bio.indiana.edu/gal4.ht

Staining of imaginal discs with acridine orange

Imaginal discs were prepared from the 3rd-instar larvae. Dissected discs were placed immediately into *Drosophila* cell culture medium (4°C), and then transferred with 50 μl cell culture medium onto a slide. After rinsing the discs with 100 μl medium, they were stained with 1 μg/ml acridine orange (Sigma) for 5 min at room temperature. The medium containing acridine orange solution was then removed, and the discs rinsed twice with PBS. Photographs were taken immediately after covering the discs with a coverslip.

Cytology of mitotic chromosomes and polytene chromosome staining

The dissection of brains from the 3rd instar-larvae and staining of mitotic chromosomes with DAPI were performed according to the procedure described by Fanti et al.[8].

Polytene chromosome squash and immunofluorescent staining were performed as described elsewhere[1]. The antibody against di-metH3K9 (metH3K9) was purchased from Upstate (1:50 dilution). acH4K16 (Abcam) was used at 1:100 dilution. The monoclonal antibody against HP1-C1A9 (a gift from Sarah C.R. Elgin) was used at 1:1 dilution. Secondary antibodies coupled to FITC (green, 1:100 dilution) and anti-rabbit Texas red (red, 1:300 dilution) were purchased from Milan. The DNA staining marker DAPI (Sigma) was used at a concerntration of 1×10^{-4} μg/μl. All images were taken under a deconvolution microscope (Olympus ×70), and processed using Adobe Photoshop software.

Western blotting analysis

Cell extracts used for western blotting analysis was prepared from discs of 20 3rd-instar larva. The collected discs were transferred into 100 μl lysis buffer (NP-40 buffer: 300 mM NaCl, 1% NP-40, 50 mM Tris-Cl, pH 7.8, protease inhibitor). The analysis was performed using the soluble fraction of the lysis. Twenty micrograms of protein sample was loaded onto the 15% SDS-PAGE, and then transferred onto a Hybond-P PVDF membrane.

Antibodies against the modified histones, anti-di-metH3K4 (metH3K4; 1:3,000), anti-H3S10P (H3S10P; 1:1,000), anti-di-metH3K79 (metH3K79; 1:5,000), anti-di-metH3K9 (metH3K9; 1:1,000), anti-di-metH4K20 (metH4K20; 1:1,000), and anti-acH4K8 (1:2,000), were all purchased from Upstate and used to perform immunoblotting. The loading of protein extract was monitored with anti-β-tubulin (1:500) or anti-H3 (1: dilution). Anti-acH4K16 was used at 1:1,000 dilution. Anti-HP1 antibodies (C1A9) were used at a dilution of 1:3,000. Anti-Su(var)3-9 was a gift from G. Reuter (Germany).

Microarray analysis

The extraction of total RNA was performed following a standard protocol (www.erin.utoronto.ca/~w3flyma/protocol.htm). Total RNA was isolated from two independent populations of male and female 3rd-instar larva of *HP1-21/act-Gal4* and, as controls, larval progenies from line *HP1-21* with the genotype *y w; +/+; HP1-21/*+, and larva with the genotype *y w; + /+; +/act-Gal4*. In brief, larvaa frozen in liquid nitrogen were homogenized and then resuspended in Trizol reagent by pipetting. The precipitated RNA was washed, and then dissolved in RNase-free water. Five micrograms of total RNA from each experimental sample were reverse-transcribed using the SuperScript Choice cDNA synthesis kit from Stratagene. One microgram of double-stranded cDNA was *in vitro*-transcribed using the Affymetrix IVT kit and labeled by the incorporation of biotinylated-UTP. Fifteen micrograms of cRNA were then fragmented and hybridized to Affymetrix DG GeneChips as per the manufacturer's instructions (Affymetrix, Santa Clara CA, USA).

The microarray database accession number is GSE3055

Chromatin-IP

ChIP assays were performed using formaldehyde-fixed nuclei isolated from 1,300 male and 1,300 female 3rd-instar larvae. The preparation of nuclei from larvae was performed as described[30] with some modifications. After homogenization of the larvae, the homogenized powder was resupended in 20 ml PBS buffer with 1% formaldehyde and cross-linked for 20 min at room temperature. The cross-linking was stopped by the addition of glycine (1 M) to a final concentration of 0.125 M, incubated for 10 min on ice, and spun at 1,600 g for 5 min. The pellets were then resuspended in hypotonic buffer (10 mM HEPES, pH 7.9, 1.5 mM $MgCl_2$, 10 mM KCl, protease inhibitor, 0.5 mM DTT). Subsequent procedures, such as the purification and sonication of the nuclei and IP followed a standard Upstate protocol (www.upstate.com). For each ChIP experiment, 5 μg antibodies were used. The same amount of ChIP DNA was used in all the PCR reactions for 35 cycles, which was in the linear range of amplification (Fig. 4 and data not shown). PCR products were analyzed on

agarose gels stained with ethidium bromide, and photographed. The Anti-H3 antibody was purchased from Abcam, and anti-HP1 serum (rabbit #192) was a gift from Sarah C.R. Elgin, and was further affinity-purified. The specificity of the polyclonal anti-HP1 antibody was further determined using western blotting assay, immunofluorecent staining, and pull-down analysis (see Supplementary Fig. S2 online).

References

1. James, T.C. *et al*. Distribution patterns of HP1, a heterochromatin-associated nonhistonechromosomal protein of *Drosophila*. *Eur J Cell Biol*. **50**, 170-180 (1989).

2. Eissenberg, J.C. *et al*. Mutation in a heterochromatin-specific chromosomal protein is associated with suppression of position-effect variegation in *Drosophila melanogaster*. *Proc. Natl. Acad. Sci. USA* **87**, 9923–9927 (1990).

3. Nielsen, S.J. *et al*. Rb targets histone H3 methylation and HP1 to promoters. *Nature* **412**, 561–565 (2001).

4. Lachner, M., O'Carroll, D., Rea, S., Mechtler, K., & Jenuwein, T. Methylation of histone H3 lysine 9 creates a binding site for HP1 proteins. *Nature* **410**, 116–120 (2001).

5. Grewal, S.I., & Elgin S. C. Heterochromatin: new possibilities for the inheritance of structure. *Curr. Opin. Genet. Dev.* **12**, 178-187 (2002).

6. Piacentini, L., Fanti, L., Berloco, M., Perrini, B., & Pimpinelli, S. Heterochromatin protein 1 (HP1) is associated with induced gene expression in *Drosophila* euchromatin. *J. Cell Biol*. **161**, 707-714 (2003).

7. Cryderman, D.E. *et al.* Role of *Drosophila* HP1 in euchromatic gene expression. *Dev. Dyn*. **232**, 767-774 (2005).

8. Fanti, L., Giovinazzo, G., Berloco, M., & Pimpinelli, S. The heterochromatin protein 1 (HP1) prevents telomere fusions in *Drosophila melanogaster*. *Mol. Cell* **2**, 1–20 (1998).

9. Giordano, E., Rendina, R., Peluso, I., & Furia, M. RNAi triggered by symmetrically transcribed transgenes in *Drosophila melanogaster*. *Genetics* **160**, 637-648 (2002).

10. Raftery, L.A., Sanicola, M., Blackman, R. K., & Gelbart, W. M. The relationship of decapentaplegic and engrailed expression in *Drosophila* imaginal disks: do these genes mark the anterior-posterior compartment boundary? *Development* **113**, 27-33 (1991).

11. Hauck, B., Gehring, W.J., & Walldorf, U. Functional analysis of an eye specific enhancer of the eyeless gene in *Drosophila*. *Proc. Natl.* Acad. *Sci. U S A.* **96**, 564-569 (1999).

12. Neufeld, T.P., de la Cruz, A.F, Johnston, L.A., & Edgar, B.A. Coordination of growth and cell division in the *Drosophila* wing. *Cell* **93**, 1183-1193 (1998).

13. Stennicke, H.R, Ryan, C.A., & Salvesen, G.S. Reprieval from execution: the molecular basis of caspase inhibition. *Trends Biochem. Sci.* **27**, 94-101 (2002).

14. Th'ng J.P. Histone modifications and apoptosis: cause or consequence? *Biochem. Cell Biol.* **79**, 305-311 (2001).

15. Jenuwein, T., & Allis, C.D. Translating the histone code. *Science* **293**, 1074-1080 (2001).

16. Schubeler, D. *et al*. The histone modification pattern of active genes revealed through genome-wide chromatin analysis of a higher eukaryote. *Genes Dev*. **18**,1263-1271 (2004).

17. Schotta, G. *et al*. Central role of *Drosophila* SU(VAR)3-9 in histone H3-K9 methylation and heterochromatic gene silencing. *EMBO J*. **21**,1121-1131 (2002).

18. Ebert, A*. et al.* Su(var) genes regulate the balance between euchromatin and heterochromatin in *Drosophila*. *Genes Dev*. **18**, 2973-2983 (2004). .

19. Akhtar, A., & Becker, P.B. Activation of transcription through histone H4 acetylation by MOF, an acetyltransferase essential for dosage compensation in *Drosophila*. *Mol. Cell* **5**, 367-375 (2000).

20. Christensen, T.W., & Tye, B.K. *Drosophila* MCM10 interacts with members of the prereplication complex and is required for proper chromosome condensation. *Mol. Biol. Cell* **14**, 2206-2215 (2003).

21. Bergmann *et al*. Regulators of IAP function: coming to grips with the grim reaper. *Curr. Opin. Cell Biol.* **15**, 717-724 (2003).

22. Kelley, R.L., Wang, J., Bell, L., & Kuroda, M.I. Sex lethal controls dosage compensation in *Drosophila* by a non-splicing mechanism. *Nature* **387**, 195-199 (1997).

23. Orlando, V., Strutt, H., & Paro, R. Analysis of chromatin structure by in vivo formaldehyde cross-linking. *Methods* **11**, 205-214 (1997).

24. Perrini *et al*. HP1 controls telomere capping, telomere elongation, and telomere silencing by two different mechanisms in *Drosophila*. *Mol. Cell* **15**, 467-476 (2004).

25. De Lucia, F., Ni, J.Q., Vaillant, C., & Sun, F.L. HP1 modulates the transcription of cell-cycle regulators in *Drosophila melanogaster*. *Nucleic Acids Res*. **33**, 2852-2858 (2005)

26. Delattre, M., Spierer, A., Jaquet, Y., & Spierer, P. Increased expression of *Drosophila* Su(var)3-7 triggers Su(var)3-9-dependent heterochromatin formation. *J. Cell Sci.* **117**, 6239-6247 (2004).

27. Peters, A.H. *et al*. Loss of the Suv39h histone methyltransferases impairs mammalian heterochromatin and genome stability. *Cell* **107**, 323-337 (2001).

28. Bongiorni, S., Mazzuoli, M., Masci, S., & Prantera, G. Facultative heterochromatization in parahaploid male mealybugs: involvement of a heterochromatin-associated protein. *Development* **128**, 3809-3817 (2001).

29. Shaffer, C.D., Wuller, J.M., & Elgin, S.C. Raising large quantities of *Drosophila* for biochemical experiments. *Methods Cell Biol*. **44**, 99-108 (1994).

30. Sun, F.L. *et al*. The fourth chromosome of Drosophila melanogaster: interspersed euchromatic and heterochromatic domains. *Proc Natl Acad Sci U S A.* **97**,5340-5345 (2000).

Acknowledgements: We thank Sarah C. R. Elgin for providing us with monoclonal (C1A9) and polyclonal antibodies (rabbit #192) against *Drosophila* HP1, and Gunter Rueter for generously providing antibody against *Drosophila* Su(var)3-9. Our colleagues D. Schübeler and A. Peters are gratefully acknowledged for their critical reading of the manuscript. Sara Oakeley and Helen Rothnie are acknowledged for their helps on nomenclature. This work was supported by the Novartis Research Foundation.

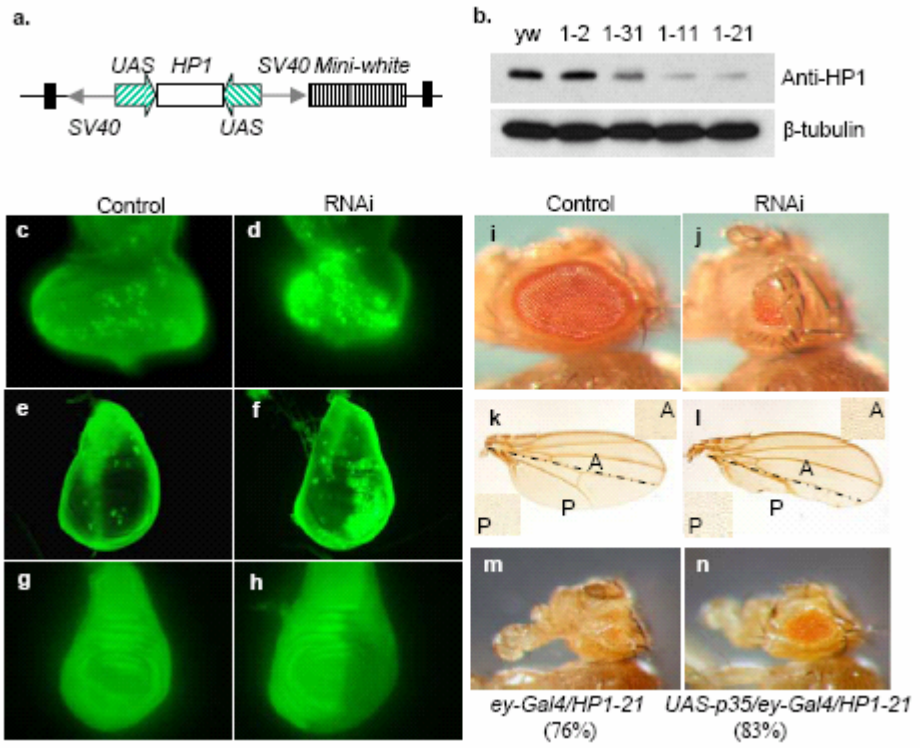

Figure 1 Depletion of HP1 causes growth defects and apoptosis in transgenic flies.

a, Schematic map of the construct used to produce *HP1* RNAi transgenic flies. The full-length *HP1* cDNA (white bar), is subcloned in *sym-pUAST* vector9. The *mini-white* reporter (shaded bar), the inverted *UAS* activator sequences (large inverted arrows), and *SV40* polyadenylation signals (grey arrows) are all indicated. The double-stranded HP1 RNA produced triggers the Dicer/siRNA machinery, resulting in degradation of endogenous HP1 mRNA10. ***b***, Reduction in HP1 levels in larval tissues using HP1 RNAi strategy. The blot was then hybridized with anti-HP1 (C1A9); anti-β-tubulin antibodies were used as loading control. yw: *y w67c23*; 1-2: HP1-2/act-Gal4 (*y w; +/+; HP1-21/act-Gal4*); 1-31: HP1-31/act-Gal4 (*y w; HP1-31/+; +/act-Gal4*); 1-11: HP1-11/act-Gal4 (*y w; HP1-11/+; +/act-Gal4*); 1-21: HP1-21/act-Gal4 (*y w; HP1-21/+; +/act-Gal4*). ***c-f***, Acridine orange (AO) staining (green) of eye (*c, d*) and wing (*e, f*) discs from female progeny of control *y w67c23* (*c, e*) and mutant (*d y w; ey-Gal4/+; HP1-21/+*; *f, y w; +/en-Gal4; HP1-21/+*) 3rd-instar larvae. ***g, h*** Expression of HP1 in control (*g*) and HP1-depleted (*h*) wing discs as indicated by monoclonal antibodies against *Drosophila* HP1 (C1A9; green). *i, j y w; +/ey-Gal4; +/HP1-21* progeny (*j*) showed eye defects in comparison with the control (*i*). ***k, l*** The anterior (A) and posterior (P) compartments of wings from control line *y w; +/+; HP1-21/+* (*k*) and HP1-21 progeny *y w; +/en-Gal4; +/HP1-21* (*l*) are indicated. The cell densities in the anterior and the posterior compartment are shown at the corners of *k* and *l*. ***m, n*** The eye defect observed in *y w; ey-Gal4/Cyo; HP1-21/+* progeny (*m*) is partially rescued by co-expression of the apoptosis inhibitor p35 (*n*); the percentage of progeny exhibiting the eye phenotype is indicated.

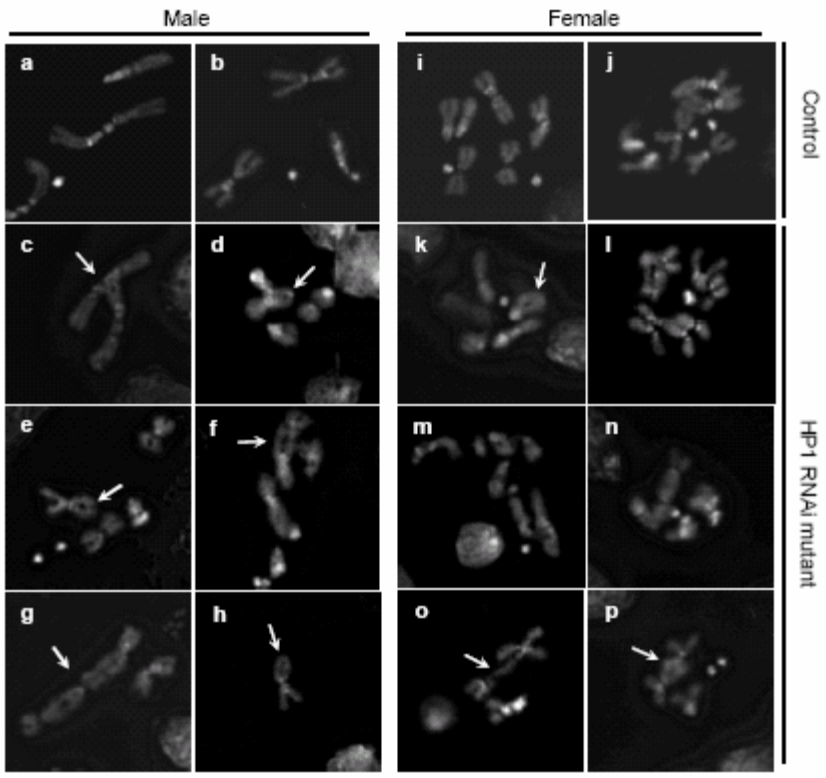

Figure 2. Depletion of HP1 causes defective mitotic chromosomes to different extents in males and females. Mitotic chromosomes from male (*a, b*) and female (*i, j*) control neuroblast cells are shown. *c-h*, *k-p* Mitotic chromosomes exhibiting defects, including fused telomeres (white arrows), in male (*c-h*) and female (*k-p*) RNAi mutant (HP1-21/act-Gal4) neuroblast cells.

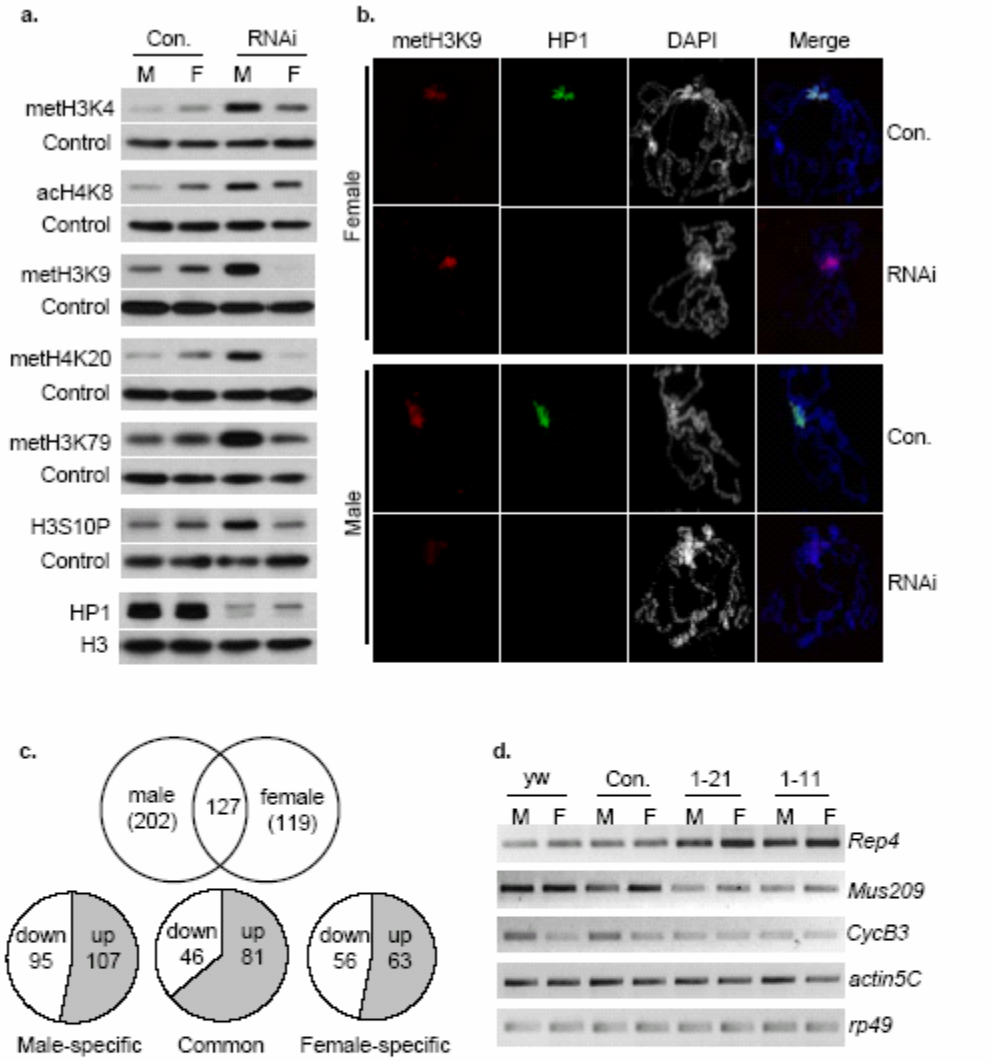

Figure 3 HP1 regulates the dynamics of histone modification and transcription sex-specifically.

a, Changes in histone modification before (con.) and after HP1 depletion (RNAi). Cell extract from control (Con.) larval discs of males (M), females (F) and the mutants depleted of HP1 (RNAi) were loaded into the 15% SDS PAGE. The names of the antibodies, including HP1 and differentially modified core histones are indicated to the left of the gels. As control, the same blot was hybridized with anti-β-tubulin. The equal loading detected by anti-β-tubulin was similar to that of anti-histone H3 (H3). ***b***, Chromatin-bound di-metH3K9 (metH3K9) is reduced in males. Polytene chromosomes from females *y w67c23* control (top row, con.), and RNAi mutant (HP1-21/act-Gal4) (second row; RNAi), and male *y w67c23* control (third row, con.), and RNAi mutant (bottom row, RNAi), are stained with anti-di-metH3K9 (metH3K9; red), anti-HP1 (C1A9, green) and DAPI (grey or blue). ***c***, Total number of genes affected by loss of HP1 in males (male) and females (female), as well as the number of genes up-regulated (up, grey) and down-regulated (down, white) in each sex. ***d***, Impact of HP1 depletion on transcription of specific genes (*Rep4*, *Mus209*, *CycB3*) as confirmed by RT-PCR. *Rep4* was commonly up-regulated, and *Mus209* was commonly down-regulated, both in males and females. *CycB3* was male-specifically down-regulated. *actin5C* and *rp49* were used as constitutively expressed controls. yw: *y w67c23*; Con.: *y w; +/+; HP1-21/+*; 1-21: *y w; +/+; HP1-21/act-Gal4*; 1-11: *y w; HP1-11/+; +/act-Gal4*.

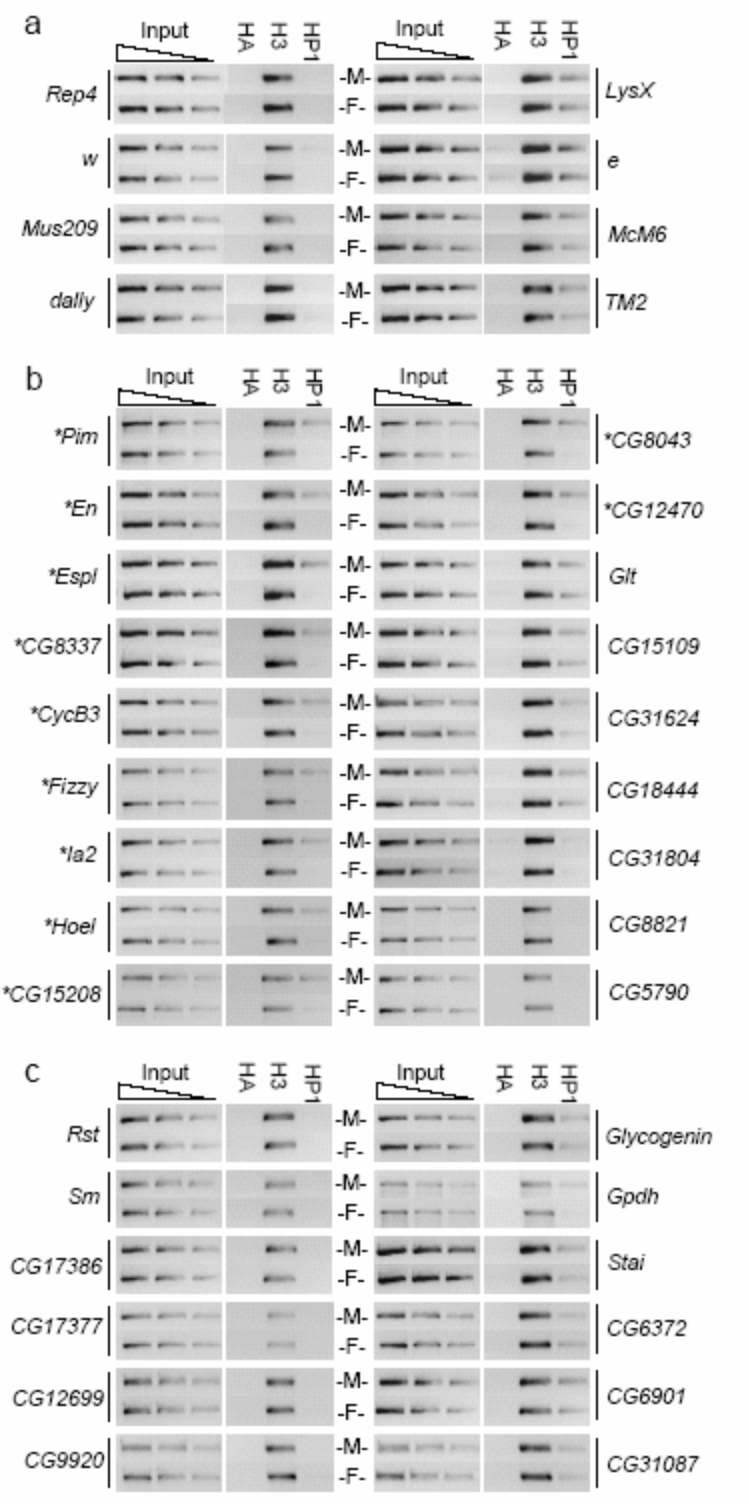
a
Input
HA
H3
HP1
Input
HA
H3
HP1
Rep4
-M-
-F-
LysX
w
-M-
-F-
e
Mus209
-M-
-F-
McM6
dally
-M-
-F-
TM2
b
Input
HA
H3
HP1
Input
HA
H3
HP1
*Pim
-M-
-F-
*CG8043
*En
-M-
-F-
*CG12470
*Espl
-M-
-F-
Glt
*CG8337
-M-
-F-
CG15109
*CycB3
-M-
-F-
CG31624
*Fizzy
-M-
-F-
CG18444
*Ia2
-M-
-F-
CG31804
*Hoel
-M-
-F-
CG8821
*CG15208
-M-
-F-
CG5790
c
Input
HA
H3
HP1
Input
HA
H3
HP1
Rst
-M-
-F-
Glycogenin
Sm
-M-
-F-
Gpdh
CG17386
-M-
-F-
Stai
CG17377
-M-
-F-
CG6372
CG12699
-M-
-F-
CG6901
CG9920
-M-
-F-
CG31087

Figure 4 A subset of genes specifically affected in males shows male-specific enhanced HP1 binding.
a-c, Physical binding of HP1 in the genes tested as determined by ChIP. ***a,*** Enrichment of HP1 in genes commonly regulated by HP1 in both males and females. ***b,*** Genes specifically affected in males. ***c,*** Genes specifically affected in females. DNA from the chromatin of male (M) and female (F) larvae is indicated. The names of the genes tested, or their CG numbers, and the antibodies used to perform the ChIP analysis are indicated. The 11 genes marked with asterisks show a severalfold enrichment of HP1 binding in males compared to females. PCR products from input DNA (representing 0.1%, 0.05%, 0.025% of total input DNA) from male and female larval chromatin are also shown. As negative and positive controls, we used polyclonal antibodies against haemagglutinin (HA) and histone H3, respectively.

Table 1. Depletion of HP1 causes altered sex ratio in *D. melanogaster*.

Parents			Number of progeny		Ratio of female/male	
male		female	Gal4	Tb	Gal4	Tb
Larval stage						
yw;+/+;act-Gal4/TM6B	x	*yw;+/+;HP1-2/HP1-2*	302	ND	1.54	ND
yw;+/+;act-Gal4/TM6B	x	*yw;HP1-31/HP1-31*	623	ND	0.92	ND
yw;+/+;act-Gal4/TM6B	x	*yw;HP1-11/SM5-Tb*	395	ND	1.03	ND
yw;+/+;act-Gal4/TM6B	x	*yw;+/+;HP1-21/HP1-21*	464	ND	1.09	ND
Adult stage						
yw;+/+;act-Gal4/TM6B	x	*yw;+/+;HP1-2/HP1-2*	912	551	1.28	1.17
yw;+/+;act-Gal4/TM6B	x	*yw;HP1-31/HP1-31*	907	521	2.37	1.27
yw;+/+;act-Gal4/TM6B	x	*yw;HP1-11/SM5-Tb*	21	526	21/0	1.26
yw;+/+;act-Gal4/TM6B	x	*yw;+/+;HP1-21/HP1-21*	0	568	0/0	1.38

Table 1. The genotype of the parents used to perform the crosses and the number of progeny from their crosses with the Gal4 driver or balancer are listed. ND: not determined. Progeny were counted at the 3rd-instar larval and at the adult stages (1-5 days old). Tb, tubby.

Figure S1

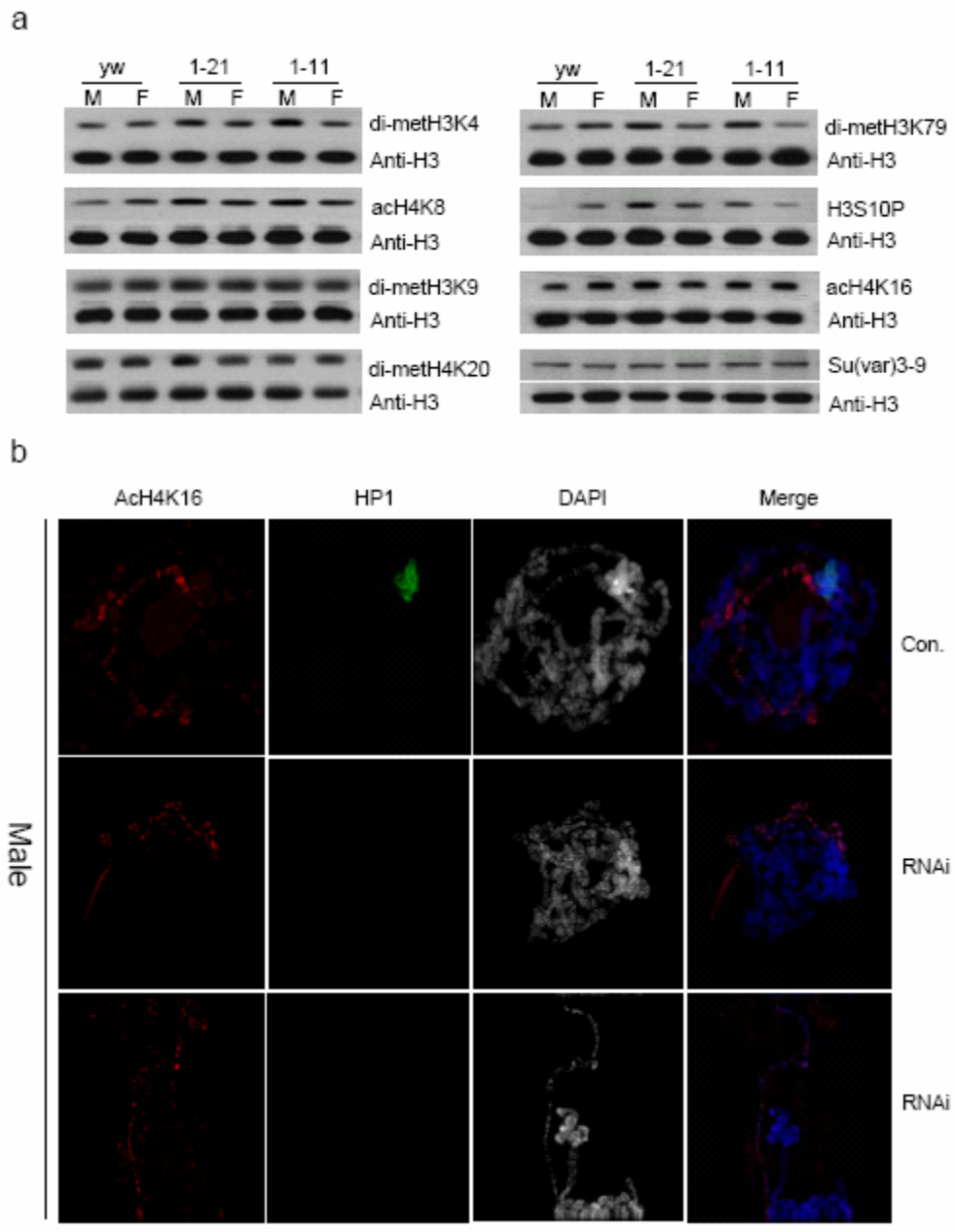
a
yw
1-21
1-11
M F M F M F
di-metH3K4
Anti-H3
acH4K8
Anti-H3
di-metH3K9
Anti-H3
di-metH4K20
Anti-H3
yw
1-21
1-11
M F M F M F
di-metH3K79
Anti-H3
H3S10P
Anti-H3
acH4K16
Anti-H3
Su(var)3-9
Anti-H3
b
AcH4K16
HP1
DAPI
Merge
Male
Con.
RNAi
RNAi

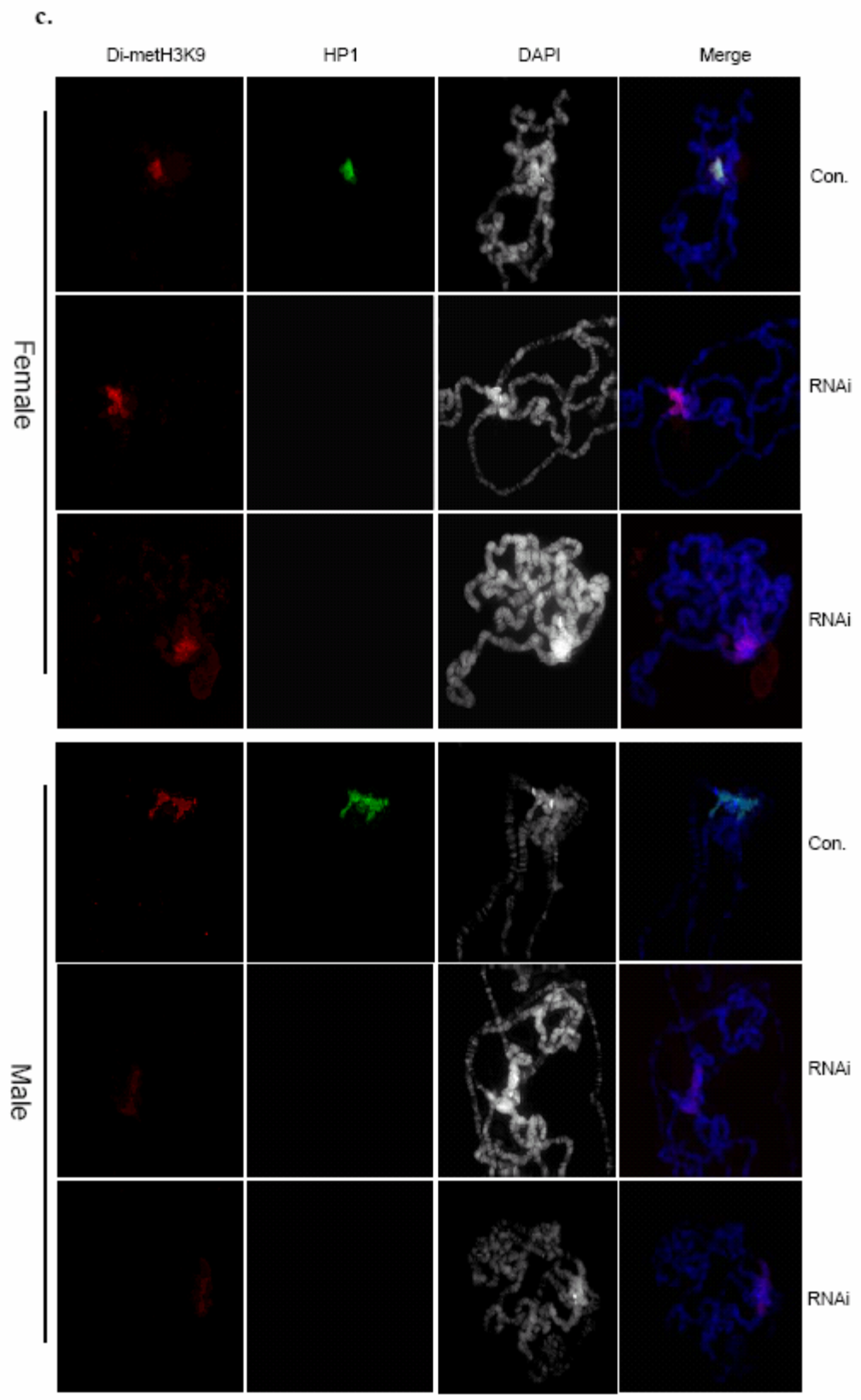
c.
Di-metH3K9
HP1
DAPI
Merge
Female
Male
Con.
RNAi
RNAi
Con.
RNAi
RNAi

Figure S1.

a, Specific increase of global histone modification in male RNAi mutants. Imaginal discs from male (M) or female (F) wild type *y w67c23* (yw) 3rd-instar and RNAi mutant 1-21/act-Gal4 (1-21) and 1-11/act-Gal4 (1-11) larvae were lysed in HEMGN buffer (25 mM HEPES, pH 7.6, 0.1 mM EDTA, 12.5 mM MgCl, 10% glycerol, 0.1% NP40, 1 mM DTT, 0.3 M KCl, proteinase inhibitor), then added to an equal volume of 2x SDS buffer (20 mM sodium phosphate, 4% SDS, 0.001% bromophenol blue, 0.2 M DTT, 2% glycerol) as described (Swaminathan et al., 2005). Aliquots (1.5 µg) of extract were resolved by 15% SDS PAGE, transferred to nylon membrane, and subjected to Western blot analysis with the antibodies indicated to detect changes in histone modification. The loading in each lane was monitored using anti-H3. For Su(var)3-9, we used 20 µg of extract (lysed in NP40 buffer) in each lane. *yw*: extracts from *y w67c23*. 1-21: *y w; +/+; HP1-21/act-Gal4*. 1-11: *y w; HP1-11/+; +/act-Gal4*.

b, The distribution of acetylated histone H4K16 (acH4K16, red) on X chromosomes from the *y w67c23* control (control) and HP1-depleted (RNAi; *y w; +/+; HP1-21/act-Gal4*) male larvae are shown. The localization of HP1 (green) and DAPI staining (grey or blue) are also indicated.

c, The distribution of di-metH3K9 (red) and HP1 (C1A9; green) on polytene chromosomes from 3rd-instar larva of *y w67c23* control (control) and HP1-depleted (RNAi; *y w; +/+; HP1-21/act-Gal4*) males and females are shown. DAPI staining is in grey or blue.

Figure S2

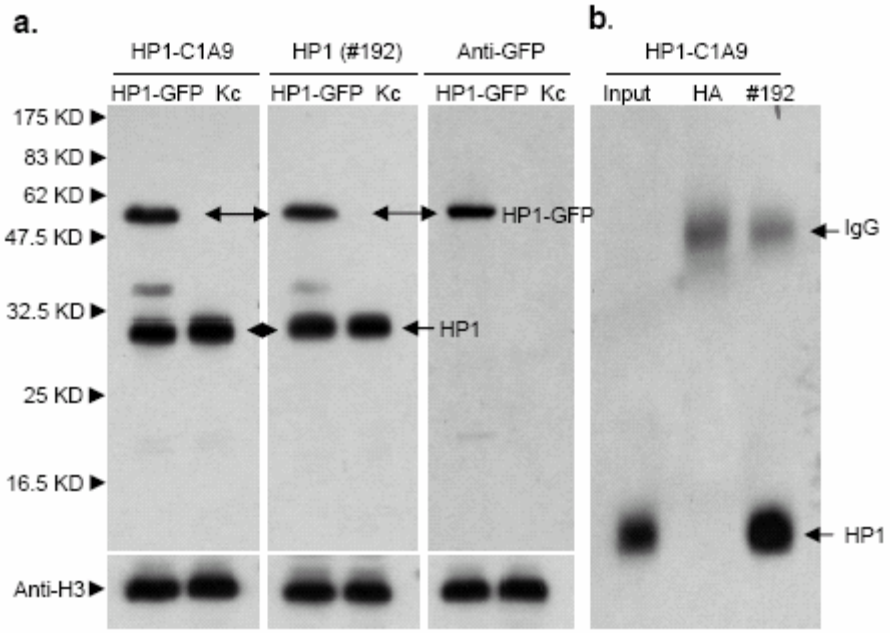
a.
HP1-C1A9
HP1 (#192)
Anti-GFP
HP1-GFP Kc
HP1-GFP Kc
HP1-GFP Kc
175 KD
83 KD
62 KD
47.5 KD
32.5 KD
25 KD
16.5 KD
Anti-H3
HP1-GFP
HP1
b.
HP1-C1A9
Input
HA
#192
IgG
HP1

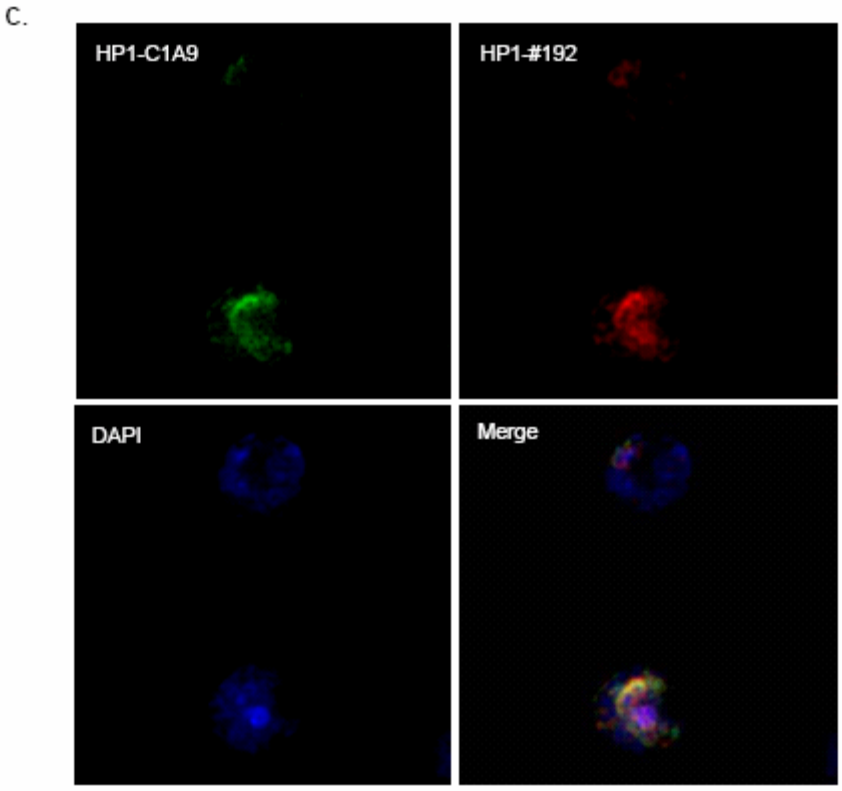
C.
HP1-C1A9
HP1-#192
DAPI
Merge

Figure S2.

a, The anti-HP1 polyclonal antibody #192 specifically recognizes HP1. Aliquots (20 µl) of whole cell extracts from wild type Kc cells or Kc cells expressing an HP1-GFP fusion protein were lysed in NP-40 buffer (see details in Methods) and resolved by 15% SDS PAGE. After transfer to nylon membrane, proteins were detected by Western blot analysis using either a monoclonal antibody against HP1 (HP1-C1A9), an affinity purified polyclonal antibody HP1 (#192), or an anti-GFP antibody. Like C1A9, the polyclonal #192 antibody recognizes both the HP1 fusion protein and native HP1 (indicated by arrows). The expression of the fusion protein HP-GFP was confirmed. Equal loading of extracts was monitored by anti-histone H3 antibody (anti-H3). The HP-GFP fusion protein construct was produced by cloning the coding sequence of GFP fused to the C-terminus of the HP1 cDNA, and then subcloning into a pIB/V5-His-TOPO vector (Invitrogen); the primer sequences used to amplify the HP1 and GFP fragments were:

b, *Drosophila* HP1 is specifically pulled down by anti-HP1 polyclonal antibody #192. Kc cell extract (600 µl; 1 µg/µl) and 5 µg of affinity purified anti-HP1 antibodies were used in each immuno-precipitation reaction. IP products were resolved by 15% SDS PAGE, and analyzed by Western blot using the C1A9 MAb. The input is also indicated. As a negative control, 5 µg of polyclonal anti-HA antibody was used to perform the IP.

c, Determining the specificity of the affinity purified #192 by immuno-localization assay. The localization of HP1 in Kc cells indicated by C1A9 (green; 1:1 dilution) and #192 (red, 1:200 dilution) is shown. DAPI staining is in blue.

Supplementary Table 1

Sample	**Control** ACT	**Control** P	**RNAi** P-ACT	**Control** ACT	**Control** P	**RNAi** P-ACT		
Sex	female	female	female	male	male	male		
Systematic	Normalized	Normalized	Normalized	Normalized	Normalized	Normalized	Genes	Products
1632974_s_at	0.818341	0.870801	1.63622	1.076176	0.800009	1.685098	CG30015	---
1634804_at	0.999851	0.889159	1.946312	0.928773	0.782684	1.543235	CG15819	---
1623160_at	0.744824	0.970921	1.872449	0.721732	1.056977	1.801354	Mmp1	Matrix metalloproteinase 1
1640235_at	1.05977	0.891314	2.27796	0.957339	0.674796	1.748936	W	Wrinkled
1628489_at	0.979296	1.000961	1.567801	0.700057	0.696493	1.489402	dally	division abnormally delayed
1623793_at	0.980343	0.999324	1.397945	0.762261	0.669639	1.384309	krz	kurtz
1623744_at	1.033307	0.944488	1.883923	0.83174	0.588497	1.234194	CG30411	---
1634960_at	1.089675	0.881497	1.578652	0.669013	0.544108	1.344912	CG14375	---
1641084_at	1.16306	0.891499	1.856376	0.905148	0.912454	1.730395	CG13897	---
1628536_s_at	1.069327	0.878623	1.93123	0.861661	0.798648	1.267846	CG11880	---
1624326_at	1.125965	0.871534	1.876165	0.717376	0.665173	1.248759	Rep4	---
1625381_at	1.048217	0.859023	4.328693	0.982669	0.845217	3.723157	Eig71Ed	Ecdysone-induced gene 71Ed
1632212_at	1.052363	0.992354	1.635651	0.629538	0.735578	1.356359	CG14401	---
1624211_at	1.106416	0.907373	2.045547	0.787148	0.834363	1.399738	CG9005	---
1640103_s_at	1.172393	0.932383	1.96205	0.596913	0.486566	1.289905	CG17224	---
1639152_at	1.259264	1.090275	1.983853	0.752154	0.700299	0.934621	Ptp52F	---
1624067_at	1.115315	0.952049	1.447368	0.583273	0.674151	1.822294	CG6704	---
1638815_at	0.745593	1.075926	3.931681	0.931672	0.764272	5.738086	CG14850	---
1633308_at	0.993128	1.012724	2.19032	0.649595	0.624732	1.315412	CG6660	---
1633857_at	0.969762	1.002456	1.337311	0.531372	0.49647	2.045065	CG13659	---
1628963_at	0.975084	1.021439	2.003125	0.651022	0.650996	2.68625	CG4716	---
1625869_at	0.077827	0.084408	0.221413	1.776744	2.212081	2.881354	Mst87F	Male-specific RNA 87F
1635007_at	1.09215	0.848432	1.569034	0.754912	0.907453	1.616827	Sulf1	Sulfated
1626917_at	1.073935	0.95176	1.319842	0.722519	0.5304	1.271276	CG31337	---
1641063_s_	0.950736	1.036622	1.573591	0.635945	0.759385	1.368085	CG3811	---
1632972_at	0.961827	0.997764	1.323816	0.600756	0.664106	1.445131	Nep3	Neprilysin 3
1630593_at	1.354255	0.388216	3.098862	0.749998	0.625669	1.881703	NLaz	Neural Lazarillo
1626884_a	0.944241	1.024499	1.383323	0.56092	0.780021	1.307579	CG32062	---
1626165_at	1.071506	1.005024	1.434974	0.47371	0.557939	0.973828	CG3754	---
1624036_at	1.167278	0.799018	1.833637	0.886051	0.68849	1.546653	CG9307	---
1633059_at	1.169202	0.691983	1.663717	0.757377	0.509284	2.593875	CG6357	---
1627499_at	1.096404	0.735495	1.9972	0.825851	0.628239	1.184454	CG2016	---
1627394_s_	1.097355	0.864671	1.99837	0.854511	0.951505	1.1915	aop	anterior open
1628224_a	1.199359	0.524757	2.295739	0.773314	0.656403	1.433567	E23	Early gene at 23
1625910_at	1.394875	0.642435	2.208411	0.656948	0.524292	1.735432	CG1773	---
1623521_at	1.402509	0.653469	3.308548	0.72202	0.472239	1.344035	CG11909	---
1624487_at	0.890195	0.383276	1.292618	1.061332	0.968253	1.937164	CG11475	---
1633293_at	1.136932	0.821836	2.825419	0.820834	0.821466	1.851492	CG10157	---
1628258_at	1.297789	0.628151	1.836855	0.727979	0.604516	1.417557	CG14526	---
1641371_at	1.299041	0.230344	5.439926	0.631828	0.69194	2.443288	CG2070	---
1637067_at	1.674959	2.24969	1.046201	0.926213	0.896153	0.669599	CG6074	---
1626031_at	1.456522	0.970836	2.335376	0.749007	0.69685	1.029225	CG12539	---

1623935_at	1.217579	0.875917	2.299987	0.505964	0.528847	1.228979	sxe2	sex-specific enzyme 2
1635894_at	1.633275	1.064108	2.137086	0.674939	0.531192	0.910006	CG30148	---
1638484_at	1.207012	0.561441	2.171237	0.887793	0.743421	1.142252	Hsp67Bc	Heat shock gene 67Bc
1637246_a	1.419818	0.640191	2.071653	0.760934	0.817836	1.153609	CG32627	---
1629056_at	0.744392	0.44282	3.586411	0.924231	1.098262	2.712335	Eig71Ea	
1638021_at	0.616442	1.51571	7.385588	0.490129	0.58158	2.137363	CG4757	---
1635522_a	1.145527	0.801308	2.8421	0.651089	0.707776	1.22168	CG12789	---
1629926_at	0.965891	0.379681	4.579994	0.972437	0.910044	1.85862	CG1342	---
1630168_at	1.644637	0.735341	2.672459	0.543462	0.613079	1.240287	CG31636	---
1634261_at	0.475769	0.34821	0.605338	1.379947	1.521158	2.120504	Cyp312a1	---
1637486_at	0.553975	0.471153	1.582642	0.975215	1.016614	1.282703	CG31698	---
1623871_at	1.632232	1.095706	2.634135	0.566678	0.552224	0.914736	CG18563	---
1634674_at	1.299541	0.566284	2.611089	0.64399	0.689124	1.932154	CG9989	---
1641304_s_at	1.08957	0.786931	2.199989	0.833831	0.902873	1.345126	CG9801	---
1625660_at	1.031463	0.887534	3.699251	0.986324	0.936989	1.325462	CG4151	---
1624889_a_at	0.999713	0.992832	1.587659	0.547834	0.844602	1.328093	l(2)k16918	---
1634547_at	1.412136	0.952002	2.334429	0.775632	0.660085	1.063299	CG32506	---
1640640_at	1.132551	0.90312	1.595592	0.542661	0.879246	1.306007	Cirl	---
1640978_at	1.18233	0.820924	1.923555	0.779189	0.481976	1.140006	CG14567	---
1628107_at	1.416074	0.88997	2.956895	0.847741	0.556481	1.151425	CG3513	---
1632457_s_at	0.999637	0.951724	1.683717	0.606333	0.851181	1.365957	mam	mastermind
1628215_s_at	1.001109	0.966274	1.390054	0.585664	0.952866	1.323838	kuz	kuzbanian
1628909_at	1.244033	0.97716	2.231814	0.823615	0.651525	1.004418	CG9686	---
1622932_s_at	1.013518	0.85522	1.510301	0.683099	0.947615	1.386796	sn	singed
1633667_at	0.945281	0.995806	1.881792	0.563733	0.992561	1.611302	Lip2	Lipase 2
1635182_at	0.97304	1.068214	1.442552	0.576294	0.925013	1.398049	wts	warts
1637032_at	0.981974	1	1.353763	0.668562	0.446958	1.164843	&bgr;4GalTB	---
1632720_at	1.032082	0.924648	1.500288	0.826551	0.602448	1.925197	LysX	Lysozyme X
1639191_at	0.598889	0.626622	0.898392	1.116301	1.545419	2.16172	CG18155	---
1638722_at	1	0.980394	1.802478	0.68102	0.485066	1.405321	CG16807	---
1626028_at	1.11137	0.966184	1.485917	0.949523	0.353828	1.419034	CG4783	---
1638959_at	1.11412	0.895942	2.322213	0.716479	0.509419	1.562364	CG8501	---
1638381_s_at	1.085623	1.131604	2.503689	0.731413	0.520432	0.973897	CG1695	---
1628150_a_at	1.036247	1.209097	2.683352	0.729322	0.44616	0.999992	CG9449	---
1630282_at	0.633773	0.543848	1.708791	1.403836	0.469698	3.371323	CG14852	---
1635987_at	0.99396	0.999999	1.465491	0.416056	0.511341	1.334831	CG12116	---
1638296_at	0.042707	0.03515	0.065842	1.960766	1.944144	2.795468	CG32064	---
1631393_at	0.180869	0.168785	0.292343	1.845201	1.783711	2.422818	CG32459	---
1639823_at	1.109305	0.044494	3.66554	0.822395	0.917921	3.03713	e	ebony
1624932_at	1.713355	1.755318	0.943082	1.049152	0.783211	0.62682	Obp49a	Odorant-binding protein 49a
632045_at	1.730983	0.875787	4.036421	0.771607	0.65904	1.065158	CG5697	---
1638575_at	1.199161	1.10205	0.781612	1.182893	0.918703	0.583618	Mcm6	Minichromosome maintenance 6
1623126_at	1.640896	1.424244	0.853701	1.103546	0.700314	0.478236	CG13912	---
1633344_at	1.763644	1.330417	0.724407	1.4686	0.813618	0.252221	CG5494	---
1624395_at	1.111283	0.931264	1.766418	0.695673	0.499452	1.067282	CG31102	---
1623545_at	1.058475	1.054492	0.683863	1.151622	0.901734	0.573257	mus209	mutagen-sensitive 209
1633272_at	1.674209	2.273213	0.625355	1.33543	0.649757	0.4337	CG9090	---

1626439_at	1.138006	1.249374	0.943805	1.039346	0.798527	0.431809	CG15353	---
1635784_a_at	1.327192	1.170296	0.814395	1.30307	0.776881	0.588201	CG32230	---
1640185_at	1.217564	1.150653	0.757802	1.178243	0.835433	0.539604	CG2076	---
1641325_s_at	1.229698	1.313734	0.537554	1.08039	0.895126	0.478822	Tm2	Tropomyosin 2
1636603_a_at	1.556157	1.521748	0.805257	1.159706	0.82068	0.500155	CG9297	---
1623398_at	3.525432	3.184863	0.733423	1.184985	0.752967	0.513904	CG4830	---
1640500_at	1.644348	1.515635	0.73563	1.277946	0.724786	0.420724	CG13678	---
1622974_at	1.383874	1.237681	0.778601	1.196202	0.608833	0.198631	CG4000	---
1623840_at	1.9638	1.743109	0.934282	1.00914	0.475414	0.282628	CG18607	---
1624362_at	1.488346	1.393918	0.711992	1.26552	0.51024	0.214742	Nplp4	Neuropeptide-like precursor 4
1626048_at	1.242472	1.394531	0.99992	0.734405	1.005037	0.428347	HLHm&ggr	
1625278_s_	1.155305	1.519901	0.651889	1.019815	0.96239	0.689676	CG31004	---
1640299_at	1.417127	1.881415	1.113963	0.909052	0.858303	0.602975	Edg91	
1623252_a	1.429108	2.171563	0.728472	1.005543	0.918109	0.576597	CG3861	---
1629747_at	1.459209	1.926453	1.12768	0.886287	0.916255	0.651169	CG8511	---
1630941_s_	1.061855	1.554466	0.764154	0.948056	1.049737	0.765467	sesB	stress-sensitive B
1626616_at	1.2111	1.670597	0.475082	0.962644	1.05547	0.334413	CG7465	---
1636813_s_	1.110539	1.654906	0.64163	1.022224	0.979193	0.827622	CG3731	---
1639457_at	1.31411	3.048061	0.918354	0.9223	1.007017	0.527304	CG32284	---
1626664_at	1.728038	2.701832	1.124239	0.913324	0.932784	0.698571	CG3285	---
1626885_at	1.32884	1.658878	1.050753	0.969911	0.843449	0.523784	CG11752	---
1631474_s_	1.556591	2.171935	0.561499	1.080445	0.921494	0.719369	l(2)k05713	---
1624101_at	1.621065	2.976731	0.875708	1.044155	0.923498	0.621571	Cyp6a23	---
1638593_a	1.153216	1.417775	0.580238	1.035028	0.955659	0.622411	ND75	
1632461_at	1.908253	2.510193	0.812523	0.996066	1.005805	0.644827	CG31233	---
1639394_at	0.821226	0.999893	0.49723	1.298658	1.265099	0.979055	m1	
1632695_at	1.461242	1.727834	1.055785	0.830094	0.913742	0.496228	CG18585	---
1638896_at	1.61802	2.797859	1.030672	0.974674	0.886479	0.403461	CG1919	---
1631639_at	1.132325	2.040704	0.662261	0.999999	0.9922	0.342951	TpnC47D	Troponin C at 47D
1641286_s_at	1.098448	0.977774	0.555477	1.212493	1.023378	0.573285	Hsp60	
1638324_s_at	0.830578	0.910929	0.587818	1.841823	1.810598	1.108604	CG6921	---
1626002_at	0.926102	0.853608	0.621802	1.779027	1.896624	1.128256	Roe1	---
1629785_a_at	1.486507	1.554845	1.186122	0.796752	0.724869	0.566048	Sp1	Buttonheat promoter construct of Schock
1622893_at	1.183933	0.91785	0.582881	1.184157	1.102222	0.177721	CG16844	---
1624509_at	2.207224	2.288856	1.446063	0.59201	0.583217	0.359523	LvpL	Larval visceral protein L
1632421_at	0.850769	0.81453	0.656415	1.613982	1.827051	1.162828	CG9531	---
1639287_at	1.421636	1.183724	0.72269	1.016998	0.99869	0.310936	CG9877	---
1636210_at	0.664466	0.700866	0.549033	2.39078	2.830486	1.343717	CG10191	---

Supplementary Table 2

Samples	**Control** ACT	**Control** P	**RNAi** P-ACT	**Control** ACT	**Control** P	**RNAi** P-ACT		
Sex	female	female	female	male	male	male		
Systematic	Normaliz	Normaliz	Normaliz	Normaliz	Normaliz	Normaliz	Genes	Products
1634828_at	1.138497	1.227905	1.547154	0.460631	0.597291	0.932611	CG7297	---
1637422_at	1.435426	0.899335	1.272348	0.625198	0.69449	1.095447	CG3246	---
1627509_s	1.000063	1.113926	0.999953	0.515819	0.551066	1.144077	hoe1	hoepel1
1636269_at	0.559449	0.458751	0.614381	1.539535	1.316554	2.626473	CG33191	---
1636217_at	1.243021	0.90129	1.193396	0.550269	0.610719	1.050972	CG30503	---
1632422_s	0.665504	0.469685	0.568136	1.378934	1.458802	2.831505	CG12901	---
1632658_a	1.238474	1.105128	1.19521	0.580854	0.470816	0.9323	CG14616	---
1630515_s	1.207252	0.825524	1.272951	0.658132	0.605456	1.416153	Glt	Glutactin
1628332_at	1.454937	1.10224	1.461827	0.549046	0.51747	0.894059	CG14990	---
1639359_at	1.111964	2.458039	1.059791	0.51153	0.661243	0.95947	CG31974	---
1640559_at	0.578779	0.443711	0.539311	1.660265	2.282655	3.925098	CG13661	---
1626022_at	1.11405	1.049804	1.081129	0.5824	0.507409	0.917446	Cyp12e1	---
1639868_at	2.506223	0.926226	2.979462	0.533028	0.609719	1.042295	CG1702	---
1626554_at	0.982199	1.473394	1.07924	0.624857	0.702578	1.298289	CG16777	---
1627514_at	0.517841	0.552544	0.614344	1.699141	1.406448	3.161904	CG14294	---
1640827_at	1.007482	1.225057	1.003691	0.637315	0.586232	1.023684	CG15422	---
1641191_s	1.501169	1.97804	1.014867	0.631832	0.552029	0.990263	Ugt36Bc	---
1635110_at	0.974161	1.031448	1.115725	0.606425	0.566759	1.178973	Cyp6a13	---
1638275_at	0.746194	1.987678	1.266803	0.793958	0.79424	1.217282	CG11699	---
1639817_at	0.40311	0.396797	0.373885	1.592287	1.784292	3.027838	Roc1b	---
1637848_at	0.473033	0.422222	0.455758	1.562466	1.804365	2.717936	CG6873	---
1629674_s	0.694778	0.531369	0.719344	1.310146	1.281715	1.776555	CG10999	---
1640703_at	0.661579	0.865062	0.783485	1.237656	1.175479	1.729995	CG30460	---
1623535_at	0.268061	0.282129	0.341801	1.925927	1.855536	4.304127	CG7164	---
1639383_a	0.429355	0.341647	0.463347	1.65997	1.71949	3.241289	CG16716	---
1632611_at	0.525052	0.460917	0.376214	2.213973	2.197892	1.448339	CG15136	---
1624908_at	0.310066	0.342689	0.359392	1.633547	1.702351	2.940303	CG15287	---
1640377_s	4.548316	1.043168	5.626966	0.588284	0.594569	0.996692	Rala	Ras-related protein
1640222_s	0.995351	1.17313	1.012957	0.663309	0.690473	1.336535	CG13124	---
1627880_at	0.625435	0.463941	0.425206	1.423089	1.684359	2.888215	CG30334	---
1635126_a	0.999724	1.47235	1.001505	0.61101	0.687253	1.960108	Ect4	---
1633858_at	0.397143	0.353089	0.329166	1.623362	1.753861	2.607259	CG4286	---
1634373_a	1.382545	2.589286	1.064705	0.584868	0.69181	0.919278	CG13492	---
1628162_at	0.890582	1.689421	1.111011	0.743486	0.704726	1.14942	CG9757	---
1627528_at	0.516774	0.430484	0.511303	1.465782	1.581117	2.47577	CG8257	---
1634645_at	0.599793	0.549337	0.527046	1.404892	1.625786	2.03236	CG31245	---
1625499_at	0.292119	0.246537	0.267923	1.673091	1.82539	2.768136	CG3809	---
1628574_at	0.386617	0.339016	0.414245	1.835226	1.623656	2.825987	CG14402	---
1639775_at	0.437656	0.367969	0.388593	1.655215	1.669799	2.515543	CG5388	---
1633373_at	0.301606	0.282188	0.301576	1.768958	1.706016	2.53164	CG2750	---
1627813_at	0.370292	0.262289	0.333854	1.734593	1.897099	3.368496	CG10113	---
1625789_at	0.128035	0.192715	0.178404	1.818588	2.685723	4.777317	CG5790	---

1633657_at	0.358232	0.228072	0.289108	1.668236	2.210892	2.964165	CG31533	---
1631316_a	0.330741	0.302044	0.334494	1.675501	1.765181	2.26575	CG6262	---
1626713_at	0.465809	0.371749	0.42098	1.560327	1.544773	2.411302	CG6629	---
1636453_at	0.269524	0.240561	0.247432	1.733926	1.763751	2.488443	CG4988	---
1624860_at	0.483276	0.424272	0.435564	1.632212	1.51263	3.031388	CG31804	---
1638077_at	0.16865	0.167319	0.174495	1.865069	2.324797	3.330489	CG7634	---
1637080_at	0.144902	0.108894	0.120541	1.903982	2.276731	3.235423	CG9129	---
1634271_at	1.622674	0.791354	1.260962	0.419312	0.461126	2.581033	Def	Defensin
1638215_at	0.197788	0.234522	0.194361	1.849549	1.854075	2.358267	CG8043	---
1624460_s	0.09042	0.11622	0.105345	3.169138	3.056181	1.944354	CG31624	---
1640373_at	0.221498	0.223912	0.194732	1.787962	2.106409	2.629912	CG4701	---
1638838_at	0.221536	0.226098	0.212189	1.842059	2.059492	2.700835	CG13030	---
1630353_at	0.172302	0.143071	0.166151	1.836416	1.959142	2.658628	---	---
1638196_at	0.968343	1.034397	1.535754	0.77946	0.769199	1.675846	&agr;Try	&agr;Trypsin
1637151_at	1.020778	1.131289	0.94479	0.643429	0.765561	1.343665	mre11	meiotic recombination 11
1634430_at	0.974672	1.022593	1.178462	0.621073	0.734278	1.258812	CG14614	---
1628715_a	0.994276	1.126906	1.262396	0.658651	0.501585	1.072213	Karl	---
1628174_at	1.024935	1.105655	0.999152	0.566652	0.636847	1.231718	CG33119	---
1634640_at	1.103929	0.952686	1.131391	0.584784	0.600475	1.171685	Cyp4ac1	---
1637378_s	0.950025	1.115921	1.301972	0.724241	0.874532	1.771718	ia2	---
1631173_at	1.282686	0.981613	1.336924	0.633175	0.515766	1.070108	CG5560	---
1638400_at	1.204586	1.209008	1.06972	0.593481	0.607088	0.99533	CG8503	---
1627041_s	1.053398	1.392524	1.097635	0.596347	0.54344	0.977152	ine	inebriated
1634818_s	1.078461	1.383598	1.033889	0.720974	0.669651	0.953106	CG2165	---
1630363_at	1.35971	0.991208	1.358309	0.635986	0.581636	1.000966	CG10469	---
1638447_s	0.814987	0.844414	0.899019	1.969783	1.74725	1.051826	CG11141	---
1630818_at	0.590667	0.755123	0.637342	1.344916	1.324608	3.281416	CG30178	---
1626949_at	1.058788	0.959397	1.235279	0.561009	0.668445	1.214061	CG11158	---
1636976_at	0.942522	1.332975	1.083361	0.47181	0.488335	1.127683	CG5322	---
1630831_at	1.160752	1.572013	0.949671	0.583995	0.65393	1.51407	CG7695	---
1636693_at	1.203243	1.207308	1.032654	0.54504	0.676676	0.984117	CG4330	---
1641476_a	0.968753	1.120143	0.999609	0.719415	0.666058	1.418425	Timp	Tissue inhibitor of metalloproteases
1638910_at	0.572329	0.880083	0.711093	1.545296	1.160023	2.536567	CG5561	---
1625133_at	1.047256	1.112631	1.359906	0.547217	0.488564	0.988549	CG14131	---
1641426_at	0.570878	0.51585	0.668131	1.323069	1.772641	3.814583	CG13843	---
1632714_at	0.892819	0.467681	1.108506	1.103782	0.907199	1.644637	CG15711	---
1635453_at	0.934229	1.033674	1.050212	0.768094	0.892067	1.562388	CG13095	---
1631755_at	1.416274	0.612959	1.630393	0.807775	0.594123	1.194539	CG1236	---
1633720_s	0.93247	1.034874	1.087201	0.74557	0.849305	1.509902	CG8795	---
1635442_a	1.253797	0.961676	1.518374	0.665202	0.507455	1.05837	GRHR	Gonadotropin-releasing hormone receptor
1639819_at	1.255755	1.018017	1.247791	0.588547	0.589824	0.940441	CG6385	---
1634854_at	0.940681	1.277133	1.011069	0.573607	0.61596	1.17578	CG16989	---
1636233_at	1.120669	1.334988	1.034354	0.710149	0.651557	0.9579	CG16995	---
1640301_a	1.017327	1.549869	1.133836	0.728488	0.7093	0.987559	Ndae1	Na<up>+</up>-driven anion exchanger 1
1633081_at	1.435331	0.998621	1.319846	0.564416	0.592122	1.019899	CG14616	---
1630088_at	1.407856	0.99084	1.559225	0.605528	0.656773	1.024734	CG16743	---

1627779_at	1.026497	1.395461	1.220284	0.650368	0.577894	0.942927	CG13295	---
1632215_at	1.272985	1.963545	1.127375	0.570047	0.632203	0.904827	CG6296	---
1641629_at	1.400433	0.980447	1.563017	0.659334	0.658821	1.063613	CG7402	---
1632533_at	1.012109	1.097129	0.95272	0.667063	0.795799	1.388428	Timp	Tissue inhibitor of metalloproteases
1639502_at	1.383666	0.761809	1.303733	0.515522	0.499669	1.656362	CG8942	---
1634826_at	0.498594	0.566959	0.521519	1.425538	1.627658	3.260269	CG13337	---
1636570_at	0.924469	1.575981	1.122115	0.678917	0.781747	1.143171	mex1	midgut expression 1
1624720_s	0.949152	1.045208	1.141367	0.972672	0.830378	1.844867	CG6043	---
1623134_at	1.755847	0.62874	1.331539	0.476328	0.37446	1.771059	CG12506	---
1632645_at	0.463765	0.382139	0.451325	1.549412	1.574763	2.886526	CG13330	---
1626996_s	1.453833	0.837586	1.462748	0.719171	0.769092	1.170887	br	broad
1631604_at	1.019418	1.30389	0.953486	0.685021	0.666571	2.924105	CG9511	---
1639396_s	0.999958	1.220766	1.02484	0.493765	0.475155	1.117975	CDase	Saccharomyces cerevisiae UAS construct a of Acharya
1633846_at	0.942016	1.013034	1.185367	0.881635	0.994253	1.819595	CG15523	---
1628100_at	0.949071	1.579419	1.316038	0.681297	0.724136	1.063142	CG8957	---
1633303_at	1.19838	1.000268	0.991872	0.566179	0.598757	1.056155	CG2989	---
1632149_at	1.26516	0.999909	0.992956	0.647386	0.664047	1.326575	CG17930	---
1628052_at	0.871212	1.159973	1.204392	0.522238	0.568828	1.199501	Cyp6a17	---
1627176_at	1.121551	1.090225	0.999927	0.554114	0.496813	0.995317	CG31431	---
1633341_s	1.0745	1.115476	1.208558	0.857501	1.076674	0.454207	dac	dachshund
1636998_at	1.165059	1.20051	1.304528	0.861076	0.99575	0.478571	sca	scabrous
1624203_s	0.996034	0.992437	1.374828	0.99973	1.043401	0.663741	Gli	Gliotactin
1636341_at	0.998048	0.781395	0.780989	2.037302	1.967886	0.969338	fzy	fizzy
1637959_at	1.286804	0.98155	0.934461	1.180061	0.897887	0.557597	CG4334	---
624815_at	0.959093	1.033467	0.737979	1.082561	1.208455	0.535991	Ssrp	Structure specific recognition protein
1631286_at	0.942757	0.66281	1.050448	1.468876	1.45808	0.973928	CG7857	---
1629738_at	0.888235	1.172719	1.128383	0.896486	1.01883	0.43602	CG14957	---
1638248_at	1.094928	1.691899	0.765887	0.999815	1.224652	0.512057	CG32350	---
1627770_at	0.929807	1.074116	1.02238	1.199601	0.911545	0.535831	Cks	Cyclin-dependent kinase subunit
1638130_at	1.110269	1.101928	0.965081	1.289383	0.986956	0.630533	CG7379	---
1630079_at	1.226067	1.077825	0.909493	1.147748	0.919387	0.534765	Atu	Another transcription unit
1623372_at	1.30069	1.027788	1.051943	0.85139	0.884628	0.516521	CG5873	---
1631542_a	1.099843	1.057532	1.002466	1.118074	0.7876	0.492354	dve	defective proventriculus
1630779_s	1.000068	0.739574	0.947613	1.839855	1.682541	0.976075	CG2061	---
1624847_at	1.042889	0.765765	0.877804	1.438906	1.538735	0.948355	CG11985	---
1632138_at	0.59933	0.654473	0.538304	2.31257	2.3334	1.187816	CG11308	---
1631344_at	1.11372	0.862382	0.927805	2.186254	2.079906	0.968716	msb1l	---
1636119_at	1.777715	0.750141	1.472341	0.997922	1.016275	0.690343	CG1468	---
1623108_at	1.018571	1.007129	0.933044	1.251494	1.028687	0.613836	geminin	Saccharomyces cerevisiae UAS construct a of Quinn
1641477_at	1.308339	0.783414	1.743275	1.013511	0.977407	0.240753	CG32447	---
1627637_at	1.31175	0.817356	0.957856	1.258758	1.048589	0.328509	d	dachs
1629708_at	0.834935	0.770151	0.886489	2.189754	2.101436	1.119744	CG8219	---
1635939_a	0.892031	0.840139	0.959293	2.606468	4.0859	1.157066	CG9641	---
1634209_at	0.886935	0.706572	0.920874	1.958051	1.501221	1.070677	pim	pimples
1630419_a	1.197338	1.664624	1.199821	0.838357	0.779253	0.521633	CG7300	---

1624333_at	1.143548	1.406426	1.097577	0.821176	0.722055	0.535167	CG9903	---
1638571_at	0.603507	0.60463	0.537373	2.924204	2.815779	1.449586	CG32588	---
1638610_at	1.222018	0.79525	1.594487	0.981566	1.038847	0.564271	CG7802	---
1636338_at	1.143326	1.905096	0.814733	0.883895	1.103375	0.40295	CG15021	---
1635621_at	0.796684	0.844642	0.746657	2.016329	1.779704	1.128829	CG13994	---
1639037_at	0.815925	0.685796	0.890173	1.810179	1.577149	1.126558	CG13588	---
1634900_at	0.478391	0.64437	0.542155	3.21293	4.178144	1.577139	CG13244	---
1640281_s	0.584353	0.651263	0.727381	2.374296	2.703836	1.286644	CG17129	---
1638417_at	1.268643	1.816765	1.231344	0.843834	0.757031	0.53819	CG31373	---
1631282_at	0.778129	0.571987	0.837697	2.370802	1.840576	1.223168	CG31088	---
1627445_s	1.161007	1.141179	1.125173	0.92991	0.99759	0.412937	en	engrailed
1627439_at	0.721968	0.520041	0.545136	2.098789	2.068712	1.194825	CG14840	---
1629966_at	1.345741	1.121961	1.33055	0.873622	0.87406	0.292649	E(spl)	Enhancer of split
1624586_a	1.871653	0.682826	1.776744	0.998713	1.000446	0.560498	Prat2	Phosphoribosylamidotransferase 2
1629771_at	1.125857	2.01925	1.045722	0.895475	1.029763	0.496127	Cyp12a5	---
1625487_at	1.857392	3.633895	1.040526	0.757834	0.896422	0.422408	CG6839	---
1630264_at	0.518224	0.604469	0.577163	2.296197	2.520681	1.413436	CG9871	---
1625639_at	0.566154	0.561424	0.559111	2.742784	2.745823	1.527008	CG6737	---
1641232_s	0.833892	0.642481	0.738272	2.08666	1.96899	1.298429	CG6999	---
1629601_at	1.258019	1.075877	1.394624	0.927091	0.887471	0.405422	m&agr;	E(spl) region transcript m&agr;
1636602_at	0.663638	0.46488	0.629918	2.417237	3.294951	1.400761	CG11253	---
1634384_at	0.684717	0.765668	0.621915	2.757313	4.318406	1.430337	CG13426	---
1629948_at	0.679758	0.729129	0.668914	1.864431	2.03322	1.202534	CG5194	---
1640161_at	1.154527	1.159234	1.054069	0.914767	0.765594	0.516546	e(y)2	enhancer of yellow 2
1628611_at	1.379751	1.149166	1.407343	0.847655	0.829364	0.579479	CG11241	---
1636672_at	1.049717	1.458438	1.372623	0.875875	0.961776	0.574992	Brd	Bearded
1636666_at	0.642987	0.578109	0.737733	2.691466	2.390727	1.381115	CG32591	---
1632755_at	1.237754	2.569543	1.137334	0.898272	0.918069	0.617774	CG31266	---
1627889_at	1.248475	0.706638	0.780686	1.23697	1.295808	0.576631	CG17826	---
1629743_at	0.49211	0.57273	0.658665	2.274368	3.082293	1.453037	CG11663	---
1635971_at	0.431106	0.44377	0.450872	2.732155	2.946484	1.701673	CG31525	---
1623940_at	0.751946	0.604503	0.669949	1.734545	1.722688	1.26238	CG9855	---
1625261_x	1.700991	1.049008	2.274244	0.968298	0.889962	0.614311	CG13722	---
1634848_at	1.5012	1.652584	1.330297	0.679671	0.737478	0.439804	CG16705	---
1626454_at	0.766227	0.70682	0.818712	2.383857	2.283235	1.190649	CycB3	
1631148_at	1.298507	2.451822	1.126872	0.92192	0.845891	0.601555	CG9673	---
1634595_at	0.345402	0.341596	0.322391	2.819397	3.235673	1.783028	CG10934	---
1629367_at	1.565391	3.151742	1.060481	0.778998	0.970349	0.582709	CG15534	---
1635937_at	2.019473	1.158181	1.770955	0.717646	0.81977	0.285343	CG4500	---
1623258_at	0.716723	0.695421	0.72098	6.60285	6.108181	1.397096	CG12493	---
1631653_at	0.573709	0.568517	0.720603	3.656307	3.907359	1.278238	CG15395	---
1629009_at	1.055542	2.387098	1.054535	0.822645	0.960849	0.525978	Cyp28a5	---
1629695_at	0.451799	0.469229	0.474739	2.237297	2.306137	1.595282	CG4686	---
1636473_at	0.161283	0.188327	0.179861	3.69965	3.333321	1.849147	CG12861	---
1625853_at	0.42831	0.389713	0.345472	2.396955	2.272434	1.629267	CG15124	---
1635598_at	0.265639	0.226295	0.241801	2.914738	3.945199	1.715307	CG18266	---
1624098_s	0.57493	0.523795	0.558949	3.095016	3.596597	1.464461	CG18675	---

1627168_at	0.234603	0.268436	0.247023	2.773634	2.853076	1.791457	CG13476	---
1626606_at	0.214716	0.27611	0.27426	4.126523	4.770064	1.690978	CG10630	---
1623565_at	1.100363	1.339411	1.476762	0.842733	0.904508	0.521229	CG17278	---
1640601_at	0.358044	0.454747	0.379	2.415174	3.27413	1.586833	CG13540	---
1624593_at	0.813126	1.105696	0.948849	1.466355	1.303135	0.316873	CG14332	---
1634694_at	0.420556	0.484194	0.555834	3.861422	3.492613	1.530931	CG12169	---
1634464_at	0.492245	0.412632	0.522583	3.611205	2.833014	1.512513	CG5338	---
1638419_at	1.261234	0.884412	0.637505	1.246063	1.077607	0.273554	Sgs1	Salivary gland secretion 1
1627972_at	1.296454	0.56826	3.838625	0.983702	1.026957	0.546037	CG9822	---
1636367_at	0.256503	0.257825	0.311275	2.477865	2.772059	1.697403	CG11018	---
1641142_at	0.093674	0.090378	0.118471	3.04001	3.570071	1.958866	CG5217	---
1628297_a	0.525875	0.505198	0.593758	2.529028	2.506777	1.460088	CG8478	---
1623326_a	0.796297	0.861577	0.887636	1.737855	1.799341	1.104606	mge	maggie
1625913_at	0.393404	0.304405	0.325634	2.197229	2.287825	1.611181	CG9970	---
1631467_at	0.203809	0.202895	0.179075	2.559926	3.156312	1.793787	CG15208	---
1625066_at	3.607408	7.305039	0.575044	0.890421	1.051062	0.396521	CG13230	---
1627105_at	0.062696	0.068037	0.092138	3.650595	5.284106	1.923884	TrxT	Thioredoxin T
1631470_at	0.349701	0.250096	0.288403	2.136964	2.263981	1.660385	CG12313	---
1627679_at	0.121466	0.138301	0.147553	2.916699	3.704197	1.94623	CG12470	---
1640525_a	0.073672	0.075594	0.083958	3.440225	4.164681	1.938241	CG15109	---
1630087_at	0.239848	0.258874	0.246279	2.897447	3.277974	1.737041	Tsp33B	Tetraspanin 33B
1631820_at	0.204445	0.159453	0.181543	3.149881	2.872178	1.889759	CG13747	---
1624534_at	1.277298	4.147042	1.355829	0.710884	0.729046	0.525904	ng1	new glue 1

Supplementary Table 3

Samples	**Control** ACT	**Control** P	**RNAi** P-ACT	**Control** ACT	**Control** P	**RNAi** P-ACT		
Sex	female	female	female	male	male	male		
Systematic	Normaliz	Normaliz	Normaliz	Normaliz	Normaliz	Normaliz	Genes	Products
1626294_a_at	0.816577	0.725342	1.758303	0.999989	1.22025	1.080601	stai	stathmin
1640228_at	0.834731	0.922138	1.839884	1.068006	0.980838	1.023371	CG11658	---
1636920_s_at	1.198263	0.80926	2.007654	0.900918	0.783768	1.167168	CG12016	---
1632204_at	0.878883	0.728054	1.995375	0.829279	1.121995	1.259486	Mmp1	Matrix metalloproteinase 1
1624464_s_at	1.056786	1.042982	1.534855	0.773162	1.029001	0.75193	Csk	C-terminal Src kinase
1633106_at	0.695286	0.647797	1.054761	1.237979	1.503177	0.902874	CG6662	---
1633337_at	1.634695	0.969966	3.393808	1.15209	0.738948	0.724107	CG17386	---
1634549_at	1.106476	1.001479	1.914625	0.722403	0.978042	0.778345	CG11750	---
1640979_at	1.107401	1.119984	1.528745	0.947554	0.553888	0.842643	CG1681	---
1633274_at	0.65642	0.683467	0.958989	1.416405	1.456475	1.064814	CG10158	---
1634597_a_at	1.254414	0.966025	2.078526	0.955692	0.76935	0.954732	CG31085	---
1623200_at	1.231976	1.087725	1.522622	0.899351	0.976256	0.732987	fng	fringe
1627645_at	1.33113	1.225492	1.806238	0.8319	0.782604	0.840431	CG9427	---
1637312_a_at	1.319216	1.039119	2.317089	0.930431	0.973444	0.901027	br	broad
1637105_at	1.138131	1.00779	1.468884	0.564966	0.868953	0.9937	rgr	regular
1637490_at	1.402391	1.107724	1.945707	0.85065	0.641725	0.732719	CG13314	---
1624432_at	1.210124	1.129622	1.769185	0.741266	0.885977	0.564329	Spz3	---
1628696_at	1.411528	1.206457	2.815346	0.708943	0.806634	0.772054	CG12643	---
1634895_s_at	0.953966	1.054428	1.256939	0.593628	0.957746	1.188902	Rab5	Rab-protein 5
1634027_at	1.264225	1.223128	1.568432	0.789158	0.471735	0.573463	CG12715	---
1635044_at	0.922197	1.06858	1.731727	0.768193	1.458411	0.62598	Hsp26	Heat shock protein 26
1639011_a_at	0.627783	0.702752	0.47389	1.328012	1.475237	1.303824	CG12162	---
1627744_at	1.184215	1.138726	1.458587	0.780799	0.533025	0.85264	CG15209	---
1635086_at	1.377316	1.239535	2.188705	0.77571	0.521594	0.738803	CG4666	---
1623699_a_at	0.242585	0.166147	0.442262	1.628364	2.205734	1.59867	sm	smooth
1634636_at	1.121444	1.261686	1.844805	0.778717	0.580293	0.912483	CG6426	---
1640760_at	0.532522	0.541265	0.765437	1.81279	2.436251	1.246545	CG17838	---
1636825_at	0.28445	0.2771	0.383354	1.772741	2.310216	1.851725	CG3492	---
1628512_at	0.39437	0.390359	0.498406	1.518373	2.238492	2.242699	CG7441	---
1625031_at	0.503813	0.509313	0.705578	1.304562	1.600725	1.349832	CG7841	---
1629240_at	0.034822	0.043274	0.082694	1.926429	2.656543	2.805659	Mst84Dc	Male-specific RNA 84Dc
1625214_at	0.172876	0.17147	0.232763	1.805449	2.437206	2.813603	CG31363	---
1639425_at	0.041495	0.038873	0.063606	1.95927	2.184512	2.483019	CG18662	---
1633068_at	0.02045	0.020152	0.045967	1.963219	2.939649	2.369777	CG4750	---
1640084_a_at	0.352735	0.310528	0.463866	1.603894	2.005323	2.024929	CG8712	---
1632993_at	0.010515	0.011857	0.034073	2.01371	2.750673	2.672569	CG6372	---
1638626_a_at	0.024601	0.022696	0.041902	1.983048	2.811763	2.643939	CG17377	---
1626292_at	0.025146	0.027407	0.043877	1.98281	2.824406	2.763026	CG4439	---
1636364_a_at	0.026315	0.022602	0.055454	1.967022	3.094271	3.407489	CG17376	---
1634719_at	0.017809	0.020531	0.041025	2.113904	2.738388	2.006681	CG9920	---
1628448_at	0.238953	0.258787	0.326284	1.886107	1.699544	1.750076	CG31473	---
1634274_s_at	0.079205	0.090864	0.13389	1.970287	2.064161	2.118649	CG14305	---

1636172_at	0.021788	0.025919	0.053777	2.173244	3.118572	1.950572	CG12699	---
1629670_at	0.02244	0.022936	0.05132	1.988781	2.411567	2.736545	CG17376	---
1633776_s_at	0.040722	0.038009	0.051711	1.979524	2.435491	2.636274	Mst35Ba	Male-specific-transcript-35Ba
1634244_s_at	0.083488	0.086957	0.105861	1.90998	2.1906	2.510196	CG31639	---
1631435_at	1.073813	1.192882	1.568681	0.728387	0.924233	0.741152	CG7988	---
1641221_at	0.891261	0.744418	1.11847	1.156808	0.568867	1.34425	CG4362	---
1628323_s_at	1.086352	0.999994	1.357496	0.990414	0.74124	0.664095	ogre	optic ganglion reduced
1632593_at	1.180724	1.208929	1.512775	0.884619	0.576578	0.786868	CG32147	---
1629683_at	1.162432	1.025669	1.471934	0.974129	0.638407	0.680486	br	broad
1629271_at	1.054586	0.941349	2.019907	0.769117	0.84528	1.03411	CG10444	---
1627646_at	1.095888	1.088941	1.857075	0.950738	0.864833	0.90609	CG5134	---
1630167_at	1.188508	1.041586	1.497598	0.988838	0.786688	0.589432	Pcd	pterin-4a-carbinolamine dehydratase
1626079_a_at	0.999969	0.927834	1.886941	0.98285	0.829417	1.187378	CG2201	---
1631635_at	0.942957	1.087632	1.41536	1.102889	0.679233	0.619163	CG7294	---
1639138_at	0.580355	0.524007	0.790201	1.211932	1.43395	1.477268	CG5524	---
1627293_at	1.111995	1.012109	2.416399	0.813024	0.725316	0.999186	CG14439	---
1626623_at	1.183396	1.175414	1.699122	0.813561	0.586839	0.867489	CG11670	---
1639532_at	1.07064	1.006847	1.75015	0.996922	0.548136	0.826642	CG5391	---
1626617_at	1.15721	0.99996	1.564352	0.996681	0.6954	0.667244	dx	deltex
1625366_at	1.195027	1.154401	1.676264	0.629202	0.857615	0.75232	rst	roughest
1623732_at	1.254056	1.291684	1.783271	0.704051	0.619692	0.812997	CG31410	---
1638879_a_at	1.69729	1.574618	1.077109	0.842051	0.733138	0.779842	CG33012	---
1623151_a_at	1.616404	1.967147	0.999951	1.051735	0.801611	0.935218	CG2010	---
1631993_s_at	1.373901	1.230707	0.808298	1.352948	0.731975	0.558509	Ald	Aldolase
1628231_at	1.633078	1.785855	0.92746	0.957885	0.854867	1.002193	Ac76E	Adenylyl cyclase 76E
1631234_at	1.255264	1.420603	0.645256	0.973697	0.808537	1.064926	CG18173	---
1639033_at	1.771328	1.851214	0.956416	1.019835	0.854731	0.896596	l(2)01289	---
1640672_at	1.340984	1.680152	0.943149	1.039549	0.797424	0.642289	CG11015	---
1628099_at	0.815699	0.917292	0.570757	1.089874	1.412671	1.223667	bor	belphegor
1629474_at	1.519691	1.72275	0.921802	0.999836	0.860074	0.726354	CG11368	---
1636311_at	2.090893	1.466116	0.602774	1.034334	0.85914	0.734983	Gpdh	Glycerol 3 phosphate dehydrogenase
1637057_at	1.784222	1.967689	1.155093	0.974777	0.687113	0.95008	nrm	neuromusculin
1630065_at	2.236448	1.75123	1.252572	0.880446	0.842944	0.89653	CG6912	---
1637496_at	1.566212	1.634955	0.898933	1.122811	0.619954	0.703805	CG30219	---
1633581_at	1.689526	1.72163	0.970994	1.040001	0.687064	0.494024	CG32571	---
1626524_at	1.354559	1.2736	0.931118	1.047848	0.55351	0.640912	CG16996	---
1626098_at	1.532344	1.810746	1.158172	0.840583	0.747901	0.9048	CG11453	---
1633039_at	1.54013	2.049906	1.150618	0.772553	0.954054	0.746514	CG5646	---
1624636_at	1.723929	1.541309	1.090799	0.872511	0.7096	0.700213	ACXD	---
1635000_at	1.395375	1.662625	0.714024	1.033243	0.899335	0.787802	Glycogenin	Glycogenin
1635674_at	2.154353	1.69126	1.02581	0.965684	0.88566	0.983464	CG6901	---
1636995_at	1.536122	1.808379	1.034964	0.809625	0.710933	0.934909	CG7440	---
1630815_at	1.11463	1.289857	0.81327	0.769417	0.496631	1.443477	CG14277	---
1633032_s_at	1.327681	1.507486	1.030867	0.639933	0.82641	0.980339	CG8177	---
1623690_at	1.538779	1.729647	1.065983	0.928188	0.751412	0.926748	CG17190	---
1633036_s_at	1.718747	1.91739	1.029278	0.986732	0.85868	0.819046	CG32495	---

1630038_at	1.705771	1.60234	1.138266	0.895286	0.594336	0.519069	pyd3	---
1638225_a_at	1.667043	1.840429	1.195251	0.847807	0.696914	0.801254	inx7	---
1627890_at	1.639188	1.403809	0.993399	1	0.554384	0.580926	GstD10	Glutathione S transferase D10
1635736_at	1.866627	1.439804	1.022228	0.96065	0.490774	0.851517	CG5157	---
1635140_at	2.524727	1.833957	0.95472	1.037444	0.525243	0.608899	CG15515	---
1624290_at	1.330696	1.437641	0.908317	0.87679	0.698515	1.081978	CG4752	---
1639911_at	1.520744	1.69439	0.913107	1.080895	0.684614	0.644967	CG17029	---
1625265_at	1.593632	1.522232	1.040191	0.93869	0.594802	0.585787	CG9119	---
1624195_at	1.322784	1.520784	1.104946	0.820321	0.704327	0.891737	sug	---
1625476_a_at	1.457532	1.229693	0.876899	1.13665	0.538783	0.705001	CG1674	---
1622902_at	1.380614	1.435575	1.017004	0.945858	0.596002	0.628466	Pbprp5	Pheromone-binding protein-related protein 5
1640632_at	1.460377	1.588815	0.730476	1.140391	0.822717	0.689504	SdhB	Succinate dehydrogenase B
1630964_at	1.539103	1.429378	1.131798	0.8901	0.68888	0.876481	CG15211	---
1625128_a_at	1.188173	1.254307	0.924279	1.045925	0.623265	0.64697	CG2249	---
1633251_at	1.514767	1.497135	1.06281	0.938199	0.611084	0.599144	CG15829	---
1624569_at	1.746918	1.957987	0.968601	1.033232	0.735045	0.720008	CG31087	---
1626503_at	1.652613	1.740611	0.956738	1.047636	0.777109	0.743767	CG2254	---
1634739_a_at	1.266601	1.188387	0.54845	1.258916	0.794586	0.629424	Pfk	Phosphofructokinase
1628751_at	0.797059	0.718483	0.506318	1.229214	1.355042	1.235022	CG8728	---
1625362_at	1.446542	1.352393	0.9833	1	0.618843	0.751954	Gclc	Glutamate-cysteine ligase catalytic subunit
1624662_at	2.562315	2.910169	1.117506	0.892076	0.743364	0.898395	CG3106	---
1638246_at	2.119031	2.378839	0.727027	1.277094	0.489833	0.366958	CG5804	---
1624957_a_at	1.415632	1.513884	1.002502	0.598109	0.979192	0.726092	Tequila	---
1625949_at	1.50885	1.345054	0.941147	1.060273	0.622059	0.672589	Gpdh	Glycerol 3 phosphate dehydrogenase
1637772_at	1.583713	1.575473	0.914271	1.115723	0.637459	0.593358	CG4726	---
1639584_at	1.35358	1.461216	1.129847	0.875326	0.613238	0.636772	Cyp4ad1	---
1632849_at	1.33318	1.385558	0.653642	1.433696	0.628524	0.065943	nol	no optic lobe
1635253_a_at	1.60214	1.723768	0.960998	1.035023	0.853862	0.70162	CG7010	---
1635331_at	1.47399	1.610612	0.861356	1.140297	0.474764	0.496925	CG8510	---
1639974_a_at	0.419931	0.396365	0.285059	1.857547	1.960496	1.612398	CG6569	---
1626829_s_at	0.41165	0.39166	0.308328	2.243655	1.68713	2.667335	CG3494	---

Supplementary Tables 1-3.

The genes/predicted transcripts (with known CG number) commonly affected in both males and females (Supplementary Table 1), specifically affected in males (Supplementary Table 2), and specifically affected in females (Supplementary Table 3) after depletion of HP1, are listed. ACT: control RNA samples from *y w; + /+; +/act-Gal4*; P: control RNA samples from *y w; +/+; HP1-21/+*; P-ACT: RNA samples from RNAi mutant *HP1-21/act-Gal4.* The sex origin of each sample used to perform the microarray is indicated. The Affymetrix tile number of each

gene/predicted transcript (Systematic), and the CG number are included in the table. Normaliz: normalized expression value. All the listed genes that are specifically affected in either males or females passed the ANOVA test. Notably, the HP1 preferentially bound genes in males, such as *pim, CycB3, Fzy, CG15208* and *CG12470*, are highly transcribed in wild type males than in females arguing a positive role of HP1 in their transcription. 50% of HP1-positive genes are down-regulated in the absence of HP1 also support that HP1 plays a distinct role in the transcription of euchromatic genes than its role in heterochromatin packaging. The females showed no sign of preferential enrichment of HP1 is consistent with the idea that HP1 may utilize a different mechanism in males and females. However, secondary effects loss of HP1, including sex-biased changes in dynamics (e.g. histone modification) may alter the accessibility of activators or repressors to chromatin, should not be excluded.
Microarray analysis was performed using DrosophilaGenome1 (DG1) GeneChips™ (Affymetrix, Santa Clara, USA). Total RNA was isolated from two independent populations of male and female 3rd-instar larvae of *HP1-21/act-Gal4*, and as controls, larval progenies from line *HP1-21* with the genotype *y w; +/+; HP1-21/*+, and larvae with the genotype *y w; + /+; +/act-Gal*; 15 μg of total RNA from each sample was reverse-transcribed and 5 μg of biotin-labeled cRNA was fragmented and hybridized to the Affymetrix *DrosophilaGenome* (DG) GeneChips. Expression values were estimated using the robust multi-chip average method with quantile normalization as implemented in the R BioConductor package (Irizarry et al., 2003, Nucleic Acid Res 31:e15). These data were then imported into GeneSpring 7 (Agilent Technologies) with the default per chip and per gene normalization steps. We compared changes in gene expression between males and females at the late larval stage. Genes were considered to have significantly ($p < 0.05$) changed in their expression values if they reached an expression value of >50 in one or more conditions, changed in expression by at least 1.5-fold, and passed a one-way ANOVA ($p<0.05$), A Benjamini and Hochberg false discovery rate correction was applied to deal with multiple testing errors. To find the origins of the significant changes, we performed a Tukey *post-hoc* analysis on the ANOVA results.

Primer sequences

ChIP primers

CG6372
Forward primer 5'-ATCCGTGTAGGCCATGGAAA-3'
Reverse primer 5'-TGCGAGGCGTATGAACGCT-3'

CG17377
Forward primer 5'-CGGCTGGAAAGGATGCATAC-3'
Reverse primer 5'-CTGAAAAGAGGATCGCTTATC-3'

CG9920
Forward primer 5'-CGTTGGACATCGTTTCTTAAG-3'
Reverse primer 5'-AAGATGTATGCGTTTGCTTGG-3'

CG12699
Forward primer 5'-GCTGTGGTTGTATCAGCATC-3'
Reverse primer 5'-TTGTACTTCCTACTTGAACGG-3'

CG6901
Forward primer 5'-CGGTGAAGACACTAGTATCTA-3'
Reverse primer 5'-TTGATGCGGGTAAAGTATCCT-3'

CG31087
Forward primer 5'-ATCCGCACTCACCAATCAGT-3'
Reverse primer 5'-GCCACCTATGCTTGATGTTG-3'

CG31804
Forward primer 5'-GGCCAAAAAACTTGCCGCAA-3'
Reverse primer 5'-TGGATGCACTTTGCCTGGTA-3'

CG31624
Forward primer 5'-CAAAACAGGGCAGCTATCGA-3'
Reverse primer 5'-CGGAAACGCTTCCTTCTGC-3'

CG18444
Forward primer 5'-GATGTTGGCAGAGTAGATGG-3'
Reverse primer 5'-ATTGCGTCGCAGGTGTAAAG-3'

CG15208
Forward primer 5'-TTGGCCAAGTAGAGAATCTGA-3'
Reverse primer 5'-TGTCATTCAGGCCGCAGTTA-3'

CG12470
Forward primer 5'-GCTGTTTACGAGCACCAAAC-3'
Reverse primer 5'-GGAATATGCCGAGCTTCCAA-3'

CG15109
Forward primer 5'-GAAAAGGTCGCCACAAATGG-3'
Reverse primer 5'-AACGTATACTTACACCCAAGG-3'

Rep4
Forward primer 5'-CAGAGCCAGGAACTTTCAGC-3'
Reverse primer 5'-TGAGAAGCGCGAAAAATGCC-3'

W
Forward primer 5'-CCTGCACTTTGTTGGCACTT-3'
Reverse primer 5'-TCACTCAGCTATTACAGGGTA-3'

dally
Forward primer 5'-CATTTCAGATTGCGCCCTTG-3'
Reverse primer 5'-TCAGGTCGAGGAAATGCACT-3'

LysX
Forward primer 5'-CCATAGTCGTTGGATCCATC-3'
Reverse primer 5'-GACGACATCATCCAGTCTGT-3'
e
Forward primer 5'-ATCTGTGGCCGTTTCACACT-3'
Reverse primer 5'-CGCATATGGGTATGTGTGGT-3'

Mcm6
Forward primer 5'-GGGCGAACTATCGGTCTTAA-3'
Reverse primer 5'-GAGCATCTGCCACATCCATT-3'

Tm2
Forward primer 5'-GCGAGAGTGCTGTGAGTAAA-3'
Reverse primer 5'-TGAAAATCCTGGCGTGACCA-3'
rst
Forward primer 5'-CCACTGGTAATCCACACCAA-3'
Reverse primer 5'-ACATAGAACAGAGGTTGCATC-3'
stai
Forward primer 5'-GGCGCCATCTCTTTTCCAC-3'
Reverse primer 5'-ACACACTGATCTGCACTTTGT-3'
sm
Forward primer 5'-CTCGATGCGTATGCGTACG-3'
Reverse primer 5'-TTTTGACCACAGTACGCTGC-3'

CG17386
Forward primer 5'-GAGAAGGAGAAGGAGAAAGG-3'

Reverse primer 5'-CCCAGCTGAGAGTCCATCG-3'

Glycogenin

Forward primer 5'-CGTGACTATATACCCTGTGTA-3'
Reverse primer 5'-ACGAAATGGAAGGATAGGCG-3'

pim

Forward primer 5'-CGTGGTATAAAATACGGTGGA-3'
Reverse primer 5'-CGGGGTTATTCCAGGAGT-3'

en

Forward primer 5'-TACTTCGGAATCGCAGCG-3'
Reverse primer 5'-AGTTCGCTGGGGACACAGT-3'

spl

Forward primer 5'-CCAGGGAGCGGTATAAAAGG-3'
Reverse primer 5'-CGTGGAATTGCTGCAAGTTC-3'

CG8337

Forward primer 5'-AGCGCACAGGAAATGCACTT-3'
Reverse primer 5'-GGTTGGTGGTCCAGAAGAAG-3'

CycB3

Forward primer 5'-CCTGGAGTCCTCGTCTCC-3'
Reverse primer 5'-CAGCTGCTCGAGGCTACTT-3'

fzy

Forward primer 5'-AAATCGCTGGAGCACGTCTT-3'
Reverse primer 5'-TTCCGCTCTTTTCTGGTGTC-3'

ia2

Forward primer 5'-ACTTTCACACGCACACAAGTT-3'
Reverse primer 5'-CTGATGGGCTGTAAGCGAAA-3'

hoe1

Forward primer 5'-TCTCCTGCAGCTTCGTCTG-3'
Reverse primer 5'-TTTCCACACTTTCCACAGCG-3'

Glt

Forward primer 5'-AAACGGAGGGAACGGAATCT-3'
Reverse primer 5'-GTTCACCCTTCATTCCCGAT-3'

CG8043

Forward primer 5'-CGGGCGTATGGAATCCTCA-3'
Reverse primer 5'-CGGCTAGAAACAATCGGC-3'

Gpdh

Forward primer 5'-GGCGCCACAACTGCTCAC-3'
Reverse primer 5'-CTCGCTGATGTGCTTCCTC-3'

RT-PCR

Rep4
Forward primer 5'-GCAATCATGTCACCGACAAC-3'
Reverse primer 5'-ACTTTTCCGGATGCTGTTCG-3'

mus209
Forward primer 5'-CAAGCCACCATCCTGAAGAA-3'
Reverse primer 5'-TCCTGGTCGAGGTTCATCAG-3'

CycB3
Forward primer 5'-ATCACAAGCGGGCATCATCA-3'
Reverse primer 5'-TTCTTAGCATCCATCAGGGC-3'

actin5C
Forward primer 5'-TGTGACGAAGAAGTTGCTGC-3'
Reverse primer 5'-ATCCAGACGCAGGATGGCA-3'

Rp49
Forward primer 5'-ATCGTGAAGAAGCGCACCAA-3'
Reverse primer 5'-AACGCGGTTCTGCATGAGC-3'

2852–2858 *Nucleic Acids Research, 2005, Vol. 33, No. 9*
doi:10.1093/nar/gki584

HP1 modulates the transcription of cell-cycle regulators in *Drosophila melanogaster*

Filomena De Lucia*, Jian-Quan Ni, Catherine Vaillant and Fang-Lin Sun

Friedrich Miescher Institute for Biomedical Research, Maulbeerstrasse 66, CH-4058 Basel, Switzerland

Received April 11, 2005; Revised and Accepted April 29, 2005

ABSTRACT

Heterochromatin protein 1 (HP1) was originally described as a non-histone chromosomal protein and is required for transcriptional gene silencing and the formation of heterochromatin. Although it is localized primarily at pericentric heterochromatin, a scattered distribution over a large number of euchromatic loci is also evident. Here, we provide evidence that *Drosophila* HP1 is essential for the maintenance of active transcription of euchromatic genes functionally involved in cell-cycle progression, including those required for DNA replication and mitosis. Depletion of HP1 in proliferating embryonic cells caused aberrant progression of the cell cycle at S phase and G2/M phase, linked to aberrant chromosome segregation, cytokinesis, and an increase in apoptosis. The chromosomal distribution of Aurora B, and the level of phosphorylation of histone H3 serine 10 were also altered in the absence of HP1. Using chromatin immunoprecipitation analysis, we further demonstrate that the promoters of a number of cell-cycle regulator genes are bound to HP1, supporting a direct role for HP1 in their active transcription. Overall, our data suggest that HP1 is essential for the maintenance of cell-cycle progression and the transcription of cell-cycle regulatory genes. The results also support the view that HP1 is a positive regulator of transcription in euchromatin.

INTRODUCTION

Chromatin in higher eukaryotes is subdivided into different functional compartments termed heterochromatin and euchromatin (1). Heterochromatin differs from euchromatin in its DNA composition, replication timing, condensation throughout the cell cycle, and its ability to silence euchromatic genes placed adjacent to or within its territory, often described as position-effect-variegation (PEV) (2).

Heterochromatin protein 1 (HP1) was the first protein identified in *Drosophila melanogaster* as a heterochromatin-associated protein (3); the corresponding gene has been cloned from a number of organisms and is highly conserved from yeast to human (4). Polytene chromosome staining showed that, in *Drosophila*, HP1 is distributed mainly in pericentric heterochromatin, telomeric heterochromatin, the banded small fourth chromosome (5–8), as well as ~200 individual loci scattered throughout the euchromatic chromosomal arms (5). The gene encoding HP1 in *D.melanogaster*, *Su(var)2-5*, was isolated as a suppressor of PEV (9–11). The protein contains a highly conserved motif, the chromo (chromatin organization modifier) domain, similar to Polycomb (Pc), a repressor of homeotic genes (12). The association between HP1 and pericentric heterochromatin is believed to occur via the chromo domain of HP1 and the N-terminal tail of histone H3 methylated at lysine 9 (13,14), generated by histone methyltransferase-Su(var)3-9, a partner of HP1 in pericentric heterochromatin (15). The C-terminal chromo 'shadow' domain of HP1 interacts with other silencing complexes to suppress local transcriptional activity (15–18). However, studies of HP1 chromosomal distribution also showed that HP1 does not always co-localize with lysine 9 methylated histone H3 or Su(var)3-9, especially in euchromatic regions (19–21); in some cases, HP1 is found directly bound to DNA (22,23). All these features argue for distinct roles for HP1 in chromatin and in epigenetic gene regulation.

HP1 is believed to be an essential structural protein protecting the integrity of chromosomes during cell division (8,24). *Swi6*, the homolog of HP1 in fission yeast, is dispensable for survival, but its deletion results in lagging chromosomes during anaphase, and a high rate of chromosome loss (25,26). Mutations of HP1 in *D.melanogaster* result in late larval lethality, chromosome breakages/loss, telomere fusion and a high frequency of cells with abnormal anaphase (8,27). Null alleles of the HP1 functional partner in mice (*SUVAR39*) also showed various chromosomal defects (28), supporting a conserved role for heterochromatin proteins in the regulation of chromosome

*To whom correspondence should be addressed. Tel: +41 (0) 61 697 7590; Fax: +41 (0) 61 697 3976; Email: menita.delucia@fmi.ch
Correspondence may also be addressed to Fang-Lin Sun. Tel: +41 (0) 61 697 7590; Fax: +41 (0) 61 697 3976; Email: fang-lin.sun@fmi.ch

dynamics during cell-cycle progression. However, the mechanism(s) involved remains to be understood.

In this study, we utilized *Drosophila* embryonic Kc cells and an RNA interference (RNAi)-based approach to demonstrate that HP1 plays an important role at S phase and G2/M phases during the cell cycle. We further show that nearly one-third of known/predicted cell-cycle regulators require HP1 to maintain their active transcription. These genes include *MCMs*, *Orc4*, *CDC45L*, *INCENP*, *Aurora B*, *CAF1*, *Bub1*, *Bub3* and a few other cell-cycle regulators. ChIP analysis suggests that HP1 plays a direct role in their transcription. Therefore, the results of this study provide an alternative explanation for the specific role of HP1 in the regulation of chromatin dynamics and in cell-cycle progression.

MATERIALS AND METHODS

RNAi in Kc cells

Drosophila Kc cells were routinely cultured at 25°C in Schneider *Drosophila* medium (GIBCO) supplemented with 10% fetal calf serum, 160 μg/ml penicillin, 250 μg/ml streptomycin, and 4 mM L-glutamine. Double-stranded RNA (dsRNA) of HP1 was generated by incubation of single-stranded RNA in annealing buffer (100 mM potassium acetate, 30 mM HEPES-KOH, pH 7.4, 2 mM magnesium acetate) for 3 min at 95°C and then placed in a beaker with water at 75°C and allowed to cool slowly to room temperature. The detailed procedure of RNAi was carried out according to the established protocols (http://dixonlab.biochem.med.umich.edu). Briefly, Kc cells were seeded in a six-well dish using serum-free medium at 1×10^6 cells/ml. HP1 dsRNA (5 μg/ml) was added to the cultured Kc cells. After 60 min at room temperature, 2 ml of medium containing 10% serum was added to each well and the plates transferred to 25°C for up to 8 days. Western blotting and RT–PCR were carried out using the extract/total RNA isolated from control and dsRNA-treated cells on days 2, 6 and 8.

Cell-cycle and apoptosis analysis

The procedure for flow cytometric analysis of Kc cells followed that in the manual provided with the BrdU flow kit (BD PharMingen). The cells were fed with BrdU for 4 h, then scraped and collected. Fluorescence was measured using a FACSCalibur (Becton Dickinson). Data collection and analysis were performed using CellQuest software.

Electrophoresis and immunoblotting

Cell extracts (15 μg) were fractionated by 10% SDS–PAGE, then transferred to Hybond-P PVDF membranes (Amersham) and probed with primary antibodies (CIA9), and secondary antibodies (anti-rabbit or anti-mouse horseradish peroxidase-conjugated IgG), obtained from Jackson Immunoresearch Laboratories. Enhanced chemiluminescence reagents (Amersham Pharmacia Biotech) were used for signal detection.

For the analysis of H3 ser10 phosphorylation, we used whole-cell extracts from 700 000 Kc cells (control and RNAi at day 8). Western blotting was performed using polyclonal antibodies against ser10-phosphorylated histone H3 at a dilution of 1:1000 (Upstate). Kc control cells arrested in mitosis by incubation in 25 μM colchicine (Sigma) for 24 h were also analyzed for comparison.

Immunofluorescence

Kc cells were seeded onto polylysine slides, fixed with 4% formaldehyde for 15 min and permeabilized with 0.5% Triton X-100 for 5 min. The incubation with primary antibodies was carried out in blocking solution for 1 h.

For staining of mitotic cells, the cells were permeabilized using PBST (PBS containing 0.3 % Triton X-100) and stained with polyclonal antibody against *Drosophila* Aurora B at 1:200 dilution and monoclonal mouse at anti-β-tubulin 1:300 dilution (Chemicon International) as primary antibodies. Secondary antibodies were anti-rabbit coupled with Alexa 488 (1:500) and anti-mouse coupled to Alexa 546 (1:500) (Molecular Probes, Eugene, Oregon). Images were acquired using a confocal LSM510 META microscope (Zeiss). Stacks of images were analyzed using the IMARIS 4.0 program (Media cybernetics, Carlsbad, CA).

Antibodies

Affinity-purified polyclonal antibodies of HP1 (rabbit #192 and #187, 5 μg) and 5 μg of polyclonal anti-HA antibodies (Sigma) were used in each ChIP reaction. The specificity of the HP1 polyclonal antibodies was determined using various approaches, including western blotting assay, immunofluorescence staining and immunoprecipitation to pull down HP1 (data not shown). The monoclonal antibody HP1–CIA9 (5) was used at a dilution of 1:20 in immunoblotting assays.

Microarray analysis and RT–PCR

Total RNA was isolated from control and HP1-depleted Kc cells at day 8 using an RNeasy kit (Qiagen). RNA labeling and microarray data analysis followed the standard protocol from Affymetrix. We used ANOVA ($P < 0.001$) to assess the expression confidence for each gene.

For RT–PCR analysis, poly(A)$^+$ mRNA was purified with the Oligotex Direct mRNA kit (Qiagen) according to the manufacturer's instructions. The purified poly(A)$^+$ RNA was reverse transcribed using the Thermoscript kit (Invitrogen). The cDNA was then used for PCR amplification for 35 cycles with gene-specific primers. PCR products were scanned after electrophoretic separation with a Typhoon Scanner, quantified using ImageQuant software (Amersham Biosciences) and normalized for amplification of the *Actin5c* transcript. The sequence of primers used for RT–PCR and ChIP analysis are provided in the Supplementary Material.

ChIP

ChIP was performed according to Orlando *et al*. (29) and the protocol provided by Upstate (www.upstate.com) with some modifications. In brief, $1–2 \times 10^8$ Kc cells were prepared and fixed in 1% formaldehyde. Nuclei were isolated according to a standard procedure in Current Protocols (http://www3.interscience.wiley.com), then resuspended in 1.7 ml of lysis buffer (50 mM Tris, pH 8.0, 10 mM EDTA, 1% SDS and protease inhibitors) and sonicated using a Branson sonifier 250. Chromatin fractions in the size range 0.2–0.8 kb were used to perform immunoprecipitation experiments. We used

5 µg affinity-purified polyclonal antibodies (#192 and #182 for HP1; HA antibody for control) and 1 ml of salmon sperm DNA/protein-A-agarose (Upstate) pre-cleared chromatin lysate in each reaction. The mixture was then rotated at 4°C overnight and the recovered beads were washed twice with 1 ml of Low salt buffer (Upstate), once with High salt buffer (Upstate), once with LiCl buffer (Upstate) and twice with TE at 4°C for 8 min. ChIP DNA was extracted according to the standard procedures (29).

RESULTS

Depletion of HP1 in *Drosophila* Kc cells

Various chromosomal defects in the cell cycle have been observed in embryos or larval tissues of *Drosophila* HP1 mutants (8,27). However, the presence of maternally loaded HP1 in embryos and the lethality of HP1 mutants at late larval stages have so far precluded a systematic study of the role of HP1 in cell-cycle regulation. Therefore, we used *Drosophila* Kc cells, a cell line derived from *Drosophila* embryos, as a model system to address this problem. HP1 transcripts were depleted using an RNAi-based approach (see Materials and Methods). The reduction in HP1 expression was measured both by RT–PCR and by western blotting analysis (Figure 1A). A significant reduction in the HP1 expression was already evident after 2 days treatment with HP1 dsRNA. Cells at day 8 showed a reduction in HP1 of ~90% (Figure 1A) and were therefore used in all subsequent experiments.

Cell-cycle progression at S and G2/M phase is altered in the absence of HP1

The impact of HP1 loss on the cell cycle of Kc cells was determined using cell-cycle profile analysis of HP1-depleted and control cells. The percentage of cells in S phase was determined by BrdU incorporation, and total DNA content by 7-amino-actinomycin (7-AAD). The results showed that the depletion of HP1 (day 8) caused a decrease in S-phase cells of at least 4-fold, and a 2-fold decrease in G2/M-phase cells (Figure 1B), although no significant effect was found at the G1 phase. In addition, depletion of HP1 caused a greater than 7-fold increase in the number of apoptotic cells. These results, therefore, confirm that HP1 is an important regulator during the cell cycle, especially at the S and G2/M phases.

Cell-cycle regulators require HP1 to maintain their active transcription

To ask whether the cell-cycle defects were due to changes in the transcription of genes functionally involved in S phase and the G2/M phase, we next assessed global changes in gene transcription following depletion of HP1. Expression profile analysis was performed using total RNA isolated from both HP1-depleted Kc cells and control Kc cells, and an Affymetrix *Drosophila* chip. For each experiment, we used total RNA isolated from two independent HP1-depleted and control samples, and at least two independent experiments were performed.

The microarray analysis showed that loss of HP1 function in Kc cells resulted in alterations in transcription of >500 genes: ~400 genes were down-regulated and ~120 genes

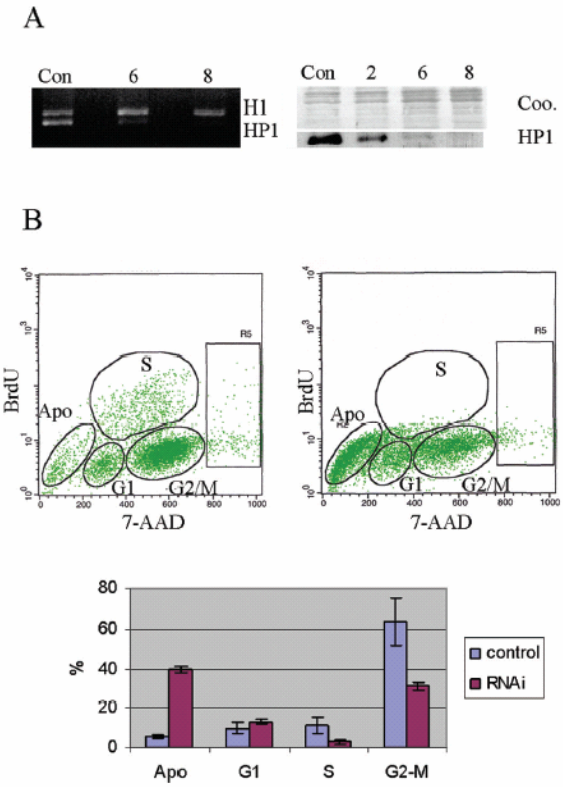

Figure 1. Depletion of HP1 alters cell-cycle progression. (**A**) Expression of HP1 after treatment with dsRNA in Kc cells. Left panel: changes in *HP1* expression after RNAi monitored by RT–PCR analysis of RNA extracted from control (Con) and RNAi-treated cells (at 6 and 8 days). Histone *H1* was used as a positive control. Right panel: western blotting with anti-HP1 antibodies (C1A9) of extracts from control (Con) and RNAi-treated cells (at 2, 6 and 8 days). Equal loading of cell extracts (15 µg of protein extract in each lane) was monitored with Coomassie blue (Coo.) staining. (**B**) Ablation of HP1 in Kc cells results in loss of cells in S and G2/M phase. Control Kc cells (left panel) and HP1-depleted Kc cells (right panel) were labeled with BrdU and 7-AAD. The fractions of cells in apoptosis (Apo), G1 phase (G1), S phase (S) and G2/M phase (G2/M) are all indicated. R5 represents over-replicated cells. Approximately 25 000 gated cell events were measured in each experiment. The comparison of cell numbers ($n = 2$) at different stages of the cell cycle in controls and cells after HP1 depletion is shown on the bottom panel of the figure. %, percentage of cells.

were up-regulated (>1.5-fold, ANOVA). The function of these genes ranged from cellular enzymes, signal transduction molecules, and membrane and cell structural proteins, to nucleic acid-binding proteins and cell-cycle regulators (Figure 2A). At the chromosomal level, the genes targeted by HP1 appeared to be distributed along all euchromatic chromosomal arms (data not shown), supporting a global role of HP1 in euchromatic gene regulation (20).

Among 60 known/predicted genes associated with DNA replication function, 15 were down-regulated in the absence of HP1 (Figure 2B). These included *McM2*, *McM5*, *McM6* and *CDC45L*, which are required for processive DNA replication and correct chromosome condensation (30–32). Other genes involved in DNA replication, such as components of the

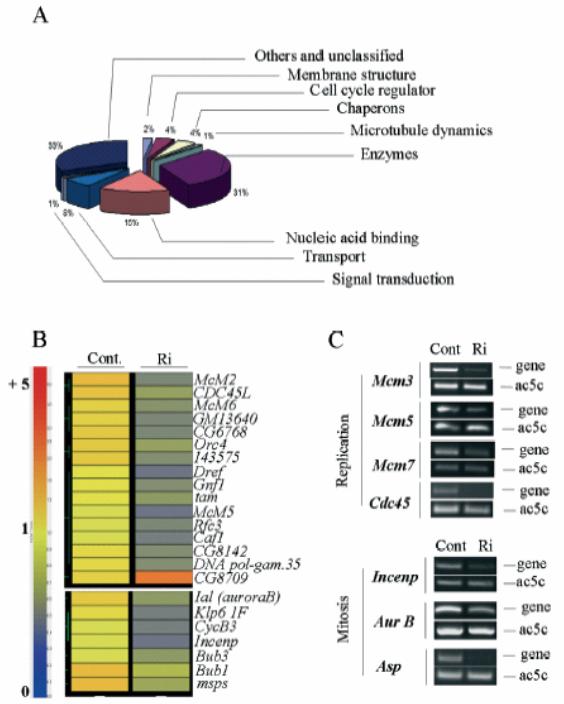

Figure 2. (**A**) Functional clusters of HP1-regulated genes in *Drosophila*. The molecular functions and the percentage of the total for each group are indicated. (**B**) Changes in the expression of genes essential for DNA replication (upper panel) and mitosis (lower panel) after RNAi treatment (Ri) compared with control cells (Cont.). The names of the genes are indicated. Expression levels are indicated by a color scale, with light blue/gray, indicating low expression and yellow/red higher expression (0- to 5-folds). (**C**) RT–PCR confirmation of the change in the expression of selected genes after HP1 ablation in Kc cells. Expression of the genes in controls (Cont.) and after RNAi (Ri) is shown. The expression level of *Actin 5c* (ac5c), used as an internal control, is also indicated.

origin recognition complex (Orc)—*Orc4*, *Caf1*, *Gnf1*, *Dref1*, *DNA polymerase-γ* and *Tam*—were also down-regulated (Figure 2B). Aurora B and inner centromere protein (INCENP), known to be required for kinetochore assembly, chromosome condensation and bipolar chromosome attachment during mitosis (33), also showed a reduction in transcription. A similar loss of transcription was observed in *Bub1* and *Bub3* (Figure 2B), encoding mitotic checkpoint control proteins (34,35). Loss function of Bub1 has been shown to cause chromatin bridges to extend between the two separating groups of chromosomes, and extensive chromosome fragmentation in anaphase cells (35).

We confirmed the changes in the transcription of cell-cycle regulators using semi-quantitative RT–PCR, which gave results consistent with the microarray analysis. In addition, cell-cycle regulator genes, such as *McM3*, *McM7* and *Asp* (abnormal spindle), were also confirmed to be down-regulated (Figure 2C). Collectively, these results demonstrate that HP1 is indeed involved in the regulation of transcription of cell-cycle regulators.

HP1 is required for Aurora B distribution and histone H3 phosphorylation

INCENP is localized to the centromeric region of chromosomes at metaphase and the spindle midzone at anaphase, which then targets Aurora B, a kinase essential for histone H3 ser10 phosphorylation, to these sites (36). Loss of function of both these 'chromosomal passenger' proteins causes abnormal chromosomal segregation at metaphase, as well as certain cytokinesis defects (36,37). The loss of transcription of both *INCENP* and *Aurora B* after depletion of HP1, therefore, raised the possibility that localization of Aurora B (Figure 3 and data not shown) may be altered. Staining of HP1-depleted Kc cells with anti-Aurora B antibodies indeed revealed an altered localization of Aurora B and, in a number of cases, a complete loss of Aurora B (Figure 3A). Consistent with the loss function of Aurora B, the spindles in the metaphase cells were also disorganized, with a large number of cells showing an altered prometaphase chromosome alignment (Figure 3A). Some showed extensive chromosome fragmentation (Figure 3B), or the presence of a third spindle pole-like structure as indicated by beta-tubulin (Figure 3A). At telophase, we observed defective separating cells with an extra cell envelope-like structure without nuclei (Figure 3A). Chromatin bridges or lagging chromatids at telophase were also evident in some cells (Figure 3C); however, in some cases, localization of Aurora B appeared not to be affected, arguing that other pathways are possibly involved.

We next analyzed changes in histone H3 serine 10 phosphorylation, since the loss of transcription of *INCENP* is known to affect localization of Aurora B (33), which is essential in the regulation of histone H3 phosphorylation (36). Total cell extracts from HP1-depleted Kc cells were analyzed by western blotting (Figure 3D). The results indeed showed a severalfold reduction in H3 ser10 phosphorylation after depletion of HP1, consistent with the functional disruption of INCENP and Aurora B in the absence of HP1.

HP1 directly targets genes encoding cell-cycle regulators in euchromatin

To test whether the loss of transcription of genes involved in DNA replication and mitosis was a direct effect of the loss of HP1, we performed a ChIP analysis to determine whether HP1 is physically associated with these genes. Chromatin lysates from formaldehyde-fixed Kc cells were sonicated into small chromatin fragments (0.2–0.8 kb) and immunoprecipitated with polyclonal antibodies against *Drosophila* HP1. As a control, we used a mock precipitation (beads only) and polyclonal antibodies against HA. Our ChIP results showed that known transposable elements distributed in heterochromatin, such as *F-element*, *TART* and *1360* (7,38), were all enriched in HP1 binding (Figure 4), which is also consistent with a previous study (20).

Using the same ChIP DNA material, we then attempted to determine whether HP1 was enriched in genes involved in DNA replication. Primers were designed to cover the promoter regions of selected genes. The results showed that *McM3*, *McM5* and *Tam* were all enriched in HP1 binding (Figure 4). However, *McM7* appeared to be HP1-negative, although its

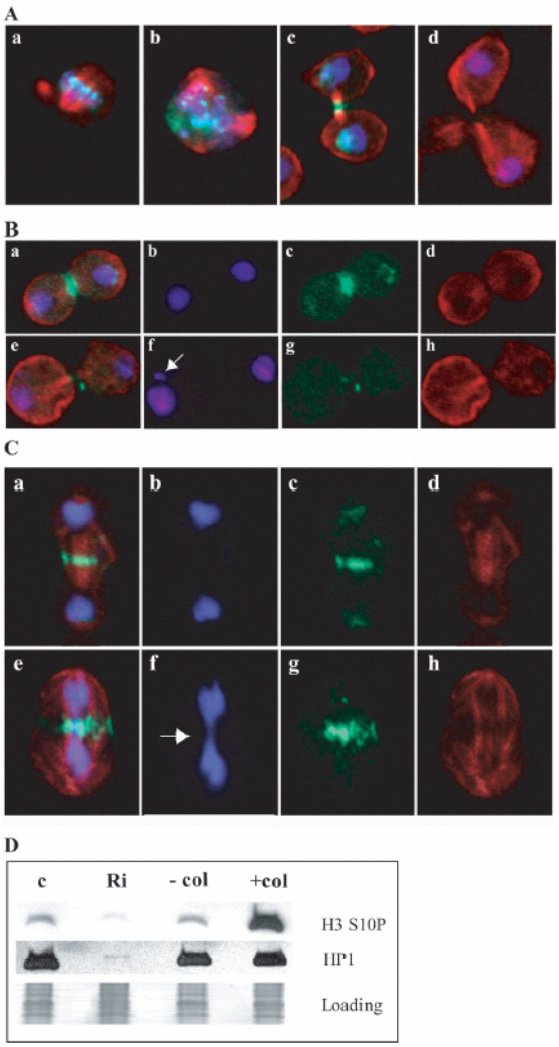

Figure 3. (**A**) Ablation of HP1 causes defects at metaphase (*a*, *b*) and telophase (*c*, *d*). Control cells at metaphase and telophase are shown in *a* and *c*; *b* and *d* show cells after HP1–RNAi. Microtubules are indicated by anti-beta-tubulin (red), anti-Aurora B (green), and DNA is indicated by DAPI (blue). (**B**) Abnormal telophase in HP1-depleted cells. Control cells are shown in *a–d*. HP1-depeleted cells are shown in *e–h*. The white arrow in *f* indicates chromosome loss/chromatin breakage. (**C**) Defective anaphase in HP1-depleted cells. Control cells are shown in *a–d*. HP1-depleted cells are shown in *e–h*. The white arrow in *f* indicates a chromatin bridge at anaphase. (**D**) Depletion of HP1 causes loss of H3 ser10 phosphorylation. Total cellular proteins from HP1–RNAi cells (Ri) and control cells (C) were used for western blotting using antibodies recognizing ser10-phosphorylated histone H3. Extracts from cells treated with colchicine (+Col) or not (−Col) were used as controls.

transcription was also affected by the loss of HP1 function. Genes essential for mitosis, such as *Aurora B*, were also HP1-positive (Figure 4). These results demonstrate that these cell-cycle regulator genes are directly targeted by HP1 in their promoter regions.

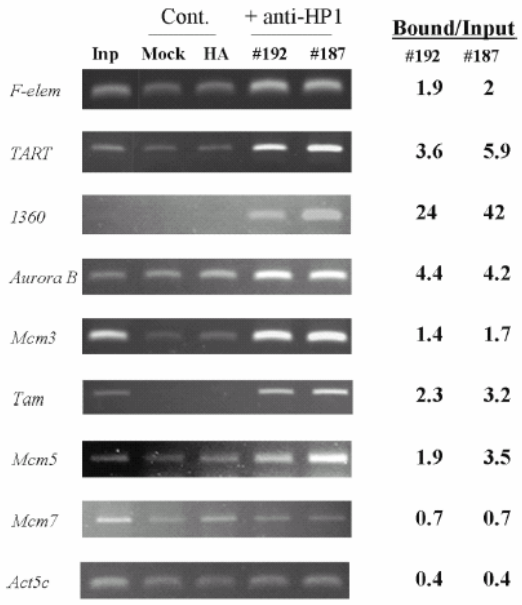

Figure 4. HP1 is physically associated with genes encoding cell-cycle regulators. Enrichment of HP1 in the genes tested was determined using PCR amplification of ChIP DNA precipitated with control and anti-HP1 antibodies (#192 and #187). Primers were designed to cover the promoter region of the genes (see Supplementary Material). The PCR products from the input (Inp) DNA are shown in the lane to the left of the gel. 1:300 dilution was used for genes *Aurora B*, *McM3*, *Tam*, *McM5*, *McM7* and *Act5c*. 1:1500 dilution used for *F-element*, *TART* and *1360* because of their high copy number in the genome. The PCR products from the controls (mock beads and anti-HA) and that from ChIP DNA using anti-HP1 are shown in agarose gels. The names of the individual gene or heterochromatin repeats analyzed are indicated. PCR amplification was performed for 35 cycles. The ratio between the intensities of the PCR products of HP1 ChIP DNA and input DNA is indicated on the right.

DISCUSSION

In this study, we used microarray and RT–PCR techniques to demonstrate that transcription of cell-cycle regulators is misregulated in the absence of HP1. Certain defects in S phase may be a direct consequence of the loss of transcription of DNA replication genes such as *McM2*, *McM5*, *McM6*, *CDC45L*, *Orc4* and others, since these genes have been functionally implicated in the initiation of DNA replication and/or the progression of replication forks (39). Depletion or mutation of these genes has been shown to result in DNA damage (32), the blockage of replication forks (39), increased chromosome loss/genome instability, and defective condensation (30).

The reduction in the number of cells in G2/M phase may be a consequence of the reduction in transcription or functional disruption of *INCENP*, *Aurora B*, *Bub1*, and *Bub3* (34,36). Chromosome segregation defects, such as chromosome fragmentation and chromatin bridges in anaphase/telophase cells, and certain cytokinesis defects in HP1-depleted cells, mimic the phenotype of cells with loss function of INCENP, Aurora B or Bub1 (35–37). The mislocalization of Aurora B in the absence of HP1 is also consistent with the loss of transcription and functional disruption of *INCENP* (37), and the reduction in *Aurora B* transcription may be partially responsible for the

observed chromosomal defects, including loss of histone H3 phosphorylation at serine 10.

HP1 is also known to physically interact with certain components of replication complexes such as ORCs and MCMs (30,40,41), with the inner centromere protein INCENP (42) and the chromatin assembly factor CAF1 (43) promoting delivery of HP1 to heterochromatin sites (44). Loss of HP1 is, therefore, expected to cause disruption to such HP1-associated complexes, and will partially contribute to the chromatin/chromosomal defects in HP1 mutants (8,27) and HP1-depleted Kc cells. It is therefore well possible that the loss of transcription of these cell-cycle regulator genes, and consequent disruption of HP1 functional complexes or heterochromatin structure, all contributed to the cell-cycle defects observed.

The ChIP assay supports the hypothesis that the loss of transcription of cell-cycle regulator genes is a direct effect of the lack of HP1. *Aurora B*, *McM3*, and *McM5* were all bound by HP1 at their promoter regions, although other cell-cycle regulators, such as *McM7*, were HP1-negative, implying that the altered transcription in these genes might be a secondary effect of the loss of HP1.

A previous study in *Drosophila* Kc cells (20) employed an approach based on the ectopic expression of a fusion protein of HP1 with a prokaryotic DNA adenine methyltransferase and identified a number of methylated targets in the genome. In this study, *MCM3* and *MCM5* were not found to be methylated, indicating lack of association with HP1. On the other hand, heterochromatin repeats, such *F-element* and *1360*, were consistently found to be HP1-enriched both here and in the previous study. It remains to be determined whether these discrepancies are due to the different experimental systems used. However, we note that the previous study was performed using a cDNA array, while we observe binding of endogenous HP1 at the promoter of these genes. Similarly, another study using chromatin immunoprecipitation in larvae also showed few HP1-positive genes that were not detected in Kc cells by the Dam ID approach (21).

A large number of genes affected by the loss of *D.melanogaster* HP1 in larval tissues (21) seem to be different from that in embryonic Kc cells. The change in the transcription of *Aurora B* and few cell-cycle regulators reported in this study is also not found among the HP1-affected genes at larval stage (21). This may be due to specific role(s) of HP1 in different stages of development. Alternatively, it is also possible that the impact of HP1 in the transcription of cell-cycle regulators in proliferating cells is underestimated when performing the analyses on larval tissues, and thus on mixed populations of both proliferating and differentiating/differentiated cells.

HP1 is generally known as a transcriptional repressor, as supported by several lines of evidence: silencing of a euchromatic reporter gene in heterochromatin requires HP1 (10,11), tethering of HP1 next to a euchromatic reporter gene causes silencing (45), and the repression of genes within euchromatic region 31 bound by HP1 is relieved in the absence of HP1 (46). In contrast, genes in heterochromatin, known as heterochromatic genes, such as *light* and *rolled*, seem to require HP1 to maintain their active transcription (47,48). The level of transcription of heterochromatic genes was dramatically reduced in a mutated HP1 background (47–49). It was therefore proposed that HP1 may function as a positive regulator of transcription of these genes (50,51), although the exact regulation mechanism remains unclear. A study of heat-shock genes found that HP1 is associated with RNA transcripts in the coding region, and is also a positive regulator of their transcription (52,53). The chromatin association of HP1 at the promoter region of active euchromatic genes demonstrated from this work and others, and its independence from histone H3K9 methylation (21), all suggest that mechanism whereby HP1 modulates transcription of euchromatic genes is potentially distinct from its role in heterochromatin formation.

Collectively, the results of this study demonstrate that HP1 plays an essential role in cell-cycle progression, and support the view that HP1, in addition to its role in heterochromatin, can act as a positive transcriptional regulator of euchromatic genes.

SUPPLEMENTARY MATERIAL

Supplementary Material is available at NAR Online.

ACKNOWLEDGEMENTS

The authors would particularly like to thank Sarah Elgin for providing them the polyclonal sera against HP1 (rabbit #187 and #192) and David M. Glover for his kindness in providing them the polyclonal antibody against *Drosophila* Aurora B. The authors also thank their colleagues Robert Hubert and Edward A. Oakeley for help with the microarray analysis, and Dirk Schübeler for stimulating discussion and critical reading of the manuscript. Funding to pay the Open Access publication charges for this article was provided by Novartis Research Foundation.

Conflict of interest statement. None declared.

REFERENCES

1. Heitz,E. (1928) Das heterochromatin der moose. *I. Jahrb. Wiss. Botanik*, **69**, 762–818.
2. Grewal,S.I. and Elgin,S.C. (2002) Heterochromatin: new possibilities for the inheritance of structure. *Curr. Opin. Genet. Dev.*, **12**, 178–187.
3. James,T.C. and Elgin,S.C. (1986) Identification of a nonhistone chromosomal protein associated with heterochromatin in *Drosophila melanogaster* and its gene. *Mol. Cell. Biol.*, **6**, 3862–3872.
4. Singh,P.B. and Georgatos,S.D. (2002) HP1: facts, open questions, and speculation. *J. Struct. Biol.*, **140**, 10–16.
5. James,T.C., Eissenberg,J.C., Craig,C., Dietrich,V., Hobson,A. and Elgin,S.C. (1989) Distribution patterns of HP1, a heterochromatin-associated nonhistone chromosomal protein of *Drosophila*. *Eur. J. Cell. Biol.*, **50**, 170–180.
6. Sun,F.L., Cuaycong,M.H., Craig,C.A., Wallrath,L.L., Locke,J. and Elgin,S.C. (2000) The fourth chromosome of *Drosophila melanogaster*: interspersed euchromatic and heterochromatic domains. *Proc. Natl Acad. Sci. USA*, **97**, 5340–5345.
7. Sun,F.L., Haynes,K., Simpson,C.L., Lee,S.D., Collins,L., Wuller,J., Eissenberg,J.C. and Elgin,S.C. (2004) *cis*-Acting determinants of heterochromatin formation on *Drosophila melanogaster* chromosome four. *Mol. Cell. Biol.*, **24**,, 8210–8220.
8. Fanti,L., Giovinazzo,G., Berloco,M. and Pimpinelli,S. (1998) The heterochromatin protein 1 prevents telomere fusions in *Drosophila*. *Mol. Cell*, **2**, 527–528.
9. Sinclair,D.A.R., Mottus,R.C. and Grigliatti,T.A. (1983) Genes which suppress position-effect variegation in *Drosophila melanogaster* are clustered. *Mol. Gen. Genet.*, **191**, 326–333.
10. Eissenberg,J.C., James,T.C., Foster-Hartnett,D.M., Hartnett,T., Ngan,V. and Elgin,S.C. (1990) Mutation in a heterochromatin-specific chromosomal protein is associated with suppression of position-effect

variegation in *Drosophila melanogaster*. *Proc. Natl Acad. Sci. USA*, **87**, 9923–9927.
11. Eissenberg,J.C., Morris,G.D., Reuter,G. and Hartnett,T. (1992) The heterochromatin-associated protein HP-1 is an essential protein in *Drosophila* with dosage-dependent effects on position-effect variegation. *Genetics*, **131**, 345–352.
12. Paro,R. and Hogness,D.S. (1991) The Polycomb protein shares a homologous domain with a heterochromatin-associated protein of *Drosophila*. *Proc. Natl Acad. Sci. USA*, **88**, 263–267.
13. Lachner,M., O'Carroll,D., Rea,S., Mechtler,K. and Jenuwein,T. (2001) Methylation of histone H3 lysine 9 creates a binding site for HP1 proteins. *Nature*, **410**, 116–120.
14. Bannister,A.J., Zegerman,P., Partridge,J.F., Miska,E.A., Thomas,J.O., Allshire,R.C. and Kouzarides,T. (2001) Selective recognition of methylated lysine 9 on histone H3 by the HP1 chromo domain. *Nature*, **410**, 120–124.
15. Schotta,G., Ebert,A., Krauss,V., Fischer,A., Hoffmann,J.E., Rea,S., Jenuwein,T., Dorn,R. and Reuter,G. (2002) Central role of *Drosophila* Su(var)3-9 in histone H3-K9 methylation and heterochromatic gene silencing. *EMBO J.*, **21**, 1121–1131.
16. Richards,E.J. and Elgin,S.C. (2002) Epigenetic codes for heterochromatin formation and silencing: rounding up the usual suspects. *Cell*, **108**, 489–500.
17. Delattre,M., Spierer,A., Tonka,C.H. and Spierer,P. (2000) The genomic silencing of position-effect variegation in *Drosophila melanogaster*: interaction between the heterochromatin-associated proteins Su(var)3-7 and HP1. *J. Cell Sci.*, **113**, 4253–4261.
18. Vaute,O., Nicolas,E., Vandel,L. and Trouche,D. (2002) Functional and physical interaction between the histone methyltransferase Suv39H1 and histone deacetylases. *Nucleic Acids Res.*, **30**, 475–481.
19. Cowell,I.G., Aucott,R., Mahadevaiah,S.K., Burgoyne,P.S., Huskisson,N., Bongiorni,S., Prantera,G., Fanti,L., Pimpinelli,S., Wu,R. *et al.* (2002) Heterochromatin, HP1 and methylation at lysine 9 of histone H3 in animals. *Chromosoma*, **111**, 22–36.
20. Greil,F., van der Kraan,I., Delrow,J., Smothers,J.F., de Wit,E., Bussemaker,H.J., van Driel,R., Henikoff,S. and van Steensel,B. (2003) Distinct HP1 and Su(var)3-9 complexes bind to sets of developmentally coexpressed genes depending on chromosomal location. *Genes Dev.*, **17**, 2825–2838.
21. Cryderman,D.E., Grade,S.K., Li,Y., Fanti,L., Pimpinelli,S. and Wallrath,L.L. (2005) Role of *Drosophila* HP1 in euchromatic gene expression. *Dev. Dyn.*, **232**, 767–774.
22. Zhao,T., Heyduk,T., Allis,C.D. and Eissenberg,J.C. (2000) Heterochromatin protein 1 binds to nucleosomes and DNA *in vitro*. *J. Biol. Chem.*, **275**, 28332–28338.
23. Perrini,B., Piacentini,L., Fanti,L., Altieri,F., Chichiarelli,S., Berloco,M., Turano,C., Ferraro,A. and Pimpinelli,S. (2004) HP1 controls telomere capping, telomere elongation, and telomere silencing by two different mechanisms in *Drosophila*. *Mol. Cell*, **15**, 467–476.
24. Kellum,R. (2003) HP1 complexes and heterochromatin assembly. *Curr. Top. Microbiol. Immunol.*, **274**, 53–77.
25. Ekwall,K., Javerzat,J.P., Lorentz,A., Schmidt,H., Cranston,G. and Allshire,R. (1995) The chromodomain protein Swi6: a key component at fission yeast centromeres. *Science*, **269**, 1429–1431.
26. Bernard,P., Maure,J.F., Partridge,J.F., Genier,S., Javerzat,J.P. and Allshire,R.C. (2001) Requirement of heterochromatin for cohesion at centromeres. *Science*, **294**, 2539–2542.
27. Kellum,R. and Alberts,B.M. (1995) Heterochromatin protein 1 is required for correct chromosome segregation in *Drosophila* embryos. *J. Cell Sci.*, **108**, 1419–1431.
28. Peters,A.H., O'Carroll,D., Scherthan,H., Mechtler,K., Sauer,S., Schofer,C., Weipoltshammer,K., Pagani,M., Lachner,M., Kohlmaier,A. *et al.* (2001) Loss of the Suv39h histone methyltransferases impairs mammalian heterochromatin and genome stability. *Cell*, **107**, 323–337.
29. Orlando,V., Strutt,H. and Paro,R. (1997) Analysis of chromatin structure by *in vivo* formaldehyde cross-linking. *Methods*, **11**, 205–214.
30. Christensen,T.W. and Tye,B.K. (2003) *Drosophila* MCM10 interacts with members of the prereplication complex and is required for proper chromosome condensation. *Mol. Biol. Cell*, **14**, 2206–2215.
31. Rowles,A. and Blow,J.J. (1997) Chromatin proteins involved in the initiation of DNA replication. *Curr. Opin. Genet. Dev.*, **7**, 152–157.
32. Bailis,J.M. and Forsburg,S.L. (2004) MCM proteins: DNA damage, mutagenesis and repair. *Curr. Opin. Genet. Dev.*, **14**, 17–21.
33. Adams,R.R., Carmena,M. and Earnshaw,W.C. (2001) Chromosomal passengers and the (aurora) ABCs of mitosis. *Trends Cell Biol.*, **11**, 49–54.
34. Sharp-Baker,H. and Chen,R.H. (2001) Spindle checkpoint protein Bub1 is required for kinetochore localization of Mad1, Mad2, Bub3, and CENP-E, independently of its kinase activity. *J. Cell Biol.*, **153**, 1239–1250.
35. Basu,J., Bousbaa,H., Logarinho,E., Li,Z., Williams,B.C., Lopes,C., Sunkel,C.E. and Goldberg,M.L. (1999) Mutations in the essential spindle checkpoint gene bub 1 cause chromosome missegregation and fail to block apoptosis in *Drosophila*. *J. Cell Biol.*, **146**, 13–28.
36. Giet,R. and Glover,D.M. (2001) *Drosophila* aurora B kinase is required for histone H3 phosphorylation and condensin recruitment during chromosome condensation and to organize the central spindle during cytokinesis. *J. Cell Biol.*, **152**, 669–682.
37. Mackay,A.M., Ainsztein,A.M., Eckley,D.M. and Earnshaw,W.C. (1998) A dominant mutant of inner centromere protein (INCENP), a chromosomal protein, disrupts prometaphase congression and cytokinesis. *J. Cell Biol.*, **140**, 991–1002.
38. Pimpinelli,S., Berloco,M., Fanti,L., Dimitri,P., Bonaccorsi,S., Marchetti,E., Caizzi,R., Caggese,C. and Gatti,M. (1995) Transposable elements are stable structural components of *Drosophila melanogaster* heterochromatin. *Proc. Natl Acad. Sci. USA*, **92**, 3804–3808.
39. Labib,K., Tercero,J.A. and Diffley,J.F. (2000) Uninterrupted MCM2-7 function required for DNA replication fork progression. *Science*, **288**, 1643–1647.
40. Pak,D.T., Pflumm,M., Chesnokov,I., Huang,D.W., Kellum,R., Marr,J., Romanowski,P. and Botchan,M.R. (1997) Association of the origin recognition complex with heterochromatin and HP1 in higher eukaryotes. *Cell*, **91**, 311–323.
41. Huang,D.W., Fanti,L., Pak,D.T., Botchan,M.R., Pimpinelli,S. and Kellum,R. (1998) Distinct cytoplasmic and nuclear fractions of *Drosophila* heterochromatin protein 1: their phosphorylation levels and associations with origin recognition complex proteins. *J. Cell Biol.*, **142**, 307–318.
42. Ainsztein,A.M., Kandels-Lewis,S.E., Mackay,A.M. and Earnshaw,W.C. (1998) INCENP centromere and spindle targeting: identification of essential conserved motifs and involvement of heterochromatin protein HP1. *J. Cell Biol.*, **143**, 1763–1774.
43. Shibahara,K. and Stillman,B. (1999) Replication-dependent marking of DNA by PCNA facilitates CAF-1-coupled inheritance of chromatin. *Cell*, **96**, 575–585.
44. Quivy,J-P., Roche,D., Kirschner,D., Tagami,H., Nakatani,Y. and Almouzni,G. (2004) A CAF-1 dependent pool of HP1 during heterochromatin duplication. *EMBO J.*, **23**, 3516–3526.
45. Li,Y., Danzer,J.R., Alvarez,P., Belmont,A.S. and Wallrath,L.L. (2003) Effects of tethering HP1 to euchromatic regions of the *Drosophila* genome. *Development*, **130**, 1817–1824.
46. Hwang,K.K., Eissenberg,J.C. and Worman,H.J. (2001) Transcriptional repression of euchromatic genes by *Drosophila* heterochromatin protein 1 and histone modifiers. *Proc. Natl Acad. Sci. USA*, **98**, 11423–11427.
47. Clegg,N.J., Honda,B.M., Whitehead,I.P., Grigliatti,T.A., Wakimoto,B., Brock,H.W., Lloyd,V.K. and Sinclair,D.A. (1998) Suppressors of position-effect variegation in *Drosophila melanogaster* affect expression of the heterochromatic gene light in the absence of a chromosome rearrangement. *Genome*, **41**, 495–503.
48. Hearn,M.G., Hedrick,A., Grigliatti,T.A. and Wakimoto,B.T. (1991) The effect of modifiers of position-effect variegation on the variegation of heterochromatic genes of *Drosophila melanogaster*. *Genetics*, **128**, 785–797.
49. Lu,B.Y., Emtage,P.C., Duyf,B.J., Hilliker,A.J. and Eissenberg,J.C. (2000) Heterochromatin protein 1 is required for the normal expression of two heterochromatin genes in *Drosophila*. *Genetics*, **155**, 699–708.
50. Wakimoto,B.T. (1998) Beyond the nucleosome: epigenetic aspects of position-effect variegation in *Drosophila*. *Cell*, **93**, 321–324.
51. Eissenberg,J.C. and Elgin,S.C. (2000) The HP1 protein family: getting a grip on chromatin. *Curr. Opin. Genet. Dev.*, **10**, 204–210.
52. Piacentini,L., Fanti,L., Berloco,M., Perrini,B. and Pimpinelli,S. (2003) Heterochromatin protein 1 (HP1) is associated with induced gene expression in *Drosophila* euchromatin. *J. Cell Biol.*, **161**, 707–714.
53. Kellum,R. (2003) Is HP1 an RNA detector that functions both in repression and activation? *J. Cell Biol.*, **161**, 671–672.

IV. References

Adamietz, P. and Rudolph, A. (1984). J Biol Chem. **259**, 6841-6846.

Adhvayu, K.K., *et al.,* (2005). Eukaryot Cell. **4**, 1455-1464.

Ahmad, K. and Henikoff S., (2002). Proc. Natl. Acad. Sci. U.S.A. **99**, 16477.

Akimitsu N., *et al*., (2003), Genes Cells. **8**, 393-402

Alami, R., *et al*., (2003). Proc Natl Acad Sci U S A. **100**, 5920-5925.

Alejandro, C., *et al*., (2003). MCB. **23**, 8626-8636.

Alfonso, P.J., *et al*., (1994). J Mol Biol. **236**, 189-198.

Allan, J., *et al*., (1980). Nature. **288**, 675-679.

Allan, J., *et al*.,(1986). J Mol Biol. **187**, 591-601.

Allfrey, V.G., *et al.*, (1964). Proc Natl Acad Sci U S A. **51**, 786-94.

Alonso, A., *et al*., (1988). EMBO J. **7**, 3003-3008.

Allshire, R., *et al*., (2002). Science. **297**, 1818-1819.

Alvarez-Gonzalez, R., *et al*., (1994). Mol Cell Biochem. **138**, 33-37.

Ananthanarayanan, M., *et al*., (2004). J Biol Chem. **279**, 54348-54357.

Anderson, J.D., *et al*., (2001). J Mol Biol. **307**, 977-985.

Andrei, *et al*., 2004

Arents, G., *et al*., (1991). Proc Natl Acad Sci U S A. **88**, 10148-10152.

Arion, D., *et al*., (1988). Cell. **55**, 371-378.

Ayyanathan, K., *et al*., (2003). Genes Dev. **17**, 1855-1869.

Bakin, R.E., *et al*., (2004). J Biol Chem. **279**, 51218-51225.

Bannister, A.J., *et al*., (2001). Nature. **410**, 120 -124.

Barnes, P.J., *et al.,* (2005). Eur Respir J. **25**, 552-563.

Bassing, C.H., *et al*., (2003). Cell. 114, **359**-370.

Bassing and Alt, *et al.,* (2004). DNA Repair (Amst.) **3**, 781-796.

Beisel, c., *et al*., (2002). Nature. **419**, 857-862.

Berger, S.L., (2002). Curr Opin Genet Dev. **12**, 142-148.

Bernstein, B.E., *et al*., (2002). Proc Natl Acad Sci U S A. **99**, 8695-8670

Bharath, M.M., *et al*., (2002). Proteins. **49**, 71-81.

Bhat, K.P., *et al.*, (2004). EMBO J. **23**, 2402-2412.

Boulikas, T., (1989). Proc Natl Acad Sci U S A. **86**, 3499-3503.

Boulias, K., *et al.*, (2004). Nucleic Acids Res. **32**, 6096-6103.

Bohm, L., *et al*., (1997). Biochim Biophys Acta. **1334**, 149-154.

Boggs, B.A., *et al.*, (2002). Nat Genet. **30**, 73-76.

Bredehorst, R., *et al*., (1981). Eur J Biochem. **120**, 267-274.

Briand, G., *et al*., (1980). FEBS Lett. **112**, 147-151.

Briggs, S.D., *et al*., (2002). Nature. **418**, 498.

Brogna, S., *et al*., (2002). Mol Cell. **10**, 93-104.

Brown, J.L., *et al*., (1998). Mol Cell. **1**, 1057-1064.

Burzio, L.O., *et al*., (1979). J Biol Chem. **254**, 3029-3037.

Byrd, K.N., et al., (2003). Proc Natl Acad Sci U S A. **100**, 11535-11540

Carvell, T., *et al.,* (2002), Cancer Research. **62**, 6456-6461.

Cao, R., *et al*., (2002). Science. **298**, 1039-1043.

Celeste, A., *et al*., (2003). Nat Cell Biol. 5**, 675**-679.

Christophe, T., *et al.*, (2005). Mol Cell. **18**, 617-622.

Chen, H.W., *et al*., (1997). Cell. 569-580.

Chen, H.Y., *et al*., (1998). J Biol Chem. **273**, 13165-13169.

Cheung, P., *et al*., (2000). Cell. **103**, 263-271.

Cheung, W.L., *et al.,* (2005). Curr Biol. **15**, 656-660.

Cheutin, T., *et al.*, (2003). Science. **299**, 721-725.

Choi, H.S., *et al.,* (2005). J Biol Chem. **280**, 13545-13553.

Clark, D.J., *et al*., (1988). EMBO J. **7**, 69-75.

Clayton, A.L. *et al*., (2000). EMBO J. **19**, 3714-3726.

Clements, A., *et al*., (2003). Mol Cell. **12**, 461-473.

Clore, *et al*., (1987). EMBO J. **6**, 1833-1842.

Couture, J.F., *et al.,* (2005). Genes & Dev. **19**, 1455-1465.

Covic, M., *et al*., (2005). EMBO J. **24**, 85-96.

Crane-Robinson, C., (1999). Bioessays. **21**, 367-371.

Crosio, C., *et al*., (2000). Nat Neurosci. **3**, 1241-1247.

Cuthbert, G.L., *et al.*, (2004). Cell. **118**, 545-553.

Czermin, B., *et al*., (2002). Cell. **111**, 185-196.

Daniel, J.A., *et al*., (2004). J. Biol. Chem. **279**, 1867-1871.

David, A.F., *et al.,* (2003). Cell. **114**, 673-688.

De Napoles, M., *et al*., (2004). Dev Cell. **7**, 663-676.

De Souza, C.P., *et al*., (2000). Cell. **102**, 293-302.

Dietmar, E., *et al*., (2004). Cell. **29**, 969-979.

Ding, H.F., *et al*., (1997). Mol Cell Biol. **17**, 5843-5855.

Dokmanovic, M., *et al.,* (2005). J Cell Biochem. **96**, 293-304.

Dover, J., *et al*., (2002). J Biol Chem. **277**, 28368-28371.

Durrin, L.K., *et al*., (1991). Cell. **65**, 1023-1031.

Dyda, F., *et al*., (2000). Annu. Rev. Biophys. Biomol. Struct. **29**, 81-103.

Ezhkova, E., *et al*, (2004). Mol Cell. **13**, 435-442

Fan, Y., *et al*., (2001). Mol. Cell. Biol. **21**, 7933-7943.

Fan, Y., *et al*., (2002). Nat Struct Biol. **9**, 172-176.

Faraone-Mennella, M.R., *et al*., (2005). Biochem Cell Biol. **83**, 396-404.

Fernandez-Capetillo, *et al.*, (2004). DNA Repair (Amst.). **3**, 959-967.

Feng, Q., *et al*., (2002). Curr Biol. **12**, 1052-1058.

Festenstein. R., *et al*.,(1999). Nat Genet. **23**, 457-461.

Filipowicz, W., (2005). Cell. **122**, 17-20.

Fischle, *et al*., (2003). Nature. **425**, 475-479.

Foster, E.R., *et al*., (2005). FEBS J. **272**, 3231-3240.

Gary, J.D., *et al*., (2003). Prog Nucleic Acid Res Mol Biol. **61**, 65-131.

Giannattasio, M, *et al*., (2005). J Biol Chem. **280**, 9879-9886.

Giordano, A., *et al*., (1999). J. Cell. Physiol. **181**, 218-230.

Golderer, G. and Grobner, P., (1991). Biochem J. **277**, 607-610.

Goodman, R.H. and Smolik, S., (2000). Genes Dev. **14**, 1553-1577.

Goto, H., *et al*., (1999). J Biol Chem. **274**, 25543-25549.

Goytisolo, F.A., *et al.,* (1996). The EMBO Journal. **15**, 3421-3429.

Graziano, V., *et al*., (1994). Nature. **368**, 351-354.

Green, C.M. and Almouzni G., (2002). EMBO Rep. **3**, 28-33.

Grewal, S.I., *et al*., (2002). Curr Opin Genet Dev **12**, 178-187.

Grewal, S.I., *et al.*, (2003). Science. **301**, 798-802.

Grigliatti, T., (1991). Methods Cell Biol. **35**, 587-627.

Guidez, F., *et al*., (2005). Mol Cell Biol. **25**, 5552-5566.

Gunjan, A., *et al*., (2001). J Biol Chem. **276**, 3635-3640.

Halmer, L., *et al*., (1996). Nucleic Acids Research. **24**, 1420-1427.

Hampsey, M., and Reinberg D., (2003). Cell. **113**, 429-432.

Hansen, J.C., (2002). Annu Rev Biophys Biomol Struct. **31**, 361-392.

Hansol, L., et al., (2004). Science. **304**, 1675-1678.

Hara, R., *et al.,* (2000). Mol Cell Biol. **20**, 9173-9181.

Hartman, P.G., *et al*., (1977). Eur J Biochem. **77**, 45-51.

Hayes, J.J., (1996). Biochemistry. **35**, 11930-11937.

Heard, E., *et al.*, (2001). Cell. **107**, 727-738.

Hecht, A., *et al*., (1995). Cell. **80**, 583-592.

Heitz, E., (1928). Jahrb Wiss Botanik. **69**, 762-818.

Henikoff, S., (1995). Curr. Top. Microbiol. Immunol. **197**, 193-208.

Henikoff, S., *et al*., (2005). Annu Rev Cell Dev Biol.

Henry, K.W., *et al.*, (2003). Genes Dev. **17**, 2648-2663.

Hill, C.S., *et al*., (1989). EMBO J. **8**, 2591-2599.

Horard, B., *et al*.,(2000). Mol Cell Biol. **20**, 3187-3197.

Hsu, J.Y., *et al*., (2000). Cell. **102**, 279-291.

Huyen, Y., et al., (2004). Nature. **432**, 406-411.

Hwang, W.W., *et al*., (2003). Mol Cell. **11,** 261-266.

Lacoste, N., et al., (2002). J Biol Chem. **277**, 30421-30424.

Lachner, M., et al., (2001). Nature. **410**, 116-120.

Lugar, *et al*., (1997). Nature **389**, 251-260.

Iizuka, M., *et al*., (2003). Curr Opin Genet Dev **13**, 154-160.

James, A.B., *et al.*, (2004). Curr Biol. **14**, R759-761.

Janknecht, R. and Hunter T., (1996). Curr. Biol. **6**, 22-23.

Jason, L.J., *et al*., (2002). Bioessays. **24**, 166-174.

Jason, L.J., *et al.,* (2005). J Biol Chem. **280**, 4975-4982.

Jenuwein, T. and Allis C.D., (2001). Science. **293**, 1074-1080.

Jiang, G., *et al*., (2004). J Cell Biochem. **93**, 286-300.

Jorgensen, P., *et al.*, (2004). Cell Growth. **329**-370 b.

Judd, C.R., *et al.*, (2002). Genes & Dev. **16**, 2225-2230.

Karras, G.I., *et al.*, (2005). EMBO J. **24**, 1911-1920.

Kasten, M.M., *et al*., (1997). Mol Cell Biol. **17**, 4852-4858.

Kayne, P.S., *et al*, (1988). Cell. **55**, 27-39.

Khadake, J.R. and Rao, M.R., (1995). Biochemistry. **34**, 15792-15801.

Khochbin, S., *et al.*, (2001). Curr Opin Genet Dev. **11**, 162-166.

Konishi, A., *et al*., (2003). Cell. **114**, 673-688.

Kornberg, R.D., *et al.*, (1999). Cell. **98**. 285-294.

Kosmoski, J.V., *et al*., (2001). Proc Natl Acad Sci U S A. **98**, 10113-10118.

Kreimeyer, A., *et al*., (1984). J Biol Chem. **259**, 890-896.

Krogen, N.J., et al., (2003). Mol Cell Biol. **23**, 4207-4218

Kuo, M.H., *et al*., (2000). Mol Cell. **6**, 1309-1320.

Kuzmichev, A., *et al*., (2004). Mol Cell. **14**, 183-193.

Kuzmichev, A., *et al*., (2002). Genes Dev. **16**, 2893-2905.

Lee, D.Y., *et al.*, (1993). Cell. **72**, 73-84.

Lennox, R.W. and Cohen L.H., (1983). J. Biol. Chem. **258**, 262-268.

Lennox, R.W. and Cohen, L.H. (1984). Dev Biol. **103**, 80-104.

Liang, S.H., *et al*., (2001). Eur J Biochem. **268**, 2779-2783.

Lim, J.H., *et al.*, (2004). Mol Cell. **15**, 573-584.

Ling, X., *et al*., (1996). Genes Dev. **10**, 686-699.

Lin, Q., *et al*., (2000). Mol. Cell. Biol. **20**, 2122-2128.

Litt, M.D., *et al.*, (2001). Science. **293**, 2453-2455.

Li, Y., *et al.*, (2003). Development. **130**, 1817-24.

Liu, X. and Smerdon MJ., (2000). J Biol Chem. **275**, 23729-23735.

Lo, W.S., *et al.*, (2000). Mol Cell. **5**, 917-926.

Lohrum, M.A., *et al*., (2003). Cancer Cell. **3**, 577-587.

Lu, X., and Hansen, J.C., *et al*., (2004). J Biol Chem. **279**, 8701-8707.

Lundgren, M., *et al*., (2000). Cell. **103**, 733-743.

Mann, R.K., *et al*., (1992). EMBO J. **11**, 3297-3306.

Masumoto, H., *et.al*., (2005). Nature. **436**, 294-298.

McBride, A.E., *et al*., (2001). Cell. **106**, 5-8.

McKittrick, *et al*., (2004). Proc Natl Acad Sci U S A. **101**, 1525-1530.

McMahon, K.K., *et al*., (1993). Biochem J. **293**, 789-793.

Mermoud, J.E., *et al.*, (2002). Curr Biol. **12**, 247-251.

Meyer-Ficca, M.L., *et al*., (2005). Chromosoma. **114**, 67-74.

Min, J., et al., (2003). Genes Dev. **17**, 1823-1828.

Miranda, T.B., *et al*., (2004). J Biol Chem. **279**, 22902-22907.

Mizzen, C.A., *et al.*, (1996). Cell. **87**, 1261-1270.

Smith, M.M., (2002). Curr. Opin. Cell Biol. **14**, 279 .

Mochizuki, K., *et al.*, (2002). Cell. **110**, 689–699.

Mulholland, N.M., *et al*., (2003). Genes Dev. **17**, 2741-2746.

Muller, H.J., (1930). J Genet. **22**, 299–334.

Nakayama, T., *et al*., (2001). J Biochem (Tokyo). **129**, 491-499.

Nakamura, T., *et al*., (2002). Mol Cell. **10**, 1119-1128.

Ng, H.H., *et al*., (2002). J Biol Chem. **277**, 34655-34657.

Ng, H.H., *et al*., (2003a). Mol Cell. **11**, 709-719.

Ng, H.H., *et al*., (2003b). Proc Natl Acad Sci U S A. **100**, 1820-1825.

Nielsen, A.L., et al., (2001). Mol Cell. **7**, 729-739.

Nishioka, K., *et al.*, (2002a). Mol Cell. **9**, 1201-13.

Nishioka, K., *et al*., (2002b). Genes Dev. **16**, 479-489.

Noma, K., *et al*., (2001). Science. **293**, 1150-1155.

Normura, M., (2001). Cold Spring Harb. Symp. Quant. Biol. **66**, 555-565.

Nowak, S.J. and Corces V.G., (2000). Genes Dev. **14**, 3003-3013.

Odintsova, T.I., *et al.*, (2003). J Protein Chem. **22**, 249-258

Ogata, N., *et al*., (1980). J Biol Chem. **255**, 7610-7615.

Oren, M., (2003). Cell Death Differ. **10**, 431-442.

Pada, F., *et al*., (2005). Chromosome Res. **13**, 57-72.

Pascreau, G., *et al*., (2003). Prog Cell Cycle Res. **5**, 369-374.

Patterton, H.G., *et al*., (1998). J Biol Chem. **273**, 7268-7276.

Peters, A.H., *et al.*, (2003). Nat Genet. **30**, 77-80.

Peterson, and Cote, (2004). Genes Dev. **18**, 602-616.

Pham, A.D. and Sauer F., (2000). Science. **289**, 2357-2360.

Plath, K., *et al*., (2003). Science. **300**, 131-135.

Pray-Grant, M.G., *et al.*, (2005). Nature. **433**, 434-438.

Pruss, D., *et al*., (1996). Science. **274**, 614-617.

Ramakrishnan, V., *et al*., (1993). Nature. **362**, 219-223.

Rea, S., *et al*., (2000). Nature. **406**, 593-599.

Redon, C., *et al*., (2002). Curr. Opin. Genet. Dev. **12**, 162.

Rice, J.C., *et al*., (2003). Mol Cell. **12**, 1591-1598.

Reid, J.L., *et al.*, (2000). Mol Cell. **6**, 1297-1307.

Reinhart, B.J., et al., (2002). Science. **297**, 1831

Richard, G., *et al.*, (2005). Molecular and Cellular Biology. **25**, 6123-6139.

Robzyk, K., *et al*., (2000). Science. **287**, 501-504.

Sanders, S.L., *et al.*, (2004). Cell. **119**, 603-614.

Santos-Rosa, H., *et al*., (2002). Nature. **419**, 407-11.

Sarg, B., *et al.,* (2004). J Biol Chem. **279**, 53458-53464.

Sassone-Corsi, P., *et al*., (1999). Science. **285**, 886-891.

Schubeler, D., *et al.*, (2004). Genes Dev. **18**, 1263-7121.

Schubeler, D., *et al*., (2000). Mol Cell Biol. **20**, 9103-9112.

Schuman, E.M., *et al*., (1994). Proc Natl Acad Sci U S A. **91**, 11958-11962.

Schneider, R., *et al.*, (2002). Trends Biochem Sci. **27**, 396-402.

Sewack, G.F., *et al*., (2001). Mol Cell Biol. **21**, 1404-1415.

Seligson, D.B., *et.al*., (2005). Nature. **435**, 1262-1266.

Shanower, G.A., *et al.,* (2005). Genetics. **169**, 173-184.

Shen, X., *et al*., (1995). Cell. **82**, 47-56.

Shen, X., & Gorovsky M. A., (1996). Cell. **86**, 475-483.

Shi, Y., et al., (2004). Cell. **119**, 941-953.

Shikama, N., *et al*., (1997). Trends Cell Biol. **7**, 230-236.

Shroff, R., *et al.*, (2004). Curr Biol. **14**, 1703-1711.

Schultz, D.C., *et al*., **(**2002). Genes Dev. **16**, 919-932.

Silva, J., *et al.*, (2003). Dev Cell. **4**, 481-495.

Simon, J.A., *et al*., (2002). Curr Opin Genet Dev. **12**, 210-218.

Sims, R.J., *et al.*, (2003). Trends Genet. **19**, 629-639.

Sirotkin, A.M., *et al*., (1995). Proc. Natl. Acad. Sci. USA. **92**, 6434-6438.

Smerdon, M.J. and Conconi A., (1999). Prog Nuc Aci Res Mol Biol. **62**, 227-255.

Spencer, V.A., *et al*., (1999). Gene. **240**, 1–12.

Stallcup, M.R., (2001). Oncongene. **20**, 3014-3020.

Strahl, B.D., (2000). Nature **403**, 41–45.

Sugasawa, K., *et al*., (1993). J Biol Chem. **268**, 9098-9104.

Suka, N., *et al.*, (2001). Mol Cell. **8**, 473-479.

Sullivan, B.A., *et al.*, (2004). Nat Struct Mol Biol. **11**, 1076-1083.

Sun, Z.W., *et al.*, (2002). Nature. **418**, 104-108.

Suzuki, M., *et al*., (1989). EMBO J. **8**, 797-804.

Suzuki, M., *et al*., (1993). Protein Eng. **6**, 565-574.

Swaminathan, J., *et al.*, (2005). Genes Dev. **19**, 65-76.

Tachibana, M., *et al*, (2001). J Biol Chem. **276**, 25309-25317.

Taddei, A., *et al.*, (2001). Nat Cell Biol **3**, 114-120.

Tanaka, M., *et al*., (2001). Development. **128**, 655-664.

Thompson, J.S., *et al*., (1994). Nature. **369**, 245-247.

Thomson, S., *et al*., (1999). EMBO J. **18**, 4779-4793.

Thomas, *et al*., (1992). Nucleic Acids Res. **20**, 187-194.

Thomas, J.O., (1999). Curr. Opin. Cell Biol. **11**, 312-317.

Tikoo, K. and Ali, Z, (1997). Biochem J. 322 , **281**-287.

Toleman, C., *et al.*, (2004). J Biol Chem. **279**, 53665-53673.

Torben, L., *et al*., (2005). Antimicro. Agents and Chemotherapy. **49**, 2399-2406.

Trewick, S.C., *et al*., (2005). EMBO Rep. **6**, 315-320.

Tschochner, H., *et al*., (2003). Trends Cell Biol. **13**, 255-263.

Tse, C., *et al*., (1998). Mol Cell Biol. **18**, 4629-4638.

Tsuchiya, M. and Shimoyama M. (1994). Mol Cell Biochem. **138**, 113-118.

Tuck, M.T., *et al.*, (1985). J Biol Chem. **260**, 7114-7121.

Turner, B.M., (2000). Bioessays. **22**, 836-845.

Unal, E., *et al*., (2004). Mol Cell. **16**, 991-1002.

Vakoc, C.R., *et al.*, (2005). Mol Cell. **19**, 381-391.

Van Holde, K., (1989). Chromatin.

Van Holde, K., (1998). Chromatin.

Van, Leeuwen F., *et al*., (2002). Cell. **109**, 745-756.

Vandel, L., *et al*., (2001). Mol Cell Biol. **21**, 6484-6494.

Vernet, G., *et al*., (1990). Biochim Biophys Acta. **1048**, 281-289.

Vila, R., *et al*., (2000). Protein Sci. **9**, 627-636.

Vila, R., *et al*., (2001). J Biol Chem. **276**, 46429-46435.

Visochek, L., *et al*., (2005). J Neurosci. **25**, 7420-7428.

Volpe, T.A., *et al*., (2002). Science. **297**, 1833-1837.

Vogelauer, M., *et al*., (2000). Nature. **408**, 495-498.

Wang, H., *et al*., (2004). Nature. **431**, 873-878.

Wang, J., Nemoto E, Dennert G. (1996). J Immunol. **156**, 2819-2827.

Wang, X., *et al.*, (2000). J Biol Chem. **275**, 35013-35020.

Wang, Z.F., *et al*., (1997). J. Mol. Biol. **271**, 124-138.

Wang, Z.G., *et al*., (1991). J Biol Chem. **266**, 22472-22478.

Warner, J.R., (1999). Trends Biochem. Sci. **24**, 437-440.

Wassenegger, M., (2005). **122**, 13-16

Wei, Y., *et al*., (1999). Cell. **97**, 99-109.

Wielckens, K., *et al*., (1982). J Biol Chem. **257,** 12872-12877.

Wilmut, I., *et al.*,(2002). Nature. **419**, 583-586.

Wolffe, A.P., (1997). Int J Biochem Cell Biol. **29**, 1463-1466.

Wolffe, A.P., (1998). Proc. Natl. Acad. Sci. U.S.A. **61**, 379-422.

Wood, A., *et al*., (2003). Mol Cell. **11**, 267-274.

Wysocka, J., *et al.*, (2005). Cell. **121**, 859-872.

Yael, K.K., *et al*., (2005). The EMBO Journal. **24**, 2138-2149.

Ye, J., *et al.,* (2005). Mol Cell. **18**, 123-130.

Yutaka, K. et al., (2004). Proc. Natl. Acad. Sci. U.S.A. **101**, 7398-7403.

Yu, Y.C., *et al.*, (2005). Proc. Natl. Acad. Sci. U.S.A. **102**, 8650-8655.

Zarbock ,*et al*., (1986). Proc. Natl. Acad. Sci. U.S.A. **83**, 7628-7632.

Zengel, J.M., *et al.*, (2003). RNA. **9**, 1188-1197.

Zegerman, P., *et al*., (2002). J Biol Chem. **277**, 11621-11624.

Zhang, Y. and Reinberg, D., (2001). Genes Dev. **15**, 2343-2360

Zhang, Y. (2003). Genes Dev. **17**, 2733-2740.

Zhang, Y., *et al*., (2003). Mol. Cell. Biol. **23**, 8902-8912

Zhang, Y., *et al.*, (2004). J. Biol. Chem. **279**, 21866-21872.

Zhou, Y.B., *et al*.,(1998). Nature. **395**, 402-405.

Zolkiewska, A., *et al*., (1992). Proc Natl Acad Sci U S A. **89**, 11352-11356.

Zolkiewska, A., Moss J. (1993). J Biol Chem. **268**, 25273-25276.

Zlatanova, J., (1992). J Cell Sci. **103**, 889-895.

Zlatanova, J. and Doenecke D., (1994). *FASEB J.* **8**, 1260-1268.

Zlatanova, J., *et al*., (2000). FASEB J. **14**, 1697-1704.